Spring 5-17-2010

The Role of Akt2 in Hepatic Lipid Metabolism

Karla F. Leavens
Universiy of Pennsylvania, karlafl@mail.med.upenn.edu

The Role of Akt2 in Hepatic Lipid Metabolism

Abstract
Insulin drives the global anabolic response to nutrient ingestion, regulating both carbohydrate and lipid metabolism. When insulin resistance occurs in Type 2 Diabetes Mellitus, dysregulation of both of these processes ensues, resulting in hyperglycemia and lipid abnormalities. One of the most prevalent morbidities associated with insulin resistance is the abnormal accumulation of triglycerides in the liver, called hepatic steatosis, though the underlying pathogenesis of this accumulation remains unclear. There is certainly an inappropriate increase in de novo lipogenesis in the livers of individuals with hepatic steatosis, but the insulin signaling pathway involved in the control of normal, and therefore abnormal, lipogenesis remain undefined. Previous studies have demonstrated that Akt2 is critical to insulin's control of glucose metabolism, but its role in lipid metabolism has remained controversial. Here we show that Akt2 is required for hepatic lipid accumulation in obese, insulin-resistant states induced by either leptin-deficiency or high fat diet feeding. Leptin-deficient ob/ob mice lacking hepatic Akt2 failed to amass triglycerides in their livers, associated with and most likely due to a decrease in lipogenic gene expression and de novo lipogenesis. However, Akt2 is also required for steatotic pathways unrelated to fatty acid synthesis, as mice fed high fat diet had reduced liver triglycerides in the absence of hepatic Akt2 but did not exhibit changes in lipogenesis. In addition, we show that Akt2 is a requisite component of the normal insulin signaling pathway that controls de novo lipogenesis in lean non-steatotic livers. Following high-carbohydrate feeding, influx of glucose and secretion of insulin induce hepatic de novo lipogenesis in normal animals. However, liver-specific Akt2 null mice failed to induce de novo lipogenesis in response to high-carbohydrate feeding. These data demonstrate that Akt2 is required for the insulin-dependent regulation of hepatic lipid metabolism both in normal livers and during insulin resistance. These studies contribute to our understanding of insulin's control of metabolism, and may potentially aid in the development of therapeutics for diseases that are increasing in prevalence around the world.

Degree Type
Dissertation

Degree Name
Doctor of Philosophy (PhD)

Graduate Group
Cell & Molecular Biology

First Advisor
Morris J. Birnbaum

Keywords
diabetes, lipid metabolism, Akt, obesity, hepatic steatosis

Subject Categories
Cardiovascular Diseases | Endocrine System Diseases

THE ROLE OF AKT2 IN HEPATIC LIPID METABOLISM

Karla Fitzgerald Leavens

A DISSERTATION

in

Cell and Molecular Biology

Presented to the Faculties of the University of Pennsylvania

in Partial Fulfillment of the Requirements for the Degree of Doctor of Philosophy

2010

_____

Morris J. Birnbaum, M.D., Ph.D., Dissertation Advisor, Professor of Medicine

_____

Daniel S. Kessler, Ph.D., Graduate Group Chairperson, Associate Professor of Cell and Developmental Biology

Dissertation Committee Members

Mark L. Kahn, M.D., Professor of Medicine

Mitchell A. Lazar, M.D., Ph.D., Professor of Medicine

Daniel J. Rader, M.D., Professor of Medicine

Doris A. Stoffers, M.D., Ph.D., Associate Professor of Medicine

Acknowledgements

The work in this thesis could not have been performed without the help of many many individuals. The establishment of the protocol for measuring *de novo* lipogenesis *in vivo* in collaboration with Dr. Stephen Previs at Case Western Reserve School of Medicine has been especially essential. The impact of this work would have been greatly diminished without this technique and thank you to Dr. Previs for the development and initial studies, and to Dr. John Millar with whom we have an ongoing collaboration; and thank you to their respective GC/MS technicians, Paul Miller and Kevin Trindade. Thank you Dr. Gerald Shulman for his intellectual input and the measurement of hepatic long-chain fatty acid CoAs. Thank you to Ravindra Dhir and all of the Mouse Phenotyping, Physiology and Metabolism core for the clamp and energy expenditure experiments, and a special thanks to the core director, Dr. Rexford Ahima for his input and advice, both scientific and worldly. A general thanks to all of the labs of the world-class Institute of Diabetes, Obesity and Metabolism, especially the labs of Drs. Lazar, Stoffers, Ahima, Kaestner, Rader, and Thompson for their valuable help. I hope that I am fortunately enough in the future to come across another consortium of labs that has the warmth and collaborative sprit as the IDOM community.

Thank you to the members of my thesis committee, Drs. Mark Kahn, Mitch Lazar, Daniel Rader, and Dorris Stoffers for their invaluable advice, support, and focus. I would like to thank Dr. Lee Witters for introducing me to a career in medicine and the MD/PhD program at Penn for allowing me to pursue it. Thank

you to all the supportive staff and surrogate guardians in the MD/PhD and CAMB programs, especially Maggie Krall and Meagan Schofer.

Thank you to all of the members of the Birnbaum lab, past and present, especially the core members, Bob, Maureen, Qingwei, and Cass: without all of you, the lab would implode. I am eternally grateful for my graduate student colleagues, Catie, Justin, and Sarah: nothing improves productivity like grad student lunch. Thank you to Danish Saleh, who endured my first attempt at becoming a mentor. I must thank Dr. Rachael Easton: words cannot describe how important she was in the success of my tenure in the Birnbaum Lab. I am forever indebted to Dr. Morrie Birnbaum for his mentoring and support: I entered his lab as a fledgling scientist and emerge being able to critically think for myself. I cannot image that I could have possibly received better training in any other lab at Penn or beyond.

I would like to thank all of my family and friends, both scientific and non-scientific alike, for their encouragement, fun, and whiskey-identifying skills. Thank you to Rob for his humor, support and being the best part of my day through this whole process. And finally, thank you to my parents, who have always loved and supported me in whatever I do, and have made me the person I am today.

ABSTRACT

THE ROLE OF AKT2 IN HEPATIC LIPID METABOLISM

Karla Fitzgerald Leavens

Morris J. Birnbaum

Insulin drives the global anabolic response to nutrient ingestion, regulating both carbohydrate and lipid metabolism. When insulin resistance occurs in Type 2 Diabetes Mellitus, dysregulation of both of these processes ensues, resulting in hyperglycemia and lipid abnormalities. One of the most prevalent morbidities associated with insulin resistance is the abnormal accumulation of triglycerides in the liver, called hepatic steatosis, though the underlying pathogenesis of this accumulation remains unclear. There is certainly an inappropriate increase in *de novo* lipogenesis in the livers of individuals with hepatic steatosis, but the insulin signaling pathway involved in the control of normal, and therefore abnormal, lipogenesis remain undefined. Previous studies have demonstrated that Akt2 is critical to insulin's control of glucose metabolism, but its role in lipid metabolism has remained controversial. Here we show that Akt2 is required for hepatic lipid accumulation in obese, insulin-resistant states induced by either leptin-deficiency or high fat diet feeding. Leptin-deficient *ob/ob* mice lacking hepatic Akt2 failed to amass triglycerides in their livers, associated with and most likely due to a decrease in lipogenic gene expression and *de novo* lipogenesis. However, Akt2 is also required for steatotic pathways unrelated to fatty acid synthesis, as mice

fed high fat diet had reduced liver triglycerides in the absence of hepatic Akt2 but did not exhibit changes in lipogenesis. In addition, we show that Akt2 is a requisite component of the normal insulin signaling pathway that controls *de novo* lipogenesis in lean non-steatotic livers. Following high-carbohydrate feeding, influx of glucose and secretion of insulin induce hepatic *de novo* lipogenesis in normal animals. However, liver-specific *Akt2* null mice failed to induce *de novo* lipogenesis in response to high-carbohydrate feeding. These data demonstrate that Akt2 is required for the insulin-dependent regulation of hepatic lipid metabolism both in normal livers and during insulin resistance. These studies contribute to our understanding of insulin's control of metabolism, and may potentially aid in the development of therapeutics for diseases that are increasing in prevalence around the world.

Table of Contents

List of Figures

List of Tables

Chapter 1:

General Introduction

Preface

Though nutrition is essential to our survival, it has become the leading cause of death in the developed world. Cardiovascular disease and other diseases of over-nutrition dominate the health care systems of high- and middle-income countries, accounting for over 20 percent of mortality (WHO, 2008). Meanwhile, the incidence of these diseases is increasing in low-income countries, even while diseases associated with malnutrition are still prevalent. Physiologic processes evolved to maximize energy storage in a world where sustenance was scarce are now resulting in obesity and Type 2 Diabetes Mellitus (T2DM) in the face of surplus.

Among its numerous functions, the mammalian liver serves both as a repository for stored nutrients and an organ that senses, integrates and controls the metabolic state of the organism. As a metabolic tissue, the liver responds to multiple inputs, including hormones, neuronal impulses and nutrients. Understanding how the liver processes these diverse inputs becomes even more challenging when one considers pathological states associated with over-nutrition. Hepatic insulin signaling serves to coordinate energy allocation and storage upon food ingestion. During times of nutritional abundance, insulin signals to the liver to halt catabolism and to stimulate anabolism, resulting in the conversion of substrate into triglyceride for local storage as well as export. However, when this point of regulation goes awry due to the insulin resistance of T2DM, and it becomes difficult to distinguish protective from maladaptive processes. Hepatic insulin resistance can simultaneously result in the dysregulation of both catabolism, leading to the excessive output of glucose, and anabolism, driving the accumulation of lipid in the liver. Thus an understanding of hepatic insulin signaling and its regulation of metabolism are required for the development of therapies to combat the most common pathologies facing the world.

The regulation of whole-body metabolism by insulin

Introduction to insulin's control of anabolism

Insulin signaling is necessary for the regulation of growth and metabolism, and the signaling components of this pathway are conserved across species. In mammals, the metabolic role of insulin has been defined predominantly in terms of glucose and lipid homeostasis. Nutrient influx after a meal stimulates secretion of insulin from the β-cells of the pancreas, promoting nutrient uptake in peripheral metabolic tissues and suppressing energy production by the liver (Saltiel, 2001). This process is tightly regulated so that nutrient intake and storage are perfectly balanced. Insulin promotes the uptake of dietary glucose into muscle and adipose by stimulating the translocation of the glucose transporter, Glut4, to the cell surface (Nelson and Cox, 2008). The uptake of dietary lipids by peripheral tissues is also regulated by insulin, which stimulates the production of lipoprotein lipase (LPL) by endothelial cells proximal to peripheral tissues. LPL hydrolyzes triglycerides into fatty acids, which are permeable to the cell membrane and can be taken up into adipocytes to be re-esterified and stored or into muscle cells to be oxidized for energy (Ginsberg et al., 2005). Simultaneously, in order to prevent release of those stored fatty acids back into the circulation, insulin blocks lipolysis in adipocytes by inhibiting hormone-sensitive lipase (HSL).

However, while insulin stimulates the storage of nutrients by its effects in the periphery, a major site of insulin's action on metabolism is the liver. Insulin blocks hepatic glucose production, which is high during fasting, by inhibiting gluconeogenes and glycogenolysis (Saltiel, 2001). Additionally, insulin switches the liver from oxidation of fatty acids to synthesis of fatty acids from excess dietary nutrients. Insulin controls these processes in the liver by a variety of signaling pathways, involving a complex network of intracellular mediators that control cytoplasmic and transcriptional targets,

which will be described in greater detail in a later section. Overall, hepatic insulin signaling is essential to the maintenance of energy homeostasis through its regulation of glucose and lipid metabolism.

Impairments in insulin's control of metabolism occurs in Type 2 Diabetes Mellitus (T2DM)

T2DM results from a combination of impaired insulin secretion and action: insulin resistance results in reduced insulin action, leading to the need for increased insulin secretion from the pancreas, further contributing to resistance. The onset of T2DM theoretically occurs when insulin secretion can no longer compensate for increasing insulin resistance (Ahren, 2005). When this occurs, carbohydrate and lipid metabolism are no longer properly regulated, resulting in hyperglycemia and dyslipidemia. While the underlying cause of insulin resistance has not been defined, it is evident that there is an inherit defect in insulin signaling. The curve for glucose disposal in response to increasing doses of insulin is not only shifted to the right in diabetic patients, indicating a reduced responsiveness to insulin, but the maximum rate of disposal is decreased, indicating that resistance cannot be overcome by merely increasing insulin levels (Kolterman et al., 1981). Therefore, as exogenous insulin is not a cure, a better understanding of the causes of insulin resistance is required for the development of therapeutics for T2DM.

Insulin was originally discovered in the 1920s as the active compound secreted by the pancreas that could reverse the effects of Type 1 Diabetes Mellitus, resulting from auto-immune destruction of pancreatic β-cells (Nelson and Cox, 2008). Prior to the discovery of insulin, Type 1 diabetic patients were profoundly hyperglycemic and unable to store any glucose in the absence of insulin, resulting in glycosuria and ketosis from

high levels of fatty acid oxidation, all of which were reversed with insulin treatment. As the most noticeable and profound effect of insulin treatment was control of hyperglycemia in Type 1 diabetics, the study of insulin's role in the regulation of glucose metabolism has dominated. As such, most of the treatment in Type 2 diabetic patients has focused on control of glucose homeostasis. However, in a seminal essay, McGarry argued persuasively that the view T2DM as a disease of glucose metabolism is purely historical, and that the lipid abnormalities are equally intrinsic to the pathophysiology (McGarry, 1992). Though glucose levels remain a major focus in the control of type 2 diabetics, cardiovascular disease remains the leading cause of death in these patients, and determining the causes of these lipid abnormalities is the key to understanding much of the pathology associated with this disease.

Insulin's control of hepatic glucose metabolism

Insulin promotes glycogen synthesis and inhibits gluconeogenesis in the liver

During the transition from fasting to the fed state, insulin stimulates glycogen synthesis while simultaneously inhibiting hepatic gluconeogenesis and glycogen breakdown, resulting in suppression of hepatic glucose production (reviewed in Saltiel, 2001). Net glycogenesis occurs via posttranslational activation of synthesis and inhibition of breakdown, whereas termination of gluconeogenesis depends on the transcriptional suppression of gluconeogenic genes. Glycogen is synthesized by glycogen synthase, which is inhibited by phosphorylation by glycogen synthase kinase-3 (GSK3) and other kinases, such as protein kinase A (PKA); alternatively, glycogen is degraded by glycogen phophorylase, which is stimulated by phosphorylation by phosphorylase kinase (Nelson and Cox, 2008). Insulin signaling results in the phophorylation and inhibition of GSK3 and activation of protein phosphatase 1 (PP1),

promoting the dephosphorylation and subsequent activation of glycogen synthase. Concurrently, PP1 dephosphorylates glycogen phosphorylase, resulting in reduced activity (Nelson and Cox, 2008). However, most of the regulation of glycogen cycling has been described in muscle, and it is unclear whether regulation in the liver proceeds in exactly the same manner. Regardless, combined influx of glucose and insulin to the liver results in increased glycogen synthase flux and decreased glycogen phosphorylase flux, leading to the net storage of glycogen (Petersen et al., 1998).

During fasting, gluconeogenesis is amped up by the expression of critical genes such as those encoding the enzymes phosphoenolpyruvate carboxykinase (PEPCK) and glucose 6-phosphatase (G6Pase). PEPCK catalyzes an irreversible reaction at the start of gluconeogenesis and G6Pase catalyzes the dephosphorylation of newly-made glucose so that it can be released into the bloodstream (Nelson and Cox, 2008). Upon feeding when glucose and insulin levels rise, the expression of these two genes is rapidly turned off in response to the activation of insulin signaling and diminishing levels of intracellular cyclic AMP from decreasing glucagon signaling (Granner and Pilkis, 1990). The insulin signaling cascade controlling this suppression proceeds predominately through inhibition of forkhead box O1 (FoxO1) and peroxisome proliferator-activated receptor-γ coactivator-1α (PGC-1α), two proteins required in the induction of *PEPCK* and *G6Pase* expression (reviewed in Gross et al., 2008).

However, while insulin regulates the expression of genes associated with gluconeogenesis, recent studies have questioned how this directly relates to metabolic fluxes. While *PEPCK* mRNA levels are decreased to 50% by insulin during hyperinsulinemic euglycemic clamp, mice with just 10% residual expression of *PEPCK* are viable and only exhibit a 40% reduction in gluconeogenesis (Burgess et al., 2007; Sun et al., 2002). Additionally, Burgess and colleagues reported that flux through the

TCA cycle better correlates with gluconeogenic flux than does hepatic PEPCK protein content, arguing that insulin's suppression of hepatic glucose production extends beyond its conventional suppression of gluconeogenic gene expression (Burgess et al., 2007). Emerging evidence suggests that insulin may instead act by rapidly turning off hepatic glucose production from glycogenolysis by switching from glycogen breakdown to synthesis (Ramnanan et al., 2010).

Hyperglycemia

Though insulin's control of hepatic glucose metabolism is likely more complex than its influence on gluconeogenic gene expression, the outcome in T2DM is obvious: an insulin-resistant liver fails to suppress hepatic glucose output (reviewed in Saltiel, 2001). The persistence of hepatic glucose output following a meal compounds diminished glucose uptake into muscle and adipose tissue, resulting in postprandial hyperglycemia. Gluconeogenesis is inappropriately increased in states of insulin resistance due to lack of insulin signaling: disruption of hepatic insulin signaling at the level of the insulin receptor results in increased *PEPCK* and *G6Pase* expression and an inability of insulin to suppress hepatic glucose output (Michael et al., 2000).

Insulin's control of hepatic lipid metabolism

Insulin promotes de novo lipogenesis while inhibiting fatty acid oxidation and very low density lipoprotein (VLDL) export

Following food intake, insulin stimulates the liver to switch from fatty acid oxidation to fatty acid synthesis. When carbohydrate flux into the liver is high after a meal, insulin promotes the synthesis of fatty acids from excess substrates, called *de novo* lipogenesis. These fatty acids, along with dietary fatty acids, are esterified into

triglycerides and eventually exported in very low density lipoproteins (VLDL) for storage and utilization by peripheral tissues. Insulin regulates *de novo* lipogenesis through the upregulation of the genes encoding lipogenic enzymes, as described below in more detail. As fatty acid synthesis proceeds, accumulation of malonyl-CoA, a precursor of fatty acids synthesis, directly inhibits carnitine palmitoyltransferase-1 (CPT1), a transporter that shuttles fatty acids into the mitochondria, the rate-limiting step of fatty acid oxidation (Nelson and Cox, 2008). Simultaneously, insulin turns off β-oxidation of fatty acids though its inhibition of PGC-1α, a master regulator of fatty acid oxidation (reviewed in Lin et al., 2005).

While insulin stimulates lipogenesis and thus increases lipid substrates for VLDL particles, it also appears to acutely decrease VLDL secretion (reviewed in Sparks and Sparks, 1994). Insulin inhibits the release of VLDL in perfused rat liver and *in vivo* in rats injected with glucose to stimulate insulin production (Chirieac et al., 2000; Sparks et al., 1989). VLDL assembly requires the presence of both of its substrates, hepatic lipids and apolipoprotein B (apoB), and insulin likely functions by inhibiting the latter. Most regulation of apoB is thought to occur post-translationally, as increased fatty acid delivery to the liver by infusion in mice causes an increase in apoB secretion but not an increase in apoB mRNA levels (Zhang et al., 2004b). Insulin may work to suppress VLDL secretion directly by increasing degradation of apoB: in primary rat hepatocytes, the inhibition of apoB secretion by insulin correlates with an increase in intracellular degradation of apoB (Sparks and Sparks, 1994). Correspondingly, mice lacking the hepatic expression of the insulin receptor have increased apoB levels in their serum (Biddinger et al., 2008). Though the precise mechanism is unclear, insulin's effect on apoB degradation may be mediated through phosphoinositide 3-kinase (PI3K) signaling

as inhibition of PI3K by wortmannin results in increased VLDL production and secretion *in vivo* (Chirieac et al., 2006).

Dyslipidemia

Type 2 diabetic patients have characteristic lipid abnormalities, called diabetic dyslipidemia; this is a triad of increased levels of triglycerides in VLDL, high or normal levels of low density lipoprotein (LDL) cholesterol, and low levels of high density lipoprotein (HDL) cholesterol is known to be highly atherogenic (Taskinen, 2003). The presence of insulin resistance and diabetic dyslipidemia is one of the major risk factors in the development of atherosclerosis and other cardiovascular disease (Isomaa et al., 2001; Reilly and Rader, 2003). While high serum cholesterol levels have been recognized as a major risk factor for cardiovascular disease and LDL has been the major target of lipid-lowering therapy, hypertriglyceridemia is emerging as another major risk factor. Though these particles are not thought to be directly atherogenic, increased VLDL levels can lead to the generation of small, dense LDL through the action of cholesteryl ester transfer protein (CEPT) (Ginsberg et al., 2005). These small, dense cholesterol ester-depleted LDL particles are highly atherogenic, and low levels of HDL cholesterol can also result from this CEPT-mediated process. Thus, elevated serum triglycerides are considered to be an independent risk factor for heart disease, though the pathogenesis remains unclear.

Hypertriglyceridemia is thought to be caused in the insulin-resistant state by VLDL overproduction in the liver (Taskinen, 2003). There are three major sources of triglyceride for hepatic VLDL, all of which have been shown to be upregulated in insulin-resistant states: fatty acid flux from adipose to the liver, hepatic uptake of VLDL remnants, and *de novo* lipogenesis (reviewed in Ginsberg et al., 2005). Studies using a

fructose-fed hamster model of insulin resistance and dyslipidemia showed that VLDL overproduction may result from decreased apoB degradation normally induced by insulin (Taghibiglou et al., 2000). When hepatic insulin signaling is improved pharmacologically in this model, apoB degradation increases, and VLDL secretion decreases (Carpentier et al., 2002). However, which process actually drives hypertriglyceridemia present in T2DM remains unclear: leptin-deficient obese *ob/ob* mice have massively increased rates of *de novo* lipogenesis but do not exhibit increased VLDL triglyceride or apoB levels (Li et al., 1997; Wiegman et al., 2003). Regardless, insulin still fails to effectively inhibit VLDL secretion in *ob/ob* livers under hyperinsulinemic euglycemic clamp conditions, and this may be the point of dysregulation that leads to hypertriglyceridemia in this model (Wiegman et al., 2003). Alternatively, triglyceride secretion from perfused liver from Zucker Diabetic Fatty (ZDF) rats is 5 times greater than that from lean rats, and their secreted VLDL particles had increased apoB content (Azain et al., 1985). Therefore the precise pathogenesis underlying VLDL oversecretion in T2DM remains unclear.

Hepatic steatosis

Another lipid abnormality associated with insulin resistance is the accumulation of lipid, mostly triglycerides, in the liver, called hepatic steatosis. Hepatic steatosis is thought to be relatively benign, but can progress to inflammatory steatohepatitis, fibrosis, and cirrhosis. This entire spectrum is termed non-alcoholic fatty liver disease (NAFLD), and is likely present in 14% to 24% of the general population (reviewed in Browning and Horton, 2004). However, when obese individuals are considered, the prevalence rises to between 57% and 74% (Angulo, 2002). Thus, as the prevalence of obesity and T2DM increase, so will the number of people with hepatic steatosis and other NAFLDs. While it

is unclear what mediates the progression of hepatic steatosis to more serious disease, increasing prevalence of NAFLD will result in increasing numbers of patients with end-stage liver disease: NAFLD is already becoming a dominant indication for liver transplant (Browning and Horton, 2004).

The underlying pathogenesis of hepatic steatosis remains undefined, though it is clearly associated with states of hepatic insulin resistance. There are increased sources of fatty acids for esterification into triglycerides in insulin-resistant livers (reviewed in Ginsberg et al., 2005). Insulin is less able to block lipolysis in adipose tissue through its inhibition of HSL, resulting in increased hydrolysis of triglycerides and increased non-esterified fatty acid (NEFA) levels for the liver to take up from the serum (Adeli et al., 2001). Insulin promotes *de novo* lipogenesis in a normal liver; thus, in the presence of insulin resistance, hepatic lipid synthesis should be impaired. Unexpectedly, insulin's promotion of lipogenesis is maintained and even enhanced by hyperinsulinemia occurring in T2DM. Furthermore, hyperglycemia may enhance pathological lipid accumulation in T2DM as the excess glucose provides increased substrate for *de novo* lipogenesis. Additionally, fatty acid oxidation is decreased in insulin-resistant livers, though whether this is due to inhibition by *de novo* lipogenesis or secondary to mitochondrial overload and oxidative stress is unclear (Angulo, 2002; Browning and Horton, 2004; Parekh and Anania, 2007). Regardless, ketogenesis is decreased by 40% in ZDF rats and malonyl-CoA, an precursor of lipogenesis and inhibitor of fatty acids oxidation, is increased (Azain et al., 1985).

Selective insulin resistance: insulin signaling is simultaneously defective to glucose metabolism and enhanced to lipid metabolism

Hepatic insulin resistance has been classically defined as an inability of insulin to suppress hepatic glucose output, as measured by hyperinsulinemic euglycemic clamp. Since insulin signaling normally induces *de novo* lipogenesis in the liver, this pathway should be impaired as well in states of insulin resistance. However, the existence of hepatic steatosis refutes this assumption and, unlike insulin signaling to glucose homeostasis, insulin's promotion of lipogenesis is preserved, driving synthesis and contributing to the accumulation of triglyceride in the liver. This phenomenon has been termed selective insulin resistance where the insulin signaling pathways inhibiting glucose metabolism are impaired while those stimulating lipid metabolism are preserved (Brown and Goldstein, 2008).

It is this phenomenon that drives the devastating co-existence of hyperglycemia and hypertriglyceridemia in T2DM. As pointed out by Brown and Goldstein, mice lacking the insulin receptor in the liver, so-called "pure hepatic insulin-resistant" mice, ironically exhibit a less severe condition consisting of hyperglycemia but hypotriglyceridemia (Brown and Goldstein, 2008). Therefore, there must be a bifurcation of insulin signaling below the level of the insulin receptor into two distinct pathways: one that suppresses glucose metabolism and is lost in insulin-resistant states and one that stimulates lipid synthesis and is retained in insulin-resistant states. It is apparent that glucose metabolism is controlled distally by FoxO1 and lipid metabolism by sterol regulatory element-binding protein-1c (SREBP1c), but the point at which signaling diverges is unknown.

De novo lipogenesis: a site of dysregulation in insulin resistance

Mechanism and control of fatty acid synthesis

Acetyl-CoA is formed in the mitochondria from pyruvate by pyruvate dehydrogenase and can enter the citric acid cycle for eventual oxidation and generation of energy (Nelson and Cox, 2008). However, following a meal, more acetyl-CoA is produced in the liver than needs to be oxidized for energy production: this excess acetyl-CoA is converted into fatty acids by *de novo* lipogenesis. The primary source of substrate for fatty acid synthesis in the liver is glucose, but fructose, galactose, lactate, pyruvate and amino acids also contribute to the pool of acetyl-CoA (Hillgartner et al., 1995). In the cytosol, acetyl-CoA carboxylase (ACC) converts acetyl-CoA into malonyl-CoA, the major source of carbon for fatty acid synthesis. This step is also the major site of regulation of *de novo* lipogenesis. Acetyl-CoA must be exported from the mitochondria as citrate and converted back into acetyl-CoA by ATP citrate lyase (ACL), an enzyme activated by insulin (Nelson and Cox, 2008). Citrate allosterically activates ACC while simultaneously inhibiting flux through glycolysis; conversely, ACC is allosterically inhibited by the end product of fatty acid synthesis, palmitoyl-CoA. ACC is also inhibited by phosphorylation induced by glucagon signaling and other pathways that inhibit fatty acid synthesis, such as AMP-activated protein kinase (AMPK) (Hillgartner et al., 1995).

The 2-carbon units provided by malonyl-CoA are joined and reduced sequentially by fatty acid synthase (FAS), eventually forming the saturated 16-carbon fatty acid palmitate. Palmitate is the major product of *de novo* lipogenesis, but also serves as a substrate for elongases and desaturases, such as stearoyl-CoA desaturase-1 (SCD1), for the generation of longer chain and unsaturated fatty acids. In the liver, most fatty acids are joined to a glycerol backbone by acyltransferases to generate triglycerides for storage. Accumulating malonyl-CoA shuts off β-oxidation by inhibiting CPT1 so that

futile cycling of fatty acid synthesis and breakdown does not occur (Nelson and Cox, 2008).

The transcription of multiple lipogenic enzymes, including *FAS, SCD1, ACC, ACL,* glycerol phosphate acyltransferase (*GPAT)*, glucokinase (*GCK*), and liver pyruvate kinase (*L-PK*), are upregulated in response to feeding. These simultaneous increases in expression are designed to increase the concentration of lipogenic enzymes thus allowing increased flux through lipogenesis in the presence of excess carbohydrates (reviewed in Postic and Girard, 2008). Inhibition or deletion of many of these target genes themselves, including *SCD1, ACC,* and *GPAT* can also prevent animals from developing hepatic steatosis due to leptin-deficiency or diet-induced obesity (DIO) by either decreasing lipogenesis or increasing flux of fatty acids into β-oxidation (Cohen et al., 2002; Gutierrez-Juarez et al., 2006; Harada et al., 2007; Jiang et al., 2005; Mao et al., 2006; Miyazaki et al., 2007; Neschen et al., 2005; Ntambi et al., 2002; Savage et al., 2006). The influences of both insulin and glucose on lipogenic gene expression are controlled by two distinct transcription factors: insulin via SREBP1c and glucose via carbohydrate response element-binding protein (ChREBP) (Dentin et al., 2004; Koo et al., 2001). These two factors coordinately stimulate lipogenic gene expression in response to both the nutrient influx and increased insulin secretion that occur during feeding.

De novo lipogenesis is inappropriately elevated in livers of patients with hepatic steatosis

Rates of hepatic *de novo* lipogenesis are fairly low in normal lean individuals, as measured by contribution to the fatty acids in hepatically-derived VLDL. Under post-absorptive conditions in humans, only approximately 4% of triglycerides secreted into the serum come from *de novo* lipogenesis, while 50% can be attributed to NEFA re-

esterification (Diraison and Beylot, 1998). *De novo* synthesis of fatty acids increases following food intake, rising from approximately 5% of fatty acids in VLDL to approximately 23% post-prandially at the peak, occurring just over 4 hours after meals (Timlin and Parks, 2005). Diets rich in carbohydrates can further stimulate *de novo* lipogenesis in normal individuals, and have been reported to result in a 10-fold increase (Schwarz et al., 1995). However, even under these conditions, *de novo* lipogenesis only accounts for the synthesis of 5 grams of fatty acids per day (Schwarz et al., 1995).

Though *de novo* lipogenesis may be low in lean individuals, it still contributes significantly to hepatic steatosis in the presence of obesity and insulin resistance. Individuals with existing hepatic steatosis should have very low rates of *de novo* lipogenesis as there are already ample stores of triglycerides in their livers. However, lipogenesis is inappropriately elevated in the livers of patients with hepatic steatosis, accounting for approximately 25-30% of the total hepatic triglyceride content and a three-fold increased contribution to VLDL triglyceride secretion (Diraison et al., 2002; Diraison et al., 2003; Donnelly et al., 2005; Forcheron et al., 2002). Normal individuals exhibit a cycling of their rates of hepatic *de novo* lipogenesis, corresponding to food intake and elevations in serum insulin levels (Timlin and Parks, 2005). However, Donnelly et al. reported that in individuals with NAFLD, *de novo* lipogenesis is elevated even during fasting and exhibits no diurnal variation (Donnelly et al., 2005). Triglycerides secreted from the perfused livers of ZDF rats contain 5-fold higher levels of *de novo* synthesized fatty acids compared with lean rats (Azain et al., 1985). Even following the consumption of a low-carbohydrate high-fat diet, which is known to decrease lipogenesis in lean individuals, hyperinsulinemic obese individuals have 3- to 5-fold higher rates of lipogenesis than lean or obese but normoinsulinemic individuals (Hillgartner et al., 1995; Schwarz et al., 2003). Similar results have been reported in

ZDF rats, which exhibit high rates of *de novo* lipongenesis that are not suppressed by high-fat feeding as observed in lean rats (Lee et al., 2000).

The control of lipogenic gene expression by two transcription factors: SREBP1c and ChREBP

Much research has been directed towards determining the transcriptional control of *de novo* lipogenesis by insulin and glucose via SREBP1c and ChREBP, respectively (Koo et al., 2001; Postic et al., 2007; Postic and Girard, 2008). Though each transcription factor is required for the maximal accumulation of hepatic triglyceride during insulin resistance in mice, the relative roles of these two transcription factors in the development of hepatic steatosis and under more physiological conditions remains unclear (Dentin et al., 2006; Postic and Girard, 2008; Yahagi et al., 2002).

Sterol regulatory element-binding protein-1c (SREBP1c)

The SREBP family members are synthesized as precursor molecules in the endoplasmic reticulum and proteolytically cleaved to release active amino-terminal transcript factors that translocate to the nucleus (reviewed in Horton, 2002). There are two SREBP1 isoforms generated by alternative splicing: SREBP1a is more active than SREBP1c in cultured cells and activates genes for both triglyceride and cholesterol synthesis, while SREBP1c only activates triglyceride synthetic genes (Shimano et al., 1996; Shimano et al., 1997a). Transgenic mice overexpressing the active nuclear transcription factor fragment of SREBP1a (nSREBP1a) have fattier livers, increased hepatic cholesterol and triglyceride levels, and increased lipogenic gene expression compared with mice overexpressing nSREBP1c (Shimano et al., 1996; Shimano et al., 1997a; Shimomura et al., 1997). However, though SREBP1a is more active and the

more highly expressed variant in cultured cell lines, SREBP1c is expressed at 9-fold higher levels in the liver (Shimomura et al., 1997). Alternatively, the other SREBP isoform, SREBP2 preferentially activates genes of cholesterol synthesis, as transgenic nSREBP2 mice have hepatic steatosis due to massive cholesterol accumulation without a significant increase in hepatic triglyceride content (Horton et al., 1998b).

Insulin increases *SREBP1c* mRNA levels, resulting in a parallel increase of lipogenic target genes, and, conversely, *SREBP1c* expression is low in rats with insulin-deficiency caused by streptozotocin treatment (Foretz et al., 1999; Shimomura et al., 1999b). nSREBP1c protein and lipogenic mRNAs are low in fasted animals, but refeeding with a high-carbohydrate/low-fat diet results in a 4-fold increase in both compared with pre-fasted fed conditions, whereas nSREBP2 protein and cholesterol synthetic genes only return to non-fasted levels (Horton et al., 1998a). Transgenic mice overexpressing the active nuclear transcription factor fragment of SREBP1c (nSREBP1c) in liver have hepatic steatosis, a 4-fold increase in fatty acid synthesis and increased lipogenic gene expression, which remains high even under fasting conditions (Horton et al., 1998a; Shimano et al., 1997a; Shimomura et al., 1999a; Shimomura et al., 1998). Adenoviral overexpression of nSREBP1c in streptozotocin-induced diabetic mice also induces lipogenic gene expression and increases hepatic triglyceride content (Becard et al., 2001).

The majority of *SREBP1*$^{-/-}$ mice die prior to birth, but those that do survive have decreased lipogenic gene expression during refeeding or prolonged high-carbohydrate feeding (Shimano et al., 1997b; Shimano et al., 1999). *SREBP1c*$^{-/-}$ mice do not experience embryonic lethality like the *SREBP1*$^{-/-}$ mice, but exhibit a similar reduction in lipogenic gene expression and serum triglycerides, under both fasted and refed conditions (Liang et al., 2002). Both models also have decreased serum triglycerides at

12 hours after refeeding, but only *SREBP1c*$^{-/-}$ mice have a significant reduction in hepatic triglycerides, and only after high-carbohydrate refeeding. Interestingly, cholesterol biosynthetic genes were increased in both mouse models, likely due to the compensatory upregulation of SREBP2 that occurs with loss of SREBP1 or SREBP1c (Liang et al., 2002; Shimano et al., 1999). Leptin-deficient obese *ob/ob* mice have increased mRNA and nuclear protein levels of SREBP1c and increased expression of its lipogenic targets, which correlate with the increased rates of *de novo* lipogenesis and hepatic triglyceride content of these animals (Shimomura et al., 1999a). Hepatic steatosis and lipogenic gene expression are markedly reduced in *ob/ob* mice lacking SREBP1 without causing a reduction in obesity or insulin resistance (Yahagi et al., 2002).

Though *SREBP1c* expression is important with regards to lipogenesis and hepatic steatosis, the post-translational regulation of SREBP1c is also influential. Following high-carbohydrate feeding, nSREBP1c protein increases to a much greater extent than either *SREBP1* mRNA or full-length protein (Horton et al., 1998a). Lipodystrophic mice exhibit increased hepatic lipogenesis, lipogenic gene expression and nSREBP1c protein in liver without exhibiting an increase in *SREBP1c* mRNA (Shimomura et al., 1999a). Liver-specific deletion of either SREBP cleavage-activating protein (SCAP) or Site-1 protease, two proteins required for the processing of precursor SREBP1c into active nSREBP1c, results in decreased hepatic lipid synthesis and decreased hepatic and serum triglyceride levels (Matsuda et al., 2001; Yang et al., 2001). Liver-specific deletion of SCAP also results in decreased expression of SREBP1c target genes (Kuriyama et al., 2005). As these proteins are also required for the processing of SREBP1a and SREBP2, hepatic cholesterol biosynthesis and content, and serum cholesterol are decreased as well in these mice.

Carbohydrate response element-binding protein (ChREBP)

Though SREBP1c is an important regulator of lipogenic gene expression, it is clearly not the sole influence. Liver-specific deletion of SCAP in mice eliminates most of the active nSREBP1c protein, yet some lipogenic gene expression does remain (Matsuda et al., 2001). Certain lipogenic genes (*FAS* and *ACC*) show less of a reduction than others (*GPAT*) in *SREBP1*$^{-/-}$ and *SREBP1c*$^{-/-}$ mice following high-carbohydrate refeeding (Liang et al., 2002; Shimano et al., 1999). In addition, the maximal upregulation of many lipogenic genes in primary hepatocytes requires glucose as well as insulin stimulation, and other lipogenic genes, such as *L-PK*, respond to increases in glucose rather than SREBP1c activation (Kawaguchi et al., 2001; Koo et al., 2001; Koo and Towle, 2000; Stoeckman and Towle, 2002; Yamashita et al., 2001). These observations eventually lead to the definition of the transcription factor, ChREBP that responds to increased intracellular glucose levels and, in tandem with the stimulation of SREBP1c by insulin, results in the upregulation of lipogenic genes (Dentin et al., 2004; Kawaguchi et al., 2001; Koo et al., 2001; Yamashita et al., 2001). *ChREBP*$^{-/-}$ mice have decreased basal and high-carbohydrate diet-stimulated hepatic expression of *FAS*, *ACL*, *ACC* and *L-PK*, the latter being a specific target of ChREBP, as well as having decreased lipogenesis and hepatic triglycerides on high-carbohydrate diet (Iizuka et al., 2004). These mice have normal hepatic triglyceride levels on chow diet as both lipid oxidation and synthesis are decreased, but exhibit decreased fat stores, and an inability to store and metabolize fatty acids, resulting in increased hepatic glycogen storage and dependence on carbohydrate metabolism (Burgess et al., 2008; Iizuka et al., 2004). As with *SREBP1c*, *ChREBP* is upregulated in the livers of *ob/ob* mice, and lipogenic gene expression and hepatic steatosis is reduced in *ob/ob* mice lacking ChREBP either globally or specifically in the liver. However, unlike *SREBP1*$^{-/-}$ mice on an *ob/ob*

background, ChREBP deficiency improves the insulin resistance and glucose intolerance of *ob/ob* mice, revealing different roles for these transcription factors beyond the stimulation of lipogenic gene expression (Dentin et al., 2006; Iizuka et al., 2006; Yahagi et al., 2002).

The insulin/PI3K signaling pathway

Overview of the insulin signaling cascade

Insulin signaling influences cellular processes through two major branches: signaling through phosphatidylinositol 3-kinase (PI3K) and mitogen-activated protein kinase (MAPK). Much of insulin's effects on metabolism have been attributed to signaling through PI3K, while MAPK is thought to mediate insulin's effects on growth and differentiation; the latter will not be discussed further in this overview. The major signaling components of the PI3K pathway are shown in Figure 1-1. Insulin signaling is initiated when insulin binds to its receptor present on the membrane surface of the cell (reviewed in Nelson and Cox, 2008; Taniguchi et al., 2006a). The insulin receptor is a receptor tyrosine kinase, which, upon binding of insulin, is autophosphorylated and activated. Once activated, the receptor can phosphorylate tyrosine residues on the insulin receptor substrate (IRS) molecules, leading to their activation. IRS proteins can bind and activate molecules with SH2 domains, including PI3K, a lipid kinase. PI3K phosphorylates the membrane lipid phosphatidylinositol 4,5-bisphosphate (PIP_2) converting it into 3,4,5-tiisphosphate (PIP_3); PIP_3 can be reverted back to PIP_2 by the phosphatase PTEN (Nelson and Cox, 2008). PIP_3 binds and co-localizes the 3-phosphoinositide-dependent protein kinase 1 (PDK1) and its targets, Akt and atypical protein kinase C (aPKC) at the cell membrane. These two kinases are phosphorylated

and activated, eventually leading to many of insulin's effects on glucose, lipid, and protein metabolism (Taniguchi et al., 2006a).

Akt is a major mediator of the metabolic actions of insulin

The serine-threonine kinase Akt exists as three highly related isoforms, Akt1-3, each encoded by a distinct gene. Based on studies of mice with interruptions in each locus, Akt2 is the major isoform mediating insulin's effects on glucose metabolism, whereas Akt1 and Akt3 are more important to growth (Chen et al., 2001; Cho et al., 2001a; Cho et al., 2001b; Easton et al., 2005; Garofalo et al., 2003). Each isoform contains a highly similar pleckstrin homology (PH) domain responsible for Akt's binding to PIP_3, a kinase domain, and carboxyl-terminal regulatory domain (reviewed in Hanada et al., 2004). There are two known activating phosphorylations that all Akt isoforms can undergo: PDK1 phosphorylates threonine-308 within the kinase domain and mammalian target of rapamycin complex 2 (mTORC2) phosphorylates serine-473 within the regulatory domain (Alessi et al., 1997; Hresko and Mueckler, 2005; Sarbassov et al., 2005; Stephens et al., 1998). Phosphorylation at both of these sites is thought to required for the full activation of Akt (Hanada et al., 2004). Akt exerts its effects through the activation of mTOR complex 1 (mTORC1) and the inhibition of GSK3, FoxO1, and PGC-1α. Akt is central to the hepatic actions of insulin on glucose output: the prevalent model is that activated Akt phosphorylates and inhibits the transcription factor FoxO, PGC-1α, and others, thereby terminating expression of the rate-controlling enzymes of gluconeogenesis (Gross et al., 2008; Li et al., 2007). Additionally, Akt phophorylates and inhibits GSK3, releasing its inhibition on glycogen synthase, with the net effect of insulin stimulating the production of glycogen (Cross et al., 1995; Roach, 2002). Akt also positive regulates mTOR signaling and protein synthesis by phophorylating and

inhibiting tuberous sclerosis complex-2 (TSC2), which in conjunction with tuberous sclerosis complex-1 (TSC1) negatively regulates mTORC1 (Taniguchi et al., 2006a).

Insight into insulin's control of lipid metabolism from insulin signaling mutants

Insulin Receptor

While the signal transduction pathways through which insulin controls lipid metabolism have not been fully defined, the study of rodents with mutations in the components of the insulin signaling cascade has aided in this process. Mice lacking the insulin receptor in liver (LIRKO mice) have no hepatic insulin signaling and as a result exhibit severe glucose intolerance due to an inability to suppress hepatic glucose output in response to insulin (Michael et al., 2000). Though they are able to maintain normal hepatic triglyceride levels on a chow diet, these mice have decreased *SREBP1c, SCD1, FAS, GCK,* and *L-PK* expression and well as dramatically decreased nSREBP1c protein levels (Biddinger et al., 2008; Michael et al., 2000). Decreased lipogenic gene expression coupled with increased secretion and decreased clearance of VLDL results in triglyceride-deficient cholesterol-rich VLDL particles. Though serum triglyceride levels are low and serum cholesterol levels are normal in chow-fed LIRKO mice, they do have a significantly higher propensity for developing severe atherosclerosis on an atherogenic diet, likely due to their abnormal lipoprotein profile (Biddinger et al., 2008). Similarly, mice with severely impaired insulin signaling (L1 mice) on a *Ldlr*$^{-/-}$ background exhibit decreased serum triglyceride levels along with decreased lipogenic gene expression when fed an atherogenic diet; however, these mice have reduced VLDL and serum cholesterol levels and are actually protected from the development of atherosclerosis unlike the LIRKO mice (Han et al., 2009). The differing results observed in these two models is likely due to residual hepatic insulin signaling in the L1 mice as opposed to the

complete absence of hepatic insulin signaling in the LIRKO mice. The dyslipidemia and decreased lipogenic gene expression are partially reversed by expression of constitutively active Akt in both models and by expression of dominant-negative GSK3 in the latter, but it is unclear if this was a physiological action of these proteins or a result of overexpression in the context of complete or almost complete insulin receptor deficiency (Biddinger et al., 2008; Han et al., 2009).

Insulin Receptor Substrate (IRS)

Once activated, the insulin receptor phosphorylates IRS proteins, and it has been proposed that the bifurcation of selective insulin signaling in the liver may occur at the level of these molecules, though this idea is controversial. Disruption of either *IRS1* or *IRS2* globally results in insulin resistance in both models, and overt diabetes in *IRS2*$^{-/-}$ mice, potentially confounding the interpretation of the role of each protein in hepatic lipid metabolism in whole-body null animals (Araki et al., 1994; Tamemoto et al., 1994; Withers et al., 1998). *IRS1*$^{-/-}$ mice have hypertriglyceridemia likely due to loss of IRS1 in adipose tissue and *IRS2*$^{-/-}$ mice have increased *SREBP1c, ACL,* and *FAS* expression and increased hepatic triglyceride content likely caused by leptin resistance (Abe et al., 1998; Tobe et al., 2001). High doses of leptin decrease the elevation in *SREBP1c* expression in *IRS2*$^{-/-}$ mice and leptin-deficient *ob/ob* mice exhibit decreased *IRS2* and increased *SREBP1c* expression (Kerouz et al., 1997; Shimomura et al., 1999a; Tobe et al., 2001).

Liver-specific *IRS2*$^{-/-}$ mice have normal serum NEFA and triglyceride levels, in addition to having normal lipogenic gene expression and hepatic triglyceride content (Simmgen et al., 2006). However, acute liver-specific knockdown using RNA interference (RNAi) against *IRS2* in adult mice results in increased *SREBP1c* expression

and mild fatty liver changes but no increase in hepatic triglyceride content (Taniguchi et al., 2005). Alternatively, acute liver-specific knockdown of *IRS1* by RNAi does not alter lipogenic gene expression or serum and hepatic triglyceride levels, but does cause an increase in gluconeogenic gene expression and fasting glucose levels, suggesting that IRS1 is more important to insulin's control of glucose metabolism (Taniguchi et al., 2005). However, there is likely overlap between the IRS proteins as coordinate hepatic knockdown by RNAi of *IRS1* and *IRS2* results in a more substantial increase in lipogenic gene expression, serum and hepatic triglycerides, glucose levels and gluconeogenic gene expression (Taniguchi et al., 2005).

While Taniguchi et al suggests that IRS1 controls glucose metabolism and IRS2 is more important to lipid metabolism based on acute hepatic knockdown, White and colleagues have published a series of reports arguing that IRS1 is more critical to hepatic lipid metabolism. IRS1-associated PI3K activity is highest after refeeding, coinciding with the activation of *SREBP1c* and lipogenic gene expression, while IRS2-associated PI3K activity is highest during fasting and immediately after refeeding (Horton et al., 1998a; Kubota et al., 2008). Unlike short-term hepatic knockdown, *IRS1/IRS2* liver-specific null mice have normal fasted but decreased refed *SREBP1c* expression, highlighting the potential differences resulting from genetic ablation versus adult knockdown (Dong et al., 2008). These mice lack the normal rise in *GCK*, *FAS*, and *SREBP1c* levels that occurs during refeeding in addition to having decreased serum triglycerides. The effects on serum triglycerides are reversed with the presence of one allele of either *IRS1* or *IRS2*, while the effect on lipogenic gene expression is reversed, and only partially, with one allele of *IRS1* (Guo et al., 2009). Additionally, though both *IRS1/IRS2* liver-specific null mice have impairments in the induction of lipogenic genes during the fasted to fed transition, these impairments appear to be greater for the most

part in the absence of *IRS1* (Guo et al., 2009). When fed a high fat diet, *IRS1/IRS2* liver-specific null mice have decreased hepatic triglycerides, an effect that is also observed in the *IRS1* liver-specific null, but not in the *IRS2* liver-specific null (Guo et al., 2009). Thus there is conflicting evidence for the bifurcation of insulin signaling to glucose and lipid metabolism at the level of IRS.

Phosphatidylinositol 3-kinase (PI3K)

There is evidence that PI3K may mediate insulin's effects on both VLDL secretion and lipogenesis. Acute inhibition of PI3K by wortmannin reverses insulin's suppression of hepatic VLDL production, resulting in increased serum VLDL apoB protein and triglyceride in mice (Chirieac et al., 2006). Adenoviral expression of a dominant-negative PI3K p85 regulatory subunit results in a marked decrease in phosphorylation of Akt, decreased *SREBP1c* and *GCK* expression, as well as lower serum triglycerides and NEFA, though the reduction in serum lipids is likely due to increased hyperinsulinemia driving uptake into adipose tissue (Miyake et al., 2002). A similar result is found in mice with genetic ablation of all PI3K activity in the liver, which results in decreased serum triglycerides and NEFA and decreased fasted *SREBP1c* expression as well as elevated glucose and insulin levels and increased gluconeogenic gene expression (Taniguchi et al., 2006b). Insulin-dependent induction of *SREBP1c* expression is blocked in rat hepatocytes following inhibition of PI3K with wortmannin (Li et al., 2010). Additionally, SREBP1c processing is influenced through a PI3K-dependent mechanism as wortmannin treatment of rat hepatocytes results in decreased nSREBP1c levels (Hegarty et al., 2005).

Atypical protein kinase C (aPKC)

Genetic ablation of all PI3K activity in the liver results in decreased serum triglycerides and fasted *SREBP1c* expression and decreased insulin-stimulated activity of its downstream target aPKCs, including PKCλ (Taniguchi et al., 2006b). Adenoviral overexpression of constitutively active PKCλ dramatically increases fasted *SREBP1c* expression in both liver-specific *PI3K* null and control mice, though the metabolic ramifications of this manipulation were not reported (Taniguchi et al., 2006b). Additionally, overexpression of PKCλ in primary rat hepatocytes results in increased *SREBP1c* and *FAS* expression, while overexpression of kinase-inactive PKCλ results in decreased insulin-stimulated expression (Matsumoto et al., 2003). These findings are corroborated by the liver-specific *PKCλ* null mice, which exhibit decreased hepatic *SREBP1c* expression and triglyceride content and have blunted induction of *SREBP1c*, *FAS*, and *SCD1* expression during refeeding (Matsumoto et al., 2003; Sajan et al., 2009). Additionally, hepatic adenoviral expression of a kinase-inactive aPKC results in decreased *SREBP1c* expression and nSREBP1c levels and decreased serum and hepatic triglycerides (Sajan et al., 2009). However, in the latter two models, decreased aPKC activity resulted in a simultaneous decrease in insulin levels, and thus the effects on triglyceride levels and lipogenic gene expression could be secondary to decreased insulin levels (Matsumoto et al., 2003; Sajan et al., 2009).

Akt

Akt activates the transcription of *SREBP1c* and its lipogenic targets in isolated hepatocytes and a human epithelial cell line (Fleischmann and Iynedjian, 2000; Porstmann et al., 2005; Ribaux and Iynedjian, 2003). Hepatic overexpression of constitutively active Akt (myr-Akt) results in hepatic steatosis and hypertriglyceridemia, with induction of *SREBP1c, SCD1*, and *GCK*, a smaller increase in *FAS* and no change

in *ACC* or fatty acid oxidation genes (Ono et al., 2003). However, not all of the effects of myr-Akt proceed through SREBP1c, as the induction of hepatic triglyceride accumulation, *GCK* and *FAS* expression by myr-Akt in *SREBP1* null mice is similar to that in normal mice, though the degree of hypertriglyceridemia and *SCD1* expression is dramatically reduced (Ono et al., 2003). Additionally, hepatic deficiency of PTEN, a negative regulator of Akt, also leads to increased lipogenesis, lipogenic gene expression and VLDL secretion, resulting in hepatic steatosis (Horie et al., 2004; Stiles et al., 2004). However, it has been argued that the resulting hepatic steatosis could be an off-target effect of overexpression of Akt, and not indicative of the role of Akt in normal hepatic lipid metabolism. Genetic ablation of all PI3K activity in the liver results in decreased fasted *SREBP1c* expression, an effect that is not reversed with overexpression of myr-Akt (Taniguchi et al., 2006b).

Peroxisome proliferator-activated receptor-γ coactivator-1α (PGC-1α)

PGC-1α is a transcription factor that integrates multiple inputs including insulin signaling to coordinately regulate many aspects of metabolism (reviewed in Lin et al., 2005). Expression of PGC-1α is highest in the liver during fasting and positively regulates β-oxidation and perhaps VLDL secretion while potentially inhibiting *SREBP1c* expression (Zhang et al., 2004a). Akt directly phosphorylates and inhibits PGC-1α at Ser570, impairing its ability to activate genes involved in fatty acid oxidation, in particular, medium-chain acetyl-CoA dehydrogenase (*MCAD*) (Li et al., 2007). Additionally, in primary hepatocytes, expression of PGC-1α stimulates palmitate oxidation and co-expression of myr-Akt significantly blunts this stimulation in cells expressing PGC-1α but not in those expressing a S570A mutant of PGC-1α. Akt's inhibition of PGC-1α serves as a dual regulatory step for the hepatic switch from fasting

to feeding, simultaneously turning off fatty acid oxidation and gluconeogenesis, the latter in concert with Akt's phosphorylation and inhibition of FoxO1 (Li et al., 2007).

Mice lacking PGC-1α either in the whole body or specifically in the liver develop hepatic steatosis during fasting due to decreased β-oxidation and increased lipogenic gene expression (Estall et al., 2009; Leone et al., 2005). Additionally, liver-specific *PGC-1*$\alpha^{-/-}$ mice display hypertriglyceridemia, correlating with increased apoB levels, as well as increased hepatic insulin resistance (Estall et al., 2009). Mice lacking the highly homologous protein PGC-1β also exhibit increased hepatic steatosis when fed a high fat diet due to decreased β-oxidation (Lelliott et al., 2006; Sonoda et al., 2007).

Mammalian Target of Rapamycin (mTOR)

mTOR is a serine-threonine kinase that promotes insulin/PI3K/Akt's positive effects on protein synthesis through activation of S6 Kinase (S6K) and inhibition of the translation inhibitor eIF4E-binding protein (4E-BP). The activities of both mTOR and S6K are increased in obese rats, and S6K1 activity is increased in *ob/ob* mice (Khamzina et al., 2005; Um et al., 2004). Inhibition of mTOR by rapamycin in isolated rat hepatocytes results in decreased *de novo* lipogenesis and esterification of fatty acids and increased fatty acid oxidation (Brown et al., 2007). Furthermore, rapamycin blocked the stimulation of *SREBP1c* expression by insulin in isolated rat hepatocytes and by fasting/refeeding in rats *in vivo* (Li et al., 2010). Expression of myr-Akt *in vitro* activates SREBP1 processing, *SREBP1, FAS* and *ACL* expression and leads to increased *de novo* lipogenesis, all of which are prevented by mTOR inhibition with rapamycin (Porstmann et al., 2008). This is a highly-conserved pathway for nutrient storage as *Drosophila melanogaster* deficient in dTOR have decreased lipid levels while those

deficient in 4E-BP have normal triglyceride stores but deplete them more rapidly and thus have reduced survival during starvation (Luong et al., 2006; Teleman et al., 2005).

Mice deficient for S6K1 are hyperglycemic due to reduced insulin secretion, but are small and have reduced fatty acid levels due to increased β-oxidation in adipose tissue (Pende et al., 2000; Um et al., 2004). However, it is unknown whether S6K plays a similar role in hepatic β-oxidation and it has been proposed that S6K may not have a direct role in metabolism but causes negative feedback to the insulin signaling pathway at the level of IRS1 (Um et al., 2004). This concept has been reinforced by findings in mice lacking 4E-BP1/4E-BP2 that exhibit hepatic steatosis, increased S6K activity in liver, muscle, and adipose, and increased adiposity due to a combination of decreased energy expenditure and lipolysis and an increase in re-esterfication in adipose tissue on high fat diet (Le Bacquer et al., 2007).

Forkhead box O1 (FoxO1)

FoxO1 is a transcription factor that is negatively regulated by insulin signaling through phosphorylation by Akt (Brunet et al., 1999). In the absence of insulin signaling, FoxO1 is active and elevates serum triglycerides through increasing VLDL secretion and decreasing triglyceride clearance. Overexpression of normal or constitutively active FoxO1 in liver either genetically or by adenovirus increases serum triglycerides during fasting or following an oral lipid load (Altomonte et al., 2004; Kamagate et al., 2008). This work by Dong and colleagues attributes the increase in serum triglycerides to increased VLDL production and decreased clearance of triglycerides from the bloodstream. FoxO1 directly activates the expression of microsomal triglyceride transfer protein (MTP), a protein that transfers lipids to growing VLDL particles in the liver; inhibition of MTP *in vivo* results in decreased serum triglyceride but increased hepatic

triglyceride levels (Kamagate et al., 2008; Liao et al., 2003). Mice expressing a constitutively active FoxO1 transgene have increased MTP expression, VLDL production and serum triglyceride levels (Kamagate et al., 2008). Adenoviral expression of FoxO1 in the liver also results in increased hepatic expression of apoC-III, the apolipoprotein that inhibits the enzyme responsible for the hydrolysis of circulating triglycerides, lipoprotein lipase, and thus inhibits clearance of VLDL triglycerides (Altomonte et al., 2004). Conversely, RNAi knockdown of FoxO1 in the liver increases hepatic triglyceride levels but decreases VLDL production, suggesting that the absence of FoxO1 can secondarily cause hepatic steatosis by impairing triglyceride secretion from the liver (Kamagate et al., 2008).

FoxO1 also has an influence on lipogenic and β-oxidative gene expression, however it is unclear whether this is a primary action of FoxO1. RNAi knockdown of FoxO1 in the liver decreases *FAS* and *ACC* expression, while hepatic expression of constitutively active FoxO1 by adenovirus results in increased lipogenic gene and decreased β-oxidative gene expression (Kamagate et al., 2008; Matsumoto et al., 2006). However, hepatic steatosis occurs in both cases, attributed to decreased VLDL secretion in the absence of FoxO1 and to increased lipid synthesis and decreased oxidation in the presence of constitutively active FoxO1 (Kamagate et al., 2008; Matsumoto et al., 2006). Interestingly, the latter mice also exhibit a compensatory increase in IRS2 protein levels and phosphorylation of Akt, so the hepatic steatosis resulting from constitutively active FoxO1 expression may be secondary to the upregulation of another Akt-dependent pathway. This same group reported that FoxO1 deletion fails to reverse the blunted refeeding-stimulated expression of *SREBP1c* or decrease in serum triglyceride levels in double *IRS1*/*IRS2* null livers, though it is able to partially restore VLDL triglyceride secretion, arguing that FoxO1 is a component of IRS-dependent VLDL secretion but not

of IRS-dependent lipogenesis (Dong et al., 2008). However, Zhang et al reported the opposite in their transgenic mice expressing constitutively active FoxO1 in liver, which have decreased hepatic expression of *SREBP1c* and its lipogenic targets, decreased lipogenesis following feeding and decreased serum triglyceride levels during fasting and feeding (Zhang et al., 2006). Though these mice do not exhibit differential activation of other insulin signaling pathways, they are markedly glucose-intolerant and insulin-resistant (Zhang et al., 2006). Thus, it is unclear whether a directly action of FoxO1 is to modulate the expression of lipogenic genes

Glycogen synthase kinase 3 (GSK3)

As its name indicates, GSK3 phosphorylates and inhibits glycogen synthase in the absence of insulin signaling; upon nutrient influx, GSK3 is inhibited via phosphorylation by Akt, mediating insulin's stimulation of glycogen production (Cross et al., 1995; reviewed in Roach, 2002). Though it mediates insulin's action on glycogen synthesis, a role with regards to lipid synthesis is less established. A series of reports by Ericsson and colleagues have shown that GSK3 can directly phosphorylate SREBP1, which promotes the ubiquitination and degradation of SREBP1 protein *in vitro* (Bengoechea-Alonso and Ericsson, 2009; Punga et al., 2006; Sundqvist et al., 2005). Additionally, expression of constitutively active GSK3 blocks the accumulation of nSREBP protein that occurs in cells expressing myr-Akt (Porstmann et al., 2008). This implicates a role for GSK3 in the downregulation of lipogenesis during fasting, a process that would then be turned off by insulin during feeding; however, the relevance of this pathway has yet to be shown *in vivo*.

Forkhead box A2 (Foxa2)

Foxa2 is a transcription factor and may serve as a potential pathway through which insulin regulates lipid metabolism during the fasting to feeding transition. Stoffel and colleagues have published that adenoviral overexpression of constitutively active Foxa2 in either lean or obese mice leads to increased VLDL secretion and increased β-oxidation, as assessed by gene expression and calorimetry, resulting in decreased hepatic triglyceride accumulation (Wolfrum et al., 2004; Wolfrum and Stoffel, 2006). Mice lacking one allele of *Foxa2* exhibit decreased hepatic ketogenesis and increased serum triglyceride and fatty acid levels, an effect that is enhanced by high fat diet-feeding (Wolfrum et al., 2004). Activity of Foxa2 is highest in fasted low-insulin states, but whether this and its effects on lipid metabolism are due to lack of insulin regulation or coactivation with PGC-1β remains unclear (Wolfrum et al., 2004; Wolfrum and Stoffel, 2006; Zhang et al., 2005). Additionally, whether Foxa2 is negatively regulated by insulin through phosphorylation by Akt and nuclear exclusion during refeeding remains contested, as does its role in the regulation of hepatic lipid metabolism (Wolfrum et al., 2004; Zhang et al., 2005).

Concluding remarks

While the underlying pathogenesis of hepatic steatosis remains elusive, its development is clearly associated with insulin resistance. The characterization of the insulin signaling transduction pathways that control hepatic lipid metabolism is essential to revealing novel therapeutic targets for the treatment of dyslipidemia and hepatic steatosis associated with T2DM. These signaling pathways appear to be distinct from those controlling hepatic glucose metabolism and are preserved in insulin-resistant states, leading to the proposal of selective insulin resistance in the liver. Specifically,

insulin's stimulation of *de novo* lipogenesis is preserved in T2DM, and as such, individuals with hepatic steatosis have inappropriately elevated rates of lipogenesis.

Much insulin's regulation of lipogenesis is thought to proceed through the transcription factor SREBP1c, which activates the broad transcription of genes expressing lipogenic enzymes. *SREBP1c* expression has been shown to be decreased in the absence of many components of the insulin signaling pathway, including the insulin receptor, IRS, PI3K, and aPKCs. However the consequences of this decrease on the rate of *de novo* lipogenesis are rarely investigated *in vivo*. Certainly, animals are protected against the development of hepatic steatosis in the absence of SREBP1c, corresponding to a decrease in *de novo* lipogenesis, but this has never been recapitulated in an animal deficient in a component of the insulin signaling pathway. Additionally, it is conceivable that not all regulation of *de novo* lipogenesis by insulin proceeds through *SREBP1c* expression: there are likely SREBP1c-independent controls of lipid synthesis, and *SREBP1c* mRNA levels may not always be an accurate measure of *de novo* lipogenesis. Additionally, it is unclear if other lipid metabolic processes beyond lipogenesis, such as VLDL secretion and β-oxidation, are controlled by the same pathway and if they contribute to hepatic lipid accumulation in insulin-resistant states.

At the outset of this thesis, we wanted to determine the downstream signaling pathway that insulin utilizes to promote hepatic lipid accumulation and, in particular, the induction of SREBP1c and *de novo* lipogenesis, a question for which a consensus answer had yet to emerge. Here we present an *in vivo* model that is inherently defective in insulin signaling due to loss of hepatic Akt2, and utilize these mice to evaluate the role of Akt2 in lipid synthesis and accumulation. Akt2 is the predominant isoform expressed in insulin target tissues, such as liver, muscle and adipose tissue, and *Akt2*$^{-/-}$ mice exhibit glucose intolerance and a mild diabetic phenotype (Cho et al., 2001a; Garofalo et al.,

2003). In the experiments described below, we establish a role for Akt2 in the development of hepatic steatosis in two models of insulin resistance, and in the elevation of *de novo* lipogenesis in one of these models. Additionally, we show that hepatic Akt2 is required for the induction of lipogenesis that occurs in lean animals during feeding.

Figure 1-1: The insulin/PI3K signaling pathway

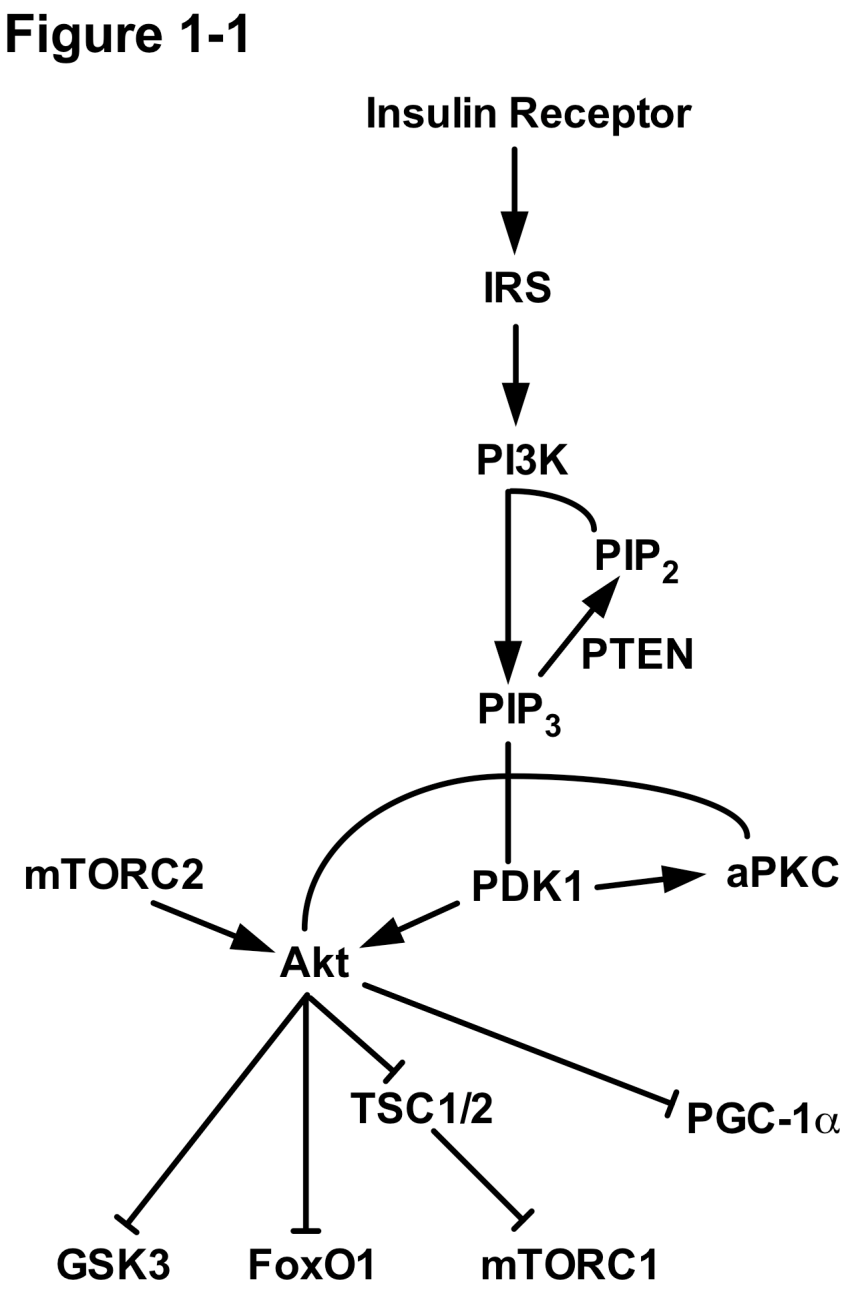

Chapter 2:

Akt2 is required for increased *de novo* lipogenesis and the development of hepatic steatosis in the *ob/ob* mouse.

Introduction

The study of lipid metabolism has relied upon the use of rodent models to characterize both normal and pathological processes. One of the most commonly used models of obesity, hepatic steaotsis, dyslipidemia, and T2DM is the *ob/ob* mouse. First described in 1950 by Ingalls et al. as a naturally occurring recessive mutation, the *ob/ob* mouse was utilized for decades prior to the characterization of the point mutation in the gene encoding leptin ($Lep^{ob/ob}$) that caused the mouse's phenotype (Bray and York, 1979; Halaas et al., 1995; Ingalls et al., 1950). Leptin is a hormone secreted by adipocytes that acts predominantly on the brain to reduce food intake and increase energy expenditure, in addition to having other influences on metabolism (reviewed in Ahima and Osei, 2004). Serum leptin levels correlate with body mass index in both humans and rodents, and administration of leptin to $Lep^{ob/ob}$ mice and humans results in weight loss and reversal of the increased food intake and decreased energy expenditure seen in leptin deficiency (Farooqi et al., 1999; Halaas et al., 1995). However, the use of leptin as a general therapy for weight loss in humans has not been successful, though it has been employed to treat congenital lipodystrophy and severe insulin resistance syndromes (Cochran et al., 2004; Petersen et al., 2002; Shimomura et al., 1999c). *ob/ob* mice are insulin-resistant, largely due to their increased adiposity, and exhibit increasing serum insulin levels throughout their life beginning around one month of age (reviewed in Bray and York, 1979). However, the severity of the insulin resistance and development of diabetes is background strain-dependent (Haluzik et al., 2004).

One of the most striking characteristics of the *ob/ob* mouse is the extreme hepatic steatosis that develops at an early age, likely due to a combination of increased *de novo* lipogenesis and esterification of elevated serum NEFA, as well as decreased fatty acid oxidation (reviewed in Bray and York, 1979). Leptin administration to *ob/ob*

mice results in decreased expression of lipogenic and cholesterol biosynthetic genes, and increased expression of fatty acid oxidation genes (Liang and Tall, 2001). Despite having elevated serum triglyceride levels, hepatic VLDL production and secretion are not drastically changed in *ob/ob* mice, indicating that these animals likely have impairments in clearance of VLDL from the circulation (Li et al., 1997; Wiegman et al., 2003). However, when subjected to hyperinsulinemic euglycemic clamp, *ob/ob* mice exhibit decreased suppression of VLDL production by insulin (Wiegman et al., 2003).

Most closely correlating with the increase in hepatic triglyceride accumulation in *ob/ob* mice is a dramatic increase in *de novo* lipogenesis in the liver, which is increased by between 10- to 23-fold per organ in *ob/ob* versus lean mice (Shimomura et al., 1999a; Wiegman et al., 2003). This increase in *de novo* lipogenesis is accompanied by increased mRNA and nuclear protein levels of SREBP1c, increased expression of *ChREBP* and upregulation of their lipogenic target genes (Dentin et al., 2006; Iizuka et al., 2006; Shimomura et al., 1999a; Yahagi et al., 2002). These two factors play an inciting role in the development of hepatic steatosis, as hepatic triglyceride levels and lipogenic gene expression are reduced in *ob/ob* mice lacking SREBP1 or ChREBP (Dentin et al., 2006; Iizuka et al., 2006; Yahagi et al., 2002). This is likely due to their influences on lipogenic gene expression and not on modulation of insulin sensitivity as deletion of ChREBP improves insulin resistance and glucose intolerance while loss of SREBP1 has no effect on insulin sensitivity. Deletion of other lipid metabolic genes, such as *PPARγ, Cidec/Fsp27*, and *SCD1,* in *ob/ob* animals can also improve the hepatic steatosis with varying affects on the diabetic phenotype (Cohen et al., 2002; Flowers et al., 2007; Matsusue et al., 2003; Matsusue et al., 2008).

In this chapter, we describe the role of hepatic Akt2 in the development of hepatic steatosis of the *ob/ob* mouse. We find that hepatic Akt2 is absolutely required

for the accumulation of hepatic triglycerides, corresponding to a requirement for the increase in lipogenic gene expression and *de novo* lipogenesis. However, while loss of hepatic Akt2 does not significantly alter the diabetic phenotype of the *ob/ob* mouse**,** $Lep^{ob/ob}$ $Akt2^{-/-}$ mice exhibit severe glucose intolerance and insulin resistance.

Results

Germline Akt2 deficiency prevents hepatic steatosis in ob/ob mice.

While the role of Akt2 in glucose homeostasis has been established, its influence on lipid metabolism *in vivo* is controversial. The first model we used to resolve this was the *ob/ob* mouse, which we initially crossed with $Akt2^{-/-}$ mice. The $Lep^{ob/ob}$ $Akt2^{+/+}$ mice were substantially heavier than $Lep^{+/+}$ $Akt2^{+/+}$ littermates at 12 weeks of age and had large, lipid-laden livers. However, deletion of both alleles of *Akt2* led to a dramatic reduction of both body and liver weight in *ob/ob* mice, with loss of one allele of *Akt2* resulting in an intermediate decrease (Figure 2-1A and 2-1B). Triglyceride accumulation in the livers of *ob/ob* mice under both fed and fasted conditions was completely prevented by loss of both alleles of *Akt2*, and, as above, mice heterozygous for Akt2 demonstrated intermediate protection from hepatic steatosis (Figure 2-1C and 2-1D).

Accumulation of hepatic triglyceride in *ob/ob* mice is associated with an increase in *de novo* lipogenesis (Shimomura et al., 1999a; Wiegman et al., 2003). Therefore, we measured hepatic fatty acid synthesis and incorporation into triglycerides using deuterated water as a biosynthetic tracer. $Lep^{ob/ob}$ $Akt2^{+/+}$ mice demonstrated greater *de novo* lipogenesis compared with $Lep^{+/+}Akt2^{+/+}$ mice, but this was reduced in both $Lep^{ob/ob}$ $Akt2^{+/-}$ and $Lep^{ob/ob}$ $Akt2^{-/-}$ mice (Figure 2-1E). Serum triglycerides were increased in both $Lep^{ob/ob}$ $Akt2^{+/-}$ and $Lep^{ob/ob}$ $Akt2^{-/-}$ relative to $Lep^{ob/ob}$ $Akt2^{+/+}$ mice, while cholesterol levels were increased in all $Lep^{ob/ob}$ mice compared with $Lep^{+/+}$ mice and modestly

decreased with loss of Akt2 under fed conditions (Figure 2-2A and 2-2B). Non-esterified free fatty acids (NEFA) were unchanged or increased in *Lep*$^{ob/ob}$ *Akt2*$^{-/-}$ compared with *Lep*$^{ob/ob}$ *Akt2*$^{+/+}$ mice while serum ketones were not changed in any group (Figure 2-2C and 2-2D).

Germline Akt2 deficiency results in severe diabetes in ob/ob mice.

Many mouse models exhibit improved hepatic insulin sensitivity in conjunction with improvements in hepatic steatosis, possibly confounding the interpretation of which preceded the other. Therefore, we wanted to characterize the state of glucose homeostasis and insulin sensitivity of the *Lep*$^{ob/ob}$ *Akt2*$^{-/-}$ mice. Deletion of Akt2 exacerbated the already impaired glucose homeostasis of the *ob/ob* mice, as indicated by an elevation in blood glucose levels both under fasted conditions and during an oral glucose tolerance test (OGTT) (Figure 2-3A and 2-3B). *Lep*$^{ob/ob}$ *Akt2*$^{+/+}$ mice exhibited hyperinsulinemia to compensate for insulin resistance at both fasting and 15 minutes post oral glucose, and *Lep*$^{ob/ob}$ *Akt2*$^{-/-}$ mice had a further increase in fasted serum insulin levels (Figure 2-3C). Interestingly, hyperglycemia was not worsened in the *Lep*$^{ob/ob}$ *Akt2*$^{+/-}$ mice, suggesting that redistribution of hepatic lipid to other organs was not the cause of the aggravated insulin resistance. Additionally, *Lep*$^{ob/ob}$ *Akt2*$^{-/-}$ mice failed to decrease their blood glucose levels during insulin tolerance tests (ITT), even at a high dose of insulin that induced glucose-lowering effects in *Lep*$^{ob/ob}$ *Akt2*$^{+/+}$ and *Lep*$^{ob/ob}$ *Akt2*$^{+/-}$ mice (Figure 2-3D and 2-3E). To determine whether the insulin resistance observed in these mice was due to hepatic or peripheral insulin resistance, *Lep*$^{ob/ob}$ *Akt2*$^{+/+}$ and *Lep*$^{ob/ob}$ *Akt2*$^{-/-}$ mice were subjected to hyperinsulinemic euglycemic clamp (Figure 2-4A). As *Lep*$^{ob/ob}$ *Akt2*$^{-/-}$ mice had reduced body weight, slightly younger *Lep*$^{ob/ob}$ *Akt2*$^{+/+}$ mice were used to better weight-match the groups. A very high level of infused insulin

(250mU/kg/min) was employed to reduce *Lep*$^{ob/ob}$ *Akt2*$^{-/-}$ mice to euglycemia. At this dose of insulin, *Lep*$^{ob/ob}$ *Akt2*$^{+/+}$ mice required a high glucose infusion rate (GIR) in order to maintain euglycemia, while *Lep*$^{ob/ob}$ *Akt2*$^{+/+}$ mice had a markedly reduced GIR, confirming that these mice were extremely insulin-resistant (Figure 2-4A). Hepatic glucose production (HGP) was increased under both basal and clamped conditions in *Lep*$^{ob/ob}$ *Akt2*$^{+/+}$ mice, while rate of disposal (Rd) of glucose into the periphery was unchanged (Figure 2-4A).

As body weight was dramatically reduced in *ob/ob* mice with loss of Akt2 (Figure 2-1A), we wanted to determine whether this was due a reduction in fat mass, lean mass, or both. Body composition was determined using the assimilation of injected D_2O from the lipogenesis assay (Figure 2-1E) into the body water compartment as described previously (McCabe et al., 2006). *Lep*$^{ob/ob}$ mice had increased fat mass by both weight and percentage, and had slightly decreased lean mass by weight compared with *Lep*$^{+/+}$ mice (Figure 2-4B). Loss of Akt2 on a *ob/ob* background resulted in both decreased fat and lean mass by weight, as well as a decrease in the percentage of body fat, indicating that these mice have an impaired ability to store fat even though they have a normal Rd by clamp (Figure 2-4A and 2-4B). However, *Lep*$^{ob/ob}$ *Akt2*$^{+/-}$ mice mice had decreased fat mass by weight and percentage, but exhibited normal lean mass by weight compared with *Lep*$^{ob/ob}$ *Akt2*$^{+/+}$ mice (Figure 2-4B).

Generation of ob/ob liver-specific Akt2 null mice.

In the experiments described above, the non-cell autonomous effects of germline deletion of Akt2 confound interpretation of changes in hepatic lipid content and metabolism. To clarify this, we generated mice with liver-specific deletion of Akt2. Mice containing an allele of *Akt2* in which exons 3 and 4 are flanked by loxP sires (*Akt2*$^{lox/lox}$)

were crossed with mice expressing Cre recombinase under the control of the albumin promoter with an alpha-fetoprotein enhancer (*AFP*). Progeny were crossed with *ob/ob* mice, and offspring were assessed for deletion of Akt2 selectively in the liver. As shown in Figure 2-5, *AFP;Akt2*$^{lox/lox}$ and *Lep*$^{ob/ob}$ *AFP;Akt2*$^{lox/lox}$ mice lacked hepatic Akt2 protein, while showing no compensatory changes in the levels of Akt1 or decrease in Akt2 protein in other tissues. While *AFP;Akt2*$^{lox/lox}$ mice exhibited no difference in body weight compared to *Akt2*$^{lox/lox}$ mice, *Lep*$^{ob/ob}$ *AFP;Akt2*$^{lox/lox}$ mice weighed less than both *Lep*$^{ob/ob}$ *Akt2*$^{lox/lox}$ and *Lep*$^{ob/ob}$ *AFP;Akt2*$^{+/+}$ mice (Figure 2-6A and 2-9A). This decrease in body weight was due to proportional reductions in both lean and fat mass, such that relative body composition remained unchanged (Figure 2-7A). The decreased body weight could not be attributed to changes in food intake or energy expenditure, which were indistinguishable in *ob/ob* mice with or without hepatic Akt2 (Figure 2-7B and 2-7C).

Loss of hepatic Akt2 reduces hepatic triglyceride levels, de novo lipogenesis and lipogenic gene expression in the ob/ob mouse.

Hepatic deletion of Akt2 resulted in decreased liver weight in the *ob/ob* mouse, due at least in part to a reduction in triglyceride content under both fed and fasted conditions (Figure 2-6B, 2-6C and 2-6D). None of these changes could be attributed to the effect of AFP Cre alone (Figure 2-9B, 2-9C, and 2-9D). The decrease in hepatic triglycerides does not solely reflect the decreased body weight in *Lep*$^{ob/ob}$ *AFP;Akt2*$^{lox/lox}$ mice, as even compared to weight-matched controls, *Lep*$^{ob/ob}$ *AFP;Akt2*$^{lox/lox}$ mice exhibited reduced hepatic triglyceride content under fed conditions (*Lep*$^{ob/ob}$ *Akt2*$^{lox/lox}$: 56.7 ± 3.34 mg/g TG, 34.9 ± 1.6 g body weight; , *Lep*$^{ob/ob}$ *AFP;Akt2*$^{lox/lox}$:12.3 ± 1.43 mg/g TG, 38.7 ± 1.1 g body weight). Fasted serum triglyceride levels were decreased in *Lep*$^{ob/ob}$ *AFP;Akt2*$^{lox/lox}$ mice compared with *Lep*$^{ob/ob}$ *Akt2*$^{lox/lox}$ mice, while fed values were

unchanged (Figure 2-8A). Serum cholesterol was decreased in *Lep*$^{ob/ob}$ mice upon liver-specific deletion of Akt2, but serum NEFA and ketones were unaffected; fasted serum ketones were decreased in all *ob/ob* mice (Figure 2-8B, 2-8C, and 2-8D). The content and distribution of long-chain fatty acyl-CoA were not significantly different among any of the genotypes, though there was a trend towards a decrease in the two monounsaturated fatty acids (MUFA) palmitoleate (C16:1) and oleate (C18:1) in *Lep*$^{ob/ob}$ *AFP;Akt2*$^{lox/lox}$ compared with *Lep*$^{ob/ob}$ *Akt2*$^{lox/lox}$ livers (Figure 2-6E). *De novo* lipogenesis was elevated in the *Lep*$^{ob/ob}$ *Akt2*$^{lox/lox}$ mice, and loss of hepatic Akt2 reversed this effect, as was previously observed with whole-body loss of Akt2 (Figure 2-6F). These results demonstrate that Akt2 is required in the liver for the increases in both hepatic *de novo* lipogenesis and triglyceride accumulation in *ob/ob* mice.

The augmented *de novo* lipogenesis in the *ob/ob* mouse is associated with an increase in lipogenic gene expression, in particular *SREBP-1c* and its transcriptional targets (Shimomura et al., 1999a). In the present studies, we confirmed the predicted increases in the mRNAs for *SREBP-1c*, *SCD1, FAS*, *ACC, ACL*, *GPAT,* and *GCK* in *Lep*$^{ob/ob}$ *Akt2*$^{lox/lox}$ livers, and moreover found that all of these increases were prevented by loss of hepatic Akt2 (Figure 2-10). Expression of *ChREBP* was unchanged, but its target *L-PK* was increased in *Lep*$^{ob/ob}$ *Akt2*$^{lox/lox}$ mice and normalized in livers from *Lep*$^{ob/ob}$*AFP;Akt2*$^{lox/lox}$ mice. *PPAR*γ and *Cidec/Fsp27*, gene products required for development of hepatic steatosis in *ob/ob* mice, were induced in *Lep*$^{ob/ob}$ *Akt2*$^{lox/lox}$ livers and this was prevented by loss of hepatic Akt2 (Figure 2-10) (Matsusue et al., 2008).

Lep$^{ob/ob}$*Akt2*$^{lox/lox}$ mice exhibited a slight increase in the expression of *PGC-1*α, which was further enhanced in *Lep*$^{ob/ob}$ *AFP;Akt2*$^{lox/lox}$ mice (Figure 2-10). However, expression of medium-chain acetyl-CoA dehydrogenase (*MCAD*), a transcriptional target of PGC-1α and rate-determining enzyme in fatty acid oxidation, was not altered in

Lep$^{ob/ob}$ *AFP;Akt2*$^{lox/lox}$ compared with *Lep*$^{ob/ob}$ *Akt2*$^{lox/lox}$ livers (Schreiber et al., 2003). Additionally, the expression of *CPT1*, another PGC-1α target, was actually decreased in *Lep*$^{ob/ob}$ *AFP;Akt2*$^{lox/lox}$ livers, while the expression of the mitochondrial gene cytochrome c oxidase subunit 7a (*Cox7a*) was not different between *Lep*$^{ob/ob}$ *Akt2*$^{lox/lox}$ and *Lep*$^{ob/ob}$ *AFP;Akt2*$^{lox/lox}$ mice (Figure 2-10) (Song et al., 2004).

While fatty acid oxidation did not appear to be altered, at least by gene expression, in *Lep*$^{ob/ob}$ *AFP;Akt2*$^{lox/lox}$ mice (Figure 2-10), we wanted to determine if triglyceride secretion was dramatically altered and therefore contributing the reduction in hepatic triglyceride accumulation. Mice were injected with poloxamer 407 (P-407), a detergent that inhibits lipoprotein lipase and triglyceride uptake in the periphery, and serum triglycerides were monitored to determine if there was greater export of triglycerides from livers lacking Akt2 (Millar et al., 2005). VLDL production secretion was not dramatically altered in *ob/ob* mice, as has been previously reported, and loss of hepatic Akt2 in *ob/ob* mice did not alter triglyceride levels (Figure 2-11) (Li et al., 1997; Wiegman et al., 2003).

Acute excision of hepatic Akt2 results in a reversal of hepatic steatosis in ob/ob mice.

While genetic loss of hepatic Akt2 prevents the accumulation of hepatic triglycerides in *ob/ob* mice, this could be due to a requirement of Akt2 either during liver development or for the initiation of hepatic steatosis. Thus, we wanted to see if acute deletion of Akt2 could reverse existing hepatic steatosis. Male *Lep*$^{ob/ob}$ *Akt2*$^{lox/lox}$ mice were injected with adeno-associated virus (AAV) expressing GFP (AAV-GFP) or Cre (AAV-Cre) at approximately 10 weeks of age, an age at which *ob/ob* mice have already developed hepatic steatosis, and sacrificed two week later under fed conditions. During this time, *Lep*$^{ob/ob}$ *Akt2*$^{lox/lox}$ mice injected with AAV-GFP exhibited a 14% increase in

body weight, while those injected with AAV-Cre only gained approximately 4% (Figure 2-12A). AAV-Cre-injected mice had a significant reduction in liver weight and hepatic triglyceride content to levels similar to those of *Lep$^{ob/ob}$ AFP;Akt2$^{lox/lox}$* mice (Figure 2-12B and 2-12C compared with 2-6B and 2-6C). Serum triglycerides, NEFA, and ketones were unchanged in mice injected with AAV-GFP versus AAV-Cre, but serum cholesterol was decreased in those injected with AAV-Cre, again following the same pattern as *Lep$^{ob/ob}$ AFP;Akt2$^{lox/lox}$* mice (Figure 2-12D to 2-12G compared with 2-8). These results indicate that the ongoing presence of Akt2 is required to maintain hepatic steatosis.

Loss of hepatic Akt2 causes hepatic insulin resistance in lean mice, but does not worsen glucose homeostasis or insulin tolerance in ob/ob mice.

As whole-body *Akt2$^{-/-}$* mice exhibit hepatic and peripheral insulin resistance, we wanted to determine if hepatic loss of Akt2 would lead to hepatic insulin resistance (Cho et al., 2001a). *Akt2$^{lox/lox}$* and *AFP;Akt2$^{lox/lox}$* male mice were subjected to hyperinsulinemic euglycemic clamp, and *AFP;Akt2$^{lox/lox}$* mice had significantly lower GIR than their *Akt2$^{lox/lox}$* littermates, indicating that loss of hepatic Akt2 does indeed to lead to insulin resistance (Figure 2-13A). While basal HGP was normal in *AFP;Akt2$^{lox/lox}$* mice, it was elevated under clamped conditions, showing that insulin's suppression of hepatic glucose production is impaired in the absence of hepatic Akt2. Additionally, loss of hepatic Akt2 also causes peripheral insulin resistance as Rd was reduced in *AFP;Akt2$^{lox/lox}$* mice (Figure 2-13A).

Since loss of hepatic Akt2 leads to insulin resistance in lean mice, it is possible that loss of Akt2 in the liver of *ob/ob* mice was leading to the severe diabetes seen in *Lep$^{ob/ob}$ Akt2$^{-/-}$* mice. *Lep$^{ob/ob}$ AFP;Akt2$^{lox/lox}$* mice had slightly increased fasted serum glucose levels compared with *Lep$^{ob/ob}$ Akt2$^{lox/lox}$* mice, and did exhibit slightly impaired

glucose tolerance by OGTT, but this was not nearly as severe as the glucose intolerance of the *Lep*$^{ob/ob}$ *Akt2*$^{+/+}$ mice (Figure 2-13B and 2-13C). As observed above, *Lep*$^{ob/ob}$ *Akt2*$^{lox/lox}$ mice exhibited hyperinsulinemia to compensate for insulin resistance during fasting and 15 minutes post oral glucose, and there was no difference due to loss of hepatic Akt2 (Figure 2-13D). ITTs were performed, and at a dose of 1 Unit of insulin per kilogram of body weight (1U/kg) in 10-week old mice, *Lep*$^{ob/ob}$ *AFP;Akt2*$^{lox/lox}$ mice had elevated glucose levels compared with *Lep*$^{ob/ob}$ *Akt2*$^{lox/lox}$ mice, though neither group responded to insulin injection by lowering their blood glucose levels (Figure 2-13E). However, when an ITT was performed using 2U/kg insulin in 8-week old mice, both *Lep*$^{ob/ob}$ *Akt2*$^{lox/lox}$ and *Lep*$^{ob/ob}$ *AFP;Akt2*$^{lox/lox}$ mice exhibited a glucose-lowering response to insulin, even though basal glucose levels were lower initially in the younger mice (Figure 2-13F). Consistent with the results of the clamp, *AFP;Akt2*$^{lox/lox}$ mice did exhibit impaired insulin tolerance compared to *Akt2*$^{lox/lox}$ mice at both doses of insulin (Figure 2-13E and 2-13F). None of the effects observed could be attributed to the effects of AFP Cre alone (Figure 2-14A, 2-14B, and 2-14C).

Loss of hepatic Akt2 decreases insulin signaling in lean mice, but does not change downstream protein phosphorylation in ob/ob livers.

In order to gain insight into the pathways that could be mediating Akt2's effect on hepatic lipid metabolism, we performed Western blots on liver extracts from *Akt2*$^{lox/lox}$ and *AFP;Akt2*$^{lox/lox}$ following intraperitoneal (IP) injection of saline or insulin (Figure 2-15A). Phosphorylation of Akt at residues S473 and T308 was increased in *Akt2*$^{lox/lox}$ mice injected with insulin, and this increase was blunted in the absence of Akt2. The same pattern held true for the phosphorylation of Proline-Rich Akt Substrate of 40kDa (PRAS), GSK3β and phospho-tuberous sclerosis complex-2 (TSC2), while

phosphorylation of FoxO1 did not appear to be decreased in the absence of hepatic Akt2. Interestingly, phosphorylation of these Akt targets was increased under basal fasted conditions in *AFP;Akt2*$^{lox/lox}$mice, suggesting relief of a negative feedback loop in the absence of Akt2 (Figure 2-15A). We also wanted to determine if loss of Akt2 had significant effects on hepatic insulin signaling in *ob/ob* mice (Figure 2-15B). In order to assess insulin signaling in both experimental groups in the presence of comparable levels of insulin and glucose, *Lep*$^{ob/ob}$ *Akt2*$^{lox/lox}$ and *Lep*$^{ob/ob}$ *AFP;Akt2*$^{lox/lox}$ mice were submitted to a hyperinsulinemic euglycemic clamp and liver extracts were prepared. Insulin signaling was significantly impaired in the insulin-resistant *ob/ob* mice, such that phosphorylation of Akt and its targets was significantly below stimulated conditions in *Akt2*$^{lox/lox}$ animals; moreover, loss of hepatic Akt2 did not reduce protein phosphorylation further (Figure 2-15B).

Discussion

In order to determine if Akt2 was involved in the development of pathological lipid accumulation, we crossed *Akt2*$^{-/-}$ mice to *ob/ob* mice. These mice are frequently used as a model of obesity and hepatic steatosis, and have decreased energy expenditure and hyperphagy, leading to excessive nutrient intake, increased adiposity, hyperglycemia, hyperinsulinemia, and insulin resistance (Bray and York, 1979). In addition to increased substrate for hepatic triglycerides from esterification of dietary and adipose fatty acids, these mice also have increased lipogenic gene expression and increased rates of lipogenesis, all likely contributing to excess lipid accumulation (Shimomura et al., 1999a; Wiegman et al., 2003). In the absence of Akt2, *ob/ob* mice failed to develop hepatic steatosis or exhibit increased *de novo* lipogenesis (Figure 2-1). However, as the *Lep*$^{ob/ob}$ *Akt2*$^{-/-}$ mice were smaller and substantially more diabetic than *Lep*$^{ob/ob}$ mice, we moved

to liver-specific *Akt2* null mice with the intent to determine the role of hepatic Akt2 without potential complications from the loss of Akt2 in extrahepatic tissues. Similar to *ob/ob* mice with whole-body loss of Akt2, $Lep^{ob/ob}$ *AFP;*$Akt2^{lox/lox}$ mice had a dramatic reduction in both *de novo* lipogenesis and hepatic triglyceride accumulation (Figure 2-6). Emphasizing the importance of Akt2 for the development of hepatic steatosis, there was an intermediate decrease in hepatic triglycerides in the $Lep^{ob/ob}$ $Akt2^{+/-}$ mouse, suggesting that Akt2 is not only required for this process but is rate-limiting. In addition, acute excision of hepatic Akt2 from the livers of $Lep^{ob/ob}$ $Akt2^{lox/lox}$ mice by AAV-Cre reversed existing steatosis, indicating that the ongoing presence of Akt2 is required for this process.

As for the mechanism of decreased lipogenesis in the $Lep^{ob/ob}$ *AFP;*$Akt2^{lox/lox}$ mice, our data suggest that Akt2 is required for the upregulation of lipogenic gene expression in the *ob/ob* mouse. It has been reported that insulin increases *SREBP1c* expression through Akt in cell lines and primary hepatocytes, though Akt never been shown to do so *in vivo* (Fleischmann and Iynedjian, 2000; Porstmann et al., 2005). In the absence of Akt2, the expression of *SREBP1c,* and its targets, *SCD-1, FAS, ACC, ACL, GPAT,* and *GCK,* failed to increase in the *ob/ob* liver (Figure 2-10). Interestingly, while we did not observe any changes in *ChREBP* expression in $Lep^{ob/ob}$ *AFP;*$Akt2^{lox/lox}$ mice, the induction of *L-PK* expression was blocked in *ob/ob* mice with loss of hepatic Akt2, suggesting an influence on lipogenesis beyond the control of *SREBP1c* expression in these mice.

While the decrease in *de novo* lipogenesis correlates with the reversal of hepatic steatosis in $Lep^{ob/ob}$ *AFP;*$Akt2^{lox/lox}$ mice, it does not exclude a role for Akt2 in the regulation of another aspect of lipid metabolism. PGC-1α regulates fatty acid oxidation in the liver, and our lab has previously reported that Akt phosphorylates and inactivates

PGC-1α, thus impairing its ability to promote fatty acid oxidation, establishing a connection between Akt and β-oxidation (Li et al., 2007). Indeed, *PGC-1α* was significantly upregulated in *Lep$^{ob/ob}$ AFP;Akt2$^{lox/lox}$* livers (Figure 2-10); however, expression of *MCAD* and *CPT1*, transcriptional targets of PGC-1α, was not increased in *Lep$^{ob/ob}$ AFP; Akt2$^{lox/lox}$* compared with *Lep$^{ob/ob}$ Akt2$^{lox/lox}$* livers (Schreiber et al., 2003; Song et al., 2004). Additionally, serum ketones and RER were not changed in these mice (Figure 2-7C and 2-8D).

Another potential pathway that could contribute to decreased hepatic triglyceride accumulation is triglyceride export from the liver. *Lep$^{ob/ob}$ Akt2$^{-/-}$* mice had elevated serum triglyceride levels, suggesting that increased in triglyceride export could decrease hepatic triglycerides by shunting them into the serum (Figure 2-2A). However in *Lep$^{ob/ob}$ AFP;Akt2$^{lox/lox}$* mice, fed serum triglyceride levels did not differ from *Lep$^{ob/ob}$ Akt2$^{lox/lox}$* mice, and fasted serum triglycerides were actually lower (Figure 2-8A). Furthermore, a triglyceride export assay using P-407 showed similar serum triglyceride levels in *ob/ob* mice with and without hepatic Akt2 (Figure 2-11). These observations suggest that increased triglyceride export does not play a role in reducing hepatic triglyceride accumulation in the absence of Akt2 in the liver. It is possible the increase in serum triglycerides observed in the *Lep$^{ob/ob}$ Akt2$^{-/-}$* mice is due to loss of Akt2 in an extrahepatic tissue, such as adipose tissue, or, alternatively, secondary to worsened glucose homeostasis.

As shown in Figure 2-3 and 2-4, deletion of Akt2 on an *ob/ob* background resulted in fasting hyperglycemia, glucose intolerance and insulin resistance considerably more severe than that in mice lacking either Akt2 or leptin. Hepatic glucose production was increased under both basal and clamped conditions in *Lep$^{ob/ob}$ Akt2$^{-/-}$* mice, while Rd of glucose into the periphery was unchanged, indicating that the

insulin resistance resulting from loss of Akt2 on an *ob/ob* background is more pronounced in the liver. However, deletion of hepatic Akt2 from *ob/ob* mice did not further contribute to diabetes as measured by OGTT and ITT, showing that the absence of hepatic Akt2 alone is not driving the severity of the diabetes in $Lep^{ob/ob}$ $Akt2^{-/-}$ mice (Figure 2-13). Some of the difference may be due to genetic background as the whole-body *Akt2* null mice are C57BL/6J and the liver-specific *Akt2* null mice are mixed; it has been shown that the severity of the insulin resistance and development of diabetes in *ob/ob* mice is strain-dependent (Haluzik et al., 2004). Nevertheless, hepatic Akt2 is required for normal insulin sensitivity in a lean liver as $AFP;Akt2^{lox/lox}$ mice have decreased GIR and suppression of HGP by clamp (Figure 2-13A).

Likely reflective of their severe diabetes and resulting inability to normally store nutrients, $Lep^{ob/ob}$ $Akt2^{-/-}$ mice exhibited a decrease in both lean and fat mass by weight (Figure 2-4B). These mice almost certainly have glycosuria, which likely contributes to caloric loss and reduction in body size in these mice. However, the reduction in adiposity does not appear to be due entirely to the severely diabetic and catabolic state of these animals as $Lep^{ob/ob}$ $Akt2^{+/-}$ mice exhibited an intermediate reduction in adiposity without a decrease in lean mass. However, whether this specific reduction in adiposity is due to heterozygote loss of Akt2 in a single tissue, specifically adipose tissue, or in the whole animal is unknown. Surprisingly, $Lep^{ob/ob}$ $AFP;Akt2^{lox/lox}$ mice also exhibited a reduction in body weight compared with $Lep^{ob/ob}$ $Akt2^{lox/lox}$ mice, but this reduction was due to an overall decrease in body size as both lean and fat mass were reduced proportionally and food intake was unaffected (Figure 2-7). This non-autonomous effect on body size does not appear to be developmental, as mature $Lep^{ob/ob}$ $Akt2^{lox/lox}$ mice gain less weight following acute excision of hepatic Akt2 (Figure 2-12).

Chapter 2 Figures

Figure 2-1: Deletion of Akt2 in *ob/ob* mice results in decreased hepatic triglycerides and *de novo* lipogenesis.

A,B. Body weight (A) and liver weight (B) of 12-week old fed male mice.

C,D. Hepatic triglyceride (TG) levels of 12-week old fed (C) and overnight fasted (D) male mice.

E. *De novo* lipogenesis: 12 week-old male mice were injected with D_2O after a 5 hour fast, sacrificed after 3 hours, and liver was removed and analyzed for palmitate by GC/MS.

All values are expressed as mean ± SEM. n=5-6; *p<0.05 vs $Lep^{+/+};Akt2^{+/+}$ and **p<0.05 vs $Lep^{ob/ob};Akt2^{+/+}$ by one-way ANOVA using Newman-Keuls post-test.

Figure 2-1

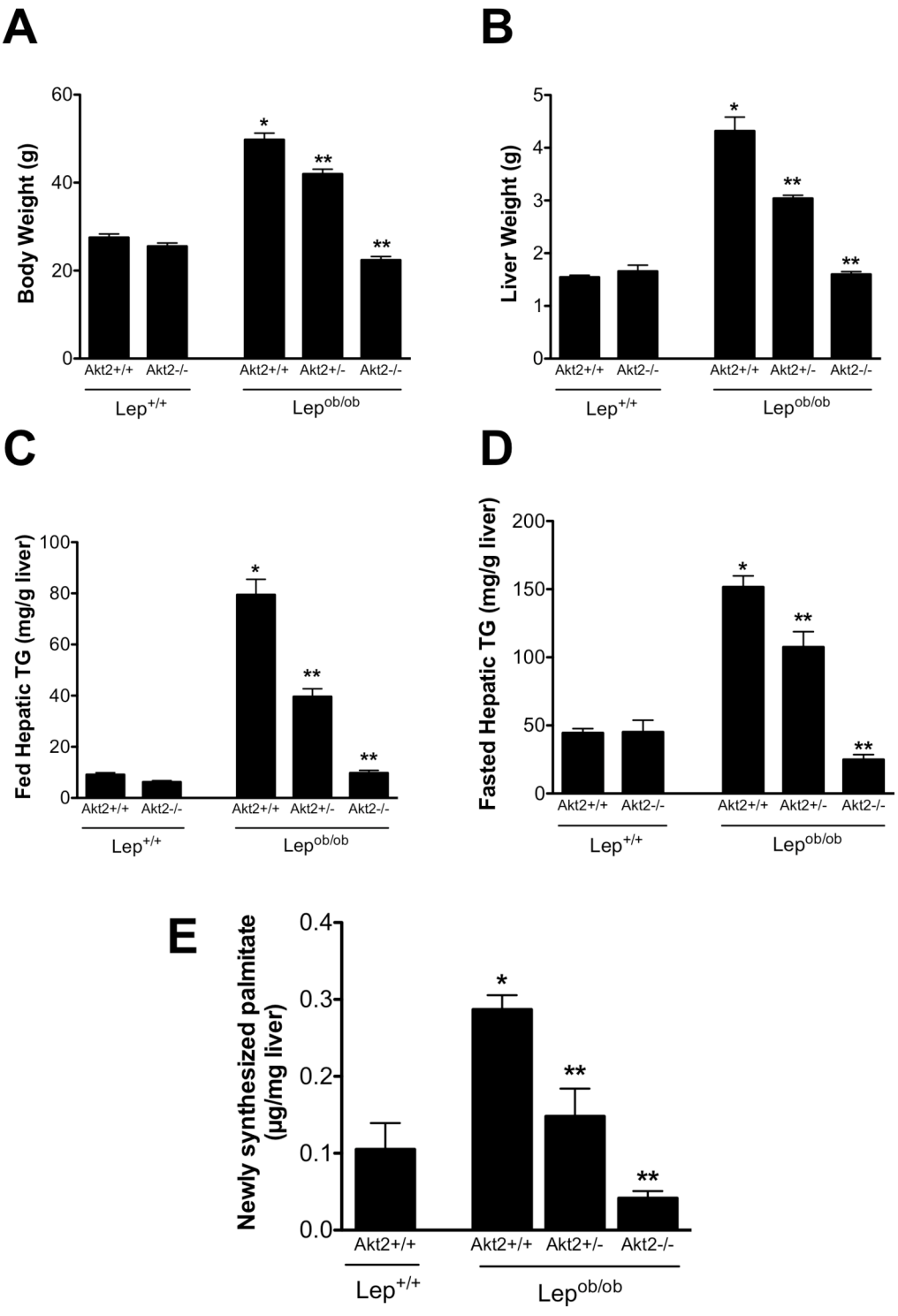
A
Body Weight (g)
60
40
20
0
*
**
**
Akt2+/+
Akt2-/-
Akt2+/+
Akt2+/-
Akt2-/-
Lep+/+
Lepob/ob
B
Liver Weight (g)
5
4
3
2
1
0
*
**
**
Akt2+/+
Akt2-/-
Akt2+/+
Akt2+/-
Akt2-/-
Lep+/+
Lepob/ob
C
Fed Hepatic TG (mg/g liver)
100
80
60
40
20
0
*
**
**
Akt2+/+
Akt2-/-
Akt2+/+
Akt2+/-
Akt2-/-
Lep+/+
Lepob/ob
D
Fasted Hepatic TG (mg/g liver)
200
150
100
50
0
*
**
**
Akt2+/+
Akt2-/-
Akt2+/+
Akt2+/-
Akt2-/-
Lep+/+
Lepob/ob
E
Newly synthesized palmitate (µg/mg liver)
0.4
0.3
0.2
0.1
0.0
*
**
**
Akt2+/+
Akt2+/+
Akt2+/-
Akt2-/-
Lep+/+
Lepob/ob

Figure 2-2: Serum measurements of *Lep$^{ob/ob}$ Akt2$^{-/-}$* mice.

Serum triglycerides (TG) (A), cholesterol (CH) (B), non-esterified fatty acids (NEFA) (C), and ketones (D) from 12 week-old fed (left) and overnight fasted (right) male mice. All values are expressed as mean ± SEM. n=6; *p<0.05 vs *Lep$^{+/+}$;Akt2$^{+/+}$* and **p<0.05 vs *Lep$^{ob/ob}$;Akt2$^{+/+}$* by one-way ANOVA using Newman-Keuls post-test.

Figure 2-2

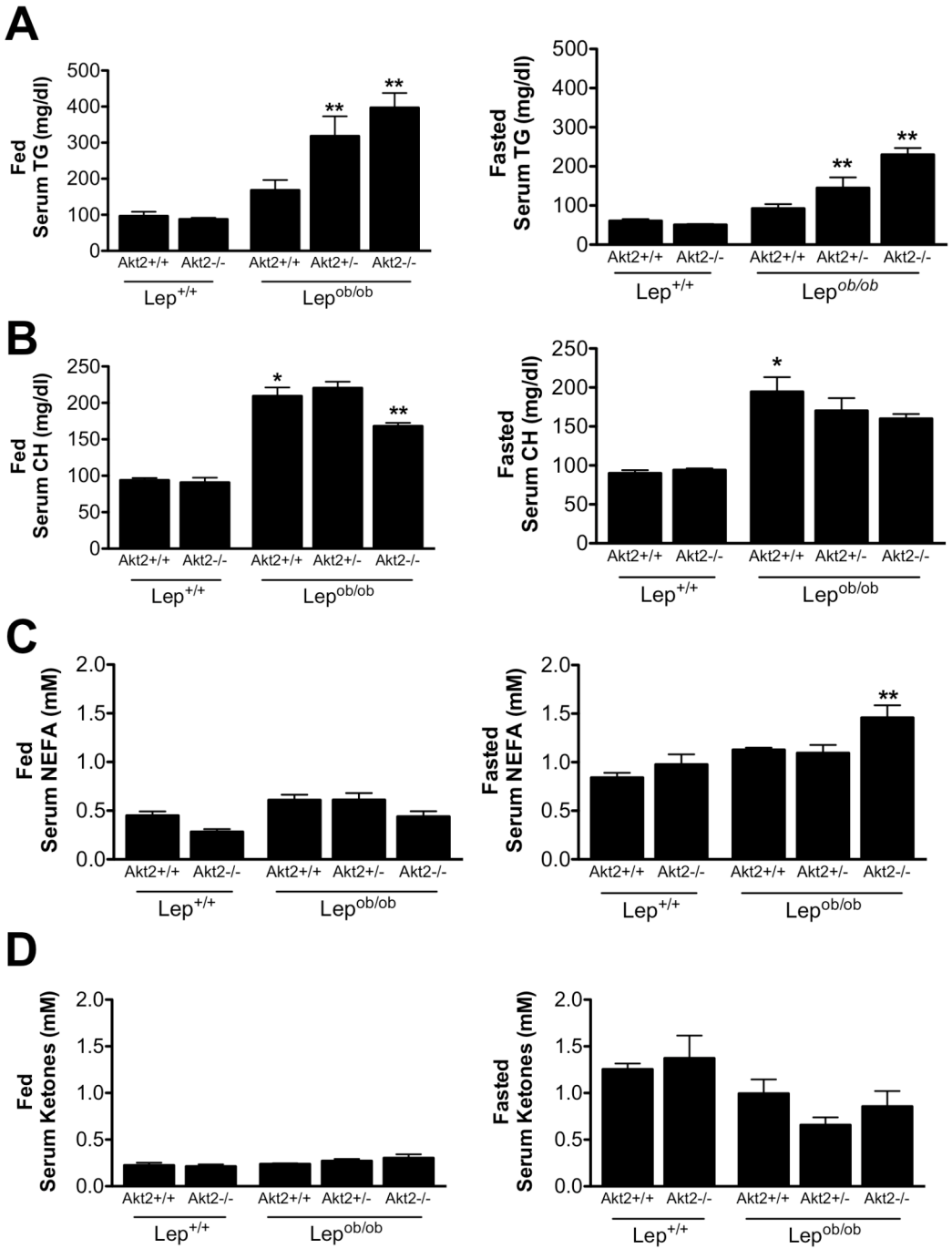
A
Fed
Serum TG (mg/dl)
500
400
300
200
100
0
**
**
Akt2+/+ Akt2-/- Akt2+/+ Akt2+/- Akt2-/-
Lep+/+
Lepob/ob
Fasted
Serum TG (mg/dl)
500
400
300
200
100
0
**
**
Akt2+/+ Akt2-/- Akt2+/+ Akt2+/- Akt2-/-
Lep+/+
Lepob/ob
B
Fed
Serum CH (mg/dl)
250
200
150
100
50
0
*
**
Akt2+/+ Akt2-/- Akt2+/+ Akt2+/- Akt2-/-
Lep+/+
Lepob/ob
Fasted
Serum CH (mg/dl)
250
200
150
100
50
0
*
Akt2+/+ Akt2-/- Akt2+/+ Akt2+/- Akt2-/-
Lep+/+
Lepob/ob
C
Fed
Serum NEFA (mM)
2.0
1.5
1.0
0.5
0.0
Akt2+/+ Akt2-/- Akt2+/+ Akt2+/- Akt2-/-
Lep+/+
Lepob/ob
Fasted
Serum NEFA (mM)
2.0
1.5
1.0
0.5
0.0
**
Akt2+/+ Akt2-/- Akt2+/+ Akt2+/- Akt2-/-
Lep+/+
Lepob/ob
D
Fed
Serum Ketones (mM)
2.0
1.5
1.0
0.5
0.0
Akt2+/+ Akt2-/- Akt2+/+ Akt2+/- Akt2-/-
Lep+/+
Lepob/ob
Fasted
Serum Ketones (mM)
2.0
1.5
1.0
0.5
0.0
Akt2+/+ Akt2-/- Akt2+/+ Akt2+/- Akt2-/-
Lep+/+
Lepob/ob

Figure 2-3: *Lep*$^{ob/ob}$ *Akt2*$^{-/-}$ mice are severely diabetic.

A-C. Fasted blood glucose levels (A) at start of 1g/kg oral glucose tolerance test (OGTT) (B) and insulin levels (C) at the start and 15 minutes post glucose load in 8-week old overnight fasted male mice. n=5-6.

D,E. Insulin tolerance tests (ITT) in 5-hour fasted male mice: 1 unit insulin/kg intraperitoneally (IP) at 10 weeks of age (D) and 2 units insulin/kg subcutaneously (subcu) at 8 weeks of age (E). n=3-9.

All values are expressed as mean ± SEM; *p<0.05 vs *Lep*$^{+/+}$*;Akt2*$^{+/+}$ and **p<0.05 vs *Lep*$^{ob/ob}$*;Akt2*$^{+/+}$ by one-way ANOVA using Newman-Keuls post-test.

Figure 2-3

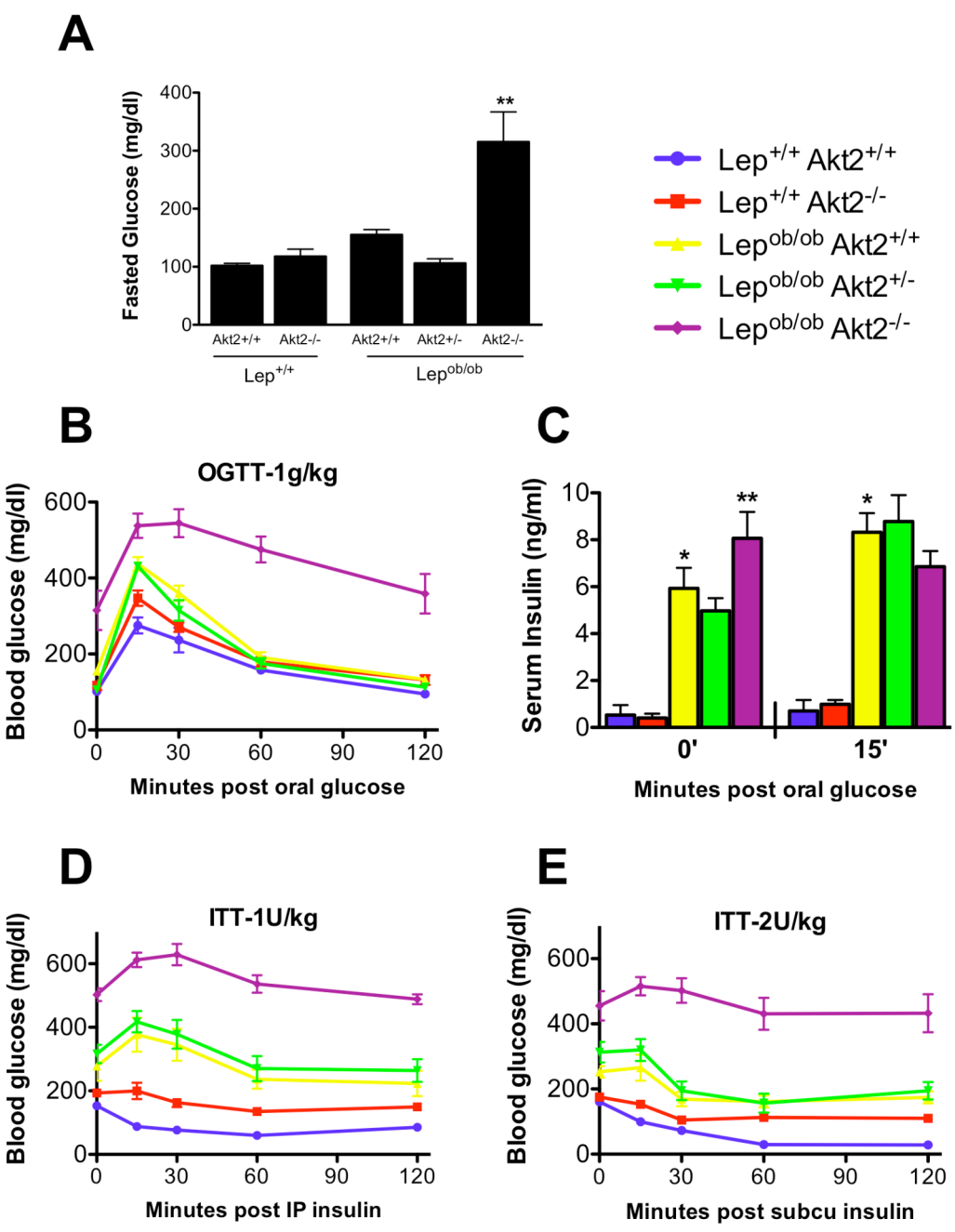
A
Fasted Glucose (mg/dl)
400
300
200
100
0
**
Akt2+/+
Akt2-/-
Akt2+/+
Akt2+/-
Akt2-/-
Lep+/+
Lepob/ob
Lep+/+ Akt2+/+
Lep+/+ Akt2-/-
Lepob/ob Akt2+/+
Lepob/ob Akt2+/-
Lepob/ob Akt2-/-
B
OGTT-1g/kg
Blood glucose (mg/dl)
600
400
200
0
0
30
60
90
120
Minutes post oral glucose
C
Serum Insulin (ng/ml)
10
8
6
4
2
0
*
**
*
0'
15'
Minutes post oral glucose
D
ITT-1U/kg
Blood glucose (mg/dl)
600
400
200
0
0
30
60
90
120
Minutes post IP insulin
E
ITT-2U/kg
Blood glucose (mg/dl)
600
400
200
0
0
30
60
90
120
Minutes post subcu insulin

Figure 2-4: *Lep*$^{ob/ob}$ *Akt2*$^{-/-}$ mice exhibit severe hepatic insulin resistance and decreased adiposity.

A. Hyperinsulinemic euglycemic clamp of 250mU insulin/kg/min on approximately 8-week old male mice. Glucose infusion rate (GIR), basal and clamped hepatic glucose production (HGP) and rate of disposal (Rd) are shown. n=4; *p<0.01 by Student's t-test.

B. Body composition of 12 week-old male mice calculated from D_2O injections expressed as mass by gram (left) and percentage of body weight (right). n=5-6; *p<0.05 vs *Lep*$^{+/+}$;*Akt2*$^{+/+}$ and **p<0.05 vs *Lep*$^{ob/ob}$;*Akt2*$^{+/+}$ for by one-way ANOVA using Newman-Keuls post-test.

All values are expressed as mean ± SEM.

Figure 2-4

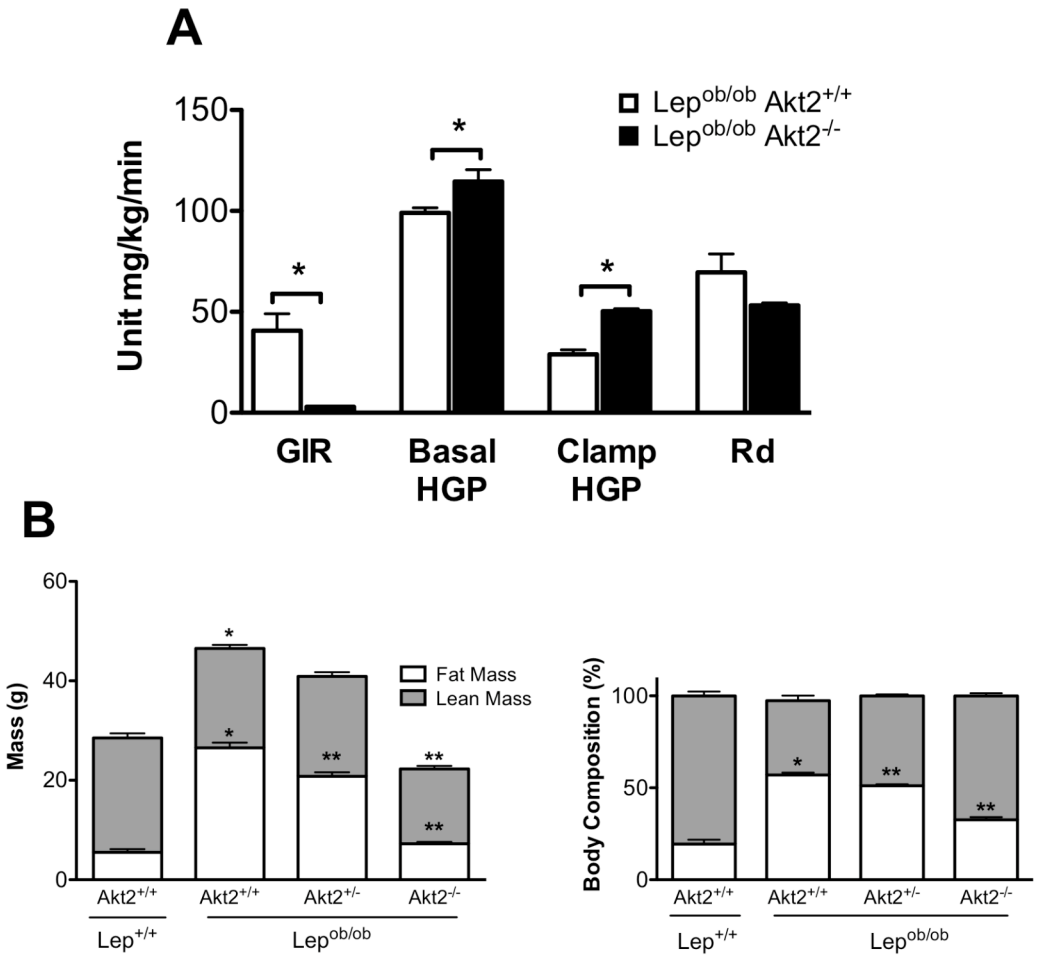
A
Lepob/ob Akt2+/+
Lepob/ob Akt2-/-
Unit mg/kg/min
150
100
50
0
*
*
*
GIR
Basal HGP
Clamp HGP
Rd
B
Mass (g)
60
40
20
0
Fat Mass
Lean Mass
Akt2+/+
Akt2+/+
Akt2+/-
Akt2-/-
Lep+/+
Lepob/ob
Body Composition (%)
100
50
0

Figure 2-5: *AFP;Akt2$^{lox/lox}$* mice lack Akt2 in the liver without change in Akt1.

A. Western blot of Akt1, Akt2, and actin from hepatic lysates from *Akt2$^{lox/lox}$*, *AFP;Akt2$^{lox/lox}$, Lep$^{ob/ob}$ Akt2$^{lox/lox}$, Lep$^{ob/ob}$ AFP;Akt2$^{lox/lox}$*, germline *Akt2$^{-/-}$* and *Akt1$^{-/-}$* mice. Each lane represents an individual mouse, and all samples were run on the same gel.

B. Western blot of Akt2 and tubulin from tissue lysates as indicated from *Akt2$^{lox/lox}$*, *AFP;Akt2$^{lox/lox}$*, and whole-body *Akt2$^{-/-}$* mice. Each lane represents an individual mouse. Abbreviations: Mus (muscle), WAT (white adipose tissue), Panc (pancreas), Kid (kidney), Spn (spleen). The arrow indicates Akt2; in some tissues there is a slightly more mobile non-specific band.

Figure 2-5

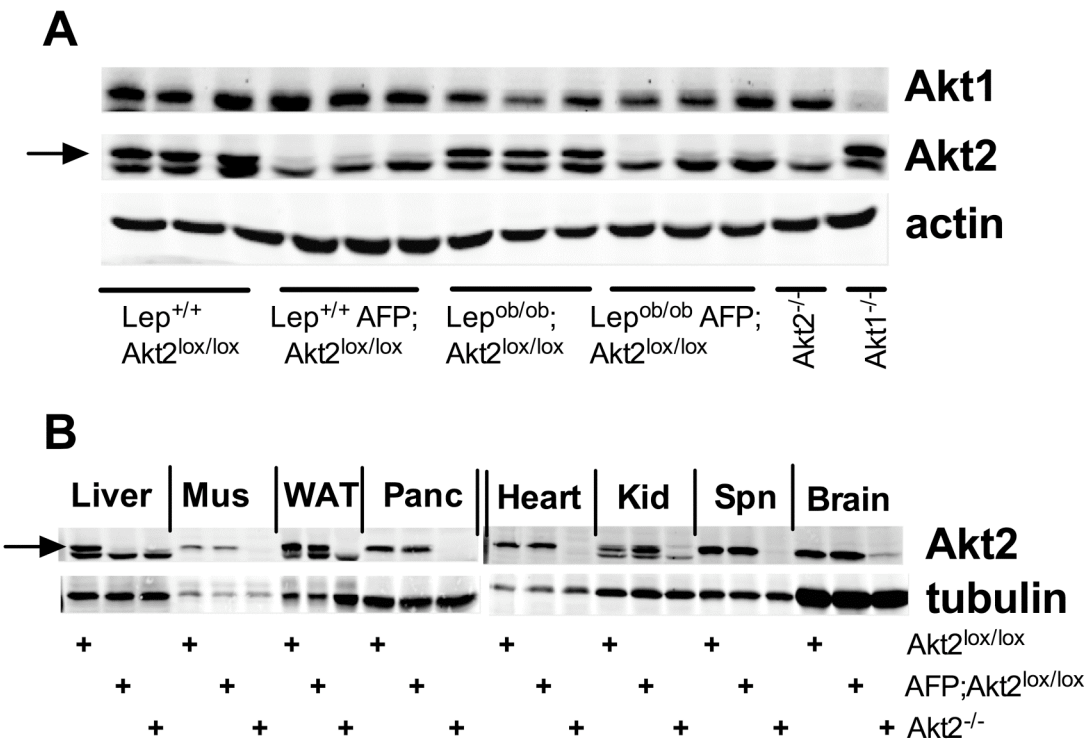
A
Akt1
Akt2
actin
Lep+/+ Akt2lox/lox
Lep+/+ AFP; Akt2lox/lox
Lepob/ob; Akt2lox/lox
Lepob/ob AFP; Akt2lox/lox
Akt2-/-
Akt1-/-
B
Liver
Mus
WAT
Panc
Heart
Kid
Spn
Brain
Akt2
tubulin
Akt2lox/lox
AFP;Akt2lox/lox
Akt2-/-

Figure 2-6: *Lep*$^{ob/ob}$ *AFP;Akt2*$^{lox/lox}$ mice have decreased hepatic triglyceride levels, which correlate with a decrease in *de novo* lipogenesis.

A,B. Body weight (A) and liver weight (B) of 12-week old fed male mice. n=6-8.

C,D. Hepatic triglyceride (TG) levels of 12-week old fed (C) and overnight fasted (D) male mice. n=6-9.

E. Hepatic long-chain fatty acid CoA (LLCoA) concentrations from 12 week-old overnight fasted male mice. n=3-4.

F. *De novo* lipogenesis measured as in Figure 2-1. n=5-6.

All values are expressed as mean ± SEM. *p<0.05 vs *Lep*$^{+/+}$*;Akt2*$^{lox/lox}$ and **p<0.05 vs *Lep*$^{ob/ob}$*;Akt2*$^{lox/lox}$ by one-way ANOVA using Newman-Keuls post-test.

Figure 2-6

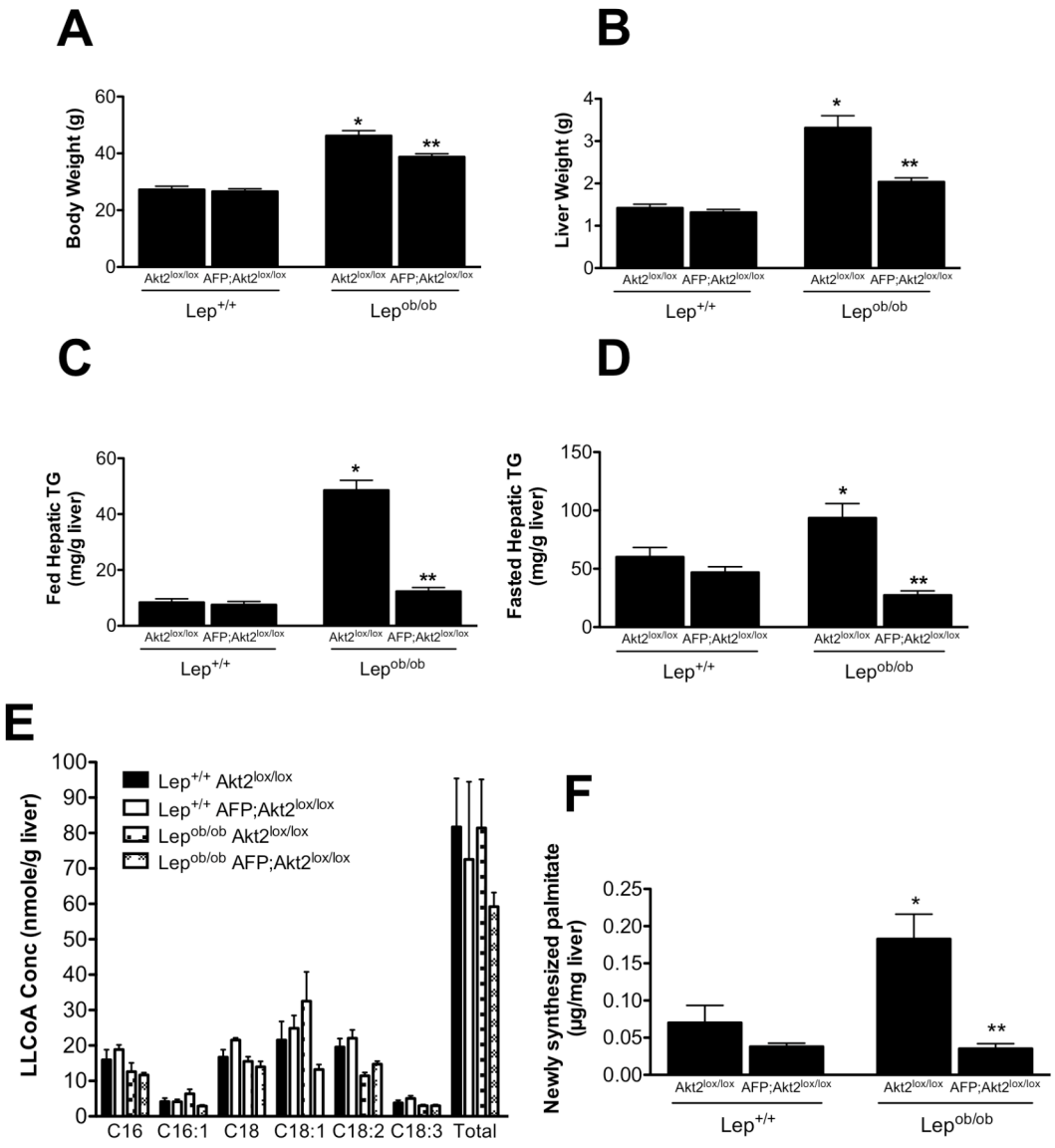
A
Body Weight (g)
60
40
20
0
*
**
Akt2lox/lox
AFP;Akt2lox/lox
Akt2lox/lox
AFP;Akt2lox/lox
Lep+/+
Lepob/ob
B
Liver Weight (g)
4
3
2
1
0
*
**
Akt2lox/lox
AFP;Akt2lox/lox
Akt2lox/lox
AFP;Akt2lox/lox
Lep+/+
Lepob/ob
C
Fed Hepatic TG (mg/g liver)
60
40
20
0
*
**
Akt2lox/lox
AFP;Akt2lox/lox
Akt2lox/lox
AFP;Akt2lox/lox
Lep+/+
Lepob/ob
D
Fasted Hepatic TG (mg/g liver)
150
100
50
0
*
**
Akt2lox/lox
AFP;Akt2lox/lox
Akt2lox/lox
AFP;Akt2lox/lox
Lep+/+
Lepob/ob
E
LLCoA Conc (nmole/g liver)
100
90
80
70
60
50
40
30
20
10
0
Lep+/+ Akt2lox/lox
Lep+/+ AFP;Akt2lox/lox
Lepob/ob Akt2lox/lox
Lepob/ob AFP;Akt2lox/lox
C16
C16:1
C18
C18:1
C18:2
C18:3
Total
F
Newly synthesized palmitate (µg/mg liver)
0.25
0.20
0.15
0.10
0.05
0.00
*
**
Akt2lox/lox
AFP;Akt2lox/lox
Akt2lox/lox
AFP;Akt2lox/lox
Lep+/+
Lepob/ob

Figure 2-7: *Lep*$^{ob/ob}$ *AFP;Akt2*$^{lox/lox}$ mice have decreased body weight and a proportional decrease in body fat content without detectable changes in energy expenditure or food intake.

A. Body composition of 12 week-old male mice.

B. 24-hour food intake of 12 week-old male mice.

C. 24-hour respiratory exchange ratio (RER) of 12 week-old male mice.

All values are expressed as mean ± SEM. n=5; *p<0.05 vs *Lep*$^{+/+}$*;Akt2*$^{lox/lox}$ and **p<0.05 vs *Lep*$^{ob/ob}$*;Akt2*$^{lox/lox}$ by one-way ANOVA using Newman-Keuls post-test.

Figure 2-7

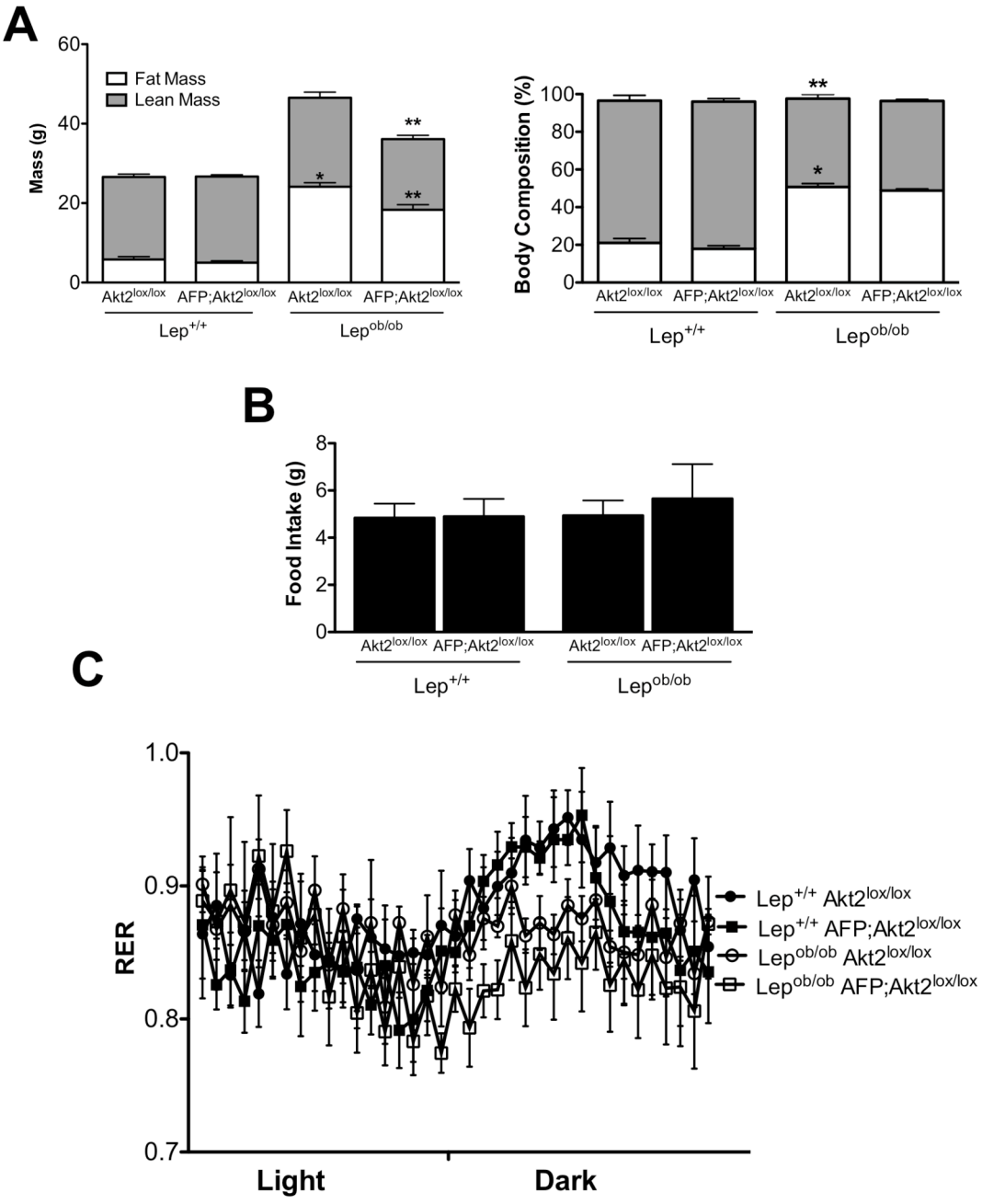
A
Fat Mass
Lean Mass
Mass (g)
60
40
20
0
Akt2lox/lox
AFP;Akt2lox/lox
Akt2lox/lox
AFP;Akt2lox/lox
Lep+/+
Lepob/ob
Body Composition (%)
100
80
60
40
20
0
B
Food Intake (g)
8
6
4
2
0
C
RER
1.0
0.9
0.8
0.7
Light
Dark
Lep+/+ Akt2lox/lox
Lep+/+ AFP;Akt2lox/lox
Lepob/ob Akt2lox/lox
Lepob/ob AFP;Akt2lox/lox

Figure 2-8: Serum measurements of *Lep$^{ob/ob}$ AFP;Akt2$^{lox/lox}$* mice.

Serum triglycerides (TG) (A), cholesterol (CH) (B), non-esterified fatty acids (NEFA) (C), and ketones (D) from 12 week-old fed (left) and overnight fasted (right) male mice. All values are expressed as mean ± SEM. n=6-9; *p<0.05 vs *Lep$^{+/+}$;Akt2$^{lox/lox}$* and **p<0.05 vs *Lep$^{ob/ob}$;Akt2$^{lox/lox}$* by one-way ANOVA using Newman-Keuls post-test.

Figure 2-8

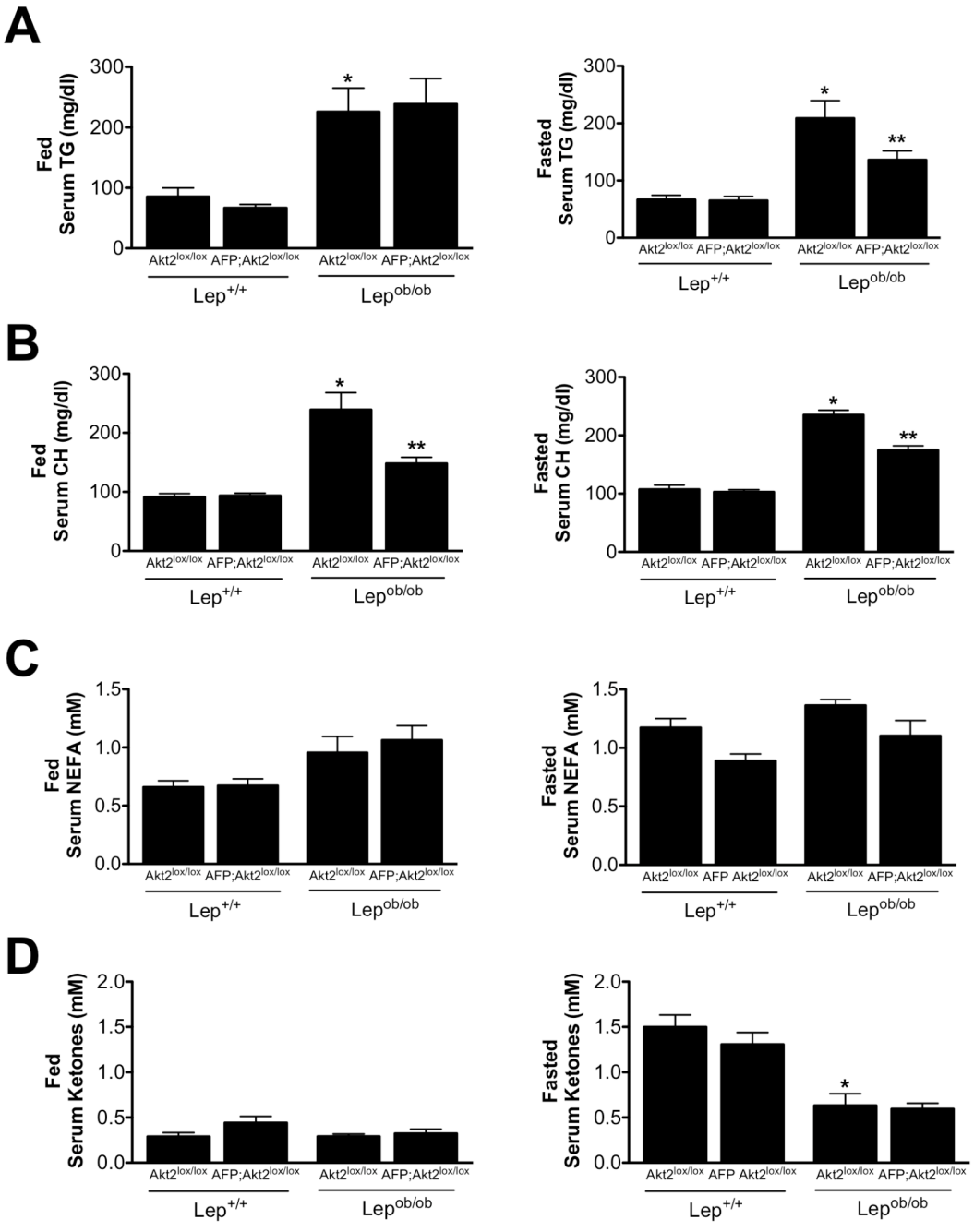
A
Fed
Serum TG (mg/dl)
300
200
100
0
*
Akt2lox/lox
AFP;Akt2lox/lox
Akt2lox/lox
AFP;Akt2lox/lox
Lep+/+
Lepob/ob
Fasted
Serum TG (mg/dl)
*
**
B
Fed
Serum CH (mg/dl)
**
Fasted
Serum CH (mg/dl)
C
Fed
Serum NEFA (mM)
1.5
1.0
0.5
0.0
Fasted
Serum NEFA (mM)
AFP
D
Fed
Serum Ketones (mM)
2.0
1.5
1.0
0.5
0.0
Fasted
Serum Ketones (mM)

Figure 2-9: AFP Cre alone does not affect body weight, liver weight, hepatic triglycerides or serum measurements in *ob/ob* mice.

All mice are 12-week old male $Lep^{ob/ob}$ mice.

A,B. Body weight (A) and liver weight (B).

Hepatic triglycerides (TG) (C), serum triglycerides (D), serum cholesterol (CH) (E), serum non-esterified fatty acids (NEFA) (F), and serum ketones (G) in fed and overnight fasted mice as indicated.

All values are expressed as mean ± SEM. n=5-7; no points are significantly different to any others within conditions ($p<0.05$ by one-way ANOVA using Newman-Keuls post-test).

Figure 2-9

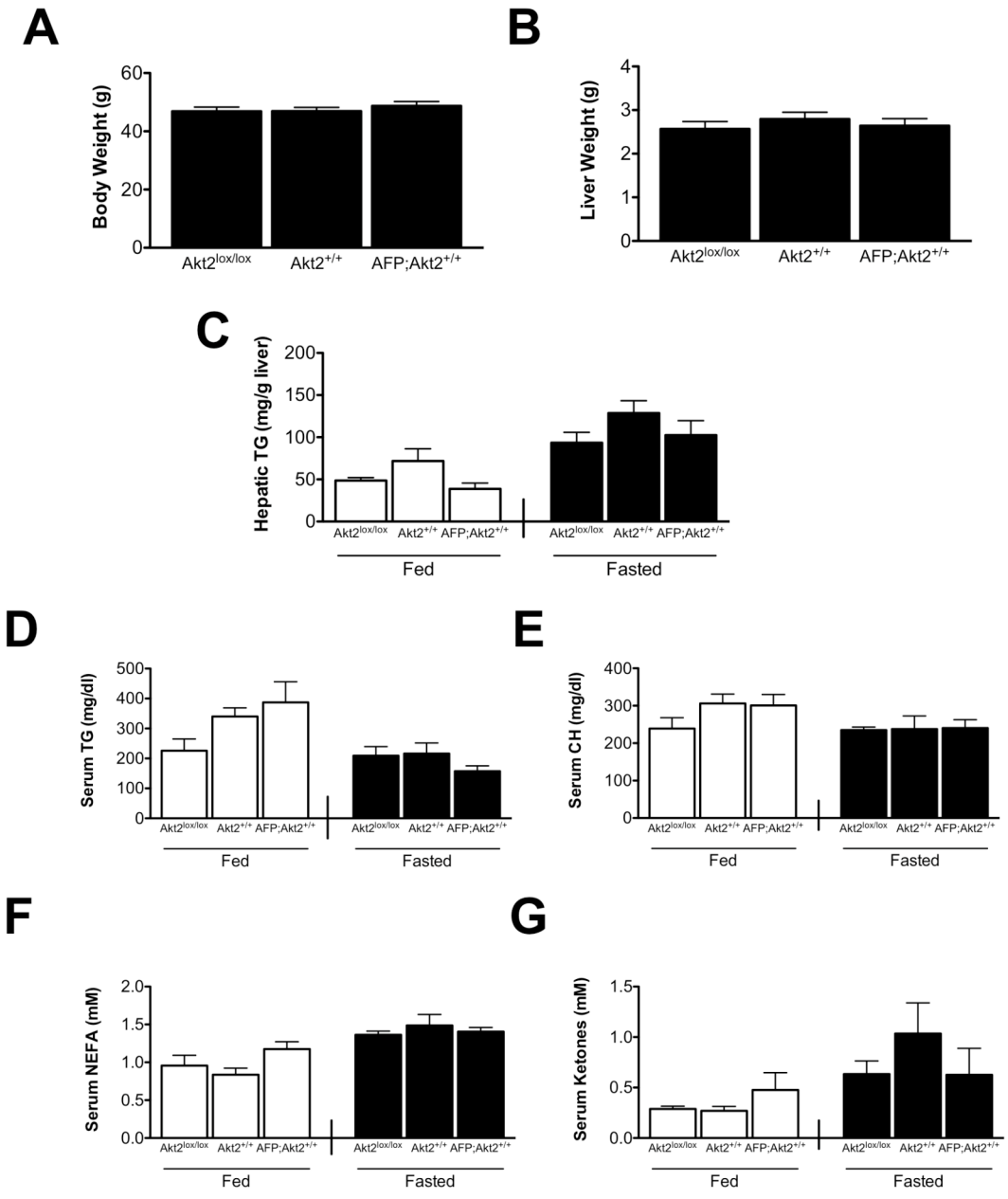
A
Body Weight (g)
60
40
20
0
Akt2lox/lox
Akt2+/+
AFP;Akt2+/+
B
Liver Weight (g)
4
3
2
1
0
Akt2lox/lox
Akt2+/+
AFP;Akt2+/+
C
Hepatic TG (mg/g liver)
200
150
100
50
0
Akt2lox/lox
Akt2+/+
AFP;Akt2+/+
Akt2lox/lox
Akt2+/+
AFP;Akt2+/+
Fed
Fasted
D
Serum TG (mg/dl)
500
400
300
200
100
0
Akt2lox/lox
Akt2+/+
AFP;Akt2+/+
Akt2lox/lox
Akt2+/+
AFP;Akt2+/+
Fed
Fasted
E
Serum CH (mg/dl)
400
300
200
100
0
Akt2lox/lox
Akt2+/+
AFP;Akt2+/+
Akt2lox/lox
Akt2+/+
AFP;Akt2+/+
Fed
Fasted
F
Serum NEFA (mM)
2.0
1.5
1.0
0.5
0.0
Akt2lox/lox
Akt2+/+
AFP;Akt2+/+
Akt2lox/lox
Akt2+/+
AFP;Akt2+/+
Fed
Fasted
G
Serum Ketones (mM)
1.5
1.0
0.5
0.0
Akt2lox/lox
Akt2+/+
AFP;Akt2+/+
Akt2lox/lox
Akt2+/+
AFP;Akt2+/+
Fed
Fasted

Figure 2-10: Hepatic gene expression in *Lep$^{ob/ob}$ AFP;Akt2$^{lox/lox}$* mice.

Hepatic gene expression as measured by Real-Time PCR of 12 week-old fed male mice. Data are presented as mRNA expression relative to that of TATA binding-protein and normalized to expression in *Akt2$^{lox/lox}$*, which is set to 1.0 using the ddCt method. All values are expressed as mean ± SEM. n=6; *p<0.05 vs *Lep$^{+/+}$;Akt2$^{lox/lox}$* and **p<0.05 vs *Lep$^{ob/ob}$;Akt2$^{lox/lox}$* by one-way ANOVA using Newman-Keuls post-test.

Abbreviations: sterol regulatory element binding protein-1c (*SREBP1c*), stearoyl-CoA desaturase-1 (*SCD1*), fatty acid synthase (*FAS*), acetyl-CoA carboxylase (*ACC*), ATP citrate lyase (*ACL)*, glycerol phosphate acyltransferase (*GPAT*), glucokinase (*GCK*), carbohydrate regulatory-element binding protein (*ChREBP*), pyruvate kinase, liver isoform (*L-PK*), peroxisome proliferator-activated receptor-γ (*PPARγ*), peroxisome proliferators-activated receptor-coactivator 1α (*PGC-1α*), carnitine palmitoyltransferase I (*CPT1*), medium-chain acetyl-CoA dehydrogenase (*MCAD*), and cytochrome c oxidase subunit 7a (*Cox7a*).

Figure 2-10

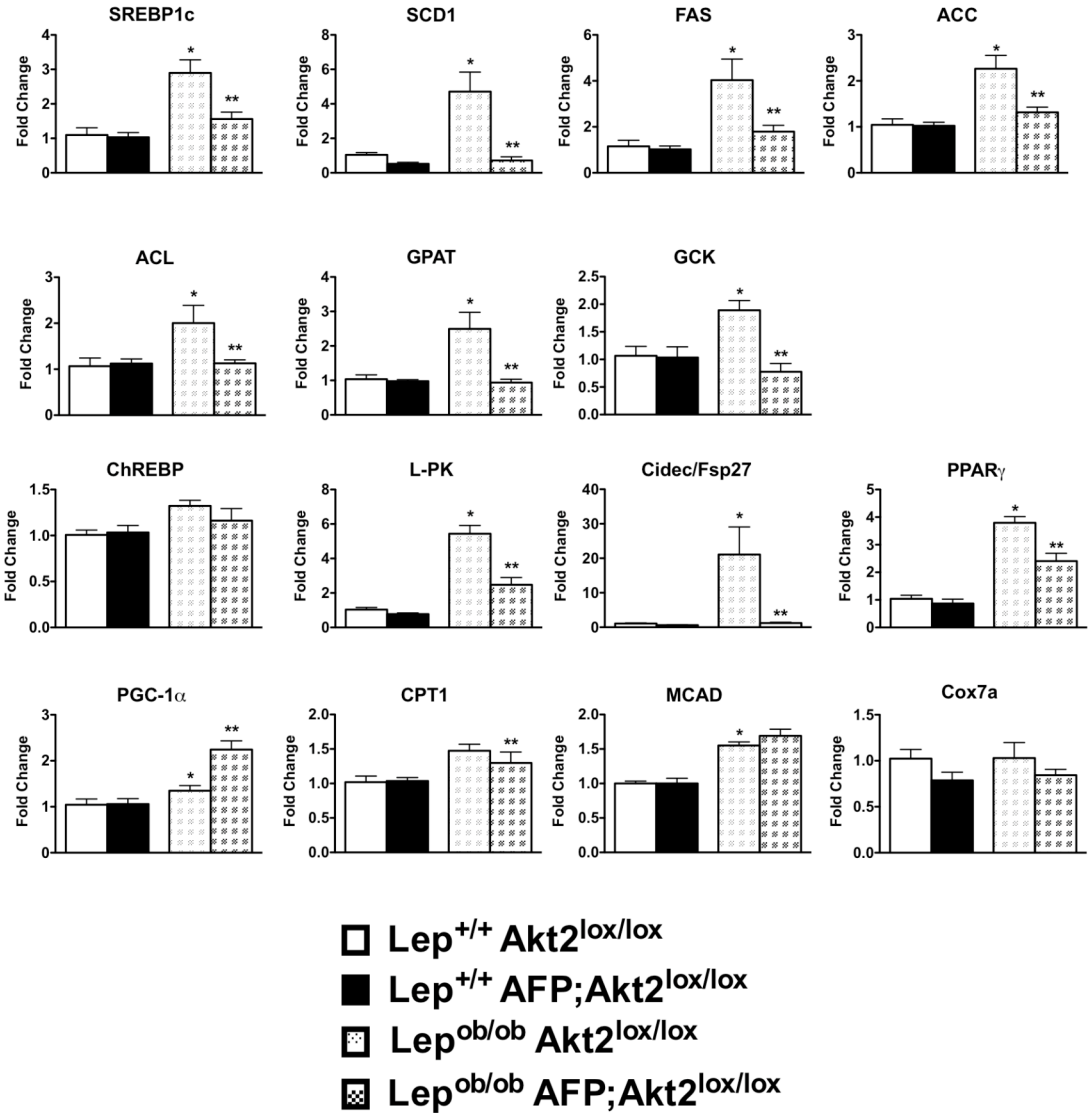
SREBP1c
SCD1
FAS
ACC
ACL
GPAT
GCK
ChREBP
L-PK
Cidec/Fsp27
PPARγ
PGC-1α
CPT1
MCAD
Cox7a
Fold Change
Lep+/+ Akt2lox/lox
Lep+/+ AFP;Akt2lox/lox
Lepob/ob Akt2lox/lox
Lepob/ob AFP;Akt2lox/lox

Figure 2-11: Loss of hepatic Akt2 does not dramatically alter triglyceride secretion in lean or *ob/ob* mice.

12-week old male mice were intraperitoneally (IP) injected with 100µl 10% poloxamer 407 (P-407) per 10 grams body weight after a 5-hour fast and serum triglycerides were measured by tail bleed at 0, 1, 2, and 4 hours after injection.

Area under the curve calculated using Graphpad Prism.

All values are expressed as mean ± SEM. n=6-9; no points are significantly different to others ($p<0.05$ by one-way ANOVA using Newman-Keuls post-test).

Figure 2-11

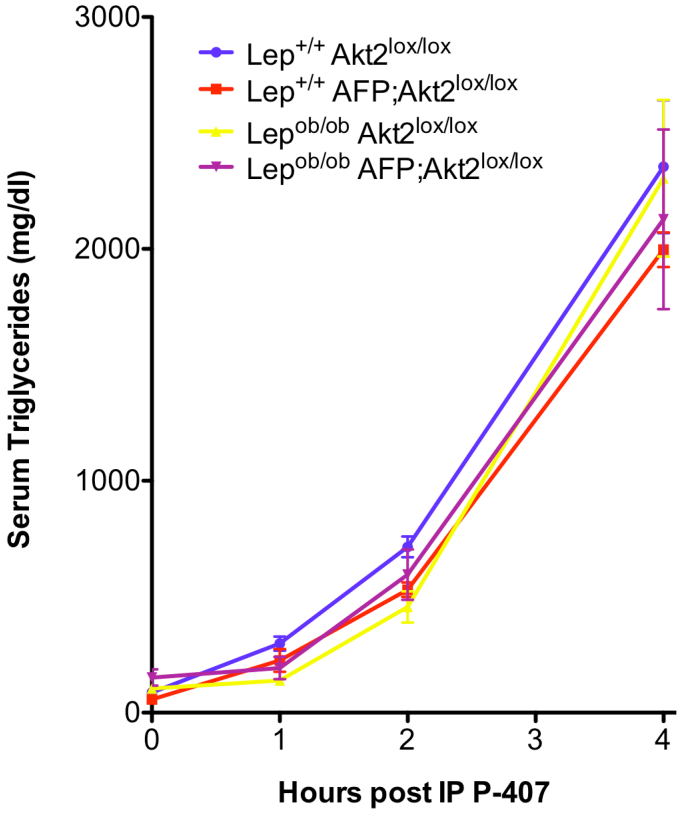
3000
2000
1000
0
Serum Triglycerides (mg/dl)
Lep+/+ Akt2lox/lox
Lep+/+ AFP;Akt2lox/lox
Lepob/ob Akt2lox/lox
Lepob/ob AFP;Akt2lox/lox
0
1
2
3
4
Hours post IP P-407

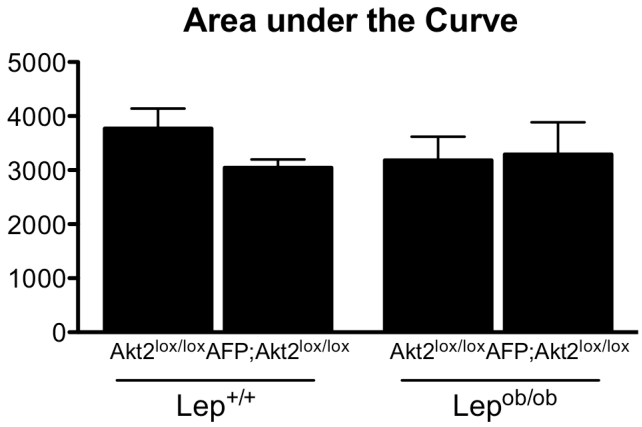
Area under the Curve
5000
4000
3000
2000
1000
0
Akt2lox/lox
AFP;Akt2lox/lox
Akt2lox/lox
AFP;Akt2lox/lox
Lep+/+
Lepob/ob

Figure 2-12: Acute excision of Akt2 reverses hepatic steatosis in *ob/ob* mice.

Male $Lep^{ob/ob}$ $Akt2^{lox/lox}$ mice were injected retro-orbitally with AAV-GFP or AAV-Cre at approximately 10 weeks of age, and were sacrificed under fed conditions 2 weeks later.

A. Body weight at time of injection and at time of sacrifice (left) and percentage change in body weight (BW) from the time of injection to sacrifice (right).

B,C. Liver weight (B) and hepatic triglycerides (TG).

D-G. Serum triglycerides (TG) (D), cholesterol (CH) (E), non-esterified fatty acids (NEFA) (F), and ketones (G).

All values are expressed as mean ± SEM. n=4; *$p<0.01$ by Student's t-test.

Figure 2-12

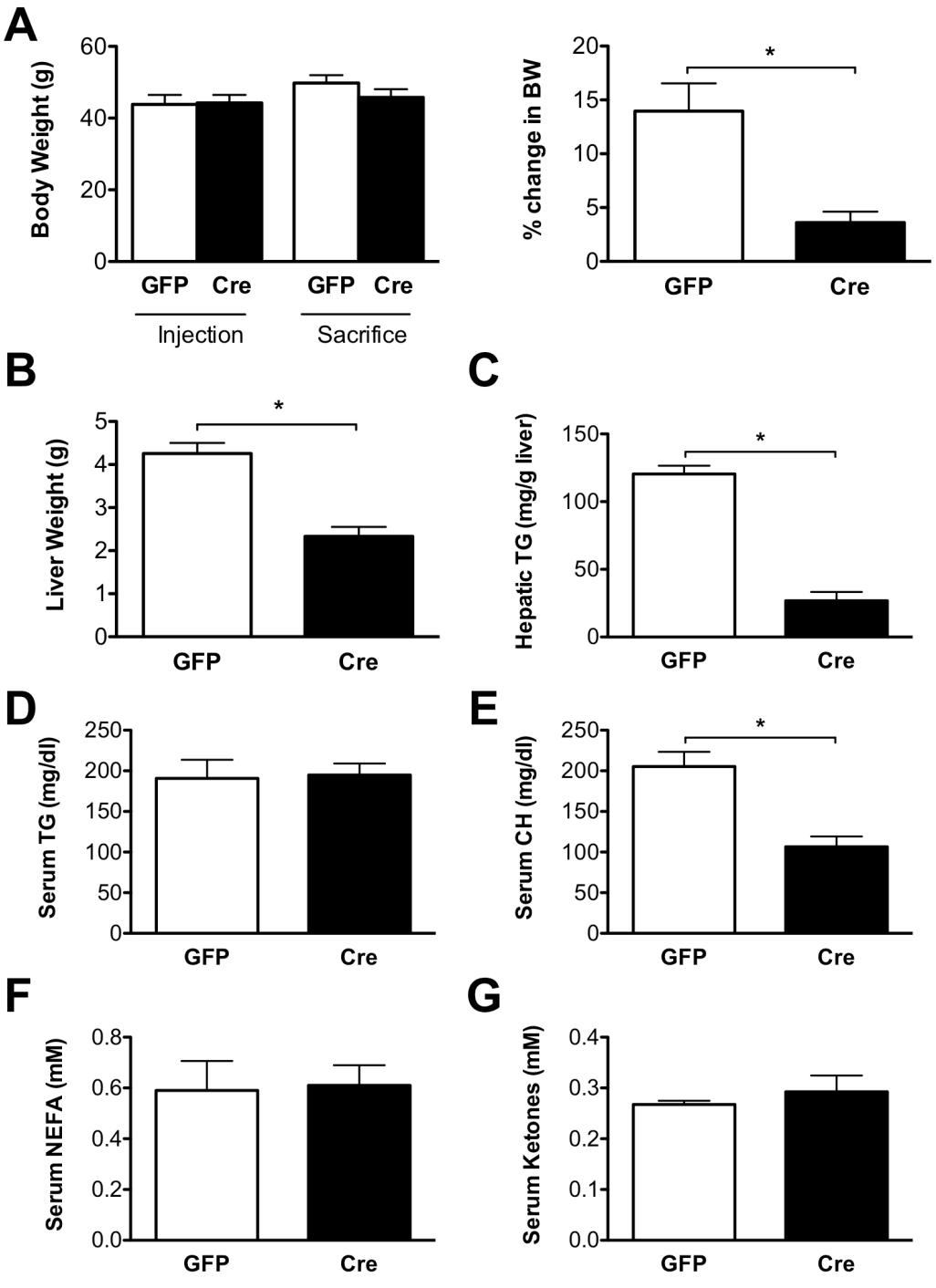
A
Body Weight (g)
60
40
20
0
GFP
Cre
GFP
Cre
Injection
Sacrifice
% change in BW
20
15
10
5
0
*
GFP
Cre
B
Liver Weight (g)
5
4
3
2
1
0
*
GFP
Cre
C
Hepatic TG (mg/g liver)
150
100
50
0
*
GFP
Cre
D
Serum TG (mg/dl)
250
200
150
100
50
0
GFP
Cre
E
Serum CH (mg/dl)
250
200
150
100
50
0
*
GFP
Cre
F
Serum NEFA (mM)
0.8
0.6
0.4
0.2
0.0
GFP
Cre
G
Serum Ketones (mM)
0.4
0.3
0.2
0.1
0.0
GFP
Cre

Figure 2-13: Loss of hepatic Akt2 causes hepatic insulin resistance in lean mice, but does not further worsen diabetes of *ob/ob* mice.

A. Hyperinsulinemic euglycemic clamp of 2.5mU insulin/kg/min on 8-week old male mice. Glucose infusion rate (GIR), basal and clamped hepatic glucose production (HGP) and rate of disposal (Rd) shown. n=4; *p<0.01 by Student's t-test.

B-D. Fasted blood glucose levels (B) at start of 1g/kg oral glucose tolerance test (OGTT) (C) and insulin levels (D) at the start and 15 minutes post glucose load in 8-week old overnight fasted male mice. n=6-9; *p<0.05 vs $Lep^{+/+};Akt2^{lox/lox}$ and **p<0.05 vs $Lep^{ob/ob};Akt2^{lox/lox}$ by one-way ANOVA using Newman-Keuls post-test.

E-F. Insulin tolerance test (ITT) in 5-hour fasted male mice: 1 unit insulin/kg intraperitoneally (IP) at 10 weeks of age (E) and 2 units insulin/kg subcutaneously (subcu) at 8 weeks of age (F). n=4-9; *p<0.05 vs $Lep^{+/+};Akt2^{lox/lox}$ and **p<0.05 vs $Lep^{ob/ob};Akt2^{lox/lox}$ by one-way ANOVA using Newman-Keuls post-test.

All values are expressed as mean ± SEM.

Figure 2-13

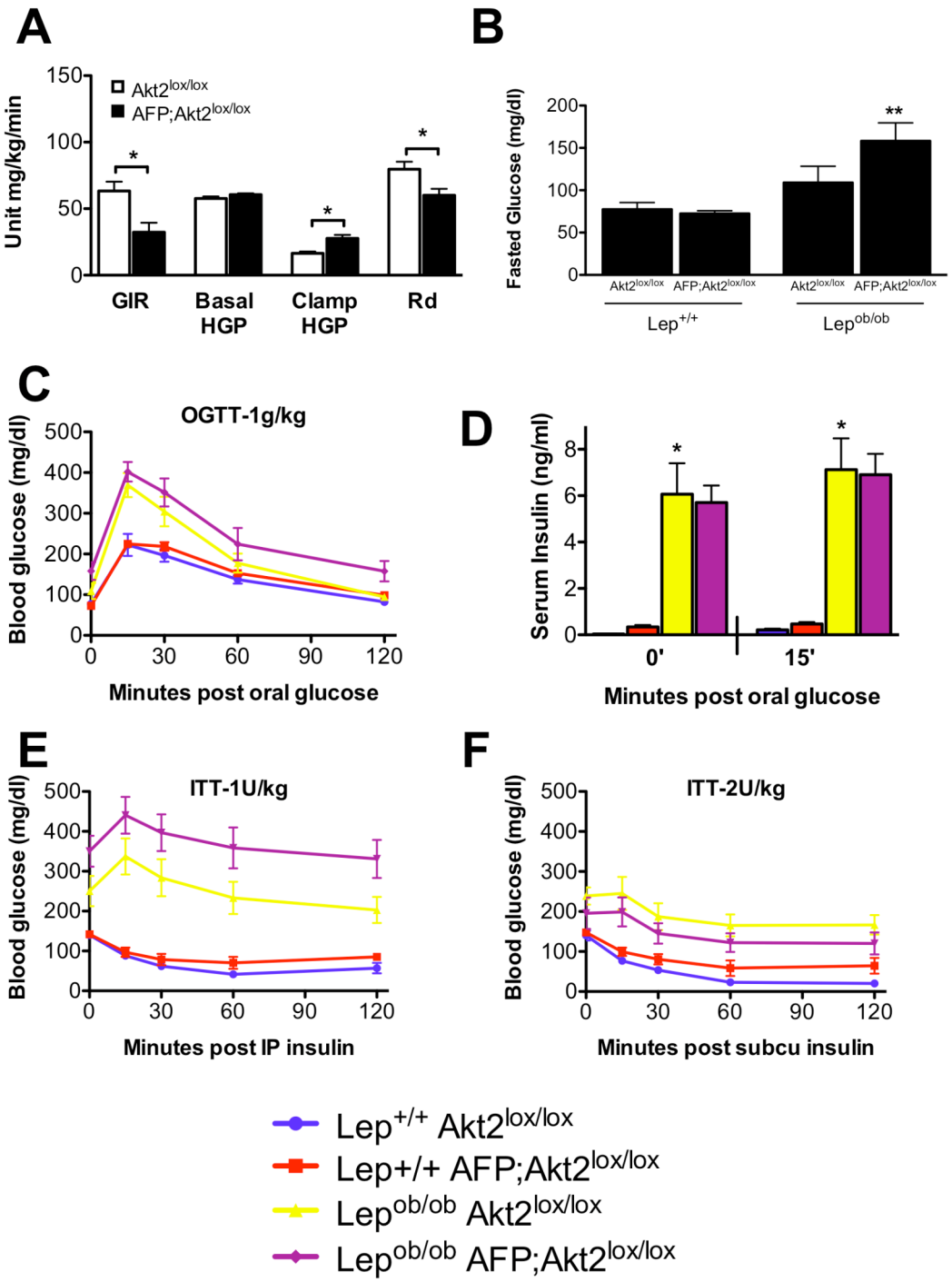
A
Unit mg/kg/min
150
100
50
0
Akt2lox/lox
AFP;Akt2lox/lox
*
*
*
GIR
Basal HGP
Clamp HGP
Rd
B
Fasted Glucose (mg/dl)
200
150
100
50
0
**
Akt2lox/lox
AFP;Akt2lox/lox
Akt2lox/lox
AFP;Akt2lox/lox
Lep+/+
Lepob/ob
C
OGTT-1g/kg
Blood glucose (mg/dl)
500
400
300
200
100
0
0
30
60
90
120
Minutes post oral glucose
D
Serum Insulin (ng/ml)
8
6
4
2
0
*
*
0'
15'
Minutes post oral glucose
E
ITT-1U/kg
Blood glucose (mg/dl)
500
400
300
200
100
0
0
30
60
90
120
Minutes post IP insulin
F
ITT-2U/kg
Blood glucose (mg/dl)
500
400
300
200
100
0
0
30
60
90
120
Minutes post subcu insulin
Lep+/+ Akt2lox/lox
Lep+/+ AFP;Akt2lox/lox
Lepob/ob Akt2lox/lox
Lepob/ob AFP;Akt2lox/lox

Figure 2-14: AFP Cre alone has no effect on GTT or ITT in lean or *ob/ob* mice.

A, B. Fasted blood glucose levels (A) at start of 1g/kg oral glucose tolerance test (OGTT) (B) in 8-week old overnight fasted male mice.

C. 1 unit insulin/kg intraperitoneally (IP) insulin tolerance test (ITT) in 10-week old 5-hour fasted male mice.

All values are expressed as mean ± SEM. n=5-9; no points are significantly different to any others ($p<0.05$ by one-way ANOVA using Newman-Keuls post-test).

Figure 2-14

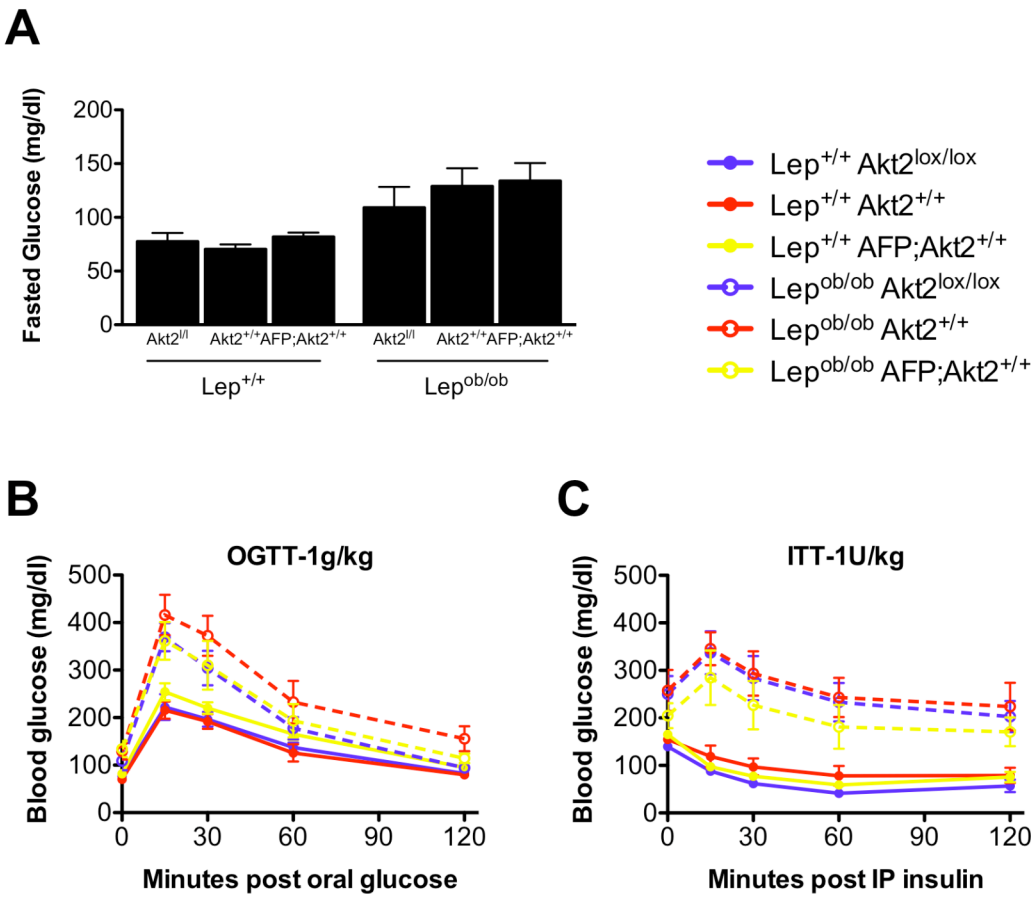
A
Fasted Glucose (mg/dl)
200
150
100
50
0
Akt2l/l
Akt2+/+AFP;Akt2+/+
Akt2l/l
Akt2+/+AFP;Akt2+/+
Lep+/+
Lepob/ob
Lep+/+ Akt2lox/lox
Lep+/+ Akt2+/+
Lep+/+ AFP;Akt2+/+
Lepob/ob Akt2lox/lox
Lepob/ob Akt2+/+
Lepob/ob AFP;Akt2+/+
B
OGTT-1g/kg
Blood glucose (mg/dl)
500
400
300
200
100
0
0
30
60
90
120
Minutes post oral glucose
C
ITT-1U/kg
Blood glucose (mg/dl)
500
400
300
200
100
0
0
30
60
90
120
Minutes post IP insulin

Figure 2-15: Hepatic insulin signaling is blunted by loss of Akt2 in the liver in lean mice, but not in *ob/ob* mice.

A. Western blot of phospho-Akt (p473 and p308) and downstream signaling targets in hepatic lysates from *Akt2*$^{lox/lox}$ and *AFP;Akt2*$^{lox/lox}$ mice. 8-week old male mice were fasted overnight and injected IP with either saline or 1U/kg insulin, then sacrificed after 20 minutes.

B. Western blot of phospho-Akt (p473 and p308) and downstream signaling targets in hepatic lysates from 8-10 week old male *Lep*$^{ob/ob}$*;Akt2*$^{lox/lox}$ and *Lep*$^{ob/ob}$ *AFP;Akt2*$^{lox/lox}$ mice under hyperinsulinemic euglycemic clamp conditions. *Akt2*$^{lox/lox}$ mice injected with saline or insulin as in A are included for comparison.

Each lane represents an individual mouse. Loading controls are included when the phospho-protein and total protein were run on different gels, though the same protein extracts were used. The arrow indicates Akt2 as there is a slightly more mobile non-specific band.

Figure 2-15

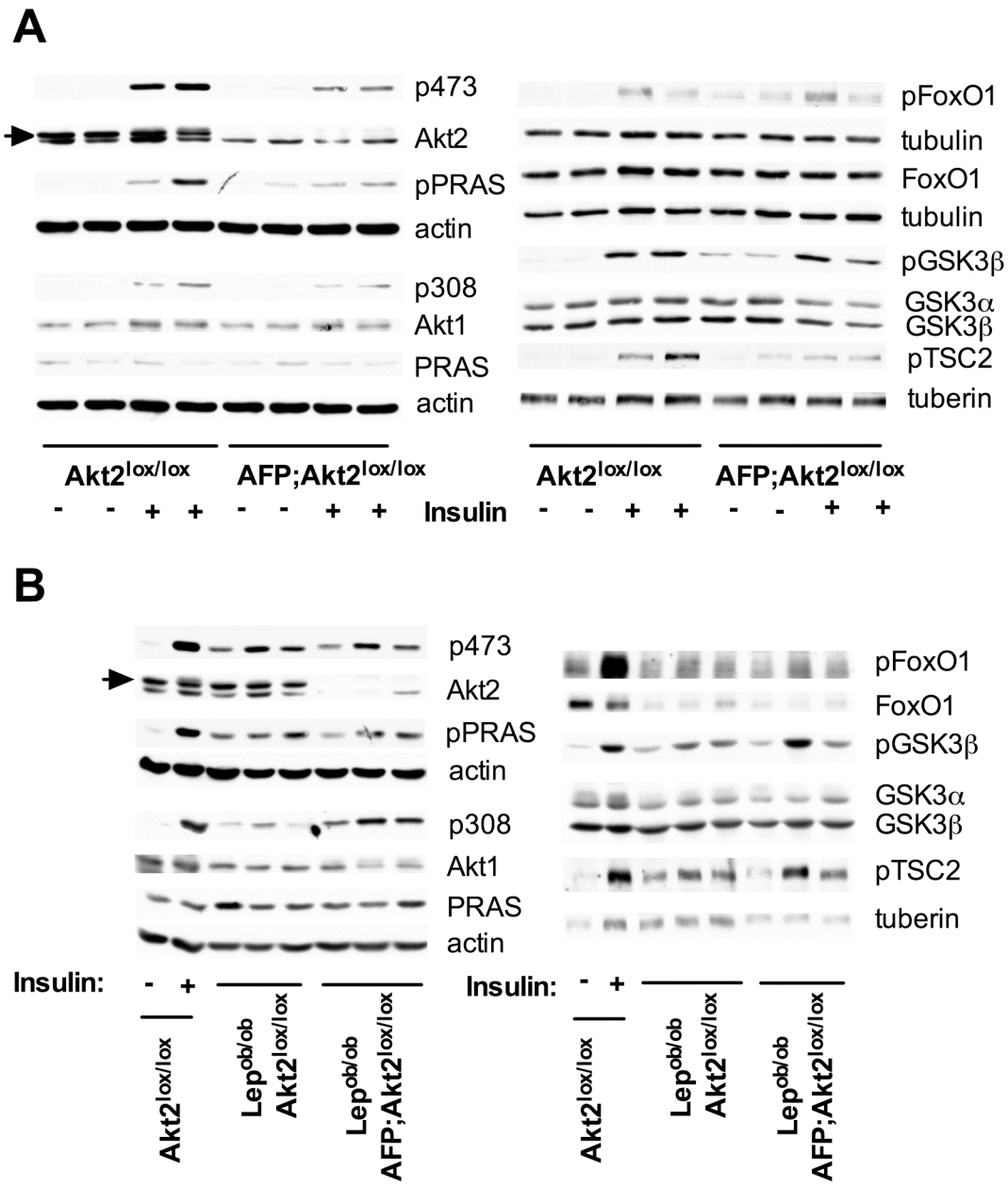
A
p473
Akt2
pPRAS
actin
p308
Akt1
PRAS
actin
pFoxO1
tubulin
FoxO1
tubulin
pGSK3β
GSK3α
GSK3β
pTSC2
tuberin
Akt2lox/lox
AFP;Akt2lox/lox
Akt2lox/lox
AFP;Akt2lox/lox
- - + + - - + + Insulin - - + + - - + +
B
p473
Akt2
pPRAS
actin
p308
Akt1
PRAS
actin
pFoxO1
FoxO1
pGSK3β
GSK3α
GSK3β
pTSC2
tuberin
Insulin: - +
Akt2lox/lox
Lepob/ob Akt2lox/lox
Lepob/ob AFP;Akt2lox/lox
Insulin: - +
Akt2lox/lox
Lepob/ob Akt2lox/lox
Lepob/ob AFP;Akt2lox/lox

Chapter 3:

Akt2 is required for the development of hepatic steatosis resulting from diet-induced obesity.

Introduction

We have shown that hepatic Akt2 is required for the development of hepatic steatosis and increased *de novo* lipogenesis that occurs in the *ob/ob* mouse (Chapter 2). However, though the *ob/ob* mouse is a robust model of obesity and hepatic steatosis, these mice lack leptin, which itself plays a role in metabolism. Thus we wanted to test the generality of the requirement of Akt2 for hepatic steatosis in another insulin-resistant model of obesity, diet-induced obesity (DIO). High-fat diets (HFD) are commonly used to induce obesity and diabetes in mice, and may be more physiologically similar to human obesity than genetic manipulations (reviewed in Collins et al., 2004). The use of HFD is advantageous as the onset of obesity and insulin resistance is gradual and often less severe than genetic causes of obesity. However, these effects are strongly influenced by genetic background and may not be solely dependent on excess energy intake (Rebuffe-Scrive et al., 1993; West et al., 1992). In addition, the majority of dietary fat in a HFD comes from a single source unlike human diets, and the particular type of fat used in the diet influences the severity of resulting insulin resistance (Buettner et al., 2006).

The Surwit HFD, originally defined in the 1980s by Richard Surwit, is both high in fat and sucrose, and rapidly induces obesity and insulin resistance in C57BL/6J mice (Surwit et al., 1988). The combination of high fat, high simple carbohydrate and low fiber resembles the type of diet that is likely a major factor in the growing prevalence of human obesity. Surwit HFD is extremely palatable to mice, resulting in hyperphagia and increased calorie intake (Surwit et al., 1995; Surwit et al., 1988). However, C57BL/6J mice still gain weight and exhibit hyperglycemia after 3 months on Surwit HFD when restricted to the same caloric intake as the control group (Petro et al., 2004). Both the obesity and diabetes can be reverse if the animals are taken off the diet and switched to

one low in fat and sucrose (Parekh et al., 1998). However, all of these effects are heavily influenced by background strain, emphasizing how complex inherited traits interact with environmental conditions. While C57BL/6J mice are very susceptible to DIO and diabetes on Surwit HFD, other strains, in particular A/J mice, are resistant (Black et al., 1998; Parekh et al., 1998; Surwit et al., 1995). This dependency on strain holds true with other high fat diets as well (West et al., 1992).

In this chapter, we describe the role of hepatic Akt2 in the development of hepatic steatosis resulting from DIO. For these studies, we used a Surwit HFD containing 58% kcal from fat (mostly coconut oil) and 25.5% kcal from carbohydrates (approximately half from sucrose) and a lard-based HFD containing 60% kcal from fat and 20% kcal from carbohydrates (approximately one-third from sucrose). HFDs containing either coconut oil or lard have been shown to increase the hepatic expression of *SREBP1c* and its lipogeneic target genes in rats (Buettner et al., 2006). We find that hepatic Akt2 is required for the accumulation of hepatic triglycerides in DIO, but this does not correspond to a decrease in *de novo* lipogenesis or lipogenic gene expression. Furthermore, lipogenic gene expression does not correlate with lipogenesis in mice fed either HFD, and mice fed lard HFD actually have decreased *de novo* lipogenesis while exhibiting hepatic steatosis. However, while loss of hepatic Akt2 does not significantly alter the diabetic phenotype of the Surwit HFD-fed mouse**,** $Akt2^{-/-}$ mice on Surwit HFD fail to gain weight but are more insulin-resistant compared with $Akt2^{+/+}$ mice.

Results

Germline Akt2 deletion decreases hepatic lipid accumulation resulting from Surwit HFD.

Male $Akt2^{+/+}$ and $Akt2^{-/-}$ mice were started on a Surwit HFD at approximately 5 weeks of age, and maintained on the diet for one or 4 months; chow-fed age-matched

male mice served as controls (for composition of Surwit HFD, see Table 6-3 in Materials and Methods). Mice on Surwit HFD steadily gained weight over time, but this increase was blunted in *Akt2*$^{-/-}$ mice, so that the weights of the two groups bifurcated during their second month on the diet (Figure 3-1A). This was not due to differences in food intake, as *Akt2*$^{-/-}$ mice actually ate more than their *Akt2*$^{+/+}$ littermates, or to significantly altered energy expenditure, as measured after 4 months on Surwit HFD (Figure 3-1B and 3-1C). The decrease in body weight of the *Akt2*$^{-/-}$ mice after 4 months on Surwit HFD could be attributed to a significant decrease in fat mass while maintaining normal lean mass by weight (Figure 3-1D).

After 4 months on Surwit diet, *Akt2*$^{+/+}$ mice gained more weight than their chow-fed counterparts, while *Akt2*$^{-/-}$ mice on HFD weighed the same as those on chow (Figure 3-2A). Though liver weight was not significantly different between any of the groups (Figure 3-2B), the increase in fed hepatic triglycerides observed in *Akt2*$^{+/+}$ mice after 4 months on the diet was abrogated with loss of Akt2 (Figures 3-2C and 3-2D). Interestingly, *Akt2*$^{-/-}$ mice on Surwit HFD for 4 months had significantly reduced fasted hepatic triglycerides compared with chow-fed *Akt2*$^{-/-}$ mice (Figure 3-2D). Germline deletion of Akt2 did not change serum triglyceride levels on Surwit HFD, but did lead to a decrease in fed serum cholesterol, fasted serum NEFA and serum ketones after 4 months on the diet (Figure 3-3A, 3-3B, 3-3C and 3-3D).

Akt2$^{-/-}$ *mice are more insulin-resistant but maintain normal glucose tolerance by increasing insulin levels on Surwit HFD.*

Akt2$^{-/-}$ mice display hepatic and peripheral insulin resistance, and have impaired glucose tolerance and hyperinsulinemia at a young age (Cho et al., 2001a). Thus, we wanted to see if the stress of a Surwit HFD would increase these glucose metabolic

impairments. *Akt2*$^{-/-}$ mice on chow did display fasting hyperglycemia, hyperinsulinemia and glucose intolerance compared with *Akt2*$^{+/+}$ mice at 2 months of age (one month on diet), but these differences were largely resolved by 5 months of age (4 months on diet) (Figures 3-4A to 3-4E). Similarly, after 4 months on Surwit HFD, *Akt2*$^{-/-}$ mice exhibited normal glucose tolerance compared with *Akt2*$^{+/+}$ mice, and actually had normal fasting glucose levels while *Akt2*$^{+/+}$ mice were hyperglycemic (Figures 3-4A, 3-4D). *Akt2*$^{-/-}$ mice on Surwit HFD eventually exhibited improved glucose tolerance compared with *Akt2*$^{+/+}$ mice on Surwit HFD likely due to increased compensation by the pancreatic β-cells (see Addendum). These effects did not appear to be the result of improved insulin sensitivity on Surwit HFD as fasted and post-glucose load insulin levels were higher in *Akt2*$^{-/-}$ versus *Akt2*$^{+/+}$ mice both after one and 4 months on Surwit HFD (Figures 3-4C and 3-4E).

To determine if *Akt2*$^{-/-}$ mice are more insulin-resistant than *Akt2*$^{+/+}$ mice on Surwit HFD, these mice were subjected to hyperinsulinemic euglycemic clamp; age-matched chow-fed *Akt2*$^{-/-}$ mice were also included to determine the contribution of HFD-feeding. After 6 weeks on Surwit HFD, *Akt2*$^{-/-}$ mice required a significantly lower GIR to maintain euglycemia than their *Akt2*$^{+/+}$ counterparts, confirming that though they had similar glucose tolerance, they were more insulin-resistant (Figure 3-4F). While basal HGP was similar, clamped HGP was increased in *Akt2*$^{-/-}$ mice on HFD compared with both *Akt2*$^{+/+}$ mice on HFD and *Akt2*$^{-/-}$ mice on chow, indicating that both Surwit HFD-feeding and loss of Akt2 leads to hepatic insulin resistance. Rd was also significantly decreased in *Akt2*$^{-/-}$ versus *Akt2*$^{+/+}$ mice on Surwit HFD, showing that *Akt2*$^{-/-}$ mice had peripheral insulin resistance despite gaining less fat mass on HFD. However, as GIR and Rd were similar in *Akt2*$^{-/-}$ mice on Surwit HFD and chow, this increase in peripheral insulin resistance was likely due to loss of Akt2 in peripheral tissue Figure 3-4F).

AFP;Akt2$^{lox/lox}$ mice display decreased hepatic triglycerides on Surwit HFD without significant changes in de novo lipogenesis or lipogenic gene expression.

As in the previous *ob/ob* experiments, we wanted to determine if the requirement for Akt2 in hepatic triglyceride accumulation resulting from Surwit HFD was cell-autonomous. Starting at approximately 5 weeks of age, we fed male *AFP;Akt2$^{lox/lox}$* mice Surwit HFD for one or 4 months and used chow-fed age-matched male mice as controls. During this period, there were no differences in the weight gained on Surwit HFD between *Akt2$^{lox/lox}$* mice and *AFP;Akt2$^{lox/lox}$* mice or in liver weight between any of the groups (Figure 3-5A, 3-5B, and 3-6A). *AFP;Akt2$^{lox/lox}$* mice did not differ from *Akt2$^{lox/lox}$* mice with regards to food intake, energy expenditure, or body composition (Figures 3-6B, 3-6C, and 3-6D). After one month on Surwit HFD, *Akt2$^{lox/lox}$* mice had significantly increased fed hepatic triglyceride levels compared to their chow-fed counterparts, an effect that was partially ameliorated by loss of hepatic Akt2 (Figure 3-5C). This difference could not be attributed to an effect of AFP Cre alone (Figure 3-8). The same held true after 4 months on Surwit HFD, as the 4-fold increase in fed hepatic triglycerides in *Akt2$^{lox/lox}$* mice was reduced by approximately 25% with loss of hepatic Akt2. Total long chain fatty acyl-CoA and linoleoyl-CoA (C18:2) were decreased in livers from mice on Surwit HFD, as the latter is an essential fatty acid and its abundance is relatively low in coconut oil, the major source of fat in the Surwit diet. However, there were no differences between mice having or lacking hepatic Akt2 (Figure 3-5D). While there were no differences in serum triglycerides, fed serum cholesterol was increased after 4 months and NEFA were increased after both one and 4 months on HFD in mice with or without Akt2 in the liver (Figure 3-7A to 3-7C and 3-7E to 3-7G).

While there was a significant increase in *de novo* lipogenesis in livers from mice on a Surwit HFD, this was not prevented by deletion of Akt2 (Figure 3-5E). Lipogenic

gene expression paralleled this finding, as there was no decrease in hepatic expression of *SREBP-1c* or its targets in *AFP;Akt2*$^{lox/lox}$ fed Surwit HFD for one month; in fact there was a slight increase in *SREBP1c, FAS, ACC* and *L-PK* expression (Figure 3-9). However, only *SCD1* showed a significant increase in livers from *Akt2*$^{lox/lox}$mice on Surwit HFD compared chow-fed animals. Additionally, there were no changes in the expression of *PGC-1*α*, CPT-1, MCAD,* or *Cox7a* in the *AFP:Akt2*$^{lox/lox}$ livers (Figure 3-9). Though fed and fasted serum ketones were similar at one month, fed levels were slightly elevated after 4 months in *AFP;Akt2*$^{lox/lox}$ mice compared with *Akt2*$^{lox/lox}$ mice on Surwit HFD (Figure 3-7D and 3-7H). Nonetheless, β-oxidation in Surwit HFD-fed mice did not appear to be significantly altered by loss of hepatic Akt2 as RER was unchanged (Figure 3-6C). As neither *de novo* lipogenesis nor fatty acid oxidation appeared to be changed in *AFP;Akt2*$^{lox/lox}$ mice on Surwit HFD, we wanted to determine if triglyceride secretion could be responsible for the reduction in hepatic triglyceride accumulation. However, triglyceride secretion from the liver did not appear to be altered in mice fed Surwit HFD for 4 months or lacking hepatic Akt2 as measured by serum triglyceride accumulation following P-407 injection (Figure 3-10).

Loss of hepatic Akt2 does not impair glucose tolerance or insulin sensitivity on Surwit HFD.

As described in Chapter 2, loss of hepatic Akt2 results in both hepatic and peripheral insulin resistance in lean mice but does not seem to further progress the diabetic phenotype of the *ob/ob* mouse (Figure 2-12). Thus, we wondered if loss of hepatic Akt2 in mice on Surwit HFD would have an effect on glucose tolerance and insulin resistance. Male mice were subjected to GTT after 4 months on Surwit HFD; age-matched chow-fed male mice were used as controls. Though mice on Surwit HFD

did not exhibit fasting hyperglycemia, they did have impaired glucose tolerance; loss of hepatic Akt2 did not have an effect (Figure 3-11A and 3-11B). Chow-fed *AFP;Akt2*$^{lox/lox}$ mice trended towards increased fasting insulin levels, and there was a trend for Surwit HFD insulin levels at fasting and 15 minutes post-glucose load to be increased above *Akt2*$^{lox/lox}$ chow levels; however, none of these differences were significant (Figure 3-11C). In order to measure insulin sensitivity, *Akt2*$^{lox/lox}$ and *AFP;Akt2*$^{lox/lox}$ mice were subjected to hyperinsulinemic euglycemic clamp after 4 months on Surwit HFD. There were no differences in GIR, HGP or Rd between the 2 sets of mice, indicating that loss of hepatic Akt2 does not lead to further insulin resistance in Surwit HFD-fed animals (Figure 3-11D).

Loss of hepatic Akt2 does not change downstream protein phosphorylation in insulin-resistant Surwit HFD-fed livers.

In order to gain insight into the pathways that could be mediating the decrease in hepatic triglycerides observed in *AFP;Akt2*$^{lox/lox}$ mice fed Surwit HFD, we wanted to determine if loss of Akt2 had significant effects on hepatic insulin signaling in HFD-fed mice by Western blots (Figure 3-12). As glucose and insulin levels did not differ between *Akt2*$^{lox/lox}$ and *AFP;Akt2*$^{lox/lox}$ after one month on a Surwit HFD, liver extracts were made from these animals under fed conditions. Unfortunately, insulin signaling was significantly impaired due to the insulin resistance caused by HFD-feeding, such that phosphorylation of Akt and its targets was significantly below stimulated conditions in *Akt2*$^{lox/lox}$ animals; moreover, loss of hepatic Akt2 did not reduce protein phosphorylation further (Figure 3-12).

AFP;Akt2$^{lox/lox}$ *mice display decreased hepatic steatosis with lard HFD-feeding.*

Given the differences in phenotype between mice deficient for leptin and those fed a Surwit HFD, we tested the generality of the requirement for Akt2 in hepatic steatosis by feeding male *AFP;Akt2*$^{lox/lox}$ mice another commonly used HFD, one enriched in fat from lard (60% kcal from fat) with a mixture of both starch and sucrose (20% kcal from carbohydrates) (for composition of lard HFD, see Table 6-4 in Materials and Methods). After one month on the lard HFD, there was an increase in hepatic triglycerides in *Akt2*$^{lox/lox}$ mice, which was ameliorated by loss of hepatic Akt2 (Figure 3-13A). However, this increase in hepatic triglyceride caused by lard HFD-feeding did not correlate with an increase in *de novo* lipogenesis; in fact, lipogenesis was significantly reduced in lard HFD-fed animals and loss of hepatic Akt2 did not reduce it further (Figure 3-13B). This differs dramatically from Surwit HFD-fed animals, which exhibited an increase in *de novo* lipogenesis after both one and 4 months on HFD (Figure 3-5E). However, in both HFDs, there was a lack of correlation between *de novo* lipogenesis and hepatic lipogenic gene expression. While there was an increase in lipogenesis but no change in gene expression during Surwit HFD, there was a significant increase in *SREBP-1c* expression in the livers of *Akt2*$^{lox/lox}$ mice after one month on lard HFD even though lipogenesis was actually decreased (Figure 3-13C). This increase was significantly reduced in *AFP;Akt2*$^{lox/lox}$ mice, though other lipogenic genes were not changed in lard HFD-fed animals. Nonetheless, these data again show clearly that hepatic Akt2 is required for hepatic lipid accumulation ensuing from HFD-feeding.

As *AFP;Akt2*$^{lox/lox}$ mice did not exhibit increased hepatic triglyceride accumulation after one month on lard HFD, we wanted to determine if acute excision of hepatic Akt2 could reverse existing triglyceride accumulation from lard HFD. Therefore we fed male *Akt2*$^{lox/lox}$ mice lard HFD for one month; one group of age-matched *Akt2*$^{lox/lox}$ mice were maintained on chow as a control. After one month, one group of lard HFD-fed mice

were sacrificed while the others were injected with either AAV-GFP or AAV-Cre and kept on lard HFD for another month; chow-fed mice were injected with AAV-GFP and all AAV-injected mice were sacrificed one month later. There was a significant increase in the body weight of mice on lard HFD after two versus one month or compared with chow-fed animals; there was no effect of loss of hepatic Akt2 (Figure 3-14A). Mice injected with AAV-GFP on lard HFD for 2 months had increased liver weight compared with those fed lard HFD for one month, though their liver weight was decreased compared with chow-fed control mice (Figure 3-14B). Mice injected with AAV-Cre had decreased liver weight compared to those injected with AAV-GFP after 2 months of lard HFD, but exhibited similar liver weights to mice after one month of lard HFD (Figure 3-14B). *Akt2*$^{lox/lox}$ mice with AAV-GFP had hepatic steatosis after 2 months on lard HFD compared with chow-fed mice, and there was an increase in triglyceride accumulation from one month to two months on the HFD (Figure 3-14C). *Akt2*$^{lox/lox}$ mice injected with AAV-Cre had significantly reduced hepatic triglycerides after 2 month on lard HFD, but had levels similar to those in mice after one month on lard HFD (Figure 3-14C). This indicated that acute loss of Akt2 could ameliorate hepatic triglyceride accumulation but could not completely prevent hepatic steatosis. Serum triglycerides did not vary, but serum cholesterol was increased in all mice fed lard HFD and was partially decreased with loss of hepatic Akt2 (Figure 3-14D and 3-14E).

Discussion

As leptin signaling itself can influence metabolism, we wanted to determine if the effect of Akt2 on lipid metabolism depended on the absence of leptin; therefore, we choose two DIO models to test the role of Akt2 in another insulin-resistant context. In animals fed a Surwit HFD, loss of hepatic Akt2 significantly decreased hepatic

triglyceride accumulation, though it did not result in a complete reversal as in *ob/ob* mice. Surprisingly, it appears that Akt2 is required for lipid accumulation on Surwit HFD through a completely different mechanism than in the *ob/ob* mice as the increase in lipogenesis on Surwit HFD was not attenuated by loss of hepatic Akt2 (Figure 3-5). However, unlike *ob/ob* mice, the increase in lipogenesis did not correspond to an increase in hepatic *SREBP1c* or lipogenic gene expression, with the exception of *SCD1*, suggesting that Surwit HFD induces an increase in lipogenesis that is independent of lipogenic gene expression (Figure 3-9). Furthermore, some gene expression, such as *SREBP1c, FAS, ACC*, and *L-PK* was actually increased in *AFP;Akt2*$^{lox/lox}$ compared with *Akt2*$^{lox/lox}$ mice on Surwit HFD, suggesting that the decrease in lipid accumulation due to loss of Akt2 stimulated a compensatory upregulation of lipogenic genes.

To confirm these findings in another HFD model, we fed mice a lard-based HFD, and once again found that loss of hepatic Akt2 significantly decreased hepatic triglyceride accumulation and that this did not correlate with changes in lipogenesis (Figure 3-13). However, unlike mice fed Surwit HFD, those fed lard HFD actually exhibited decreased *de novo* lipogenesis and loss of hepatic Akt2 did not decrease this further. Despite having decreased lipogenesis, *Akt2*$^{lox/lox}$ animals on lard HFD had increased hepatic *SREBP1c* expression that was reversed with loss of hepatic Akt2, though there were not significant changes in the expression of the other lipogenic genes that were measured (Figure 3-13).

A general question in the development of hepatic steatosis is why would a liver with existing triglyceride accumulation synthesize additional lipid (Tamura and Shimomura, 2005). For example, hyperinsulinemic obese humans have higher rates of *de novo* lipogenesis on HFD than normoinsulinemic lean individuals (Schwarz et al., 2003). Additionally, HFD-feeding in mice, where animals consume a relative surplus of

dietary lipids, has been reported to induce hepatic lipogenic gene expression and even lipogenesis (Buettner et al., 2006; Oosterveer et al., 2009). One report attributes increased hepatic fatty acid synthesis predominantly to chain elongation and desaturation of exogenous fatty acids rather than actual *de novo* synthesis, as palmitate (C16:0) synthesis was unchanged, but oleate (C18:1) synthesis was increased in C57BL/6J mice fed HFD (Oosterveer et al., 2009). Though *de novo* lipogenesis was not increased in these mice, hepatic expression of *SREBP1c, SCD1, FAS, ACC1,* and *GPAT* were all elevated. While we observed an increase in *SREBP1c* expression in our lard HFD-fed mice, we did not see an increase in any other lipogenic mRNAs, and actually saw a decrease in the synthesis of palmitate (Figure 3-13). Conversely, mice fed Surwit HFD did exhibit increased palmitate synthesis in the absence of lipogenic gene upregulation. It is unclear if this difference results from the differences in the source of fat of each of the diets (coconut oil vs lard) or if the increase in sucrose content of the Surwit HFD is influencing *de novo* lipogenesis independently of dietary fat. Nonetheless, as loss of hepatic Akt2 does ameliorate hepatic steatosis in both models of DIO and does not act through *de novo* synthesis of fatty acids, exogenous fatty acid elongation and desaturation are potential mechanisms through which Akt2 could function.

While it is not possible to completely rule out lipogenesis as a cause for decreased hepatic triglyceride accumulation on either HFD, it appears that Akt2 acts through another mechanism to regulate lipid metabolism in HFD-fed mice. Other possibilities through which loss of Akt2 could lead to decreased hepatic triglyceride levels include increased β-oxidation and increased triglyceride export. However, there were no changes in any of the hepatic oxidative genes measured between *Akt2*$^{lox/lox}$ and *AFP;Akt2*$^{lox/lox}$ mice on Surwit HFD (Figure 3-9). Fed serum ketones were slightly

increased in *AFP;Akt2*$^{lox/lox}$ versus *Akt2*$^{lox/lox}$ mice on Surwit HFD for 4 months, though this is unlikely to represent a significant increase in β-oxidation as RER was indistinguishable in these two groups (Figure 3-6C, 3-7D, and 3-7H). Similarly, triglyceride export did not appear to be changed in the absence of hepatic Akt2 as serum triglycerides were not different in fed or fasted conditions or during the P-407 assay (Figure 3-7A, 3-7E and 3-10).

Interestingly, acute loss of Akt2 in lard HFD-fed animals prevented some hepatic triglyceride accumulation but could not reverse existing hepatic steatosis as it did in *ob/ob* mice. Though this result shows that the requirement for Akt2 in DIO is not restricted to liver development, it is further evidence that Akt2 regulates different lipid metabolic processes in *ob/ob* and HFD livers. Acute loss of Akt2 did not completely ameliorate triglyceride accumulation after 2 months of lard HFD (Figure 3-14); one explanation for this finding is that hepatic Akt2 could be required for a lipid metabolic process that contributes to hepatic steatosis but is not the sole cause. Surwit HFD-induced hepatic steatosis appears to be only partial regulated by Akt2 as *AFP;Akt2*$^{lox/lox}$ mice after 4 months of Surwit HFD still had increased hepatic triglycerides over chow-fed animals (Figure 3-5), and this may also be the case for lard HFD. Alternatively, Akt2-permissive hepatic steatosis could be cumulative and not dynamically influenced by Akt2 once it has developed. Regardless, Akt2 is certainly required for the full development of hepatic steatosis that results from DIO, though it is unclear how Akt2 influences hepatic lipid metabolism in this model.

Interestingly, the phenotype of *Akt2*$^{-/-}$ mice on Surwit HFD varied greatly from that of *AFP;Akt2*$^{lox/lox}$ mice on HFD, illustrating the importance of Akt2 in extrahepatic tissues. *Akt2*$^{-/-}$ mice gained significantly less weight on Surwit HFD compared with their *Akt2*$^{+/+}$ counterparts, and this was predominately due to their failure to gain fat mass (Figure 3-

1). These mice also had a reduction in serum NEFA during fasting, likely a result of their reduced fat mass (Figure 3-3C). However, though they have reduced adiposity, *Akt2*$^{-/-}$ mice still have increased hepatic and peripheral insulin resistance compared with *Akt2*$^{+/+}$ mice, suggesting that the prevention of lipid accumulation does not improve insulin sensitivity in this model (Figure 3-4F). While GIR, basal HGP and Rd were similar in *Akt2*$^{-/-}$ mice on Surwit HFD and chow, clamped HGP was elevated in Surwit HFD-fed mice (Figure 3-4F). This indicates that the most profound effect after 6 weeks of HFD is on the liver of the *Akt2*$^{-/-}$ mouse and that most of the peripheral insulin resistance is likely due to loss of Akt2 iteself in muscle or adipose tissue. Though liver-specific *Akt2* null animals exhibited hepatic insulin resistance compared with their wildtype littermates on chow (Figure 2-13A), after 4 months on Surwit HFD, there were no differences (Figure 3-11D). It is unclear whether these differences resolved over time, could be due to strain differences or whether loss of hepatic Akt2 is not additive with the stress of DIO to insulin resistance. The latter is consistent with the Western blots of insulin signaling that show that DIO blunted insulin signaling, and that loss of hepatic Akt2 had a negligible effect on this already decreased state (Figure 3-12).

In light of similar insulin sensitivity in *Akt2*$^{lox/lox}$ and *AFP;Akt2*$^{lox/lox}$ mice on Surwit HFD, it is not surprising that these mice exhibited similar glucose tolerance after 4 months on HFD (Figure 3-11). Unexpectedly, *Akt2*$^{-/-}$ and *Akt2*$^{+/+}$ mice also exhibited similar glucose tolerance after 4 months, even though *Akt2*$^{-/-}$ mice were more insulin resistant and showed impaired glucose tolerance after one month on Surwit HFD compared with *Akt2*$^{+/+}$ animals (Figure 3-4). This maintenance of GTT by *Akt2*$^{-/-}$ mice appears to be the result of increased insulin secretion, as these mice exhibited much higher serum insulin levels during GTT: thus, this elevation was an appropriate compensation for their increased insulin resistance. However, serum insulin levels in

Akt2$^{-/-}$ mice on Surwit HFD continued to increase over time so that these mice actually over-compensated and had improved glucose tolerance over their *Akt2*$^{+/+}$ counterparts on HFD: this appears to be the result of greatly increased β-cell mass (see Addendum).

Chapter 3 Figures

Figure 3-1: *Akt2*$^{-/-}$ mice gain less weight and fat mass on Surwit HFD.

Male *Akt2*$^{+/+}$ and *Akt2*$^{-/-}$ littermates were started on Surwit HFD at approximately 5 weeks of age.

A. Body weights following start of HFD.

B. 24-hour food intake of mice after 4 months on Surwit HFD.

C. 24-hour respiratory exchange ratio (RER) of mice after 4 months on Surwit HFD.

D. Body composition of mice after 4 months on Surwit HFD.

All values are expressed as mean ± SEM. n=6; *$p<0.01$ by Student's t-test.

Figure 3-1

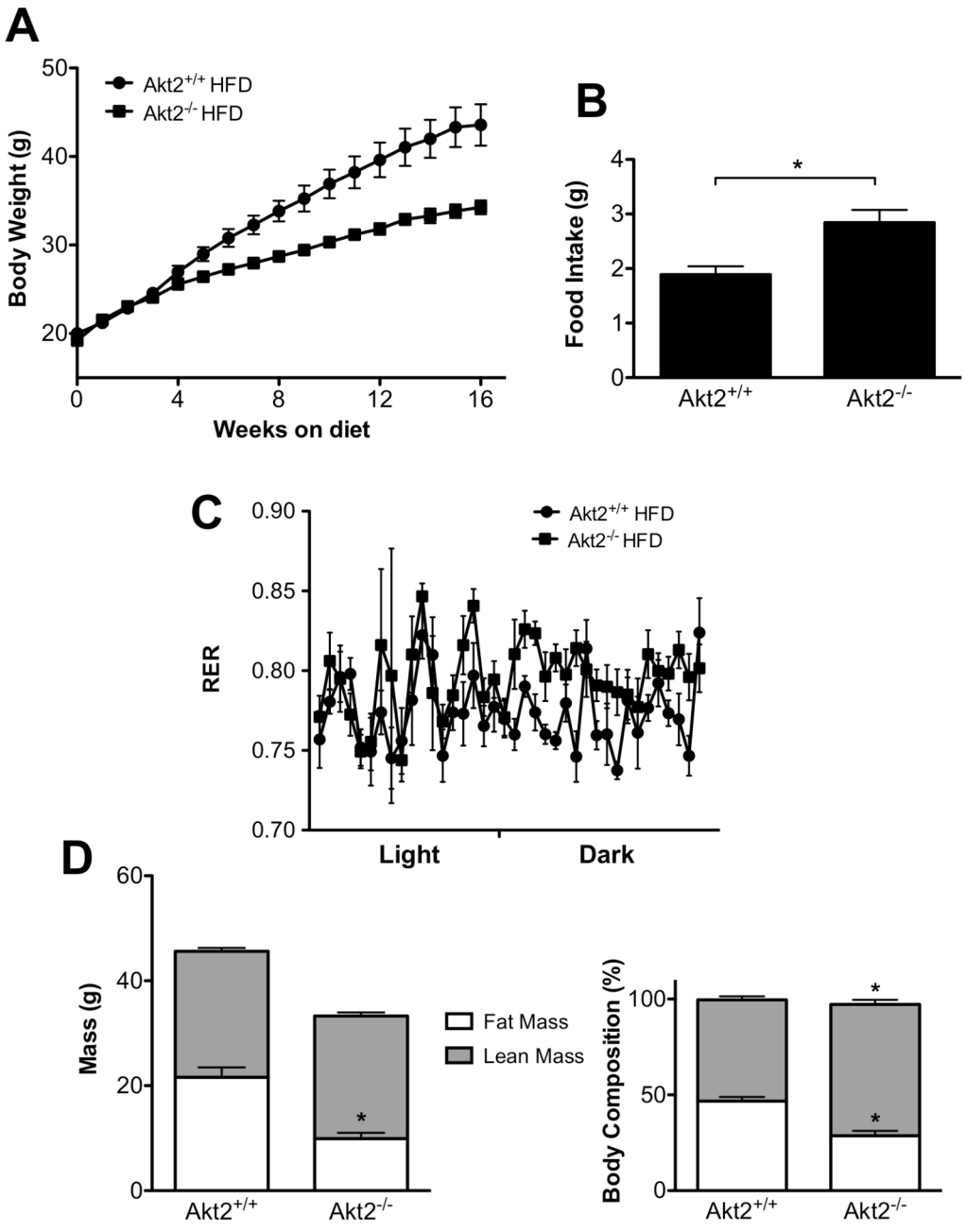
A
Akt2+/+ HFD
Akt2-/- HFD
Body Weight (g)
Weeks on diet
B
Food Intake (g)
Akt2+/+
Akt2-/-
C
RER
Light
Dark
D
Mass (g)
Fat Mass
Lean Mass
Body Composition (%)

Figure 3-2: *Akt2*$^{-/-}$ mice have decreased hepatic triglyceride levels after 4 months on Surwit HFD.

Male *Akt2*$^{+/+}$ and *Akt2*$^{-/-}$ littermates were started on Surwit HFD at approximately 5 weeks of age and sacrificed after either 1 or 4 months along with age-matched chow controls. Body weight (A), liver weight (B); hepatic triglyceride (TG) levels of fed (C) and overnight fasted (D) mice.

All values are expressed as mean ± SEM. n=5-9; *p<0.05 by one-way ANOVA using Newman-Keuls post-test.

Figure 3-2

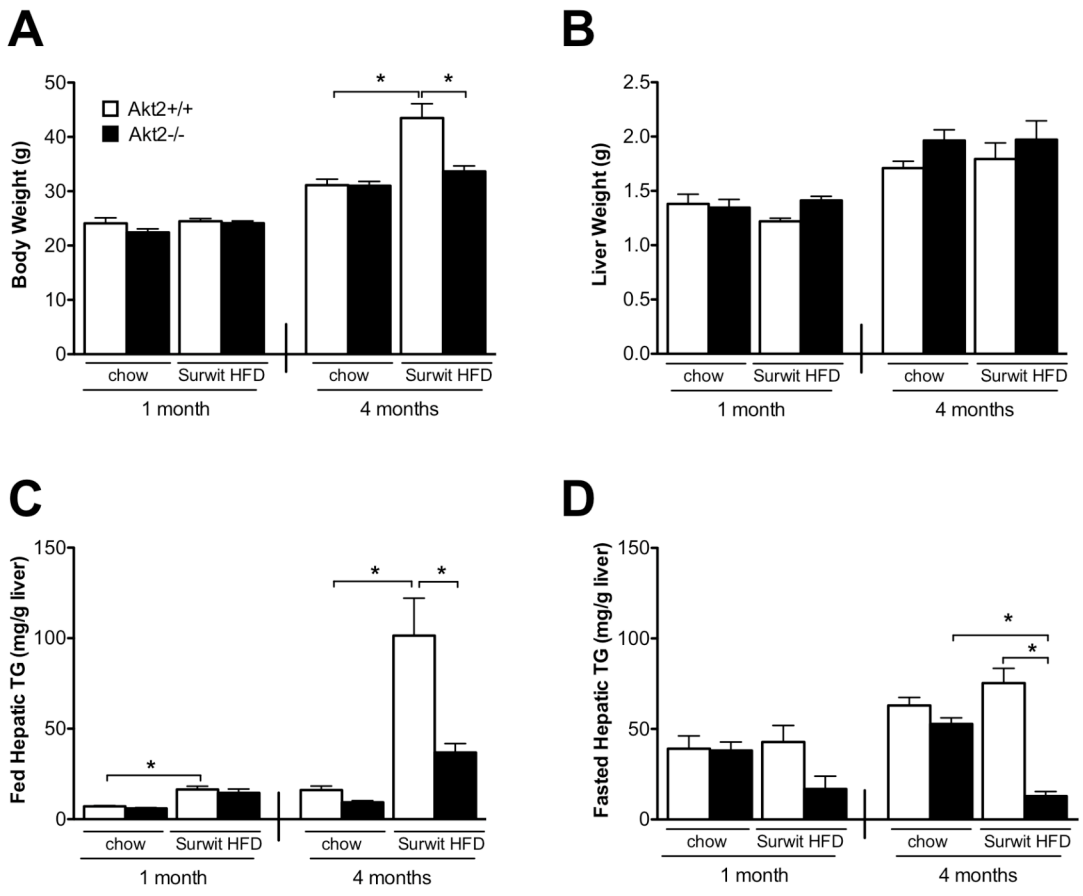
A
B
C
D
Akt2+/+
Akt2-/-
Body Weight (g)
Liver Weight (g)
Fed Hepatic TG (mg/g liver)
Fasted Hepatic TG (mg/g liver)
chow
Surwit HFD
1 month
4 months
*

Figure 3-3: Serum measurements of *Akt2*$^{-/-}$ mice on Surwit HFD.

Data from male *Akt2*$^{+/+}$ and *Akt2*$^{-/-}$ littermates started on Surwit HFD at approximately 5 weeks of age and sacrificed after 1 or 4 months on diet along with age-match chow controls.

Serum triglycerides (TG) (A), cholesterol (CH) (B), non-esterified fatty acids (NEFA) (C), and ketones (D) from fed (left) and overnight fasted (right) mice.

All values are expressed as mean ± SEM. n=5-9; *p<0.05 vs *Akt2*$^{+/+}$ chow and **p<0.05 vs *Akt2*$^{+/+}$ HFD by one-way ANOVA using Newman-Keuls post-test.

Figure 3-3

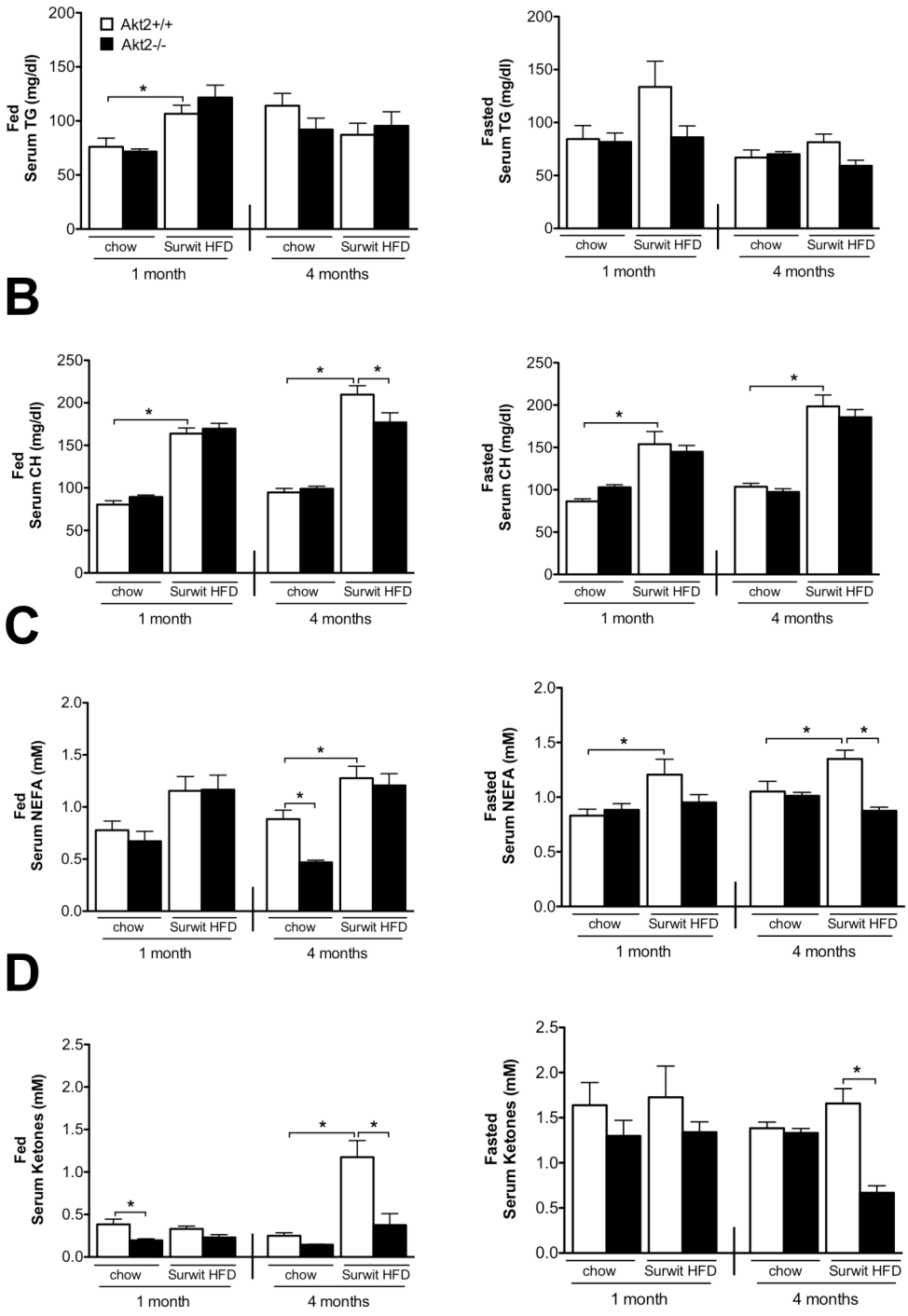
A
Akt2+/+
Akt2-/-
Fed
Serum TG (mg/dl)
Fasted
Serum TG (mg/dl)
B
Fed
Serum CH (mg/dl)
Fasted
Serum CH (mg/dl)
C
Fed
Serum NEFA (mM)
Fasted
Serum NEFA (mM)
D
Fed
Serum Ketones (mM)
Fasted
Serum Ketones (mM)
chow
Surwit HFD
1 month
4 months

Figure 3-4: *Akt2*$^{-/-}$ mice are insulin-resistant but maintain normal glucose tolerance by increasing insulin levels on Surwit HFD.

Data from male *Akt2*$^{+/+}$ and *Akt2*$^{-/-}$ littermates started on Surwit HFD or maintained on chow at approximately 5 weeks of age.

A-E. Fasted blood glucose levels (A) at start of glucose tolerance test (GTT) after 1 month (B) and 4 months (D) on Surwit HFD; insulin levels at the start and 15 minutes post glucose load (C and E). n=6-13.

F. Hyperinsulinemic euglycemic clamp of 5mU insulin/kg/min on 11-week old male mice started on Surwit HFD at 5 weeks of age along with age-match chow controls. Glucose infusion rate (GIR), basal and clamped hepatic glucose production (HGP) and rate of disposal (Rd) shown. n=4-5.

All values are expressed as mean ± SEM; *$p<0.05$ by one-way ANOVA using Newman-Keuls post-test.

Figure 3-4

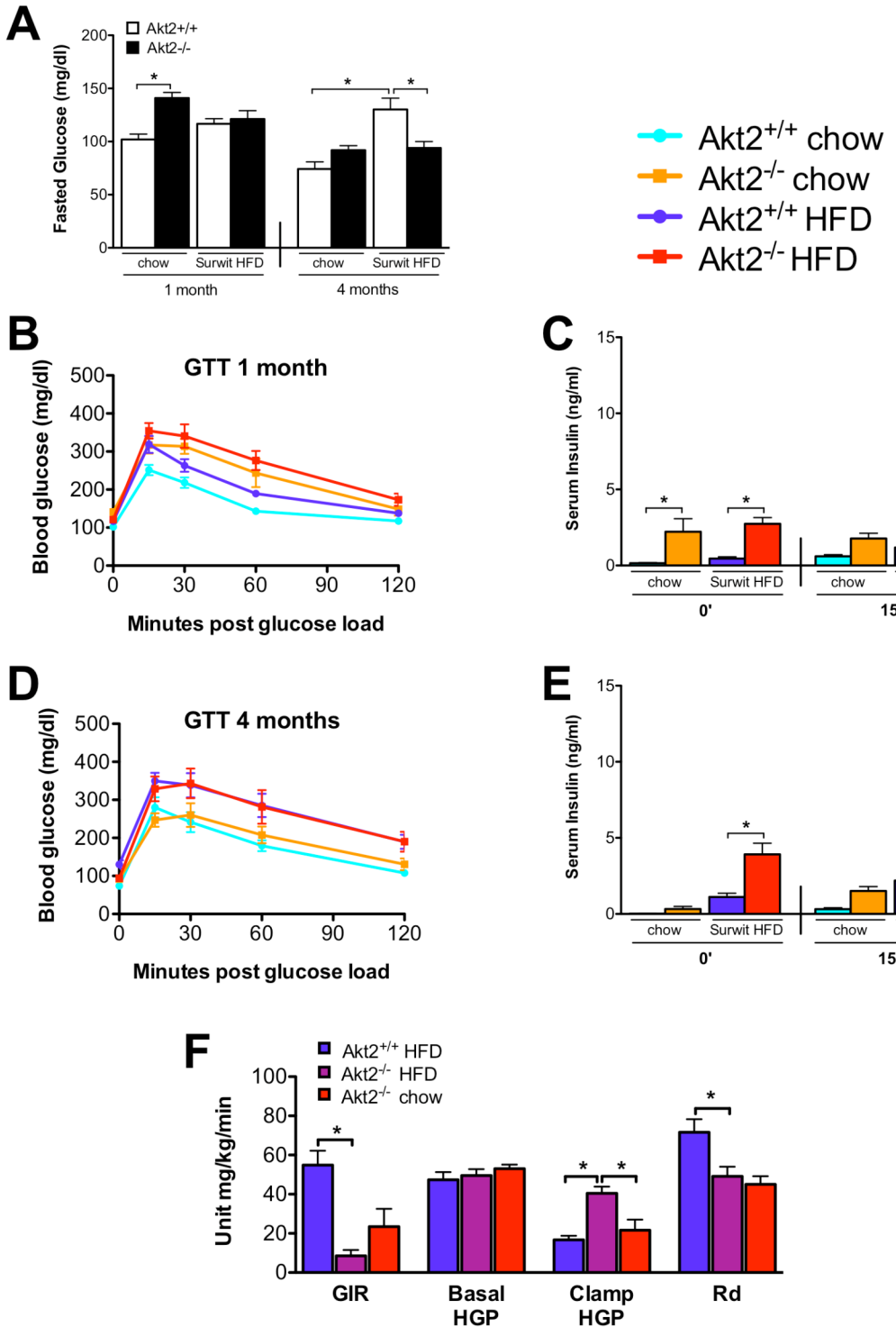
A
Akt2+/+
Akt2-/-
Fasted Glucose (mg/dl)
200
150
100
50
0
chow
Surwit HFD
chow
Surwit HFD
1 month
4 months
Akt2+/+ chow
Akt2-/- chow
Akt2+/+ HFD
Akt2-/- HFD
B
GTT 1 month
Blood glucose (mg/dl)
500
400
300
200
100
0
0
30
60
90
120
Minutes post glucose load
C
Serum Insulin (ng/ml)
15
10
5
0
chow
Surwit HFD
chow
Surwit HFD
0'
15'
D
GTT 4 months
Blood glucose (mg/dl)
Minutes post glucose load
E
Serum Insulin (ng/ml)
F
Akt2+/+ HFD
Akt2-/- HFD
Akt2-/- chow
Unit mg/kg/min
100
80
60
40
20
0
GIR
Basal HGP
Clamp HGP
Rd

Figure 3-5: *AFP;Akt2*$^{lox/lox}$ mice on Surwit HFD have decreased hepatic triglyceride levels, but do not exhibit changes in *de novo* lipogenesis.

Male mice were started on Surwit HFD at approximately 5 weeks of age and sacrificed after either 1 or 4 months along with age-matched chow controls.

Body weight (A), liver weight (B); hepatic triglyceride (TG) levels of fed mice (C). n=5-9; *p<0.05 by one-way ANOVA using Newman-Keuls post-test.

D. Hepatic long-chain fatty acyl CoA (LLCoA) concentrations from overnight fasted male mice after 1 month on Surwit HFD. n=4. *p<0.05 vs *Akt2*$^{lox/lox}$ chow by two-way ANOVA using Bonferroni post-test.

E. *De novo* lipogenesis: Male mice after 1 or 4 months on Surwit HFD or maintained on normal chow were injected with D_2O after a 5 hour fast, sacrificed after 3 hours, and liver was removed and analyzed for palmitate by GC/MS. n=5; *p<0.05 by one-way ANOVA using Newman-Keuls post-test.

All values are expressed as mean ± SEM.

Figure 3-5

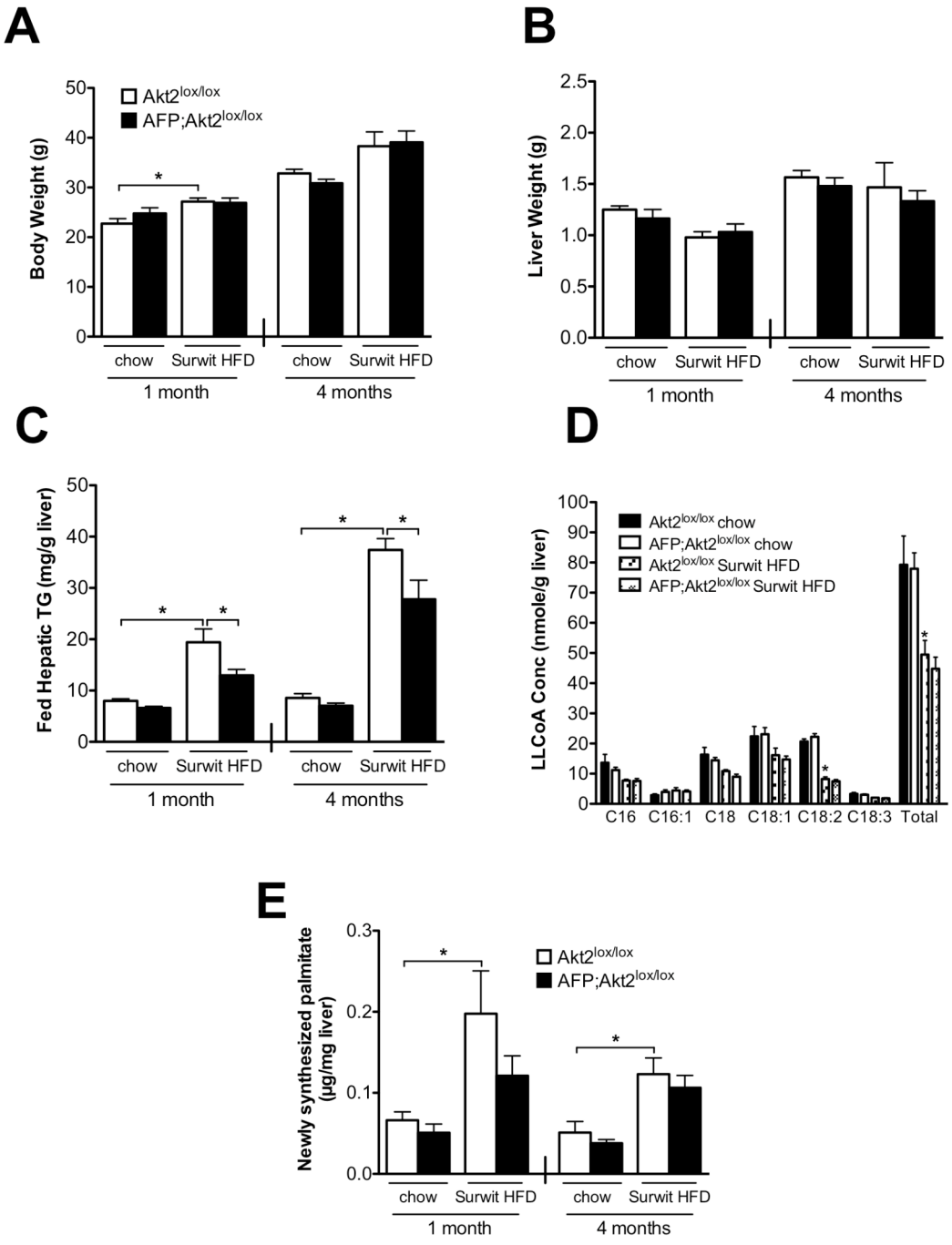
A
Akt2lox/lox
AFP;Akt2lox/lox
Body Weight (g)
chow
Surwit HFD
chow
Surwit HFD
1 month
4 months
B
Liver Weight (g)
chow
Surwit HFD
chow
Surwit HFD
1 month
4 months
C
Fed Hepatic TG (mg/g liver)
chow
Surwit HFD
chow
Surwit HFD
1 month
4 months
D
Akt2lox/lox chow
AFP;Akt2lox/lox chow
Akt2lox/lox Surwit HFD
AFP;Akt2lox/lox Surwit HFD
LLCoA Conc (nmole/g liver)
C16
C16:1
C18
C18:1
C18:2
C18:3
Total
E
Newly synthesized palmitate (µg/mg liver)
Akt2lox/lox
AFP;Akt2lox/lox
chow
Surwit HFD
chow
Surwit HFD
1 month
4 months

Figure 3-6: *AFP;Akt2*$^{lox/lox}$ mice on Surwit HFD have normal body weight, body composition and energy expenditure.

Male mice were started on Surwit HFD at approximately 5 weeks of age.

A. Body weights following start of HFD. n=7-11.

B. 24-hour food intake of mice after 4 months on Surwit HFD. n=6.

C. 24-hour respiratory exchange ratio (RER) of mice after 4 months on Surwit HFD. n=6.

D. Body composition of mice after 4 months on Surwit HFD. n=6.

All values are expressed as mean ± SEM; no points are significantly different to any others ($p<0.05$ by one-way ANOVA using Newman-Keuls post-test).

Figure 3-6

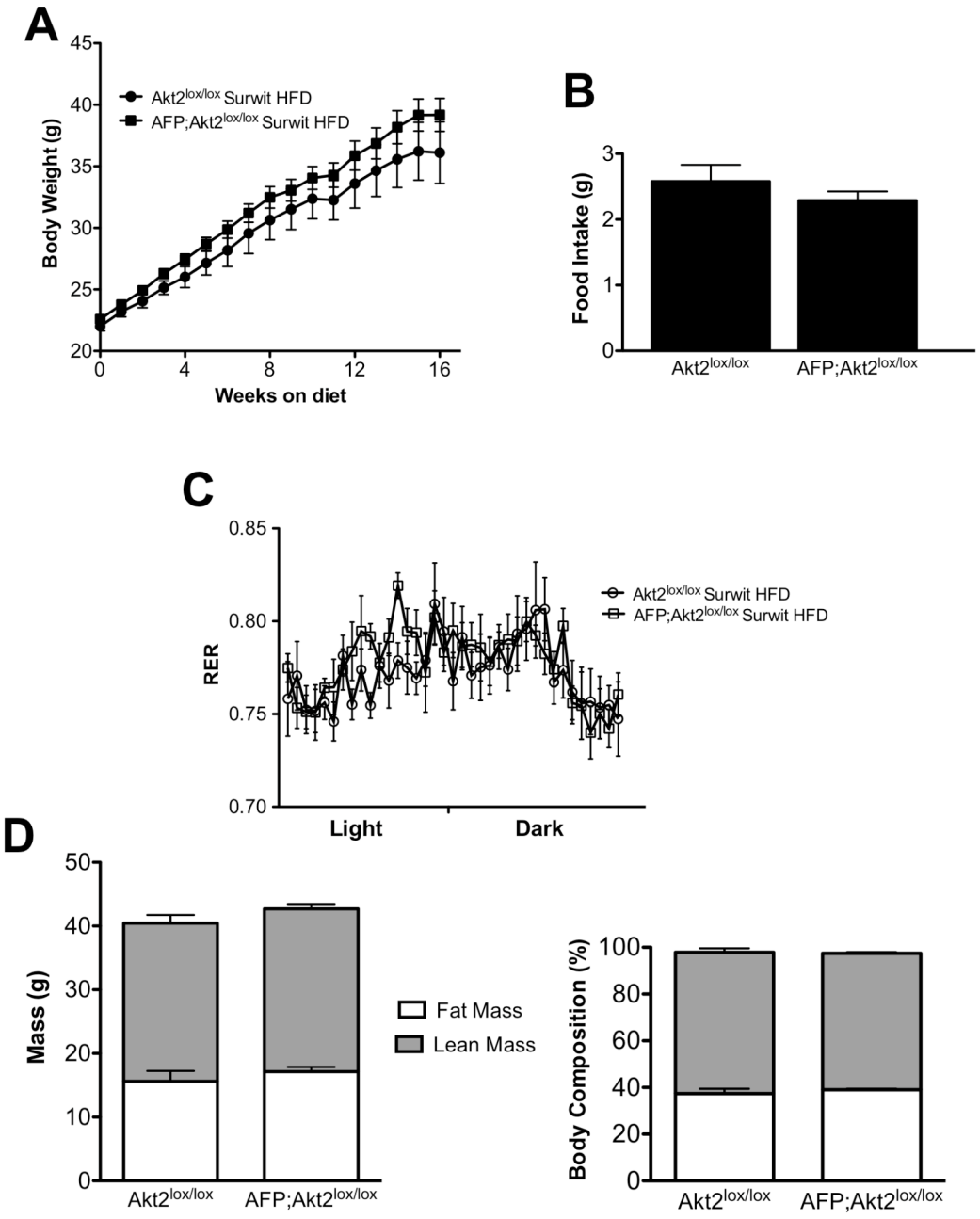
A
Body Weight (g)
Weeks on diet
Akt2lox/lox Surwit HFD
AFP;Akt2lox/lox Surwit HFD
B
Food Intake (g)
Akt2lox/lox
AFP;Akt2lox/lox
C
RER
Light
Dark
Akt2lox/lox Surwit HFD
AFP;Akt2lox/lox Surwit HFD
D
Mass (g)
Fat Mass
Lean Mass
Akt2lox/lox
AFP;Akt2lox/lox
Body Composition (%)
Akt2lox/lox
AFP;Akt2lox/lox

Figure 3-7: Serum measurements of *AFP;Akt2*$^{lox/lox}$ mice on Surwit HFD.

A-D. Data from male mice started on Surwit HFD at approximately 5 weeks of age and sacrificed after 1 or 4 months on diet along with age-match chow controls under fed conditions. Serum triglycerides (TG) (A), cholesterol (CH) (B), non-esterified fatty acids (NEFA) (C), and ketones (D).

E-H. Data from male mice started on Surwit HFD at approximately 5 weeks of age and sacrificed after 1 month on diet along with age-match chow controls after an overnight fast. Serum triglycerides (E), cholesterol (F), NEFA (G), and ketones (H).

All values are expressed as mean ± SEM. n=4-9; *p<0.05 vs *Akt2*$^{lox/lox}$ chow and **p<0.05 vs *Akt2*$^{lox/lox}$ HFD by one-way ANOVA using Newman-Keuls post-test.

Figure 3-7

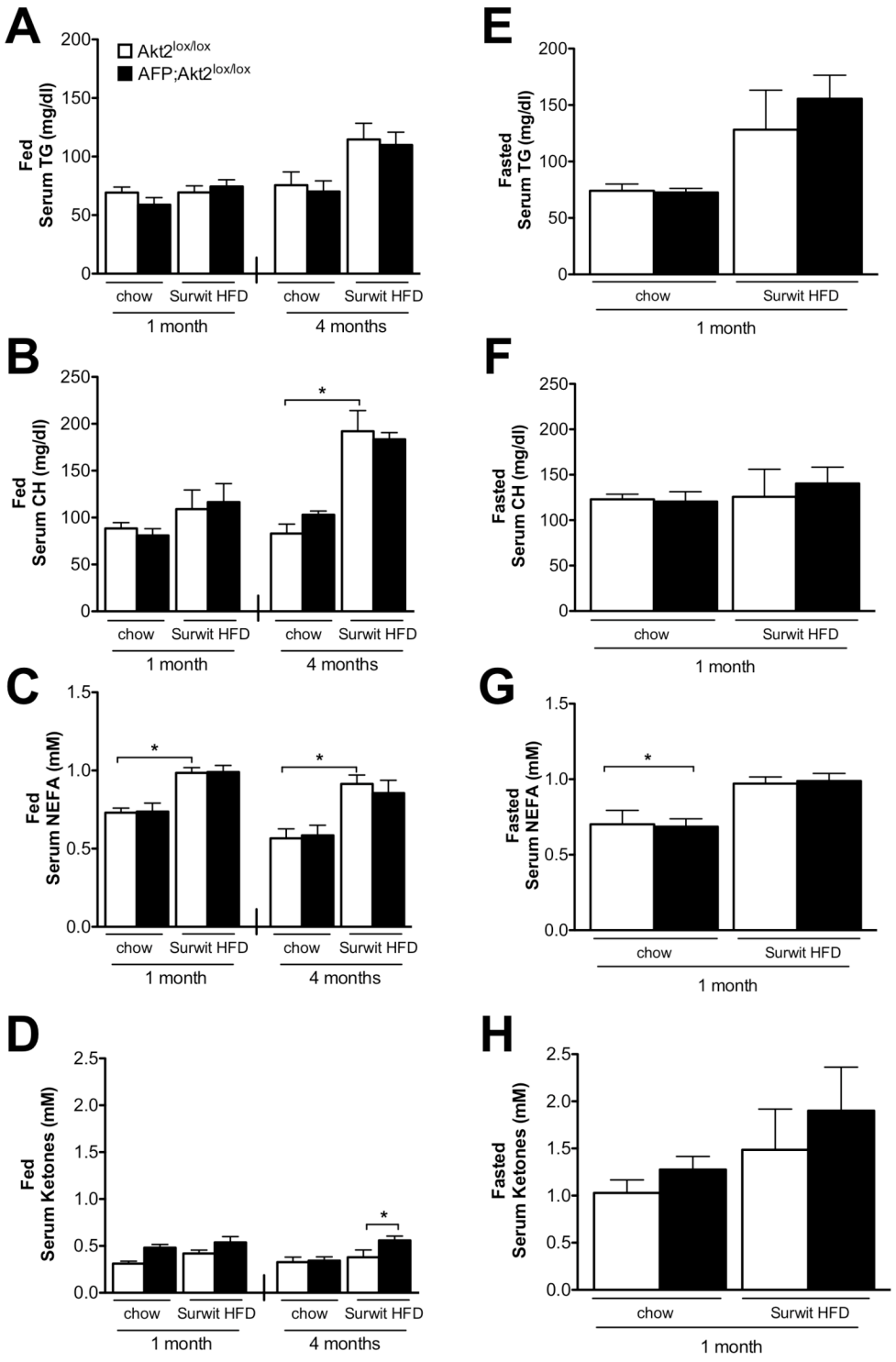
A
Akt2lox/lox
AFP;Akt2lox/lox
Fed
Serum TG (mg/dl)
200
150
100
50
0
chow
Surwit HFD
chow
Surwit HFD
1 month
4 months
B
Fed
Serum CH (mg/dl)
250
200
150
100
50
0
*
chow
Surwit HFD
chow
Surwit HFD
1 month
4 months
C
Fed
Serum NEFA (mM)
1.5
1.0
0.5
0.0
*
*
chow
Surwit HFD
chow
Surwit HFD
1 month
4 months
D
Fed
Serum Ketones (mM)
2.5
2.0
1.5
1.0
0.5
0.0
*
chow
Surwit HFD
chow
Surwit HFD
1 month
4 months
E
Fasted
Serum TG (mg/dl)
200
150
100
50
0
chow
Surwit HFD
1 month
F
Fasted
Serum CH (mg/dl)
250
200
150
100
50
0
chow
Surwit HFD
1 month
G
Fasted
Serum NEFA (mM)
1.5
1.0
0.5
0.0
*
chow
Surwit HFD
1 month
H
Fasted
Serum Ketones (mM)
2.5
2.0
1.5
1.0
0.5
0.0
chow
Surwit HFD
1 month

Figure 3-8: AFP Cre alone does not affect body weight, liver weight, hepatic triglycerides or serum measurements in mice fed Surwit HFD for one month.

Data from male mice started on Surwit HFD at approximately 5 weeks of age and sacrificed after one month on diet along with age-match chow controls under fed conditions. Body weight (A) and liver weight (B), hepatic triglycerides (TG) (C), serum triglycerides (D), serum cholesterol (CH) (E), serum non-esterified fatty acids (NEFA) (F), and serum ketones (G).

All values are expressed as mean ± SEM. n=3-5; *$p<0.05$ for both genotypes on chow vs both genotypes on Surwit HFD by one-way ANOVA using Newman-Keuls post-test. No values *Akt2*$^{+/+}$ vs AFP;Akt2$^{+/+}$ on a given diet are significantly different ($p<0.05$ by one-way ANOVA using Newman-Keuls post-test).

Figure 3-8

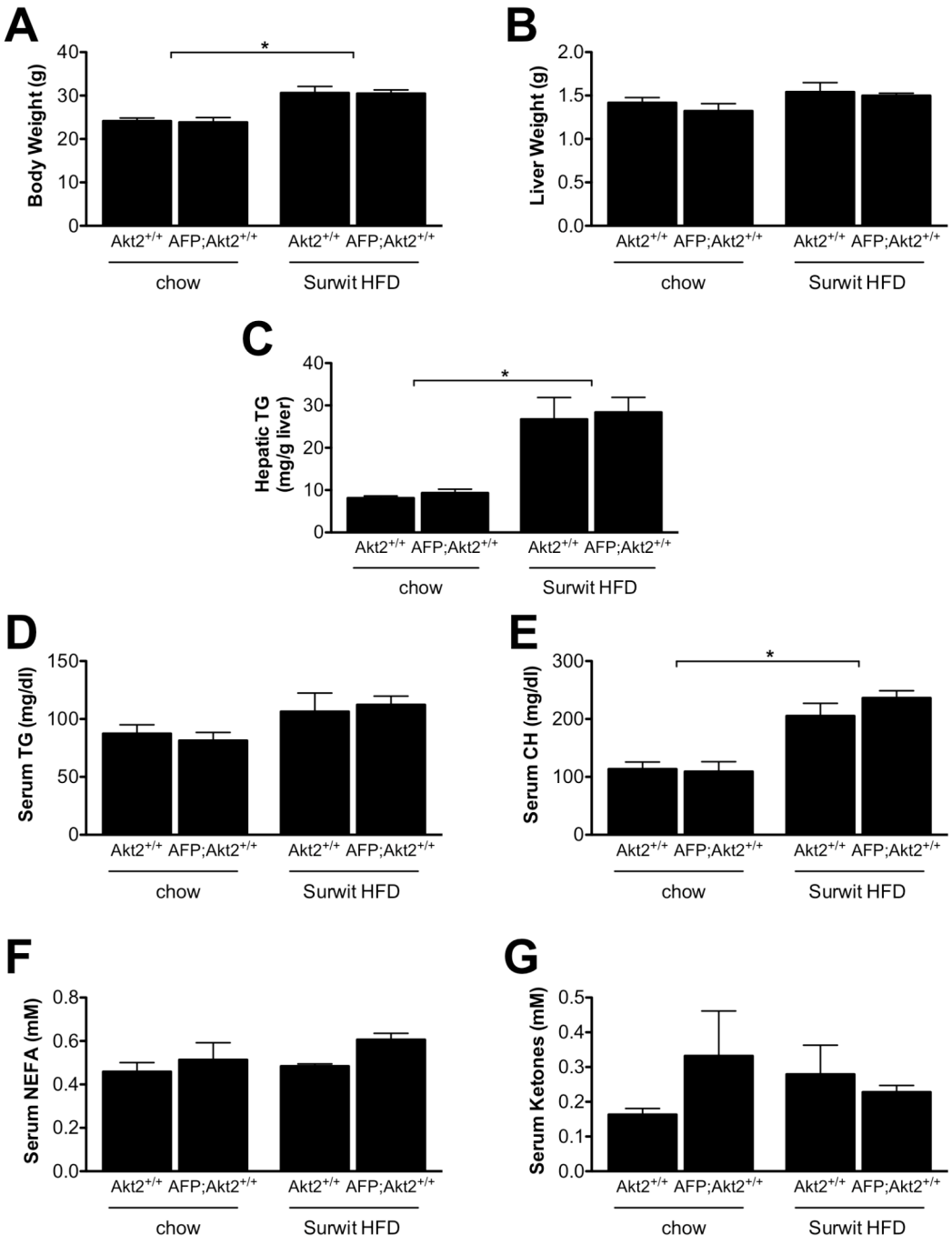
A
Body Weight (g)
40
30
20
10
0
*
Akt2+/+ AFP;Akt2+/+ Akt2+/+ AFP;Akt2+/+
chow
Surwit HFD
B
Liver Weight (g)
2.0
1.5
1.0
0.5
0.0
Akt2+/+ AFP;Akt2+/+ Akt2+/+ AFP;Akt2+/+
chow
Surwit HFD
C
Hepatic TG (mg/g liver)
40
30
20
10
0
*
Akt2+/+ AFP;Akt2+/+ Akt2+/+ AFP;Akt2+/+
chow
Surwit HFD
D
Serum TG (mg/dl)
150
100
50
0
Akt2+/+ AFP;Akt2+/+ Akt2+/+ AFP;Akt2+/+
chow
Surwit HFD
E
Serum CH (mg/dl)
300
200
100
0
*
Akt2+/+ AFP;Akt2+/+ Akt2+/+ AFP;Akt2+/+
chow
Surwit HFD
F
Serum NEFA (mM)
0.8
0.6
0.4
0.2
0.0
Akt2+/+ AFP;Akt2+/+ Akt2+/+ AFP;Akt2+/+
chow
Surwit HFD
G
Serum Ketones (mM)
0.5
0.4
0.3
0.2
0.1
0.0
Akt2+/+ AFP;Akt2+/+ Akt2+/+ AFP;Akt2+/+
chow
Surwit HFD

Figure 3-9: Hepatic gene expression in *AFP;Akt2$^{lox/lox}$* mice on Surwit HFD.

Hepatic gene expression as measured by Real-Time PCR of male mice after 1 month on Surwit HFD along with age-matched chow-fed controls sacrificed under fed conditions. Data are presented as mRNA expression relative to that of TATA-binding protein and normalized to expression in *Akt2$^{lox/lox}$* chow-fed, which is set to 1.0 using the ddC_T method.

All values are expressed as mean ± SEM. n=6; *p<0.05 vs *Akt2$^{lox/lox}$* chow and **p<0.05 vs *Akt2$^{lox/lox}$* HFD by one-way ANOVA using Newman-Keuls post-test.

Abbreviations: sterol regulatory element binding protein-1c (*SREBP1c*), stearoyl-CoA desaturase-1 (*SCD1*), fatty acid synthase (*FAS*), acetyl-CoA carboxylase (*ACC*), ATP citrate lyase (*ACL)*, glycerol phosphate acyltransferase (*GPAT*), glucokinase (*GCK*), carbohydrate regulatory-element binding protein (*ChREBP*), pyruvate kinase, liver isoform (*L-PK*), peroxisome proliferator-activated receptor-γ (*PPARγ*), peroxisome proliferators-activated receptor-coactivator 1α (*PGC-1α*), carnitine palmitoyltransferase I (*CPT1*), medium-chain acetyl-CoA dehydrogenase (*MCAD*), and cytochrome c oxidase subunit 7a (*Cox7a*).

Figure 3-9

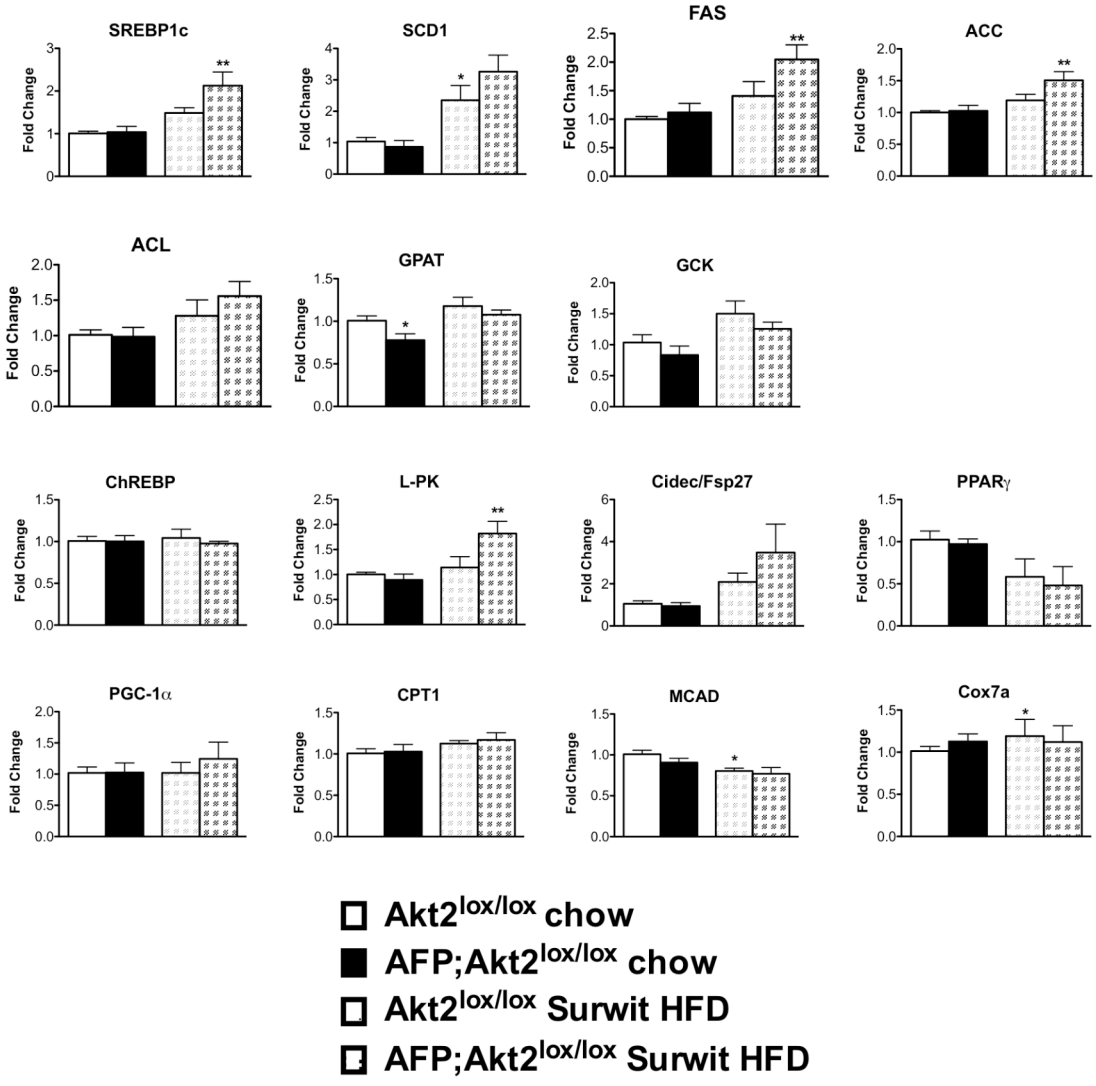
SREBP1c
SCD1
FAS
ACC
ACL
GPAT
GCK
ChREBP
L-PK
Cidec/Fsp27
PPARγ
PGC-1α
CPT1
MCAD
Cox7a
Fold Change
Akt2lox/lox chow
AFP;Akt2lox/lox chow
Akt2lox/lox Surwit HFD
AFP;Akt2lox/lox Surwit HFD

Figure 3-10: Loss of hepatic Akt2 does not dramatically alter triglyceride secretion on Surwit HFD.

Male mice were started on Surwit HFD at 5 weeks of age, and after 4 months on diet were intraperitoneally (IP) injected with 100µl 10% poloxamer 407 (P-407) per 10 grams body weight after a 5-hour fast and serum triglycerides were measured by tail bleed at 0, 1, 2, and 4 hours after injection.

Area under the curve calculated using Graphpad Prism.

All values are expressed as mean ± SEM. n=3-6; no points are significantly different to others ($p<0.05$ by one-way ANOVA using Newman-Keuls post-test).

Figure 3-10

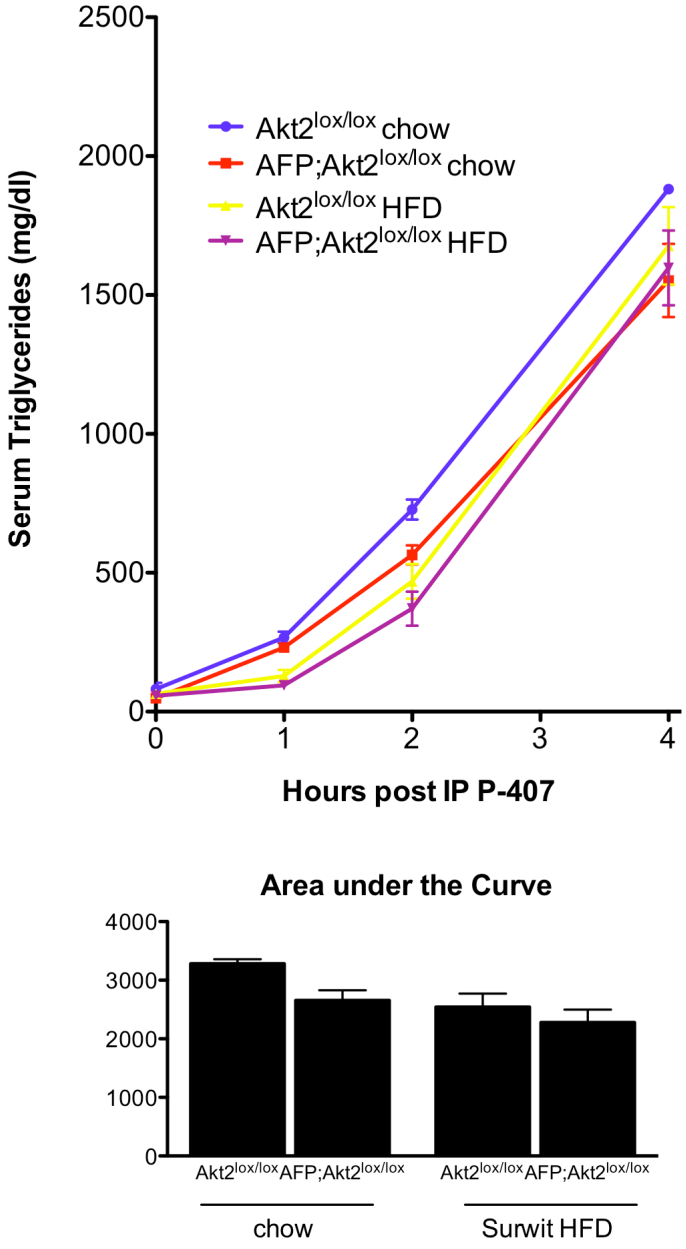
Serum Triglycerides (mg/dl)
2500
2000
1500
1000
500
0
Akt2lox/lox chow
AFP;Akt2lox/lox chow
Akt2lox/lox HFD
AFP;Akt2lox/lox HFD
0
1
2
3
4
Hours post IP P-407
Area under the Curve
4000
3000
2000
1000
0
Akt2lox/lox
AFP;Akt2lox/lox
Akt2lox/lox
AFP;Akt2lox/lox
chow
Surwit HFD

Figure 3-11: *AFP;Akt2*$^{lox/lox}$ mice have normal glucose tolerance and insulin sensitivity on Surwit HFD.

Data from male mice started on Surwit HFD or maintained on chow at approximately 5 weeks of age.

A-C. Fasted blood glucose levels (A) at start of glucose tolerance test (GTT) (B) after 1 month on Surwit HFD, and insulin levels at the start and 15 minutes post glucose load (C). n=5-6.

D. Hyperinsulinemic euglycemic clamp of 2.5mU insulin/kg/min on 22-week old male mice started on Surwit HFD at 5 weeks of age. Glucose infusion rate (GIR), basal and clamped hepatic glucose production (HGP) and rate of disposal (Rd) shown. n=4.

All values are expressed as mean ± SEM; no points are significantly different to any others ($p<0.05$ by one-way ANOVA using Newman-Keuls post-test).

Figure 3-11

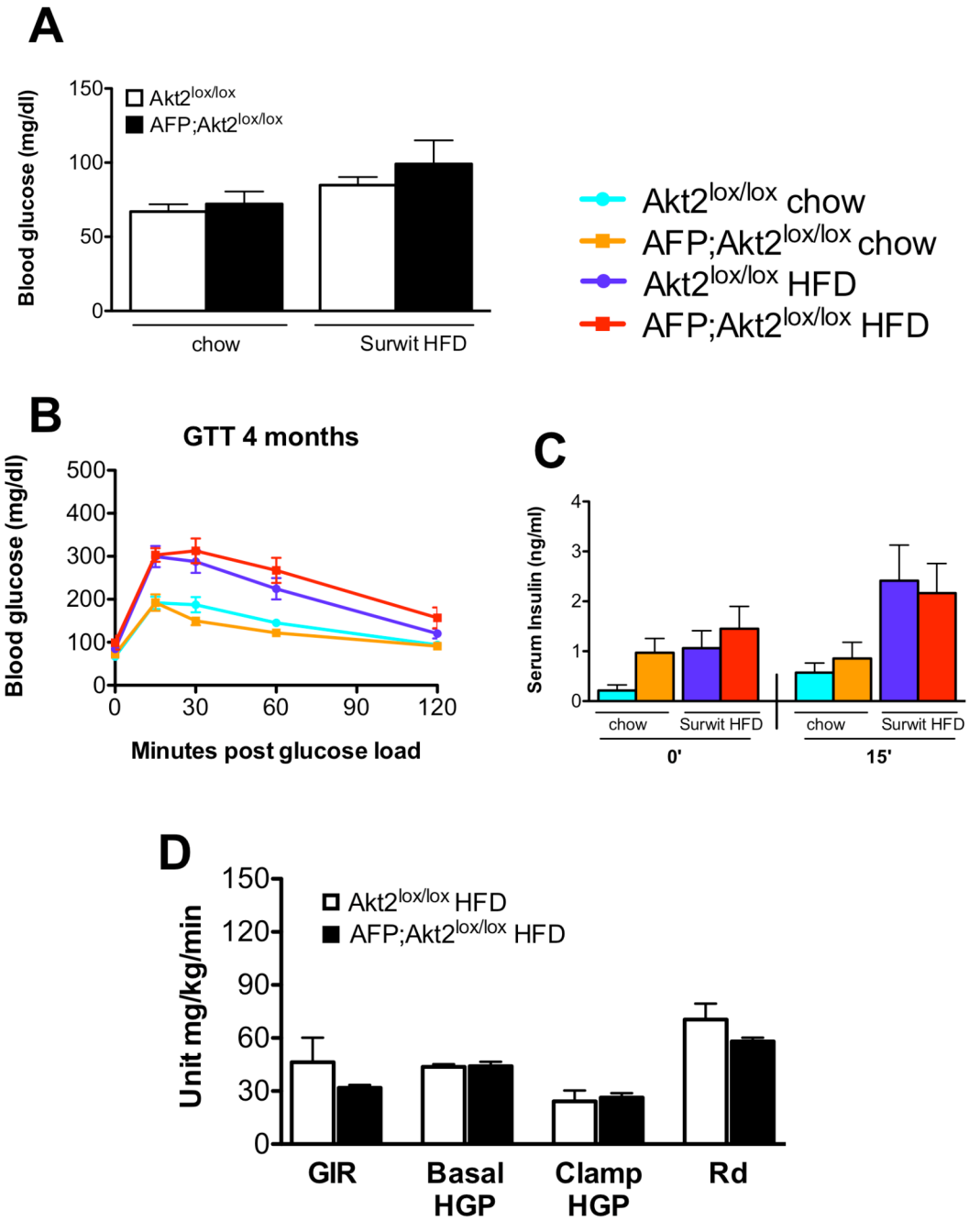
A
Blood glucose (mg/dl)
150
100
50
0
Akt2lox/lox
AFP;Akt2lox/lox
chow
Surwit HFD
Akt2lox/lox chow
AFP;Akt2lox/lox chow
Akt2lox/lox HFD
AFP;Akt2lox/lox HFD
B
GTT 4 months
Blood glucose (mg/dl)
500
400
300
200
100
0
0
30
60
90
120
Minutes post glucose load
C
Serum Insulin (ng/ml)
4
3
2
1
0
chow
Surwit HFD
chow
Surwit HFD
0'
15'
D
Unit mg/kg/min
150
120
90
60
30
0
Akt2lox/lox HFD
AFP;Akt2lox/lox HFD
GIR
Basal HGP
Clamp HGP
Rd

Figure 3-12: Hepatic insulin signaling is not blunted by loss of Akt2 in the liver of Surwit HFD-fed mice.

Western blot of phospho-Akt (p473 and p308) and downstream signaling targets in hepatic lysates from *Akt2*$^{lox/lox}$ and *AFP;Akt2*$^{lox/lox}$ mice on Surwit HFD for 1 month under fed conditions. *Akt2*$^{lox/lox}$ mice injected with saline or insulin as in Figure 2-15A are included for comparison. All samples were run on the same gel and imaged at the same exposure, but were cropped to exclude lanes in the middle, as denoted by the vertical line. Each lane represents an individual mouse. Loading controls are included when blots from different gels were used for phospho-protein and total protein, though the same protein extracts were used. The arrow indicates Akt2 as there is a slightly more mobile non-specific band.

Figure 3-12

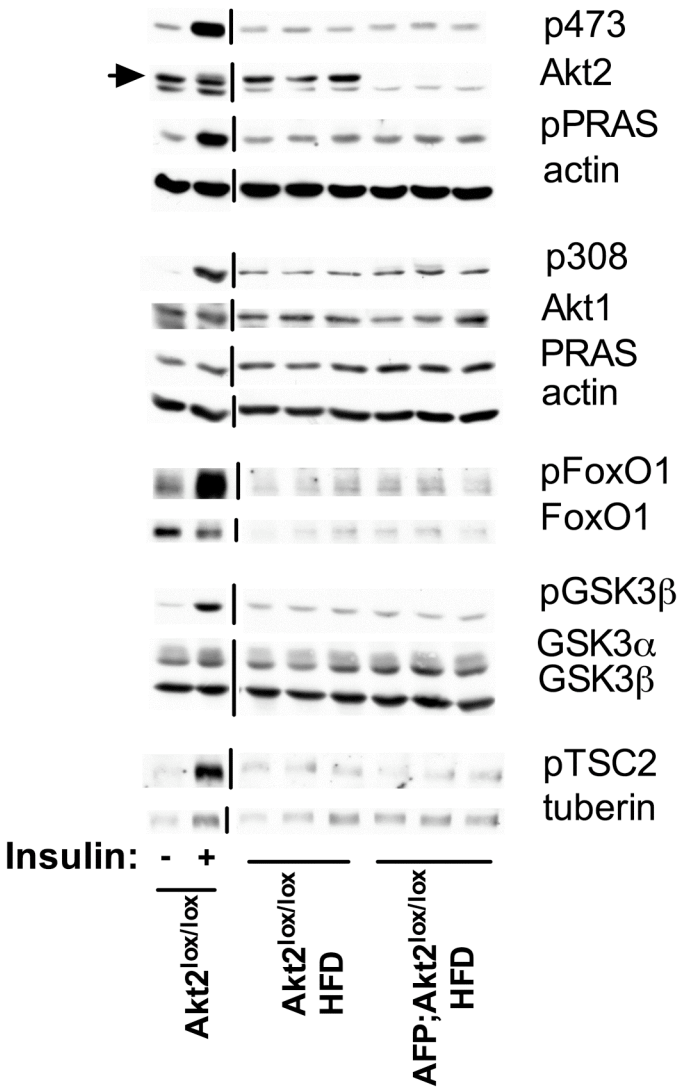
p473
Akt2
pPRAS
actin
p308
Akt1
PRAS
actin
pFoxO1
FoxO1
pGSK3β
GSK3α
GSK3β
pTSC2
tuberin
Insulin: - +
Akt2lox/lox
Akt2lox/lox HFD
AFP;Akt2lox/lox HFD

Figure 3-13: *AFP;Akt2*$^{lox/lox}$ mice on lard HFD have decreased hepatic triglyceride levels and *SREBP-1c* expression, but no alterations in *de novo* lipogenesis.

Male mice were started on HFD at approximately 6 weeks of age and sacrificed after 1 month on lard HFD under fed conditions along with age-matched chow-fed controls.

A. Hepatic triglycerides (TG).

B. *De novo* lipogenesis: Male mice after 1 month on lard HFD or maintained on normal chow were injected with D_2O after a 5 hour fast, sacrificed after 3 hours, and liver was removed and analyzed for palmitate by GC/MS. Data from chow-fed mice are the same as Figure 3-5E, as these experiments were run concurrently.

C. Hepatic gene expression as measured by Real-Time PCR. Data are presented as mRNA expression relative to that of TATA-binding protein and normalized to expression in *Akt2*$^{lox/lox}$ chow-fed, which is set to 1.0 using the ddC_T method.

All values are expressed as mean ± SEM. n=5-6; *p<0.05 vs *Akt2*$^{lox/lox}$ chow and **p<0.05 vs *Akt2*$^{lox/lox}$ HFD and ***p<0.05 for bracketed group by one-way ANOVA using Newman-Keuls post-test.

Figure 3-13

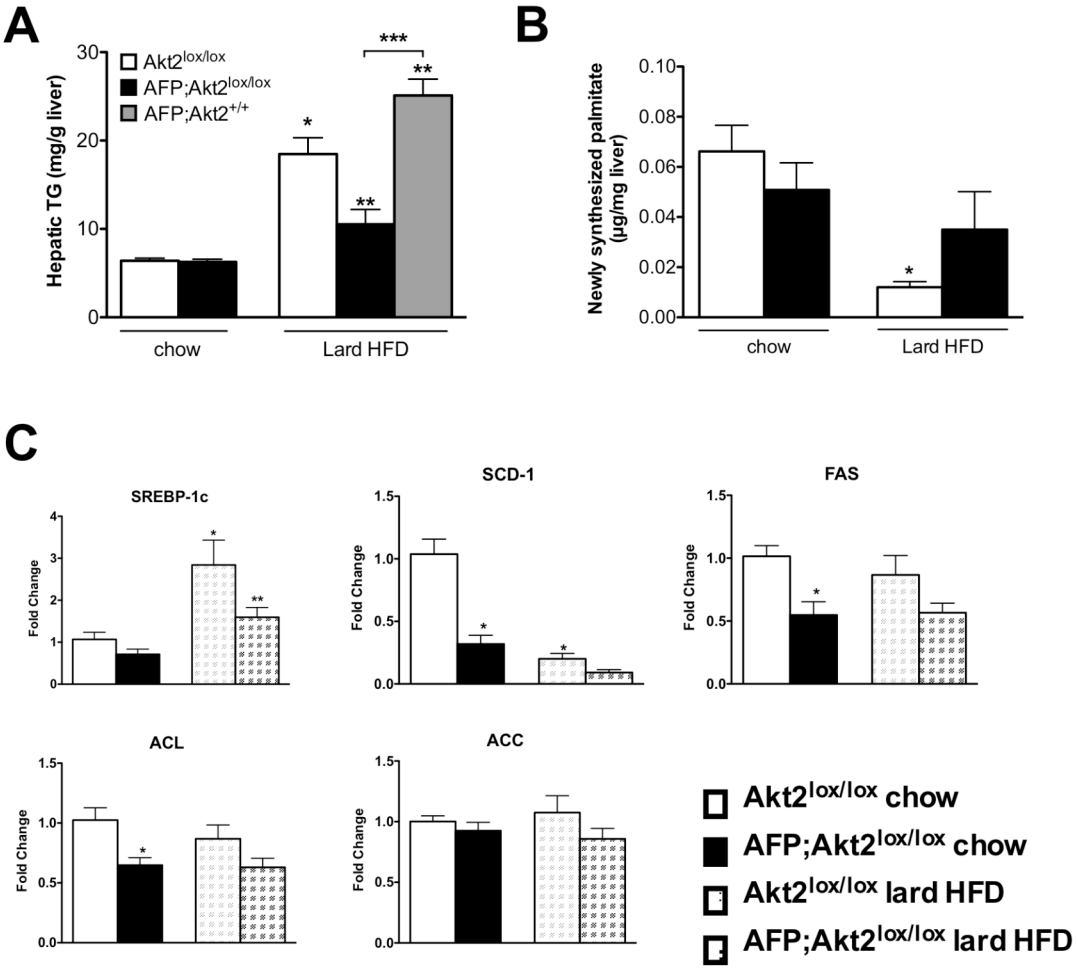
A
Hepatic TG (mg/g liver)
Akt2lox/lox
AFP;Akt2lox/lox
AFP;Akt2+/+
chow
Lard HFD
B
Newly synthesized palmitate (µg/mg liver)
chow
Lard HFD
C
SREBP-1c
SCD-1
FAS
ACL
ACC
Fold Change
Akt2lox/lox chow
AFP;Akt2lox/lox chow
Akt2lox/lox lard HFD
AFP;Akt2lox/lox lard HFD

Figure 3-14: Acute excision of hepatic Akt2 decreases hepatic triglyceride accumulation on lard HFD.

Male mice were started on lard HFD at approximately 5 weeks of age or maintained on chow. One group of mice was sacrificed after one month on lard HFD under fed conditions; all others were injected retro-orbitally with AAV-GFP or AAV-Cre. Chow-fed mice were injected with AAV-GFP; half of the remaining mice on lard HFD were injected with AAV-GFP and the other half with AAV-Cre. AAV-injected mice were then sacrificed one month later under fed conditions.

A-C. Body weight (A) and liver weight expressed as grams weight (B) and as a ratio to body weight (LW/BW) (C).

D. Hepatic triglycerides (TG) expressed as concentration per gram liver (left) and total (right).

E,F. Serum triglycerides (E) and cholesterol (CH) (F).

All values are expressed as mean ± SEM. n=4-5; all points are significantly different ($p<0.05$ by one-way ANOVA using Newman-Keuls post-test) to all others except for those marked non-significant (NS).

Figure 3-14

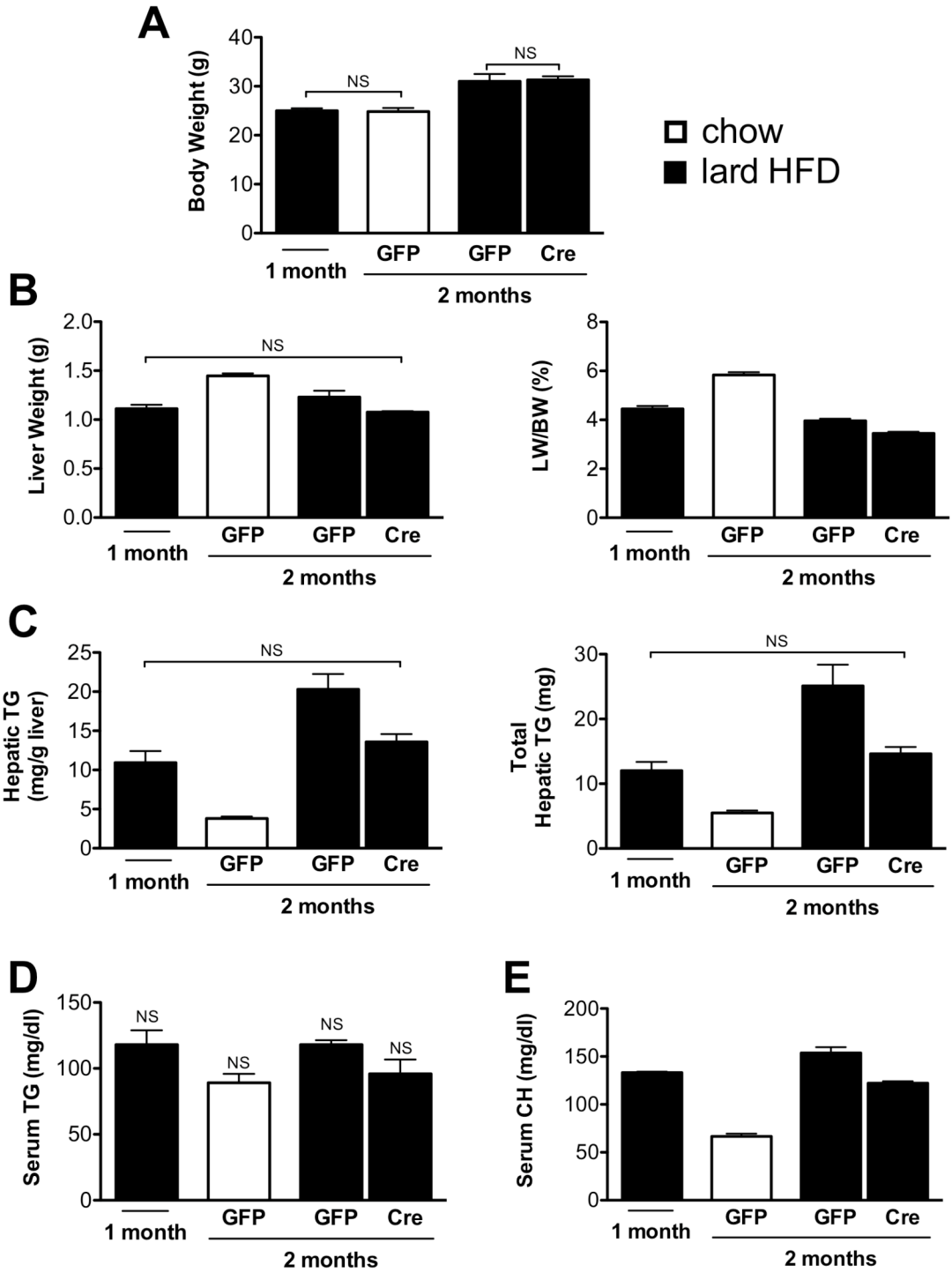
A
Body Weight (g)
40
30
20
10
0
NS
NS
chow
lard HFD
1 month
GFP
GFP
Cre
2 months
B
Liver Weight (g)
2.0
1.5
1.0
0.5
0.0
NS
LW/BW (%)
8
6
4
2
0
C
Hepatic TG (mg/g liver)
25
20
15
10
5
0
Total Hepatic TG (mg)
30
D
Serum TG (mg/dl)
150
100
50
E
Serum CH (mg/dl)
200

Chapter 4:

Akt2 is required for the induction of *de novo* lipogenesis during refeeding in lean animals

Introduction

We have shown that Akt2 is required for the development of hepatic steatosis in two different models of insulin-resistance, the *ob/ob* mouse and DIO. Additionally, Akt2 is indispensible for the elevated rate of *de novo* lipogenesis that occurs in the *ob/ob* mouse. However, the question still remains if Akt2 plays a role in normal lipid metabolism, specific the induction of *de novo* lipogenesis that occurs in lean animals without insulin resistance. In order to test the requirement for Akt2 in the regulation of lipogenesis in a lean liver, we wanted to establish a paradigm where lipogenesis would be stimulated acutely in an insulin-dependent manner. *De novo* lipogenesis is normally induced by the intake of food, when increased flux through glycolysis increases the amount of acetyl-CoA available for fatty acid synthesis. In addition, post-prandial hyperinsulinemia promotes lipogenesis, which peaks approximately 4 hours after meals in humans correlating with peak serum insulin concentrations (Timlin and Parks, 2005).

It has been long observed that high-carbohydrate diets (HCD) in particular lead to increased rates of *de novo* lipogenesis. Three to five days of high-carbohydrate consumption in humans results in up to a 10-fold increase in lipogenesis (Chong et al., 2008; Schwarz et al., 2003; Schwarz et al., 1995). Both lean and hyperinsulinemic obese individuals exhibit increased *de novo* palmitate synthesis following one to two weeks of diets high in simple carbohydrates and low in fat (Hudgins et al., 1996; Hudgins et al., 2000). Associated with this increase in lipogenesis is an increase in VLDL secretion and serum triglyceride levels. This is especially problematic for disease control in Type 2 diabetics, as long-term HCD consumption results in elevations of fasting plasma triglyceride, glucose and insulin levels in these patients (Garg et al., 1994). It has been proposed that HCDs also suppress hepatic fatty acid oxidation,

which, along with increased fatty acid synthesis, contributes to increased triglyceride secretion from the liver (Mittendorfer and Sidossis, 2001).

HCD consumption likely leads to increased rates of *de novo* lipogenesis at least in part through stimulation of gene expression: fasting followed by refeeding with a HCD leads to exponential increases in lipogenic gene expression in both humans and rodents (Horton et al., 1998a; Iritani et al., 1992). Lipogenic gene expression is coordinately upregulated in HCD-feeding by the combination of glucose through ChREBP and insulin through SREBP1c (Dentin et al., 2004; Koo et al., 2001) (and reviewed in Postic and Girard, 2008). *SREBP1c* mRNA and nuclear protein levels are very low during fasting in mice as are its lipogenic target genes; upon refeeding with a HCD, the expression of these genes rises dramatically and even increases 5- to 10- fold above fed levels (Horton et al., 1998a). In the absence of SREBP1c or ChREBP, the increase in lipogenic gene expression in response to fasting/refeeding is blunted (Iizuka et al., 2004; Liang et al., 2002; Shimano et al., 1999).

In this chapter, we show that hepatic Akt2 is required for the induction of *de novo* lipogenesis that occurs with HCD refeeding. This correlates with decreased expression of some lipogenic genes, but expression is not universally impaired in the absence of Akt2; specifically *SREBP1c* expression is not reduced by loss of hepatic Akt2. These studies also reveal additional roles for Akt2 in hepatic metabolism as liver-specific *Akt2* null mice have reduced liver weight and serum triglycerides following refeeding.

Results

HCD refeeding induces SREBP1c and lipogenic gene expression.

In order to first establish the validity of a fasting/refeeding protocol in normal mice, 8-week old C57BL/6J male mice were fasted overnight and sacrificed after various

points following refeeding with a HCD (for HCD composition, see Table 6-5 in Materials and Methods). Mice fasted overnight had low body weights, which were increased at the earliest time point (1.5 hours) following refeeding (Figure 4-1A). Upon refeeding, liver weight, both by mass and as expressed as a ratio to body weight, increased linearly over time (Figure 4-1B and 4-1C). Neither protein nor triglyceride content could account for this increase. Total protein content remained constant, whereas protein concentration per gram liver decreased with refeeding, presumably due to increasing liver weight over that time period (Figure 4-1D and 4-1E). However, hepatic triglycerides remained unchanged through the experiment, both in concentration and total (Figure 4-1F and 4-1G). The observed increase in liver weight was likely due at least partially to replenishing glycogen stores (see below).

Serum triglycerides did not significantly vary during the transition from fasting to feeding until 6 hours after refeeding, when levels spiked before returning to basal (Figure 4-2A). A similar sort of peak was observed for serum cholesterol, though this occurred much earlier, at just 1.5 hours after refeeding (Figure 4-2B). However, after this early peak, serum cholesterol was decreased after 12 hours of refeeding compared with fasting (Figure 4-2B). Both serum NEFA and ketones were elevated under fasting conditions, and decreased dramatically upon refeeding for the duration of the time points measured (Figure 4-2C and 4-2D).

SREBP1c expression was very low under fasting conditions, and increased dramatically upon refeeding as has been previously reported (Horton et al., 1998a) (Figure 4-3). Expression was maximal by 3 hours and persisted through 12 hours after refeeding. *FAS* expression also increased with refeeding but in a delayed pattern compared with *SREBP1c*, not increasing above fasting until after 6 hours, and not reaching maximal expression until 9 hours after refeeding (Figure 4-3). This lag in

expression was consistent with the time needed for additional round of transcription following SREBP1c activation and subsequent stimulation of its lipogenic targets, including *FAS.* However, mRNA levels of *SCD1*, another target gene of SREBP1c, did not change with refeeding, as has been previously reported; these reports, however, did not observe as robust an increase as with *FAS* (Horton et al., 1998a; Liang et al., 2002; Shimano et al., 1999). *GCK* mRNA also increased with refeeding, but its expression pattern was different from those of *SREBP1c* and *FAS*, reaching its highest level at 3 hours after refeeding and then decreasing over the rest of the time course (Figure 4-3).

AFP;Akt2$^{lox/lox}$ mice have smaller livers upon refeeding.

Having shown that our fasting/refeeding protocol was a robust stimulus of *SREBP1c* expression in wildtype mice, we wanted to subject the liver-specific *Akt2* null mice to this protocol. 8-week old mixed background *Akt2$^{lox/lox}$* and *AFP;Akt2$^{lox/lox}$* male littermates were used for all of the experiment described. Body weight did not differ during the refeeding time course in either group (Figure 4-4A). Blood glucose and serum insulin levels increased dramatically upon refeeding and were not affected by loss of hepatic Akt2 (Figure 4-4D and 4-4E). These levels remained elevated during the duration of the time course, indicating that the mice were likely feeding at various times, and not only acutely upon refeeding. *AFP;Akt2$^{lox/lox}$* mice were able to maintain normal glucose levels during refeeding despite exhibiting insulin resistance by hyperinsulinemic euglycemic clamp (Figure 2-12A), indicating that glucose metabolism in *AFP;Akt2$^{lox/lox}$* mice was not significantly impaired under fasting/refeeding conditions.

However, while *Akt2$^{lox/lox}$* mice had steadily increasing liver weight during refeeding, *AFP;Akt2$^{lox/lox}$* mice did not exhibit any change in liver weight (Figure 4-4B). The liver weight to body weight ratio was slightly elevated in *AFP;Akt2$^{lox/lox}$* mice 12

hours after refeeding, but it was significantly reduced compared with *Akt2*$^{lox/lox}$ mice (Figure 4-4C). As observed in the original C57BL/6J time course experiment, hepatic triglycerides did not change either in concentration or in total, while hepatic protein concentrations decreased with refeeding though total levels remained constant in *Akt2*$^{lox/lox}$ mice (Figure 4-1, 4-5A to 4-5D). Glycogen, and its associated water weight, is likely responsible for the increase in liver weight that occurs with refeeding, as glycogen, both concentration and total, increased from non-detectable levels at fasting over the course of refeeding, correlating with the increase in liver weight in *Akt2*$^{lox/lox}$ mice (Figure 4-5E and 4-5F). Total glycogen levels were decreased at 6 and 12 hours after refeeding in *AFP;Akt2*$^{lox/lox}$ mice compared with *Akt2*$^{lox/lox}$ mice, though glycogen concentrations were not significantly altered at these points (Figure 4-5E and 4-5F). Additionally, there was a trend towards decreased total levels of hepatic triglyceride and protein in *AFP;Akt2*$^{lox/lox}$ mice at 12 hours after refeeding, though their concentrations were not altered from those in *Akt2*$^{lox/lox}$ mice (Figure 4-5A to 4-5D).

Similar to those in the C57BL/6J time course experiment, serum triglycerides increased upon refeeding in *Akt2*$^{lox/lox}$ mice, though this occurred earlier at 1.5 hours after refeeding, before decreasing to a lower level at 12 hours (Figure 4-6A). This increase was not present in the absence of hepatic Akt2, as *AFP;Akt2*$^{lox/lox}$ mice exhibited fairly constant serum triglyceride levels during refeeding (Figure 4-6A). Serum cholesterol levels were not altered over time in either genotype (Figure 4-6B). Serum NEFA and ketones decreased similarly in both groups upon refeeding, though *AFP;Akt2*$^{lox/lox}$ mice exhibited a slight decrease in fasting NEFA levels compared with *Akt2*$^{lox/lox}$ mice (Figure 4-6C and 4-6D).

AFP;Akt2$^{lox/lox}$ mice have decreased de novo lipogenesis and reductions of some lipogenic gene expression during refeeding, without changes in SREBP1c expression.

We have shown that our fasting/refeeding protocol is a potent stimulus of *SREBP1c* and lipogenic gene expression (Figure 4-3); thus, it should also cause an increase in *de novo* lipogenesis. Indeed, *Akt2$^{lox/lox}$* mice refed HCD for 6 or 12 hours exhibited significantly elevated *de novo* lipogenesis compared with mice that were fasted (Figure 4-7A and 4-7B). While lipogenesis in *AFP;Akt2$^{lox/lox}$* mice was similar to that in *Akt2$^{lox/lox}$* mice under fasted conditions, it was significantly decreased upon 6 or 12 hours of refeeding (Figure 4-7A and 4-7B). Interestingly, refeeding did not stimulate an increase in lipogenesis in *AFP;Akt2$^{lox/lox}$* mice, as fasted and 6 hour refed levels were not significantly different (Figure 4-7A). AFP Cre alone did not affect lipogenesis as *AFP;Akt2$^{+/+}$* mice exhibited identical levels of lipogenesis to *Akt2$^{lox/lox}$* mice at 6 hours after refeeding (Figure 4-7A).

Consistent with our findings in C57BL/6J mice, *SREBP1c*, *FAS*, and *GCK* expression increased with refeeding, as did that of *ACL, ACC, GPAT*, in *Akt2$^{lox/lox}$* livers*;* loss of hepatic Akt2 resulted in the blunted expression of *FAS* and *ACL* (Figure 4-8). *GCK* mRNA peaked at 1.5 and 3 hours after refeeding and decreased at later time points in *Akt2$^{lox/lox}$* mice, and this peak was significantly decreased in *AFP;Akt2$^{lox/lox}$* mice, though levels at 6 and 12 hours were similar. However, *SREBP1c* mRNA increased normally in *AFP;Akt2$^{lox/lox}$* livers, as did *ACC* and *GPAT* mRNA (Figure 4-8). Expression of the ChREBP target, *L-PK*, was also normal in *AFP;Akt2$^{lox/lox}$* mice, increasing during refeeding similarly to *Akt2$^{lox/lox}$* mice. Expression of *G6Pase* was initially suppressed at 3 hours of refeeding, but then recovered at later time points; loss of hepatic Akt2 had no effect on this pattern of expression (Figure 4-8).

Discussion

In this chapter, we established a role for hepatic Akt2 in the control of normal *de novo* lipogenesis in lean animals. As the rate of lipogenesis is very low in lean animals under most conditions, we utilized a situation where lipogenesis would be maximally induced: fasting and refeeding with HCD. Overnight fasting following by HCD refeeding resulted in a profound increase in *SREBP1c* and other lipogenic gene expression (Figure 4-3 and 4-8). Paralleling this increase in lipogenic gene expression, animals exhibited an approximately 5-fold increase in *de novo* lipogenesis after 6 or 12 hours of HCD refeeding over that of fasted animals, similar to the increase that has been reported in humans with high carbohydrate consumption (Chong et al., 2008; Schwarz et al., 2003; Schwarz et al., 1995). Using this model, we showed that though *AFP;Akt2*$^{lox/lox}$ mice exhibited normal lipogenesis under fasting conditions, they lacked the induction upon refeeding (Figure 4-7). Correspondingly, lipogenesis levels at both 6 hours and 12 hours after refeeding were decreased in *AFP;Akt2*$^{lox/lox}$ mice compared with *Akt2*$^{lox/lox}$ mice. Thus, we have determined that Akt2 is required for the normal induction of *de novo* lipogenesis in response to high-carbohydrate feeding.

However, it is unclear how Akt2 actually influences lipogenesis in the fasted/refeed condition. HCD refeeding dramatically induced the expression of *SREBP1c* and other lipogenic genes; *FAS* mRNA in particular was increased 100-fold over fasted levels (Figure 4-3). The only exception was *SCD1*, though this gene as has been previously reported to be upregulated in response to HCD refeeding but to a lesser degree than other lipogenic genes (Horton et al., 1998a; Liang et al., 2002; Shimano et al., 1999). While fasted expression levels were similar in *Akt2*$^{lox/lox}$ and *AFP;Akt2*$^{lox/lox}$ mice, loss of hepatic Akt2 blunted the increase in some but not all mRNAs (Figure 4-8). Those genes whose upregulation was Akt2-dependent were *FAS*, *ACL* and *GCK*; those

that were Akt2-independent were *ACC*, *GPAT, L-PK*, and critically, *SREBP1c.* Though *SREBP1c* expression was decreased in *Lep*$^{ob/ob}$ *AFP;Akt2*$^{lox/lox}$ mice, *SREBP1c* upregulation in response to refeeding was unfettered by loss of hepatic Akt2. However, this does not exclude the possibility that Akt2 could be regulating SREBP1c through post-transcriptional regulation or enzymatic processing. However, not all SREBP1c target genes were affected in *AFP;Akt2*$^{lox/lox}$ mice; therefore, if Akt2 is acting solely through SREBP1c, either it can regulate the specificity of SREBP1c's targets or the expression of some genes can be maintained by other pathways. Additionally, *de novo* lipogenesis was increased at 6 hours in *Akt2*$^{lox/lox}$ mice though *FAS, ACC* and *ACL* expression was not significantly elevated above fasting until this point. Therefore, it is unclear whether expression of these genes truly drives the increased flux through lipogenesis during HCD refeeding, or whether the process is mostly substrate-driven. Accordingly, it is unclear whether the reduction in *FAS, ACL* and *GCK* expression in *AFP;Akt2*$^{lox/lox}$ mice is sufficient to lower lipogenesis in these mice or whether Akt2 has another effect, such as modulating enzymatic activity.

Importantly, we also show that though *AFP;Akt2*$^{lox/lox}$ mice are inherently defective in lipogenesis, this is not secondary to a decrease in glucose or insulin levels during refeeding (Figure 4-4D and 4-4E). While this would not be expected as *AFP;Akt2*$^{lox/lox}$ mice are insulin resistance by hyperinsulinemic euglycemic clamp (Figure 2-12A), it is essential to exclude this possibility. Unlike the insulin-resistant models previously used, this demonstrates that there is an impairment in lipid metabolism coinciding with normal glucose metabolism in *AFP;Akt2*$^{lox/lox}$ mice. However, though serum glucose levels were normal in *AFP;Akt2*$^{lox/lox}$ mice, it is possible that the amount available for utilization by the liver was not. The rate-limiting step for the entrance of glucose into the liver is its phosphorylation by *GCK*. *GCK* mRNA, unlike the other

lipogenic mRNAs measured, increased rapidly, peaking at 1.5 and 3 hours after refeeding (Figure 4-3 and 4-8). This occurred long before *SREBP1c* expression was maximal, likely so that the liver could take up increasing levels of glucose from the blood as it became available after refeeding. This peak was significantly reduced with the loss of hepatic Akt2, though later expression was maintained (Figure 4-8). However, it seems unlikely that this resulted in significantly altered glucose uptake into the liver, as glucose and glycogen concentrations were not altered, though total glycogen content was decreased at later time points (Figure 4-5 and not shown). Additionally, expression of *L-PK*, a transcriptional target of ChREBP, was not blunted with loss of hepatic Akt2, indicating at least that the stimulation of ChREBP activity by glucose was not decreased.

Interestingly, *AFP;Akt2*$^{lox/lox}$ mice failed to exhibit the peak in serum triglycerides that *Akt2*$^{lox/lox}$ mice did (Figure 4-6A). This peak occurred at 6 hours after refeeding in C57BL/6J mice and after 1.5 hours in mixed background *Akt2*$^{lox/lox}$ mice and disappeared by 12 hours in both groups (Figure 4-2A and 4-6A). It is unknown if this difference was due to variability in experimental groups or strain differences. Both *Akt2*$^{lox/lox}$ and *AFP;Akt2*$^{lox/lox}$ mice exhibited a constant elevation in glucose and insulin levels following refeeding, indicating that animals were likely eating a bolus of food initially followed by continued lighter feeding (Figure 4-4D and 4-4E). This behavior was perhaps responsible for some of the variability observed as there may be different feeding behavior among individual animals: in the future, it may be advantageous to feed animals a single large “meal” instead of *ad libitum*. Regardless, the most likely source of the peak in serum triglycerides is dietary: in humans, this peak occurs 2 hours post HCD consumption while maximum *de novo* lipogenesis does not occur until 4 hours (Timlin and Parks, 2005). Additionally, lipolysis in adipose tissue was suppressed with refeeding, as indicated in our mice by the abrupt fall in serum NEFA; thus, increased

exogenous fatty acids are likely to be the source of triglycerides in the peak (Figure 4-6C). *AFP;Akt2*$^{lox/lox}$ mice did not exhibit an increase in serum triglycerides following refeeding, indicating that loss of Akt2 in the liver somehow influences the handling of dietary triglycerides. Non-cell autonomous effects of Akt2 on gut function cannot be excluded, but a preliminary lipid tolerance test using gavaged olive oil suggested that there was not a defect in lipid absorption by the gut in *AFP;Akt2*$^{lox/lox}$ mice (not shown). Thus, it would be interesting to determine if Akt2 regulates the uptake and re-esterification of dietary fatty acids in the liver.

Another finding which appeared to be unrelated to Akt2's role in lipogenesis, was the failure of *AFP;Akt2*$^{lox/lox}$ mice to normally increase their liver weight upon refeeding. Liver weight was identical in *Akt2*$^{lox/lox}$ and *AFP;Akt2*$^{lox/lox}$ mice after an overnight fast, and we have not previously observed a change in fed liver weight in *AFP;Akt2*$^{lox/lox}$ mice on a normal chow diet (Figure 4-4, 2-6B and 3-8B). Therefore, it is unlikely that there is a developmental aspect to the loss of Akt2 in determining liver size or hepatic cell number, though it is possible that this difference only becomes apparent with HCD-feeding. The concentrations of glycogen, triglycerides and protein, the 3 macromolecules that make up the bulk of the liver, were unchanged during refeeding (Figure 4-5). However, total content of glycogen was decreased at 6 and 12 hours after refeeding, and there was a trend towards decreased triglyceride and protein content at 12 hours. Therefore, it appears that the absence of increasing liver weight in *AFP;Akt2*$^{lox/lox}$ mice was due primarily to decreased glycogen content, with a small contribution by triglyceride and protein content, though it is possible that decreases in all 3 macromolecules were secondary to decreased liver weight by another unknown cause.

Chapter 4 Figures

Figure 4-1: Liver weight increases with refeeding but not due to increases in triglycerides or protein.

8-week old male C57BL/6J mice were fasted overnight (4pm to 10am) and refed HCD for 0, 1.5, 3, 6, 9 or 12 hours prior to sacrifice.

A. Body weight. *$p<0.05$ by one-way ANOVA using Newman-Keuls post-test.

B, C. Liver weight expressed as grams weight (B) and as a ratio to body weight (LW/BW) (C). All time points are significantly different ($p<0.05$ by one-way ANOVA using Newman-Keuls post-test) to all others except for those marked non-significant (NS).

D. Hepatic protein expressed as concentration per gram liver. All time points are significantly different ($p<0.05$ by one-way ANOVA using Newman-Keuls post-test) to all others except for those marked NS.

E. Total hepatic protein. No time points are significantly different to others ($p<0.05$ by one-way ANOVA using Newman-Keuls post-test).

F, G. Hepatic triglycerides (TG) expressed as concentration per gram liver (F) and total (G). No time points are significantly different to others ($p<0.05$ by one-way ANOVA using Newman-Keuls post-test).

All values are expressed as mean ± SEM. n=4-6.

Figure 4-1

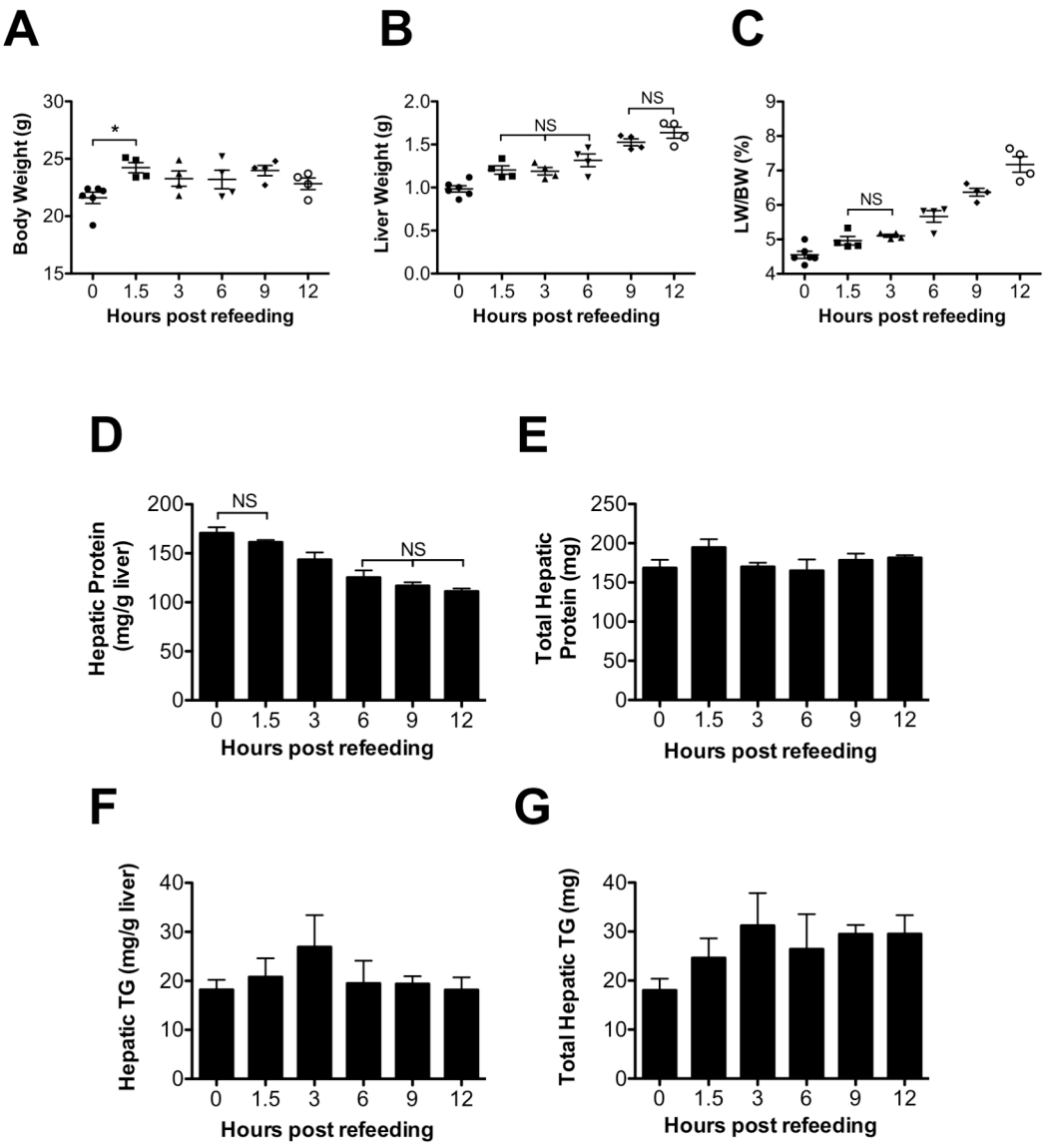
A
B
C
Body Weight (g)
Liver Weight (g)
LW/BW (%)
Hours post refeeding
*
NS
D
E
F
G
Hepatic Protein (mg/g liver)
Total Hepatic Protein (mg)
Hepatic TG (mg/g liver)
Total Hepatic TG (mg)

Figure 4-2: Serum measurements during fasting and refeeding.

8-week old male C57BL/6J mice were fasted overnight (4pm to 10am) and refed HCD for 0, 1.5, 3, 6, 9 or 12 hours prior to sacrifice.

A. Serum triglycerides (TG). 6-hour time point: *$p<0.05$ vs all other time points by one-way ANOVA using Newman-Keuls post-test.

B. Serum cholesterol (CH). *$p<0.05$ for 1.5-hour time point vs all other time points and two bracketed time points **$p<0.05$ by one-way ANOVA using Newman-Keuls post-test.

C. Serum non-esterified fatty acids (NEFA). Fasted (0 hour) time point: *$p<0.05$ vs all other time points by one-way ANOVA using Newman-Keuls post-test.

D. Serum ketones. Fasted (0 hour) time point: *$p<0.05$ vs all other time points by one-way ANOVA using Newman-Keuls post-test.

All values are expressed as mean ± SEM. n=4-6.

Figure 4-2

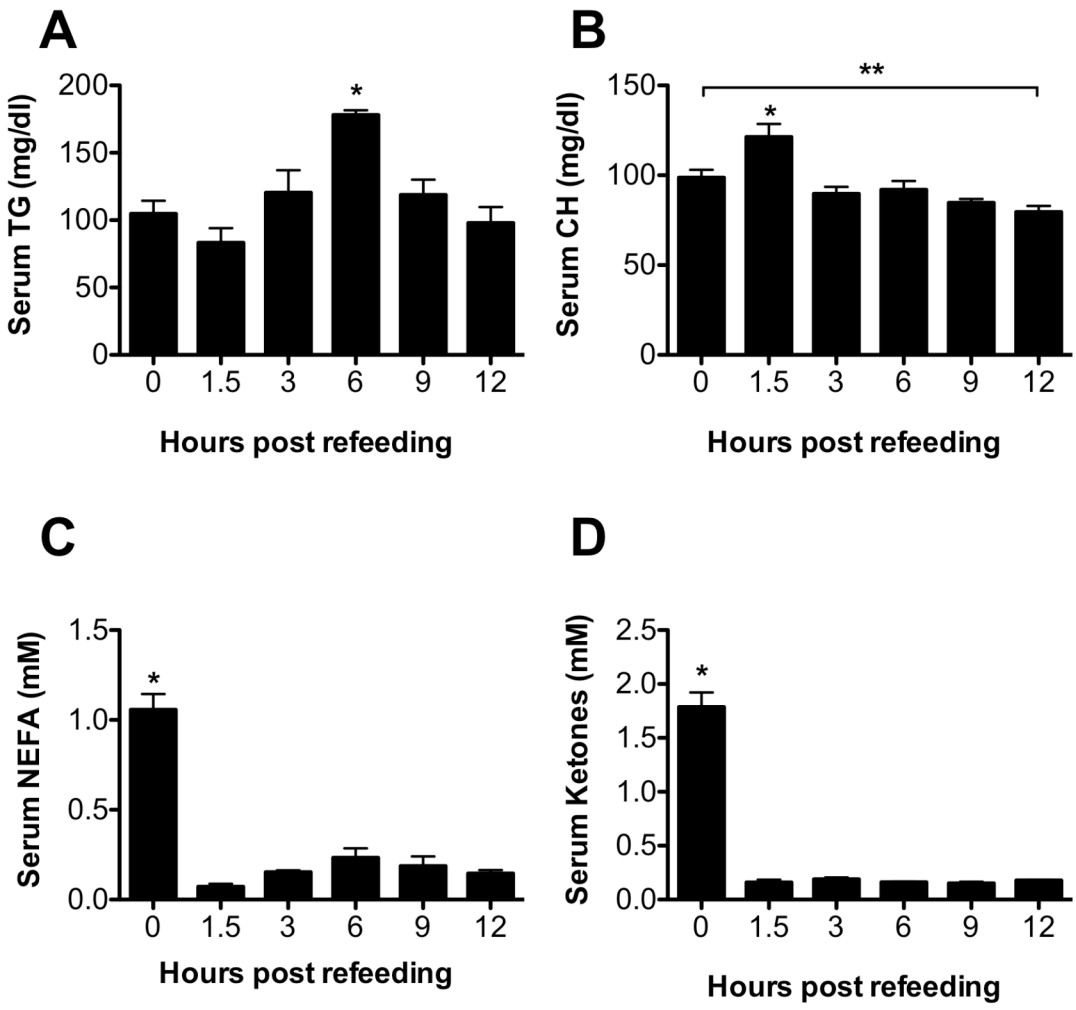
A
Serum TG (mg/dl)
200
150
100
50
0
*
0
1.5
3
6
9
12
Hours post refeeding
B
Serum CH (mg/dl)
150
100
50
0
**
*
0
1.5
3
6
9
12
Hours post refeeding
C
Serum NEFA (mM)
1.5
1.0
0.5
0.0
*
0
1.5
3
6
9
12
Hours post refeeding
D
Serum Ketones (mM)
2.5
2.0
1.5
1.0
0.5
0.0
*
0
1.5
3
6
9
12
Hours post refeeding

Figure 4-3: *SREBP1c*, *FAS*, and *GCK* expression increases with refeeding.

Hepatic gene expression as measured by Real-Time PCR of 8-week old male C57BL/6J mice fasted overnight (4pm to 10am) and refed HCD for 0, 1.5, 3, 6, 9 or 12 hours prior to sacrifice. Data are presented as mRNA expression relative to that of TATA-binding protein and normalized to expression in Fasted (0) time point, which is set to 1.0 using the ddC_T method.

All values are expressed as mean ± SEM. n=4-6; *p<0.05 vs Fasted (0) time point and **p<0.05 vs 3-hour time point by one-way ANOVA using Newman-Keuls post-test.

Abbreviations: sterol regulatory element binding protein-1c (*SREBP1c*), fatty acid synthase (*FAS*), glucokinase (*GCK*), and stearoyl-CoA desaturase-1 (*SCD1*).

Figure 4-3

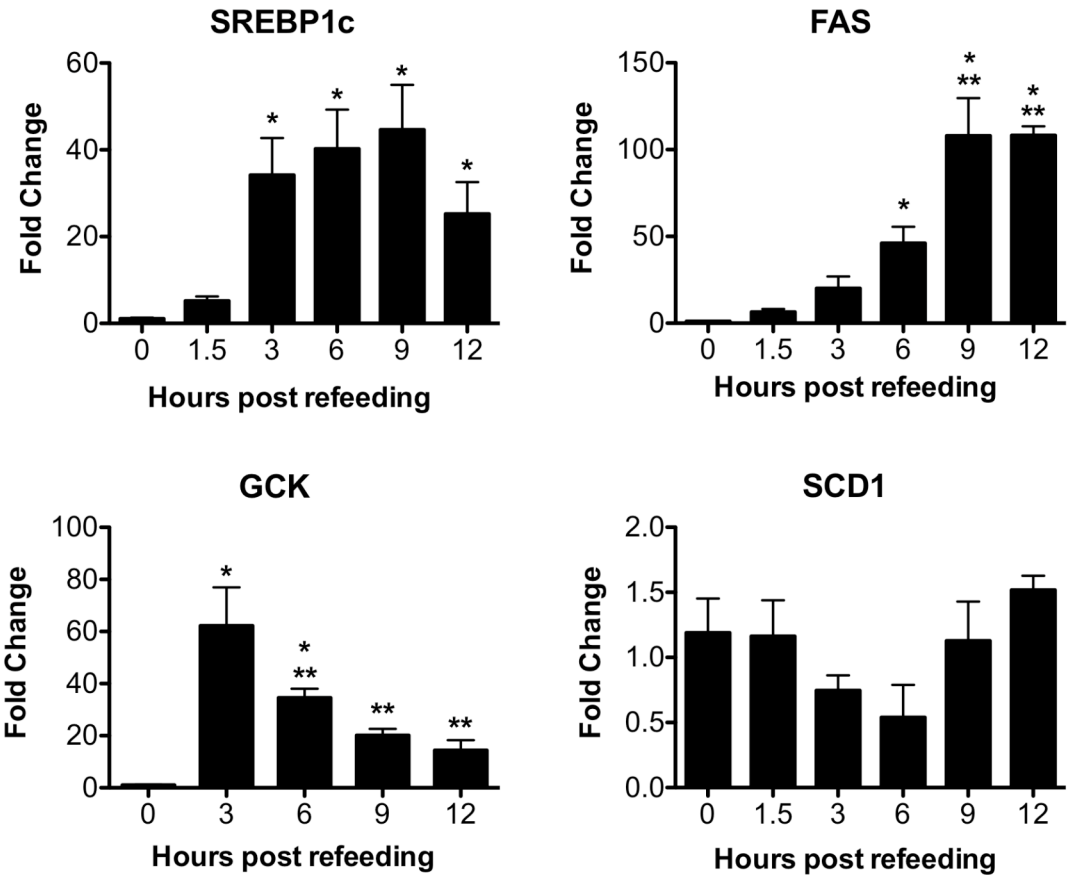
SREBP1c
Fold Change
60
40
20
0
0 1.5 3 6 9 12
Hours post refeeding
FAS
Fold Change
150
100
50
0
0 1.5 3 6 9 12
Hours post refeeding
GCK
Fold Change
100
80
60
40
20
0
0 3 6 9 12
Hours post refeeding
SCD1
Fold Change
2.0
1.5
1.0
0.5
0.0
0 1.5 3 6 9 12
Hours post refeeding

Figure 4-4: *AFP;Akt2*$^{lox/lox}$ mice gain less liver weight upon refeeding but maintain normal glucose and insulin levels.

8-week old male mice were fasted overnight (4pm to 10am) and refed HCD for 0, 1.5, 3, 6, or 12 hours prior to sacrifice.

A-C. Body weight (A), liver weight expressed as grams weight (B) and as a ratio to body weight (LW/BW) (C). *p<0.05 vs Fasted (0) time point of the same genotype and **p<0.05 of the two bracketed points by one-way ANOVA using Newman-Keuls post-test.

E, F. Blood glucose (E) and seurm insulin (F) at the time of sacrifice. Fasted (0 hour) time point: *p<0.05 vs all other time points of that same genotype by one-way ANOVA using Newman-Keuls post-test.

All values are expressed as mean ± SEM. n=5-6.

Figure 4-4

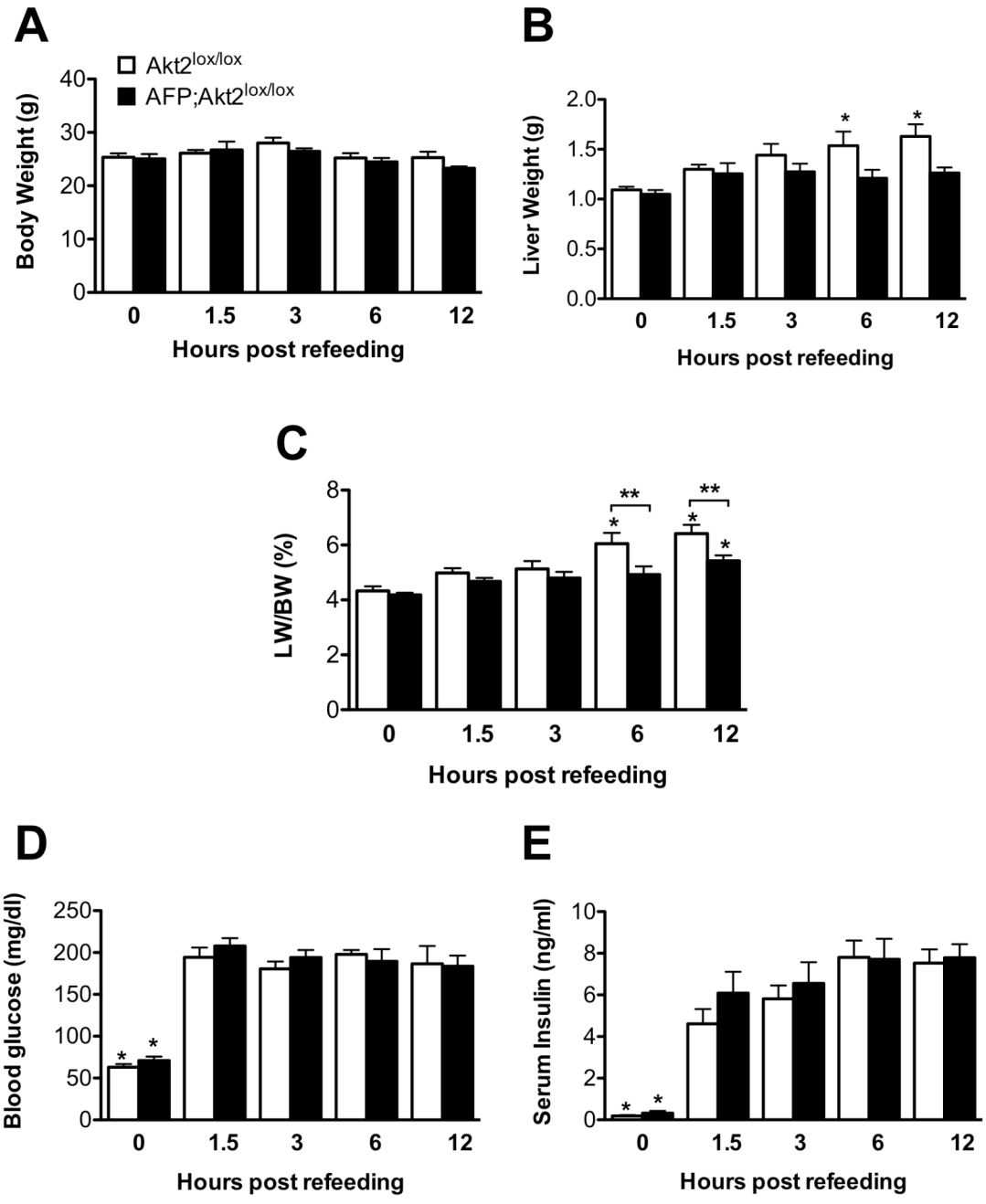
A
Akt2lox/lox
AFP;Akt2lox/lox
Body Weight (g)
40
30
20
10
0
0
1.5
3
6
12
Hours post refeeding
B
Liver Weight (g)
2.0
1.5
1.0
0.5
0.0
*
*
0
1.5
3
6
12
Hours post refeeding
C
LW/BW (%)
8
6
4
2
0
**
**
*
*
*
*
0
1.5
3
6
12
Hours post refeeding
D
Blood glucose (mg/dl)
250
200
150
100
50
0
*
*
0
1.5
3
6
12
Hours post refeeding
E
Serum Insulin (ng/ml)
10
8
6
4
2
0
*
*
0
1.5
3
6
12
Hours post refeeding

Figure 4-5: *AFP;Akt2*$^{lox/lox}$ mice maintain normal hepatic concentrations of triglyceride, protein and glycogen but have decreased glycogen content.

8-week old male mice were fasted overnight (4pm to 10am) and refed HCD for 0, 1.5, 3, 6, or 12 hours prior to sacrifice.

A, B. Hepatic triglycerides (TG) expressed as concentration per gram liver (A) and total (B). No time points are significantly different to others ($p<0.05$ by one-way ANOVA using Newman-Keuls post-test).

C. Hepatic protein expressed as concentration per gram liver. Fasted (0 hour) time point: *$p<0.05$ vs all other time points of that same genotype by one-way ANOVA using Newman-Keuls post-test.

D. Total hepatic protein. No time points are significantly different to others ($p<0.05$ by one-way ANOVA using Newman-Keuls post-test).

E, F. Hepatic glycogen expressed as concentration per gram liver (E) and total (F). Fasted (0) levels were undetectable. *$p<0.05$ by one-way ANOVA using Newman-Keuls post-test.

All values are expressed as mean ± SEM. n=5-6.

Figure 4-5

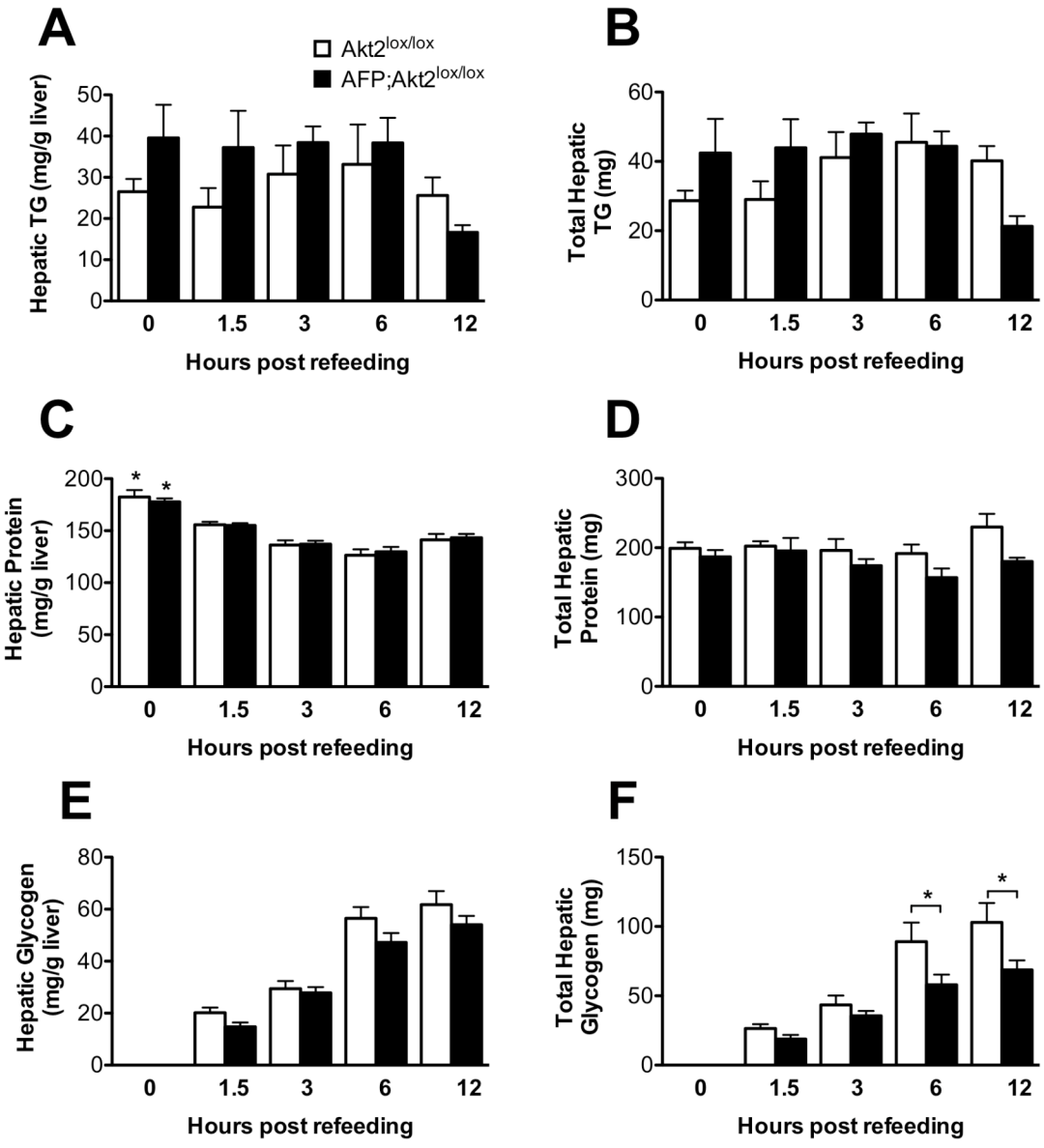
A
Akt2lox/lox
AFP;Akt2lox/lox
Hepatic TG (mg/g liver)
0
10
20
30
40
50
0
1.5
3
6
12
Hours post refeeding
B
Total Hepatic TG (mg)
0
20
40
60
0
1.5
3
6
12
Hours post refeeding
C
Hepatic Protein (mg/g liver)
0
50
100
150
200
*
*
0
1.5
3
6
12
Hours post refeeding
D
Total Hepatic Protein (mg)
0
100
200
300
0
1.5
3
6
12
Hours post refeeding
E
Hepatic Glycogen (mg/g liver)
0
20
40
60
80
0
1.5
3
6
12
Hours post refeeding
F
Total Hepatic Glycogen (mg)
0
50
100
150
*
*
0
1.5
3
6
12
Hours post refeeding

Figure 4-6: Serum measurements during fasting and refeeding in *AFP;Akt2*$^{lox/lox}$ mice.

8-week old male mice were fasted overnight (4pm to 10am) and refed HCD for 0, 1.5, 3, 6, or 12 hours prior to sacrifice.

A, B. Serum triglycerides (TG) (A) and cholesterol (CH) (B).

C, D. Serum non-esterified fatty acids (NEFA) (C) and ketones (D). Fasted (0 hour) time point: *$p<0.05$ vs all other time points of that same genotype by one-way ANOVA using Newman-Keuls post-test.

All values are expressed as mean ± SEM. n=5-6; **$p<0.05$ of the two bracketed points by one-way ANOVA using Newman-Keuls post-test.

Figure 4-6

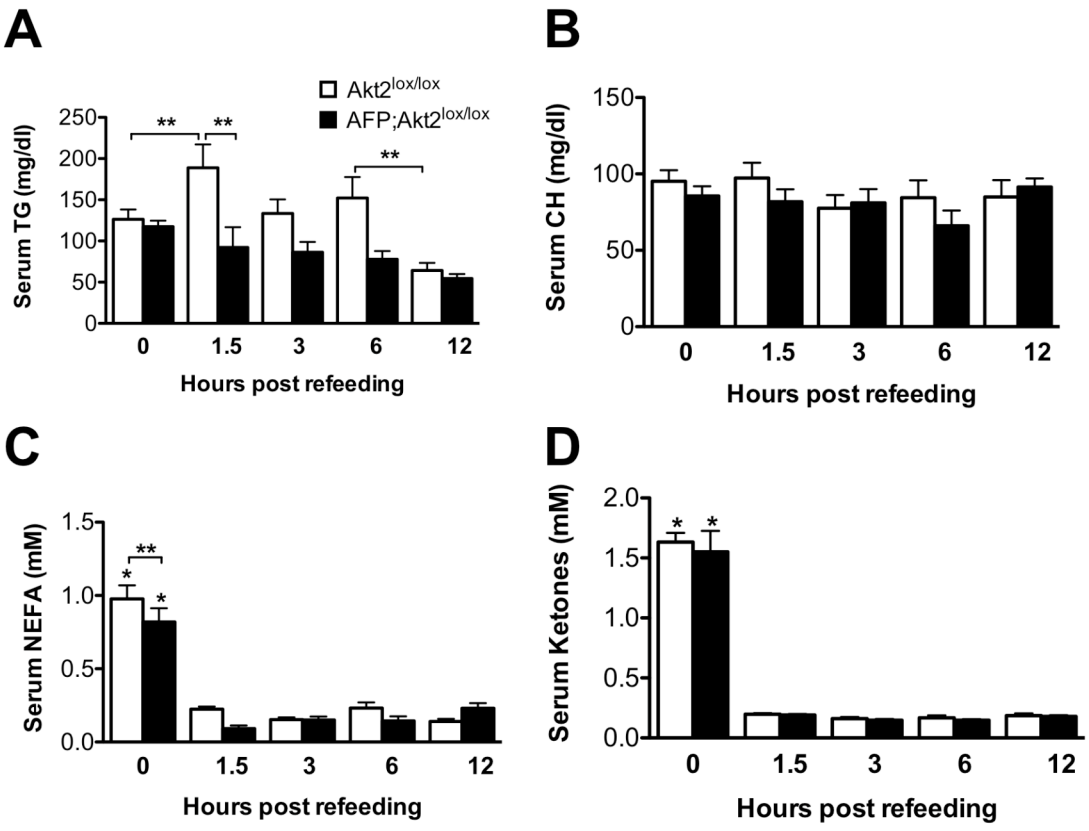
A
Akt2lox/lox
AFP;Akt2lox/lox
Serum TG (mg/dl)
250
200
150
100
50
0
**
**
**
0
1.5
3
6
12
Hours post refeeding
B
Serum CH (mg/dl)
150
100
50
0
0
1.5
3
6
12
Hours post refeeding
C
Serum NEFA (mM)
1.5
1.0
0.5
0.0
**
*
*
0
1.5
3
6
12
Hours post refeeding
D
Serum Ketones (mM)
2.0
1.5
1.0
0.5
0.0
*
*
0
1.5
3
6
12
Hours post refeeding

Figure 4-7: Refeeding-stimulated *de novo* lipogenesis is decreased in *AFP;Akt2*$^{lox/lox}$ mice.

De novo lipogenesis: 8-week old male mice were injected with D_2O at the time points described below, sacrificed after 3 or 6 hours, and liver was removed and analyzed for palmitate by GC/MS.

A. Mice were fasted overnight (4pm to 10am), refed HCD (6 hour group) or maintained fasting (Fasted), injected after 3 hours (1pm), and sacrificed 3 hours later (4pm). n=3-5; *p<0.05 by one-way ANOVA using Newman-Keuls post-test.

B. Mice were fasted overnight (4pm to 9am), refed HCD (12 hour group), injected after 6 hours (4pm), and sacrificed 6 hours later (9pm). n=5-6; *p<0.01 by Student's t-test.

All values are expressed as mean ± SEM.

Figure 4-7

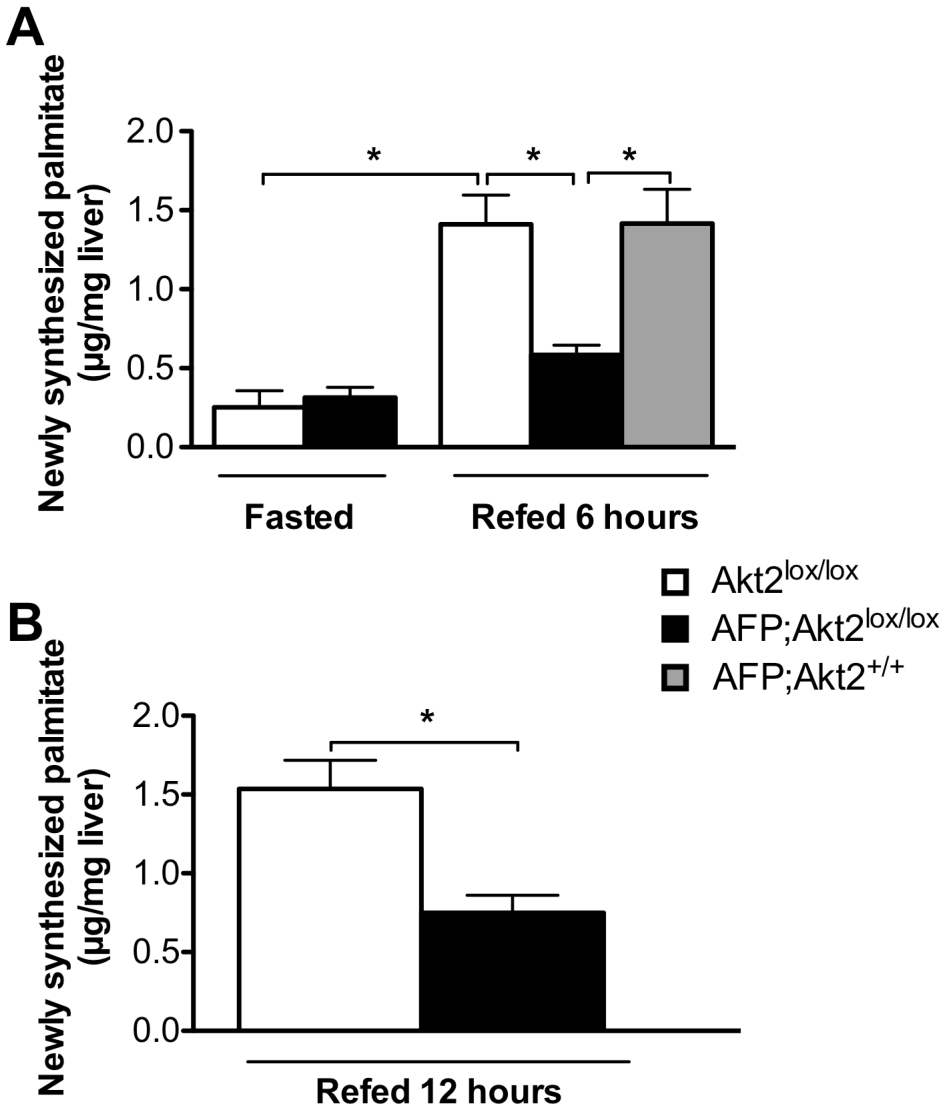
A
Newly synthesized palmitate (µg/mg liver)
2.0
1.5
1.0
0.5
0.0
*
*
*
Fasted
Refed 6 hours
Akt2lox/lox
AFP;Akt2lox/lox
AFP;Akt2+/+
B
Newly synthesized palmitate (µg/mg liver)
2.0
1.5
1.0
0.5
0.0
*
Refed 12 hours

Figure 4-8: Refeeding-stimulated increases in expression of some, but not all, lipogenic gene are Akt2-dependent.

Hepatic gene expression as measured by Real-Time PCR of 8-week old male mice were fasted overnight (4pm to 10am) and refed HCD for 0, 1.5, 3, 6, or 12 hours prior to sacrifice. Data are presented as mRNA expression relative to that of TATA-binding protein and normalized to expression in *Akt2*$^{lox/lox}$ Fasted (0) time point, which is set to 1.0 using the ddC_T method.

All values are expressed as mean ± SEM. n=5-6; *p<0.05 vs Fasted (0) time point of the same genotype and ** p<0.05 by one-way ANOVA using Newman-Keuls post-test.

Abbreviations: sterol regulatory element binding protein-1c (*SREBP1c*), fatty acid synthase (*FAS*), ATP citrate lyase (*ACL)*, acetyl-CoA carboxylase (*ACC*), glucokinase (*GCK*), glycerol phosphate acyltransferase (*GPAT*), pyruvate kinase, liver isoform (*L-PK*), and glucose-6-phosphatase (*G6Pase*).

Figure 4-8

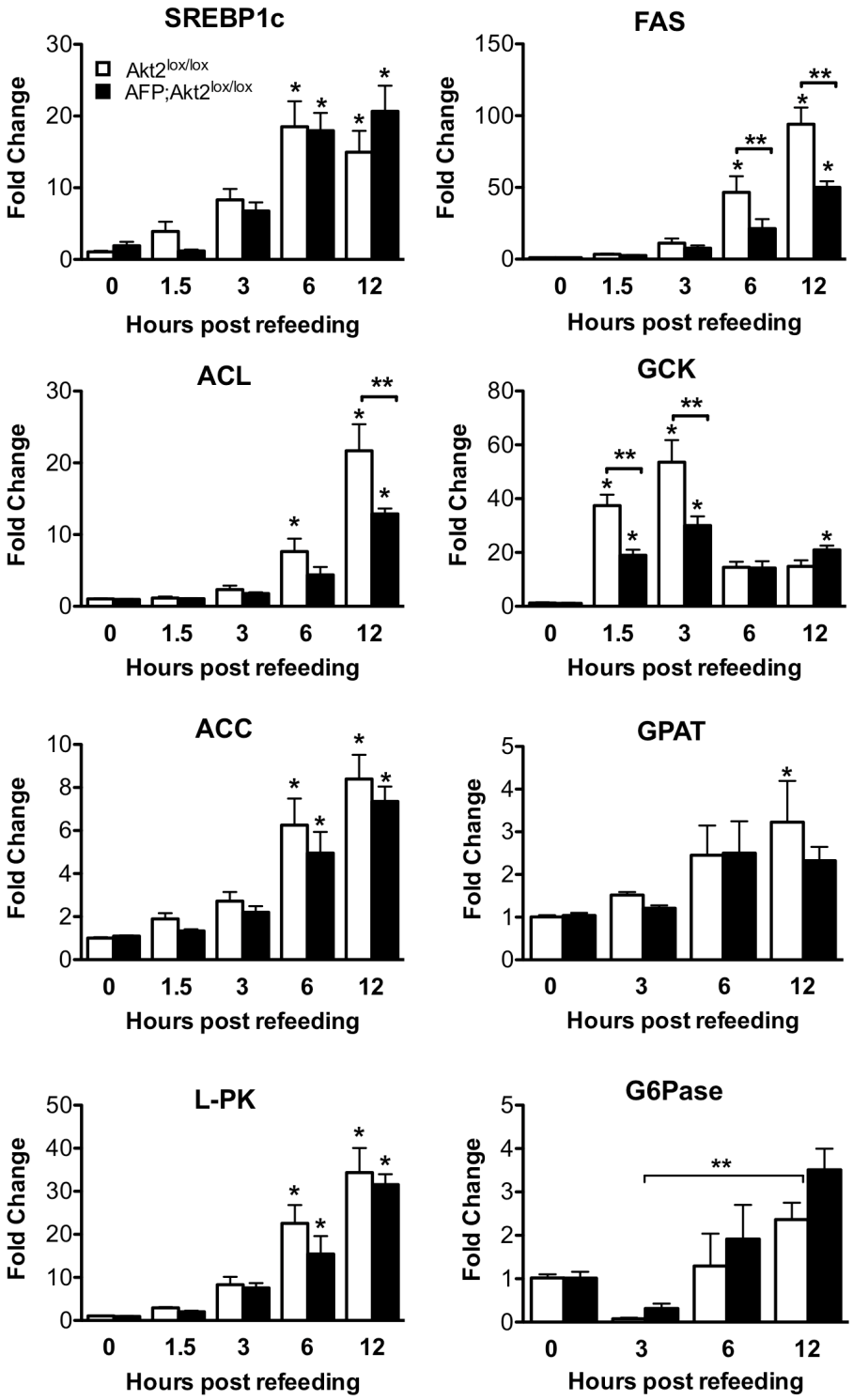
SREBP1c
FAS
ACL
GCK
ACC
GPAT
L-PK
G6Pase
Akt2lox/lox
AFP;Akt2lox/lox
Fold Change
Hours post refeeding
0
1.5
3
6
12

Chapter 5:

Summary and Speculations

Akt2 regulates hepatic lipid metabolism

Though insulin is well known to stimulate *de novo* lipogenesis in liver, the precise mechanism by which this is accomplished is not well understood. SREBP1c is clearly an important intermediate in the transcriptional control of lipogenesis, but the pathway by which insulin activates both processing and expression of SREBP1c remains uncertain (Raghow et al., 2008). To some extent, the difficulty in investigating this problem relates to the low rates of *de novo* lipogenesis in the normal postabsorptive liver, which have been estimated to contribute as little as 5% of total triglyceride fatty acids in humans (Diraison et al., 2003). For this reason, it has proven instructive to manipulate the metabolic state of experimental organisms in order to increase fat accumulation in the liver. In the present study, we have done so employing both genetic and dietary strategies and found a strong dependency on the presence of hepatic Akt2 for the development of steatosis and an absolute requirement for the increase in lipogenesis. In addition, we have established that Akt2 is required for the induction of *de novo* lipogenesis following HCD-feeding in lean animals. Thus, we can conclude that Akt2 is required definitively for full accretion of hepatic triglyceride during pathological states and as well as in normal anabolic lipid metabolism.

However, Akt2 does not influence lipid metabolism in the same manner in our three different models. In the *ob/ob* mouse, loss of Akt2 prevented any excess hepatic triglyceride accumulation and acute loss of the kinase reversed existing steatosis. The absence of hepatic steatosis was associated with decreased *de novo* lipogenesis, which appeared to be controlled at the level of *SREBP1c* expression. On the other hand, loss of Akt2 in DIO reduced hepatic triglyceride accumulation but did not completely prevent it, and *de novo* lipogenesis was unchanged in the absence of the kinase, indicating that Akt2 is required for another lipid metabolic pathway involved in steatosis. Furthermore,

Akt2 was required for the induction of *de novo* lipogenesis following HCD-refeeding in lean animals, though this did not appear to be due to a requirement for the induction of *SREBP1c* expression. Therefore, Akt2 appears to be involved in many facets of the regulation of hepatic lipid metabolism.

Akt2 is required for increased *de novo* lipogenesis in the *ob/ob* mouse, likely through SREBP1c

The role of Akt as the primary mediator of insulin's action to increase SREBP1c and promote lipogenesis has been a point of some controversy. Hepatic overexpression of constitutively active Akt increases hepatic neutral lipid dramatically by a pathway partially dependent on SREBP1c (Ono et al., 2003). Similarly, forced activation of endogenous Akt by liver-specific deletion of the lipid phosphatase PTEN produces substantial accumulation of hepatic triglyceride and increased lipogenic gene expression, though this model is complicated by the concomitant activation of other PI3K-dependent kinases (Stiles et al., 2004). On the other hand, a dominant inhibitory Akt does not block insulin's induction of *SREBP1c* in tissue culture cells and *ob/ob* mice have markedly increased *SREBP1c* mRNA in spite of significantly reduced levels of phospho-Akt (Matsumoto et al., 2002; Shimomura et al., 2000). aPKC (PKCλ/ζ) proteins have received considerable attention as obligate mediators of the effects of insulin and PI3K on anabolic lipid metabolism, and have specifically been advanced as an alternative to Akt (Matsumoto et al., 2003; Taniguchi et al., 2006b). Matsumoto et al. showed that mice with liver-specific deletion of PKCλ have decreased *SREBP1c* expression and triglyceride content, though reduced serum insulin levels complicated the interpretation of the *in vivo* findings in the study (Matsumoto et al., 2003). Kahn and colleagues undertook a different approach, eliminating both aPKC and Akt activity by

ablation of all PI3K in the liver, and then selectively introducing constitutively activate versions of the two kinases by adenovirus-mediated delivery (Taniguchi et al., 2006b). They found that aPKC, but not Akt, restored *SREBP1c* mRNA, but the effects on hepatic lipids were not reported.

The current studies do not address a potential role for aPKC and thus are compatible with a requirement for this kinase. However, in contrast to Taniguchi et al., they strongly support a critical role for Akt2. *ob/ob* mice lacking hepatic Akt2 exhibited decreased *SREBP1c* expression, decreased lipogenesis and greatly improved hepatic steatosis. Importantly, *ob/ob* mice heterozygous for *Akt2* displayed a reduction in liver triglyceride content and *de novo* lipogenesis intermediate between that in mice wildtype and null for *Akt2*. This indicates that Akt2 is not only permissive for anabolic lipid metabolism, but is actually rate-determining. Additionally, acute excision of hepatic Akt2 resulted in a reversal of hepatic steatosis, indicating that Akt2 is required for ongoing maintenance of lipid accumulation.

Our data suggest that Akt2 is required for the upregulation of lipogenic gene expression in the *ob/ob* mouse, and in Akt2's absence, lipogenic gene expression and therefore *de novo* lipogenesis are not increased. Insulin is known to regulate lipogenic gene expression through stimulating the expression of *SREBP1c*, and this has been shown to be Akt-dependent *in vitro* (Fleischmann and Iynedjian, 2000; Porstmann et al., 2005). Indeed, we found that the expression of *SREBP1c* and its lipogenic targets were decreased in $Lep^{ob/ob}AFP;Akt2^{lox/lox}$ livers. Upregulation of *SREBP1c* drives some of the hepatic lipid accumulation observed in leptin-deficiency as hepatic steatosis is markedly reduced in *ob/ob* mice lacking SREBP1, corresponding to a decrease in lipogenic gene expression, a phenotype similar to our studies in *ob/ob* mice lacking hepatic Akt2 (Yahagi et al., 2002). However, while the decreased hepatic expression of *SREBP1c*

correlates with decreased *de novo* lipogenesis in *Lep$^{ob/ob}$AFP;Akt2$^{lox/lox}$* mice, it does not prove causality between the two.

Interestingly, while we did not observe any changes in *ChREBP* mRNA in *Lep$^{ob/ob}$ AFP;Akt2$^{lox/lox}$* mice, the induction of *L-PK* expression, a lipogenic gene that is supposed to be regulated by ChREBP and not SREBP1c, was blocked in *ob/ob* mice with loss of hepatic Akt2. In addition, overexpression of constitutively active Akt promotes hepatic triglyceride accumulation through some SREBP1c-independent mechanisms, indicating that Akt2's regulation of *de novo* lipogenesis may not proceed solely through SREBP1c (Ono et al., 2003). Liver X receptors (LXR) are transcription factors activated by oxysterol ligands, and administration of LXR agonists in mice results in induction of lipogenic gene expression and hepatic steatosis (Schultz et al., 2000). LXRs are necessary for insulin-stimulated induction of *SREBP1c* expression in rat hepatocytes and sufficient to increase hepatic *SREBP1c* mRNA *in vivo* (Chen et al., 2004; Repa et al., 2000). Additionally, LXRs can induce the expression of *ChREBP* and *L-PK*, though this is likely through an increase in *ChREBP* mRNA and not through modulation of ChREBP activity (Cha and Repa, 2007; Denechaud et al., 2008). Though *L-PK* mRNA was decreased in *Lep$^{ob/ob}$AFP;Akt2$^{lox/lox}$* mice, *ChREBP* mRNA was not, indicating that Akt2 somehow influences ChREBP activity and not expression. To determine if LXR activity was altered and contributing to the regulation of lipogenic gene expression in our *Lep$^{ob/ob}$AFP;Akt2$^{lox/lox}$* mice, we could measure the expression of one of LXR's non-lipogenic targets, such as the transporters ABCG5 or ABCG8 (Tontonoz and Mangelsdorf, 2003).

Akt2 is required for the induction of *de novo* lipogenesis in lean animals by high carbohydrate-feeding, likely independent of *SREBP1c*

While Akt2 is certainly required in insulin-resistant livers for lipid metabolism and accumulation, we show that hepatic Akt2 is also required in normal livers for the induction of *de novo* lipogenesis by HCD-refeeding. Livers from animals subjected to an overnight fast had very low levels of lipogenic mRNAs and *de novo* lipogenesis, regardless of the presence or absence of Akt2. Upon refeeding with a HCD, both *de novo* lipogenesis and lipogenic gene expression increased in *Akt2*$^{lox/lox}$ mice. Hepatic Akt2 was required for the induction of *de novo* lipogenesis above fasted levels and for the full increase in the expression of some lipogenic genes. However, Akt2 was not required for the induction of *SREBP1c* expression and the universal lipogenic gene program as *AFP;Akt2*$^{lox/lox}$ mice exhibited normal increases in *SREBP1c, ACC,* and *GPAT* mRNAs. Thus, Akt2 can regulate the rate of *de novo* lipogenesis in lean animals in an *SREBP1c* expression-independent manner.

There are several possible mechanisms through which Akt2 could act to induce *de novo* lipogenesis. Akt2 could still induce *de novo* lipogenesis through the induction of *FAS*, *ACL, GCK*, and possibly other lipogenic enzyme expression though not through the control of *SREBP1c* expression. Insulin can control the processing of SREBP1c into an active transcription factor; nuclear fractionization and Western blotting could be used to determine if this processing is regulated in an Akt2-dependent manner. Additionally, Akt2 could either directly or indirectly modulate the translation or activity of key lipogenic enzymes thereby regulating flux through *de novo* lipogenesis. Though we have demonstrated that mRNAs for *FAS, ACL* and *GCK* were decreased in the absence of hepatic Akt2, we need to determine if the protein levels of these enzymes are correspondingly decreased. Activities of FAS, ACC, ACL, and GCK could be measured in the absence of Akt2 to assess whether this could be a level of control. If any lipogenic activity was decreased, add-back of that enzyme by adenoviral expression could be

performed to reverse the blunted rate of lipogenesis. Further biochemical characterization of these enzymes could also reveal whether they were Akt2 substrates and subject to regulation by the kinase.

Akt2 controls lipid accumulation by an unknown lipid metabolic process in diet-induced obesity

One surprising result of these studies is that even though the necessity of Akt2 for steatosis applies to multiple models, in DIO by high-fat feeding, hepatic triglyceride content was reduced but lipogenesis and lipogenic gene expression were unchanged in the absence of hepatic Akt2. These results contrast with those in the *ob/ob* mouse, in which the protection from steatosis is at least partially mediated through preventing the stimulation of *de novo* lipogenesis, though this does not exclude the influence of Akt2 on another lipid metabolic pathway in the *ob/ob* mouse. In DIO induced by Surwit HFD, *de novo* lipogenesis was elevated compared with chow-fed mice, but lipogenic gene expression was unchanged, and loss of hepatic Akt2 had no effect on either. In DIO induced by lard HFD, *de novo* lipogenesis was reduced compared with chow-fed mice, though once again lipogenic gene expression was largely unchanged and loss of hepatic Akt2 did not influence either. The dramatic difference in lipogenesis observed between the two diets is surprising as the contribution of fat and carbohydrates to caloric content is similar (58 and 25.5 % kcal in Surwit and 60 and 20 % kcal in lard; see Materials and Methods). The difference in sucrose content or source of fat is perhaps influencing the suppression versus the induction of lipogenesis. Regardless, Akt2 does not reduce hepatic triglyceride content in DIO through its control of *de novo* lipogenesis. Additionally, while loss of hepatic Akt2 resulted in a complete prevention of hepatic triglyceride accumulation in the *ob/ob* mouse, it only resulted in decreased accumulation

in DIO, suggesting different underlying causes. Thus, Akt2 likely mediates insulin's induction of triglyceride accumulation by stimulating fatty acid synthesis as well as processes other than *de novo* lipogenesis.

One obvious candidate mechanism is that loss of Akt2 abrogates the normal suppression of β-oxidation produced by insulin. For example, insulin suppresses the PGC-1α-dependent stimulation of fatty acid oxidation, both by reducing hepatocyte cyclic AMP and by promoting the Akt-dependent inhibition of PGC-1α activity (Li et al., 2007). However, by several criteria, an increase in β-oxidation is unlikely to explain the protection from steatosis in DIO or *ob/ob* mice. First, there were no differences in expression of hepatic oxidative genes comparing $Akt2^{lox/lox}$ to $AFP;Akt2^{lox/lox}$ mice placed on a Surwit HFD. Second, though *PGC-1α* mRNA increased in $Lep^{ob/ob}$ $AFP;Akt2^{lox/lox}$ livers, expression of the critical targets *MCAD* and *CPT1* were not elevated in parallel (Schreiber et al., 2003; Song et al., 2004). Lastly, RER and serum ketones bodies were largely indistinguishable in wildtype versus $AFP;Akt2^{lox/lox}$ mice on either an *ob/ob* background or Surwit HFD.

Another possible mechanism through which Akt2 could decrease hepatic lipid accumulation is increased triglyceride export. Insulin can suppress VLDL secretion by directly increasing apoB degradation in a PI3K-dependent manner (Chirieac et al., 2000). Han and colleagues reported decreased VLDL levels along with decreased lipogenic gene expression in mice with severely impaired insulin signaling (*L1* mice) on $Ldlr^{-/-}$ background fed an atherogenic Western diet (Han et al., 2009). VLDL levels were normalized with hepatic overexpression of constitutively active Akt, suggesting a role for Akt in the context of almost complete deficiency of the insulin receptor. $Lep^{ob/ob}$ $Akt2^{-/-}$ mice did exhibit elevated serum triglyceride levels, suggesting that an increase in triglyceride export could be partially responsible for decreasing hepatic triglycerides by

shunting them into the serum. However in *Lep*$^{ob/ob}$ *AFP;Akt2*$^{lox/lox}$ mice, fed serum triglyceride levels did not differ from *Lep*$^{ob/ob}$ *Akt2*$^{lox/lox}$ mice, and fasted serum triglycerides were actually lower; there was also no difference in *AFP;Akt2*$^{lox/lox}$ mice on Surwit HFD. Additionally, a direct measurement of triglyceride export using P-407 in both *ob/ob* and DIO mice failed to reveal a requirement for Akt2. These observations suggest that increased triglyceride export and increased β-oxidation do not play a role in reducing hepatic triglyceride accumulation in the absence of Akt2 in the liver. However, we do discuss a potential role for Akt signaling in the control of these two processes through FoxO1 and PGC-1α below.

Having likely ruled out *de novo* lipogenesis, VLDL export and β-oxidation as Akt2-regulated processes that could control hepatic lipid accumulation in DIO, we must consider other processes, less classically involved in insulin signaling. We measured *de novo* lipogenesis as the synthesis of its major product, palmitate, in our mice; however, increased hepatic fatty acid synthesis could occur through chain elongation and desaturation of exogenous fatty acids rather than through *de novo* synthesis. This has been previously reported to be the case in C57BL/6J mice fed a HFD as palmitate (C16:0) synthesis was unchanged, but oleate (C18:1) synthesis was increased; additionally hepatic expression of *SREBP1c, SCD1, FAS, ACC1,* and *GPAT* were all elevated (Oosterveer et al., 2009). However, long-chain fatty acyl-CoAs were not changed in either Surwit HFD-fed or *ob/ob* mice lacking hepatic Akt2, suggesting that Akt2 was not regulating the elongation and saturation of exogenous fatty acids, though measurement of oleate synthesis could formally rule out this possibility. However, Akt2 could be influencing the handling of exogenous fatty acids, either from the diet or from adipose tissue. While uptake and re-esterifcation of fatty acids from the serum by the liver has been considered to be a largely passive process, recent evidence has emerged

that certain conditions, such as high-fructose feeding, can actually enhance fatty acid re-esterification (Parks et al., 2008). *AFP;Akt2*$^{lox/lox}$ mice have decreased serum triglycerides following HCD-refeeding at a time when most of the triglycerides in the serum should be from a dietary source and not from *de novo* lipogenesis; this suggests that Akt2-deficient livers may have a defect in their handling of exogenous fatty acids. We are currently developing an *ex vivo* liver perfusion system that could be used to measure uptake and esterification of heavy isotope-labeled fatty acids, thus making it feasible to question whether Akt2 could control this aspect of hepatic lipid metabolism.

Selective insulin resistance revisited: bifurcation below the level of Akt

A longstanding paradox has been that people with T2DM and obesity or rodents with equivalent metabolic disorders have systemic insulin resistance in the face of increased hepatic lipogenesis, a classical insulin response (Petersen et al., 2007). Though a number of models could explain this, the concept of selective or partial insulin resistance has received increasing recent attention (Brown and Goldstein, 2008). Both humans with insulin resistance due to inherited mutations in the insulin receptor and mice with liver-specific deletion of the insulin receptor exhibit hyperglycemia and hyperinsulinemia but are protected against steatosis and hypertriglyceridemia (Biddinger et al., 2008; Semple et al., 2009). This finding is consistent with the idea that in classical "insulin-resistant" states, not all signaling is blunted, but rather some is preserved, in particular that to lipid synthesis. While it is likely that the pathways regulating glucose and lipid metabolism diverge somewhere downstream of the IRS proteins but upstream of FoxO1 and SREBP1c, respectively, the precise biochemical site is unknown (Dong et al., 2008; Kubota et al., 2008; Matsumoto et al., 2007). In the studies presented in this thesis, we have demonstrated that the point of selective insulin resistance likely lies

downstream of Akt (Figure 5-1A). Additionally, we propose a model for further study in which Akt mediates both the insulin-resistant arm to glucose output and the insulin-sensitive arm to lipid synthesis (Figure 5-1B).

Akt to FoxO1 to glucose output: the insulin-resistant branch

That Akt2 plays a role in glucose homeostasis has been established prior to the start of this thesis. Earlier reports from our group and another reported that whole-body *Akt2*$^{-/-}$ mice are mildly diabetic and exhibit impaired suppression of hepatic glucose output by insulin (Cho et al., 2001a; Garofalo et al., 2003). We have shown here that liver-specific *Akt2* null mice also failed to suppress hepatic glucose output during hyperinsulinemic euglycemic clamp, the gold standard measure of insulin resistance with regards to glucose homeostasis. *Akt2*$^{-/-}$ mice on an *ob/ob* background and on Surwit HFD exhibited increased insulin resistance by clamp compared with their *Akt2*$^{+/+}$ counterparts. *Akt2*$^{-/-}$ mice were able to compensate by increasing their serum insulin levels, while *Lep*$^{ob/ob}$*Akt2*$^{-/-}$ mice were unable to do so and succumbed to severe hyperglycemia. However, *AFP;Akt2*$^{lox/lox}$ mice on either an *ob/ob* background or Surwit HFD did not exhibit worse insulin resistance or glucose intolerance than that of their *Akt2*$^{lox/lox}$ counterparts. This clearly demonstrates that Akt2 plays a role in tissues other than the liver to regulate glucose homeostasis. It also shows that signaling through Akt in the liver is already likely to be impaired in insulin-resistant states, such that further loss of hepatic Akt2 does not have an additional effect on glucose homeostasis. Indeed, Western blotting of both *ob/ob* and Surwit HFD-fed livers showed substantial impairments in insulin signaling through Akt.

While Akt2 seems to be specifically required for the regulation of lipid synthesis, at least in *ob/ob* and HCD-refed livers, regulation of glucose metabolism is likely shared

by both Akt2 and Akt1. Though *Akt1*$^{-/-}$ mice do not exhibit impairments in glucose homeostasis, compound whole-body *Akt1*$^{+/-}$ *Akt2*$^{-/-}$ mice have severe diabetes, indicating that signaling through Akt1 controls glucose homeostasis at least somewhat in the absence of Akt2 (Chen et al., 2009; Chen et al., 2001; Cho et al., 2001b). Unpublished work being done in our group has supported this hypothesis: acute excision of both Akt1 and Akt2 in the liver results in extremely elevated blood glucose levels and complete dysregulation of the FoxO1 target gene, insulin-like growth factor binding protein-1 (*IGFBP1*) (unpublished data courtesy of Dr. Mingjian Lu). However, it is unclear whether the regulation of glucose metabolism is shared by both isoforms equally and only the amount of hepatic Akt present matters or if there is some level of isoform specificity.

The insulin signaling cascade controlling glucose metabolism is generally thought to proceed predominately through inhibition of FoxO1 (reviewed in Gross et al., 2008). Therefore, in the model of selective insulin resistance proposed in this thesis, insulin signals through Akt and FoxO1 to regulate glucose metabolism and is impaired in insulin-resistant states; this branch includes signaling through both Akt2 and Akt1 (Figure 5-1B). There is also evidence that FoxO1 mediates insulin's suppression of VLDL secretion, through insulin's suppression of FoxO1's stimulation. Overexpression of FoxO1 in liver increases serum triglycerides and conversely, hepatic RNAi knockdown of FoxO1 decreases VLDL production (Altomonte et al., 2004; Kamagate et al., 2008). As we did not observe any alterations in VLDL secretion in our Akt2-deficient mice, residual signaling through Akt1 in the "insulin-resistant" branch could be maintaining normal control of FoxO1 and VLDL secretion. In addition, Akt phosphorylates and inhibits PGC-1α, an action which should inhibit fatty acid oxidation (Li et al., 2007); however, we did not see any gross abnormalities in β-oxidation. Thus this pathway could also proceed along the "insulin-resistant" branch and receive signaling from Akt1

in the absence of Akt2. Thus, VLDL secretion and fatty acid oxidation should be investigated in the liver-specific *Akt1/Akt2* double null mice.

Akt2 (to mTOR?) to lipid synthesis: the insulin-sensitive branch

Unlike the glucose arm of insulin/Akt signaling, we propose that insulin signaling to lipogenesis runs solely through Akt2 and is maintained in insulin-resistant states (Figure 5-1B). We cannot fully discount a role of Akt1: signaling to lipid synthesis could require higher hepatic Akt levels than does that to glucose metabolism, and loss of hepatic Akt2 could decrease signaling through Akt to below what is required. Indeed $Lep^{ob/ob}Akt2^{+/-}$ mice exhibited an intermediate decrease in *de novo* lipogenesis compared with both $Lep^{ob/ob}Akt2^{+/+}$ and $Lep^{ob/ob}Akt2^{-/-}$ mice. This question could be resolved in $Lep^{ob/ob}Akt1^{-/-}$ mice, which should have approximately the same amount of residual Akt as $Lep^{ob/ob}Akt2^{+/-}$ mice, and therefore would have a similar rate of *de novo* lipogenesis.

Having established the presence of Akt2 in the pathway regulating hepatic lipogenesis, the next step is defining what is downstream. There appear to be both *SREBP1c* expression-dependent and –independent influences of Akt2 on *de novo* lipogenesis. Since the start of this thesis, mTOR has emerged as a likely downstream target of insulin signaling for the regulation of *SREBP1c* expression, though most of the published studies have relied upon chemical inhibitors of mTOR. Inhibition of mTOR by rapamycin in isolated rat hepatocytes results in decreased *de novo* lipogenesis and blocks insulin-stimulated *SREBP1c* expression; the latter is also blocked by rapamycin in fasted/refed rats (Brown et al., 2007; Li et al., 2010). Additionally, rapamycin blocks myr-Akt-induced SREBP1 processing, *SREBP1, FAS* and *ACL* expression and increase in *de novo* lipogenesis *in vitro* (Porstmann et al., 2008). However, further *in vivo* studies are required to determine if mTOR is a distal mediator of insulin's control of SREBP1c

and lipogenesis. We have already done preliminary studies in liver-specific *Raptor* null mice that are deficient in mTORC1 signaling, and have found that these mice have decreased *SREBP1c, FAS, SCD1,* and *ACL* expression under random fed conditions (unpublished data in collaboration with Dr. Min Wan). We plan on measuring *de novo* lipogenesis in these mice, and hope to use them to further define the pathway through which insulin/Akt regulates lipogenesis.

The definition of *SREBP1c*-independent influences of Akt2 signaling on *de novo* lipogenesis may prove more difficult. As discussed above, these could include the regulation of SREBP1c processing, which could be determined by nuclear fractionization and Western blotting, or modulation of lipogenic enzyme activities. Activities of FAS, ACC and ACL could be measured in either liver samples or isolated hepatocytes to assess if the absence of Akt2 has an effect. Additionally, we are planning on injecting liver-specific *Raptor* null mice with adenovirus expressing myr-Akt, which induces massive hepatic steatosis and hypertriglyceridemia (Ono et al., 2003). If Raptor-deficiency in the liver results in a complete reversal of the myr-Akt-induced hepatic steatosis, then it is unlikely that Akt2 has any direct effects on protein processing or activity. However, if there is still a residual effect of myr-Akt in the absence of Raptor on the liver, this will give us insight into those pathways that are mTOR- and possibly *SREBP1c*-independent.

The role of extrahepatic Akt2

The entire contribution of hepatic Akt2 to metabolism has not been fully elucidated in the studies described in this thesis. For example, we continually see a decrease in serum cholesterol in the absence of Akt2: serum cholesterol is reduced in both *Akt2*$^{-/-}$ and *AFP;Akt2*$^{lox/lox}$ mice on an *ob/ob* background, in *Akt2*$^{-/-}$ mice on Surwit

HFD, and in *Akt2*$^{lox/lox}$ mice on lard HFD following AAV-Cre injection. This is likely due to a role of hepatic Akt2, yet we have no data as to the mechanism. Additionally, hepatic Akt2 determines liver weight in response to HCD-refeeding by some unknown influence; hepatic Akt2 also has a non-autonomous effect on whole-body size of the *ob/ob* mouse. All of these observations warrant further investigation beyond the scope of this thesis.

Another question not fully elucidated in these studies is the role of Akt2 in extrahepatic tissues in the control of metabolism. As mentioned above, whole-body *Akt2*$^{-/-}$ mice exhibited a much more severe diabetic phenotype than *AFP;Akt2*$^{lox/lox}$ mice did on an *ob/ob* background. *ob/ob* mice null for *Akt2* also had elevated serum triglyceride levels, whereas *ob/ob* mice with liver-specific deletion of Akt2 exhibited normal or reduced circulating triglycerides. A recent study examining lipid abnormalities in humans with genetic syndromes of insulin resistance reported increased liver fat content, lipogenesis, serum triglycerides, and other severe metabolic abnormalities in several individuals with a dominant-negative mutation in *Akt2* (Semple et al., 2009). This emphasizes the role of non-hepatic tissues in determining glucose and lipid metabolism and the difficulties in interpreting data in the context of whole-body metabolism. Perhaps the most striking unexplained observation is the phenotype of *Akt2*$^{-/-}$ mice on Surwit HFD: these mice gained significantly less weight on Surwit HFD compared with their *Akt2*$^{+/+}$ counterparts, predominately due to their failure to gain fat mass. This phenotype cannot be explained by loss of hepatic Akt2 as *AFP;Akt2*$^{lox/lox}$ gain normal body weight and fat mass on Surwit HFD. Therefore, while our understanding of the role of hepatic Akt2 in the regulation of metabolism is advancing, partially due to the studies described in this thesis, our understanding of the role of Akt2 in other metabolic tissues requires further investigation.

Figure 5-1: Proposed model of Akt action

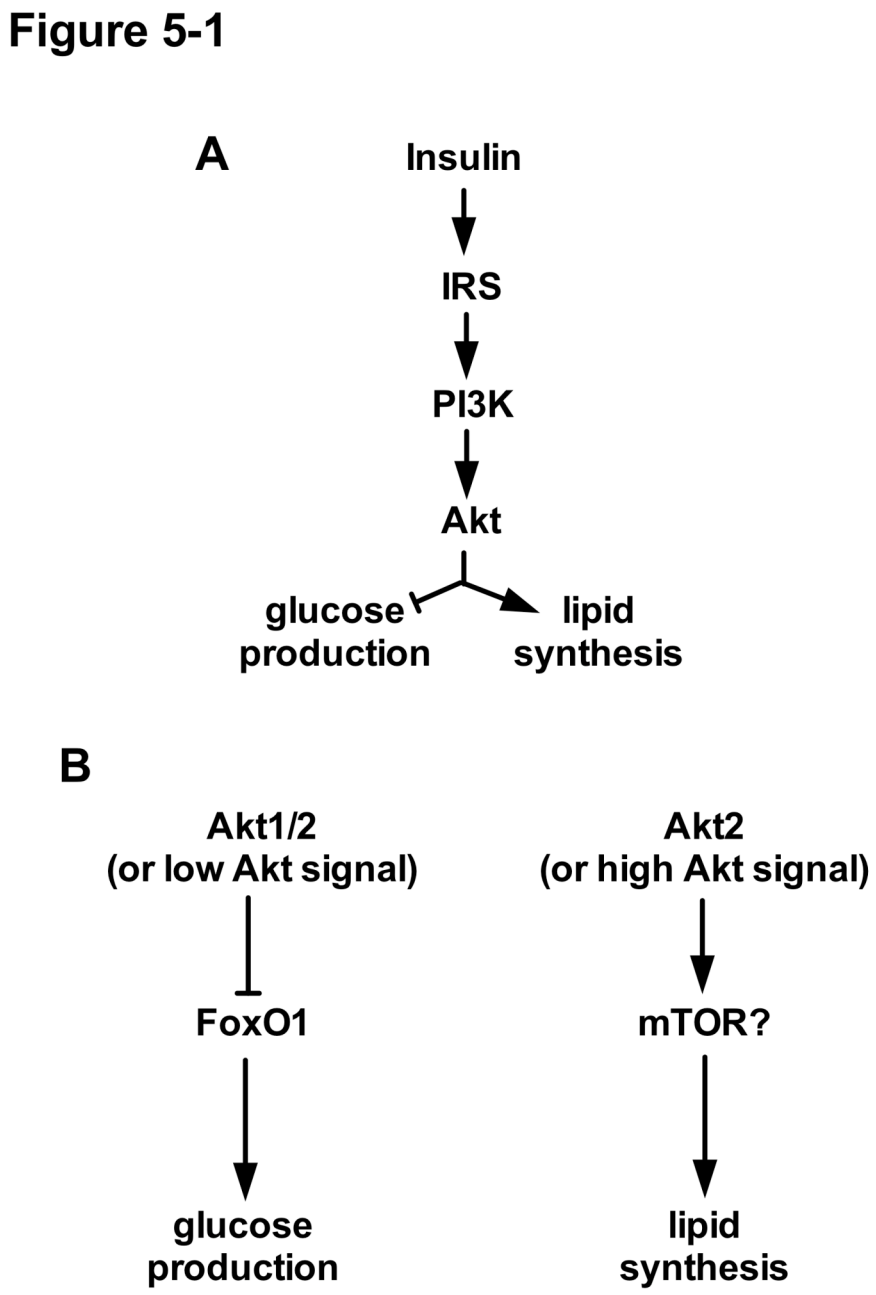

Chapter 6:

Materials and Methods

Animals

All animals were raised and treated with approval from the University of Pennsylvania in accordance with NIH guidelines. Male mice were used for all studies. Mice were reared on normal chow fed *ad libitum* unless otherwise noted under 12 hour light:dark cycles (7am:7pm) in a barrier facility. The generation of a conditional allele of *Akt2* and derivation of *Akt2* null mice have been described previously (Cho et al., 2001a). $Akt2^{-/-}$ mice were backcrossed ten generations or more to C57BL/6J mice. $Lep^{ob/+}$ mice on a C57BL/6J background were purchased from Jackson Laboratories. To generate $Akt2^{lox/lox}$ mice, mice described by Cho et al prior to *loxP* mediated recombination were mated to mice expressing a variant of the Saccharomyces cerevisiae FLP1 recombinase gene under the direction of the Gt(ROSA)26Sor promoter (FLPeR) (Jackson Laboratories), thus excising the neomycin selection cassette (Cho et al., 2001a). The *AFP Cre* mouse line was generously provided by Dr. Klaus Kaestner (Zhang et al., 2005). All $Akt2^{lox/lox}$ mice used were of a mixed background, with the exception of $Akt2^{lox/lox}$ and $Lep^{ob/ob}Akt2^{lox/lox}$ mice injected with AAVs, which had been backcrossed ten generations or more to C57BL/6J mice at that point.

Mice were fed specialized diets as noted starting at 5-6 weeks of age: composition of diets is included below as Tables 6-2 through 6-5. For fasting/refeeding protocol, mice were first acclimated to high-carbohydrate diet for 2-4 days, fasted overnight starting at 4pm, and refed at 10am the following morning for the described intervals prior to sacrifice.

Metabolic measurements and analytical procedures

All blood glucose measurements were made using a glucometer (OneTouch Ultra, Lifescan). Insulin assays were conducted on blood collected from mice by tail

bleed into heparinized tubes using an ELISA kit (Ultra Sensitive Rat or Mouse Insulin ELISA kit, Crystal Chem, Inc.). Serum triglycerides, cholesterol, free fatty acids (NEFA), and ketone bodies were analyzed from blood collected after sacrifice by cardiac puncture using colorimetric assay kits (Infinity TG and CH reagents, ThermoDMA, Inc; NEFA-HR kit, Wako; β-hydroxybutyrate LiquiColor kit, Stanbio Laboratories, respectively).

Hepatic triglycerides were measured from animals sacrificed by CO_2 inhalation, snap-frozen in liquid nitrogen, and stored at -80ºC until processed. Frozen livers were weighted and homogenized in lysis buffer (140mM NaCl, 50mM Tris, 0.1% Triton-X) using a Tissuelyser (Qiagen). Liver homogenates were then incubated at 37ºC with 1% deoxycholate, and triglycerides measured colorimetrically using Infinity Triglyceride Reagent (ThermoDMA, Inc). The same homogenates were used to measure hepatic protein content using a bicinchoninic Acid (BCA) assay (Thermo Scientific). Liver glycogen was measured using a 6% perchloric acid (PCA) extraction, followed by an amyloglucosidase digestion; glucose both from liver (pre-digestion) and glycogen (post-digestion) were analyzed using a hexokinase-based assay kit (Glucose (HK) Assay Kit from Sigma).

Hepatic long-chain fatty acyl-CoAs were isolated as previously described and measured by using an API 4000 tandem mass spectrometer (Applied Biosystems) in conjunction with 2 PerkinElmer 200 Series micro pumps and a 200 Series autosampler (PerkinElmer) (Neschen et al., 2005). This was performed in the laboratory of Gerald Shulman of Yale School of Medicine.

Adeno-associated virus (AAV) injections

In order to acutely excise Akt2, *Akt2*$^{lox/lox}$ and *Lep*$^{ob/ob}$*Akt2*$^{lox/lox}$ mice were injected with AAV2/8 expressing green fluorescent protein (GFP) or Cre recombinase under the control of the tyroxine-binding globulin (TBG) promoter. Mice were anesthetized using isoflurane, and injected retro-orbitally with 100µl of virus diluted in phospho-buffered saline (PBS) so that each mouse received a titer of 1e^{12} GC/ml. Viruses were produced by the Penn Vector Core of the Gene Therapy Program at the University of Pennsylvania.

Glucose tolerance tests (GTT) and insulin tolerance tests (ITT)

For GTT, mice were fasted overnight (approximately 5pm to 9am). 20% dextrose was injected intraperitoneally or gavaged in a dose of 1g/kg body weight. Blood glucose was measured from tail bleed at 0, 15, 30, 60 and 120 minutes, and blood was collected in heparinized tubes for insulin measurement at 0 and 15 minutes. Food was returned to animals at the end of experiment.

For ITT, mice were fasted for 5 hours (approximately 9am to 2pm). Insulin was injected intraperitoneally or subcutaneously at 1U/kg or 2U/kg body weight (Humilin, Lilly). Blood glucose was measured at 0, 15, 30, 60 and 120 minutes post injection by tail bleed. 20% glucose was on hand to give to if mouse's blood glucose level dropped below 20mg/dl. Food was returned to animals at the end of experiment.

***De novo* lipogenesis assay**

The protocols for ^{2}H-Labeling of body water, ^{2}H-Labeling and concentration of total palmitate, and rate of lipid synthesis were provided by Dr. Stephen Previs of Case Western Reserve University School of Medicine. GC/MS analysis was performed by Dr. Previs for all *ob/ob* mice and by Dr. John Millar of the GC/MS Resource of the Institute of

Diabetes, Obesity and Metabolism at the University of Pennsylvania School of Medicine for the fasted/refeeding experiment.

Animal procedure. Male mice were fasted for 5 hours (8am to 1pm), injected with D_2O (400µl per 20g body wt), and sacrificed 3 hours later. Blood was collected by cutting the aorta/IVC, using the diaphragm as a barrier to the peritoneal cavity. Liver was removed and snap-frozen in liquid nitrogen.

^{2}H-Labeling of body water. The ^{2}H-labeling of body water was determined by exchange with acetone (Yang et al., 1998). Briefly, samples were centrifuged for 1 min at ~ 12,000 g in a microcentrifuge, 40 µl of sample (or standard) was reacted with 2 µl of 10 N NaOH and 4 µl of a 5% (v/v) solution of acetone in acetonitrile for 24 h at room temperature. Acetone was then extracted by addition of 600 µl of chloroform followed by addition of ~ 0.5 g Na_2SO_4. Samples were vigorously mixed and a small aliquot of the chloroform was transferred to a GC-MS vial. Acetone was analyzed using an Agilent 5973N-MSD equipped with an Agilent 6890 GC system, a DB-17MS capillary column (30 m x 0.25 mm x 0.25 µm) was used in all analyses. The temperature program was as follows: 60ºC initial, increase by 20ºC per min to 100ºC, increase by 50ºC per min to 220ºC and hold for 1 min. The sample was injected at a split ratio of 40:1 with a helium flow of 1 ml per min. Acetone eluted at ~ 1.5 min. The mass spectrometer was operated in the electron impact mode (70 eV). Selective ion monitoring of m/z 58 and 59 was performed using a dwell time of 10 ms per ion.

^{2}H-Labeling and concentration of total palmitate. A known quantity of tissue was hydrolyzed and extracted, after adding a known amount of heptadecanoic acid.

Palmitate was analyzed as its trimethylsilyl derivative using gas chromatography-electron impact ionization mass spectrometry. The oven temperature was initially held for 1 min at 150° C, then increased by 20° C per min to 310° C and maintained for 8 min. The split ratio was 20:1 with helium flow 1 ml per min. The inlet temperature was set at 270° C and MS transfer line was set at 310° C. Under these conditions, palmitate elutes at ~ 5.7 min. The ^{2}H-enrichment was determined by using selective ion monitoring under electron impact ionization of m/z 313 and 314 (M+0 and M+1), 10 ms dwell time per ion (Brunengraber et al., 2003). The concentration of palmitate was determined by comparing the corrected abundance of m/z 313 to 314 to that of heptadecanoate (17:0, m/z 327). To account for possible differences in the ionization efficiency of each fatty acid, the profile was compared against standards prepared by mixing known quantities of each fatty acid (Brunengraber et al., 2003).

Rate of lipid synthesis. The percent contribution of newly made palmitate was determined using the equation:

% newly made palmitate = [total ^{2}H-labeling palmitate / (^{2}H-labeling body water x n)] x 100

where *n* is the number of exchangeable hydrogens, assumed to equal 22 (Diraison et al., 1997; Lee et al., 1994a; Lee et al., 1994b). The absolute amount of newly made palmitate was determined by multiplying the % newly made palmitate by the concentration of palmitate.

Hyperinsulinemic euglycemic clamps, body composition, food intake, and RER

Hyperinsulinemic euglycemic clamps**,** body composition (with the exception of that in *Lep$^{ob/ob}$Akt2$^{-/-}$* mice), food intake, and RER were performed by the Mouse

Phenotyping, Physiology and Metabolism Core at the University of Pennsylvania School of Medicine. Body composition was determined in conscious mice by nuclear MRI analysis (Echo Medical Systems); food intake and RER were assessed under conditions of free access to food and water using Comprehensive Laboratory Animal Monitoring System (CLAMS; Columbus Instruments). Oxygen consumption (VO_2) and carbon dioxide production (VCO_2) were measured in CLAMS and used to calculate respiratory quotient/RER. Body composition of *Lep*$^{ob/ob}$*Akt2*$^{-/-}$ mice was measured using the ^{2}H-labeling of body water (determination described above in *de novo* lipogenesis assay) by a known amount of injected D_2O relative to body weight as a determination of lean mass as previously described (McCabe et al., 2006).

RNA isolation and gene expression studies

Total RNA was prepared from liver using Trizol reagent (Invitrogen), followed by chloroform extraction and DNAse treatment (DNA-free kit, Ambion). cDNA was synthesized with random decamers using the RetroScript Kit (Ambion) and mixed with Brilliant SYBR Green QPCR Master Mix (Stratagene), and primers as noted in Table 6-1. Reactions were performed on an Mx3000P Quantitative PCR System (Stratagene). The relative amounts of specific transcripts were calculated using TATA binding protein (*TBP*) mRNA as an invariant control by the comparative C_T (ddC_T) method, with the control genotype set to 1.0 (either *Lep*$^{+/+}$ *Akt2*$^{lox/lox}$ or *Akt2*$^{lox/lox}$ chow-fed).

Western blotting

Mice were sacrificed and tissues snap-frozen in liquid nitrogen and stored at -80^0 C until being homogenized by Tissuelyser (Qiagen) in lysis buffer containing 140 mM NaCl, 50 mM Tris, 0.1% Triton-X, 400 mM NaF, 1x Complete protease inhibitor mixture

(Roche Applied Science) and 1x phosphatase inhibitor mixtures 1 and 2 (Sigma). Equivalent amounts of protein were subjected to SDS-polyacrylamide gel electrophoresis (PAGE) followed by transfer to nitrocellulose membranes (Whatman). Blots were probed for Akt1, pAkt (S473), pAkt (T308), PRAS, pFoxO1 (S256), FoxO1, pGSK3β (S9), pTSC2 (T1462) (Cell Signaling Technology), pPRAS (T246) (Invitrogen Corporation), GSK3α/β (Santa Cruz Biotechnology, Inc) Akt2, actin (Abcam, INC) and/or tubulin (Sigma Chemical Co) followed by horseradish peroxidase-conjugated secondary antibodies (Santa Cruz Biotechnology, Inc).

Statistics

Data are presented as mean ± SEM. Data were analyzed using one-way ANOVA using Newman-Keuls post-test, two-way ANOVA using Bonferroni post-test, or Student's t-test assuming unequal variance with 2-tailed analysis as described in the figure legends. Values of $p < 0.05$ were defined as statistically significant.

Table 6-1: Real-Time PCR primers

Sterol regulatory-element binding protein 1c (SREBP1c)	AGG CTG TAG GAT GGT GAG TGG	ACG GAG CCA TGG ATT GCA CAT TTG
Stearoyl-CoA desaturase-1 (SCD1)	CCG GAG ACC CCT TAG ATC GA	TAG CCT GTA AAA GAT TTC TGC AAA CC
Fatty acid synthase (FAS)	GCT GCG GAA ACT TCA GGA AAT	AGA GAC GTG TCA CTC CTG GAC TT
Acetyl-CoA carboxylase (ACC)	TGA CAG ACT GAT CGC AGA GAA AG	TGG AGA GCC CCA CAC ACA
ATP citrate lyase (ACL)	GCC AGC GGG AGC ACA TC	CTT TGC AGG TGC CAC TTC ATC
Glycerol phosphate acyltransferase (GPAT)	CAA CAC CAT CCC CGA CAT C	GTG ACC TTC GAT TAT GCG ATC A
Glucokinase (GCK)	GAA GAC CTG AAG AAG GTG ATG AGC	GTC TAT GTC TTC GTG CCT TAC AGG
Carbohydrate regulatory-element binding protein (ChREBP)	CTG GGG ACC TAA ACA GGA GC	GAA GCC ACC CTA TAG CTC CC
Pyruvate kinase, liver isoform (L-PK)	CTT GCT CTA CCG TGA GCC TC	ACC ACA ATC ACC AGA TCA CC
Peroxisome proliferator-activated receptor- γ (PPARγ)	GTG CCA GTT TCG ATC CGT AGA	GGC CAG CAT CGT GTA GAT GA

Cidec/Fsp27	CAG AAG CCA ACT AAG AAG ATC G	TGT AGC AGT GCA GGT CAT AG
Peroxisome proliferators-activated receptorγ-coactivator 1α (PGC-1α)	GAG AAT GAG GCA AAC TTG CTA GCG	TGC ATG GTT CTG AGT GCT AAG ACC
Carnitine palmitoyltransferase I (CPT1)	GCA GAG GCT CAC CAA GCT GTG	CTT CGT CTG GCT TGA CAT GCG
Medium-chain acetyl-CoA dehydrogenase (MCAD)	TAC CCG TTC CCT CTC ATC AA	CTT CTT CTC TGC TTT GGT CTT
Cytochrome c oxidase subunit 7a (Cox7a)	GCT GCT GAG GAC GCA AAA TGA GG	CCA TTC CCC CGC CTT TCA AG

Table 6-2: Composition of normal chow diet (Laboratory Rodent Diet #5001 from LabDiets)

	% kcal
Protein	28.5
Fat	13.5
Carbohydrates	58.0

Ingredients: ground corn, dehulled soybean meal, dried beet pulp, fish meal, ground oats, brewers dried yeast, cane molasses, dehydrated alfalfa meal, dried why, wheat germ, porcine animals fat preserved with BHA, porcine meat meal, wheat middlings, salt, calcium carbonate, DL-methionine, choline chloride, cholecalciferol, vitamin A acetate, folic acid, menadione dimethylpryimidinol bisulfite, pyridoxine hydrochloride, thiamin mononitrate, nicotinic acid, calcium pantothenate, dl-alpha tocopheryl acetate, vitamin B_{12} supplement, riboflavin, ferrous sulfate, manganeous oxide, zinc oxide, ferrous carbonate, copper sulfate, zine sulfate, calcium iodate, cobalt carbonate, sodium selenite.

Diet information reproduced from labdiet.com

Table 6-3: Composition of Surwit high fat diet (Research Diets, INC #D12331)

	% kcal
Protein	16.4
Fat	58.0
Carbohydrates	25.5

Ingredient	Grams	kcal
Casein	228	912
DL-Methionine	2	0
Maltodextrin 10	170	680
Corn Starch	0	0
Sucrose	175	700
Soybean Oil	25	225
Coconut Oil, Hydrogenated	333.5	3001.5
Mineral Mix	40	0
Sodium Bicarbonate	10.5	0
Potassium Citrate	4	0
Vitamin Mix	10	40
Choline Bitartrate	2	0

Diet information reproduced from ResearchDiets.com

Table 6-4: Composition of lard high fat diet (Research Diets, INC #D12492)

	% kcal
Protein	20.0
Fat	60.0
Carbohydrates	20.0

Ingredient	Grams	kcal
Casein	200	800
L-Cystine	3	12
Corn Starch	0	0
Maltodextrin 10	125	500
Sucrose	68.8	275.2
Cellulose	50	0
Soybean Oil	25	225
Lard	245	2205
Mineral Mix	10	0
Dicalcium Phosphate	13	0
Calcium Carbonate	5.5	0
Potassium Citrate	16.5	0
Vitamin Mix	10	40
Choline Bitartrate	2	0

Diet information reproduced from ResearchDiets.com

Table 6-5: Composition of high carbohydrate diet (Research Diets, INC #D12450B)

	% kcal
Protein	20.0
Fat	10.0
Carbohydrates	70.0

Ingredient	**Grams**	**kcal**
Casein	200	800
L-Cystine	3	12
Corn Starch	315	1260
Maltodextrin 10	35	140
Sucrose	350	1400
Cellulose	50	0
Soybean Oil	25	225
Lard	20	180
Mineral Mix	10	0
Dicalcium Phosphate	13	0
Calcium Carbonate	5.5	0
Potassium Citrate	16.5	0
Vitamin Mix	10	40
Choline Bitartrate	2	0

Diet information reproduced from ResearchDiets.com

References

Abe, H., Yamada, N., Kamata, K., Kuwaki, T., Shimada, M., Osuga, J., Shionoiri, F., Yahagi, N., Kadowaki, T., Tamemoto, H., Ishibashi, S., Yazaki, Y., and Makuuchi, M. (1998). Hypertension, hypertriglyceridemia, and impaired endothelium-dependent vascular relaxation in mice lacking insulin receptor substrate-1. J Clin Invest 101, 1784-1788.

Adeli, K., Taghibiglou, C., Van Iderstine, S.C., and Lewis, G.F. (2001). Mechanisms of hepatic very low-density lipoprotein overproduction in insulin resistance. Trends Cardiovasc Med 11, 170-176.

Ahima, R.S., and Osei, S.Y. (2004). Leptin signaling. Physiol Behav 81, 223-241.

Ahren, B. (2005). Type 2 diabetes, insulin secretion and beta-cell mass. Current molecular medicine 5, 275-286.

Alessi, D.R., James, S.R., Downes, C.P., Holmes, A.B., Gaffney, P.R., Reese, C.B., and Cohen, P. (1997). Characterization of a 3-phosphoinositide-dependent protein kinase which phosphorylates and activates protein kinase Balpha. Curr Biol 7, 261-269.

Altomonte, J., Cong, L., Harbaran, S., Richter, A., Xu, J., Meseck, M., and Dong, H.H. (2004). Foxo1 mediates insulin action on apoC-III and triglyceride metabolism. J Clin Invest 114, 1493-1503.

Angulo, P. (2002). Nonalcoholic fatty liver disease. N Engl J Med 346, 1221-1231.

Araki, E., Lipes, M.A., Patti, M.E., Bruning, J.C., Haag, B., 3rd, Johnson, R.S., and Kahn, C.R. (1994). Alternative pathway of insulin signalling in mice with targeted disruption of the IRS-1 gene. Nature 372, 186-190.

Azain, M.J., Fukuda, N., Chao, F.F., Yamamoto, M., and Ontko, J.A. (1985). Contributions of fatty acid and sterol synthesis to triglyceride and cholesterol secretion by the perfused rat liver in genetic hyperlipemia and obesity. J Biol Chem 260, 174-181.

Becard, D., Hainault, I., Azzout-Marniche, D., Bertry-Coussot, L., Ferre, P., and Foufelle, F. (2001). Adenovirus-mediated overexpression of sterol regulatory element binding protein-1c mimics insulin effects on hepatic gene expression and glucose homeostasis in diabetic mice. Diabetes 50, 2425-2430.

Bengoechea-Alonso, M.T., and Ericsson, J. (2009). A phosphorylation cascade controls the degradation of active SREBP1. J Biol Chem 284, 5885-5895.

Biddinger, S.B., Hernandez-Ono, A., Rask-Madsen, C., Haas, J.T., Aleman, J.O., Suzuki, R., Scapa, E.F., Agarwal, C., Carey, M.C., Stephanopoulos, G., Cohen, D.E.,

King, G.L., Ginsberg, H.N., and Kahn, C.R. (2008). Hepatic insulin resistance is sufficient to produce dyslipidemia and susceptibility to atherosclerosis. Cell Metab 7, 125-134.
Black, B.L., Croom, J., Eisen, E.J., Petro, A.E., Edwards, C.L., and Surwit, R.S. (1998). Differential effects of fat and sucrose on body composition in A/J and C57BL/6 mice. Metabolism 47, 1354-1359.
Bray, G.A., and York, D.A. (1979). Hypothalamic and genetic obesity in experimental animals: an autonomic and endocrine hypothesis. Physiol Rev 59, 719-809.
Brown, M.S., and Goldstein, J.L. (2008). Selective versus total insulin resistance: a pathogenic paradox. Cell Metab 7, 95-96.
Brown, N.F., Stefanovic-Racic, M., Sipula, I.J., and Perdomo, G. (2007). The mammalian target of rapamycin regulates lipid metabolism in primary cultures of rat hepatocytes. Metabolism 56, 1500-1507.
Browning, J.D., and Horton, J.D. (2004). Molecular mediators of hepatic steatosis and liver injury. J Clin Invest 114, 147-152.
Brunengraber, D.Z., McCabe, B.J., Kasumov, T., Alexander, J.C., Chandramouli, V., and Previs, S.F. (2003). Influence of diet on the modeling of adipose tissue triglycerides during growth. Am J Physiol Endocrinol Metab 285, E917-925.
Brunet, A., Bonni, A., Zigmond, M.J., Lin, M.Z., Juo, P., Hu, L.S., Anderson, M.J., Arden, K.C., Blenis, J., and Greenberg, M.E. (1999). Akt promotes cell survival by phosphorylating and inhibiting a Forkhead transcription factor. Cell 96, 857-868.
Buettner, R., Parhofer, K.G., Woenckhaus, M., Wrede, C.E., Kunz-Schughart, L.A., Scholmerich, J., and Bollheimer, L.C. (2006). Defining high-fat-diet rat models: metabolic and molecular effects of different fat types. J Mol Endocrinol 36, 485-501.
Burgess, S.C., He, T., Yan, Z., Lindner, J., Sherry, A.D., Malloy, C.R., Browning, J.D., and Magnuson, M.A. (2007). Cytosolic phosphoenolpyruvate carboxykinase does not solely control the rate of hepatic gluconeogenesis in the intact mouse liver. Cell Metab 5, 313-320.
Burgess, S.C., Iizuka, K., Jeoung, N.H., Harris, R.A., Kashiwaya, Y., Veech, R.L., Kitazume, T., and Uyeda, K. (2008). Carbohydrate-response element-binding protein deletion alters substrate utilization producing an energy-deficient liver. J Biol Chem 283, 1670-1678.

Carpentier, A., Taghibiglou, C., Leung, N., Szeto, L., Van Iderstine, S.C., Uffelman, K.D., Buckingham, R., Adeli, K., and Lewis, G.F. (2002). Ameliorated hepatic insulin resistance is associated with normalization of microsomal triglyceride transfer protein expression and reduction in very low density lipoprotein assembly and secretion in the fructose-fed hamster. J Biol Chem 277, 28795-28802.

Cha, J.Y., and Repa, J.J. (2007). The liver X receptor (LXR) and hepatic lipogenesis. The carbohydrate-response element-binding protein is a target gene of LXR. J Biol Chem 282, 743-751.

Chen, G., Liang, G., Ou, J., Goldstein, J.L., and Brown, M.S. (2004). Central role for liver X receptor in insulin-mediated activation of Srebp-1c transcription and stimulation of fatty acid synthesis in liver. Proc Natl Acad Sci U S A 101, 11245-11250.

Chen, W.S., Peng, X.D., Wang, Y., Xu, P.Z., Chen, M.L., Luo, Y., Jeon, S.M., Coleman, K., Haschek, W.M., Bass, J., Philipson, L.H., and Hay, N. (2009). Leptin deficiency and beta-cell dysfunction underlie type 2 diabetes in compound Akt knockout mice. Mol Cell Biol.

Chen, W.S., Xu, P.Z., Gottlob, K., Chen, M.L., Sokol, K., Shiyanova, T., Roninson, I., Weng, W., Suzuki, R., Tobe, K., Kadowaki, T., and Hay, N. (2001). Growth retardation and increased apoptosis in mice with homozygous disruption of the Akt1 gene. Genes Dev 15, 2203-2208.

Chirieac, D.V., Chirieac, L.R., Corsetti, J.P., Cianci, J., Sparks, C.E., and Sparks, J.D. (2000). Glucose-stimulated insulin secretion suppresses hepatic triglyceride-rich lipoprotein and apoB production. Am J Physiol Endocrinol Metab 279, E1003-1011.

Chirieac, D.V., Davidson, N.O., Sparks, C.E., and Sparks, J.D. (2006). PI3-kinase activity modulates apo B available for hepatic VLDL production in apobec-1-/- mice. Am J Physiol Gastrointest Liver Physiol 291, G382-388.

Cho, H., Mu, J., Kim, J.K., Thorvaldsen, J.L., Chu, Q., Crenshaw, E.B., 3rd, Kaestner, K.H., Bartolomei, M.S., Shulman, G.I., and Birnbaum, M.J. (2001a). Insulin resistance and a diabetes mellitus-like syndrome in mice lacking the protein kinase Akt2 (PKB beta). Science 292, 1728-1731.

Cho, H., Thorvaldsen, J.L., Chu, Q., Feng, F., and Birnbaum, M.J. (2001b). Akt1/PKBalpha is required for normal growth but dispensable for maintenance of glucose homeostasis in mice. J Biol Chem 276, 38349-38352.

Chong, M.F., Hodson, L., Bickerton, A.S., Roberts, R., Neville, M., Karpe, F., Frayn, K.N., and Fielding, B.A. (2008). Parallel activation of de novo lipogenesis and stearoyl-CoA desaturase activity after 3 d of high-carbohydrate feeding. Am J Clin Nutr 87, 817-823.

Cochran, E., Young, J.R., Sebring, N., DePaoli, A., Oral, E.A., and Gorden, P. (2004). Efficacy of recombinant methionyl human leptin therapy for the extreme insulin resistance of the Rabson-Mendenhall syndrome. J Clin Endocrinol Metab 89, 1548-1554.

Cohen, P., Miyazaki, M., Socci, N.D., Hagge-Greenberg, A., Liedtke, W., Soukas, A.A., Sharma, R., Hudgins, L.C., Ntambi, J.M., and Friedman, J.M. (2002). Role for stearoyl-CoA desaturase-1 in leptin-mediated weight loss. Science 297, 240-243.

Collins, S., Martin, T.L., Surwit, R.S., and Robidoux, J. (2004). Genetic vulnerability to diet-induced obesity in the C57BL/6J mouse: physiological and molecular characteristics. Physiol Behav 81, 243-248.

Cross, D.A., Alessi, D.R., Cohen, P., Andjelkovich, M., and Hemmings, B.A. (1995). Inhibition of glycogen synthase kinase-3 by insulin mediated by protein kinase B. Nature 378, 785-789.

Denechaud, P.D., Bossard, P., Lobaccaro, J.M., Millatt, L., Staels, B., Girard, J., and Postic, C. (2008). ChREBP, but not LXRs, is required for the induction of glucose-regulated genes in mouse liver. J Clin Invest 118, 956-964.

Dentin, R., Benhamed, F., Hainault, I., Fauveau, V., Foufelle, F., Dyck, J.R., Girard, J., and Postic, C. (2006). Liver-specific inhibition of ChREBP improves hepatic steatosis and insulin resistance in ob/ob mice. Diabetes 55, 2159-2170.

Dentin, R., Pegorier, J.P., Benhamed, F., Foufelle, F., Ferre, P., Fauveau, V., Magnuson, M.A., Girard, J., and Postic, C. (2004). Hepatic glucokinase is required for the synergistic action of ChREBP and SREBP-1c on glycolytic and lipogenic gene expression. J Biol Chem 279, 20314-20326.

Diraison, F., and Beylot, M. (1998). Role of human liver lipogenesis and reesterification in triglycerides secretion and in FFA reesterification. Am J Physiol 274, E321-327.

Diraison, F., Dusserre, E., Vidal, H., Sothier, M., and Beylot, M. (2002). Increased hepatic lipogenesis but decreased expression of lipogenic gene in adipose tissue in human obesity. Am J Physiol Endocrinol Metab 282, E46-51.

Diraison, F., Moulin, P., and Beylot, M. (2003). Contribution of hepatic de novo lipogenesis and reesterification of plasma non esterified fatty acids to plasma triglyceride synthesis during non-alcoholic fatty liver disease. Diabetes Metab 29, 478-485.
Diraison, F., Pachiaudi, C., and Beylot, M. (1997). Measuring lipogenesis and cholesterol synthesis in humans with deuterated water: use of simple gas chromatographic/mass spectrometric techniques. J Mass Spectrom 32, 81-86.
Dong, X.C., Copps, K.D., Guo, S., Li, Y., Kollipara, R., DePinho, R.A., and White, M.F. (2008). Inactivation of hepatic Foxo1 by insulin signaling is required for adaptive nutrient homeostasis and endocrine growth regulation. Cell Metab 8, 65-76.
Donnelly, K.L., Smith, C.I., Schwarzenberg, S.J., Jessurun, J., Boldt, M.D., and Parks, E.J. (2005). Sources of fatty acids stored in liver and secreted via lipoproteins in patients with nonalcoholic fatty liver disease. J Clin Invest 115, 1343-1351.
Easton, R.M., Cho, H., Roovers, K., Shineman, D.W., Mizrahi, M., Forman, M.S., Lee, V.M., Szabolcs, M., de Jong, R., Oltersdorf, T., Ludwig, T., Efstratiadis, A., and Birnbaum, M.J. (2005). Role for Akt3/protein kinase Bgamma in attainment of normal brain size. Mol Cell Biol 25, 1869-1878.
Estall, J.L., Kahn, M., Cooper, M.P., Fisher, F.M., Wu, M.K., Laznik, D., Qu, L., Cohen, D.E., Shulman, G.I., and Spiegelman, B.M. (2009). Sensitivity of lipid metabolism and insulin signaling to genetic alterations in hepatic peroxisome proliferator-activated receptor-gamma coactivator-1alpha expression. Diabetes 58, 1499-1508.
Farooqi, I.S., Jebb, S.A., Langmack, G., Lawrence, E., Cheetham, C.H., Prentice, A.M., Hughes, I.A., McCamish, M.A., and O'Rahilly, S. (1999). Effects of recombinant leptin therapy in a child with congenital leptin deficiency. N Engl J Med 341, 879-884.
Fleischmann, M., and Iynedjian, P.B. (2000). Regulation of sterol regulatory-element binding protein 1 gene expression in liver: role of insulin and protein kinase B/cAkt. Biochem J 349, 13-17.
Flowers, J.B., Rabaglia, M.E., Schueler, K.L., Flowers, M.T., Lan, H., Keller, M.P., Ntambi, J.M., and Attie, A.D. (2007). Loss of stearoyl-CoA desaturase-1 improves insulin sensitivity in lean mice but worsens diabetes in leptin-deficient obese mice. Diabetes 56, 1228-1239.
Forcheron, F., Cachefo, A., Thevenon, S., Pinteur, C., and Beylot, M. (2002). Mechanisms of the triglyceride- and cholesterol-lowering effect of fenofibrate in hyperlipidemic type 2 diabetic patients. Diabetes 51, 3486-3491.

Foretz, M., Guichard, C., Ferre, P., and Foufelle, F. (1999). Sterol regulatory element binding protein-1c is a major mediator of insulin action on the hepatic expression of glucokinase and lipogenesis-related genes. Proc Natl Acad Sci U S A 96, 12737-12742.
Garg, A., Bantle, J.P., Henry, R.R., Coulston, A.M., Griver, K.A., Raatz, S.K., Brinkley, L., Chen, Y.D., Grundy, S.M., Huet, B.A., and et al. (1994). Effects of varying carbohydrate content of diet in patients with non-insulin-dependent diabetes mellitus. JAMA 271, 1421-1428.
Garofalo, R.S., Orena, S.J., Rafidi, K., Torchia, A.J., Stock, J.L., Hildebrandt, A.L., Coskran, T., Black, S.C., Brees, D.J., Wicks, J.R., McNeish, J.D., and Coleman, K.G. (2003). Severe diabetes, age-dependent loss of adipose tissue, and mild growth deficiency in mice lacking Akt2/PKB beta. J Clin Invest 112, 197-208.
Ginsberg, H.N., Zhang, Y.L., and Hernandez-Ono, A. (2005). Regulation of plasma triglycerides in insulin resistance and diabetes. Arch Med Res 36, 232-240.
Granner, D., and Pilkis, S. (1990). The genes of hepatic glucose metabolism. J Biol Chem 265, 10173-10176.
Gross, D.N., van den Heuvel, A.P., and Birnbaum, M.J. (2008). The role of FoxO in the regulation of metabolism. Oncogene 27, 2320-2336.
Guo, S., Copps, K.D., Dong, X., Park, S., Cheng, Z., Pocai, A., Rossetti, L., Sajan, M., Farese, R.V., and White, M.F. (2009). The Irs1 branch of the insulin signaling cascade plays a dominant role in hepatic nutrient homeostasis. Mol Cell Biol 29, 5070-5083.
Gutierrez-Juarez, R., Pocai, A., Mulas, C., Ono, H., Bhanot, S., Monia, B.P., and Rossetti, L. (2006). Critical role of stearoyl-CoA desaturase-1 (SCD1) in the onset of diet-induced hepatic insulin resistance. J Clin Invest 116, 1686-1695.
Halaas, J.L., Gajiwala, K.S., Maffei, M., Cohen, S.L., Chait, B.T., Rabinowitz, D., Lallone, R.L., Burley, S.K., and Friedman, J.M. (1995). Weight-reducing effects of the plasma protein encoded by the obese gene. Science 269, 543-546.
Haluzik, M., Colombo, C., Gavrilova, O., Chua, S., Wolf, N., Chen, M., Stannard, B., Dietz, K.R., Le Roith, D., and Reitman, M.L. (2004). Genetic background (C57BL/6J versus FVB/N) strongly influences the severity of diabetes and insulin resistance in ob/ob mice. Endocrinology 145, 3258-3264.
Han, S., Liang, C.P., Westerterp, M., Senokuchi, T., Welch, C.L., Wang, Q., Matsumoto, M., Accili, D., and Tall, A.R. (2009). Hepatic insulin signaling regulates VLDL secretion and atherogenesis in mice. J Clin Invest 119, 1029-1041.

Hanada, M., Feng, J., and Hemmings, B.A. (2004). Structure, regulation and function of PKB/AKT--a major therapeutic target. Biochim Biophys Acta 1697, 3-16.
Harada, N., Oda, Z., Hara, Y., Fujinami, K., Okawa, M., Ohbuchi, K., Yonemoto, M., Ikeda, Y., Ohwaki, K., Aragane, K., Tamai, Y., and Kusunoki, J. (2007). Hepatic de novo lipogenesis is present in liver-specific ACC1-deficient mice. Mol Cell Biol 27, 1881-1888.
Hegarty, B.D., Bobard, A., Hainault, I., Ferre, P., Bossard, P., and Foufelle, F. (2005). Distinct roles of insulin and liver X receptor in the induction and cleavage of sterol regulatory element-binding protein-1c. Proc Natl Acad Sci U S A 102, 791-796.
Hillgartner, F.B., Salati, L.M., and Goodridge, A.G. (1995). Physiological and molecular mechanisms involved in nutritional regulation of fatty acid synthesis. Physiol Rev 75, 47-76.
Horie, Y., Suzuki, A., Kataoka, E., Sasaki, T., Hamada, K., Sasaki, J., Mizuno, K., Hasegawa, G., Kishimoto, H., Iizuka, M., Naito, M., Enomoto, K., Watanabe, S., Mak, T.W., and Nakano, T. (2004). Hepatocyte-specific Pten deficiency results in steatohepatitis and hepatocellular carcinomas. J Clin Invest 113, 1774-1783.
Horton, J.D. (2002). Sterol regulatory element-binding proteins: transcriptional activators of lipid synthesis. Biochem Soc Trans 30, 1091-1095.
Horton, J.D., Bashmakov, Y., Shimomura, I., and Shimano, H. (1998a). Regulation of sterol regulatory element binding proteins in livers of fasted and refed mice. Proc Natl Acad Sci U S A 95, 5987-5992.
Horton, J.D., Shimomura, I., Brown, M.S., Hammer, R.E., Goldstein, J.L., and Shimano, H. (1998b). Activation of cholesterol synthesis in preference to fatty acid synthesis in liver and adipose tissue of transgenic mice overproducing sterol regulatory element-binding protein-2. J Clin Invest 101, 2331-2339.
Hresko, R.C., and Mueckler, M. (2005). mTOR.RICTOR is the Ser473 kinase for Akt/protein kinase B in 3T3-L1 adipocytes. J Biol Chem 280, 40406-40416.
Hudgins, L.C., Hellerstein, M., Seidman, C., Neese, R., Diakun, J., and Hirsch, J. (1996). Human fatty acid synthesis is stimulated by a eucaloric low fat, high carbohydrate diet. J Clin Invest 97, 2081-2091.
Hudgins, L.C., Hellerstein, M.K., Seidman, C.E., Neese, R.A., Tremaroli, J.D., and Hirsch, J. (2000). Relationship between carbohydrate-induced hypertriglyceridemia and fatty acid synthesis in lean and obese subjects. J Lipid Res 41, 595-604.

Iizuka, K., Bruick, R.K., Liang, G., Horton, J.D., and Uyeda, K. (2004). Deficiency of carbohydrate response element-binding protein (ChREBP) reduces lipogenesis as well as glycolysis. Proc Natl Acad Sci U S A 101, 7281-7286.
Iizuka, K., Miller, B., and Uyeda, K. (2006). Deficiency of carbohydrate-activated transcription factor ChREBP prevents obesity and improves plasma glucose control in leptin-deficient (ob/ob) mice. Am J Physiol Endocrinol Metab 291, E358-364.
Ingalls, A.M., Dickie, M.M., and Snell, G.D. (1950). Obese, a new mutation in the house mouse. J Hered 41, 317-318.
Iritani, N., Nishimoto, N., Katsurada, A., and Fukuda, H. (1992). Regulation of hepatic lipogenic enzyme gene expression by diet quantity in rats fed a fat-free, high carbohydrate diet. J Nutr 122, 28-36.
Isomaa, B., Almgren, P., Tuomi, T., Forsen, B., Lahti, K., Nissen, M., Taskinen, M.R., and Groop, L. (2001). Cardiovascular morbidity and mortality associated with the metabolic syndrome. Diabetes care 24, 683-689.
Jiang, G., Li, Z., Liu, F., Ellsworth, K., Dallas-Yang, Q., Wu, M., Ronan, J., Esau, C., Murphy, C., Szalkowski, D., Bergeron, R., Doebber, T., and Zhang, B.B. (2005). Prevention of obesity in mice by antisense oligonucleotide inhibitors of stearoyl-CoA desaturase-1. J Clin Invest 115, 1030-1038.
Kamagate, A., Qu, S., Perdomo, G., Su, D., Kim, D.H., Slusher, S., Meseck, M., and Dong, H.H. (2008). FoxO1 mediates insulin-dependent regulation of hepatic VLDL production in mice. J Clin Invest 118, 2347-2364.
Kawaguchi, T., Takenoshita, M., Kabashima, T., and Uyeda, K. (2001). Glucose and cAMP regulate the L-type pyruvate kinase gene by phosphorylation/dephosphorylation of the carbohydrate response element binding protein. Proc Natl Acad Sci U S A 98, 13710-13715.
Kerouz, N.J., Horsch, D., Pons, S., and Kahn, C.R. (1997). Differential regulation of insulin receptor substrates-1 and -2 (IRS-1 and IRS-2) and phosphatidylinositol 3-kinase isoforms in liver and muscle of the obese diabetic (ob/ob) mouse. J Clin Invest 100, 3164-3172.
Khamzina, L., Veilleux, A., Bergeron, S., and Marette, A. (2005). Increased activation of the mammalian target of rapamycin pathway in liver and skeletal muscle of obese rats: possible involvement in obesity-linked insulin resistance. Endocrinology 146, 1473-1481.

Kolterman, O.G., Gray, R.S., Griffin, J., Burstein, P., Insel, J., Scarlett, J.A., and Olefsky, J.M. (1981). Receptor and postreceptor defects contribute to the insulin resistance in noninsulin-dependent diabetes mellitus. J Clin Invest 68, 957-969.
Koo, S.H., Dutcher, A.K., and Towle, H.C. (2001). Glucose and insulin function through two distinct transcription factors to stimulate expression of lipogenic enzyme genes in liver. The Journal of biological chemistry 276, 9437-9445.
Koo, S.H., and Towle, H.C. (2000). Glucose regulation of mouse S(14) gene expression in hepatocytes. Involvement of a novel transcription factor complex. J Biol Chem 275, 5200-5207.
Kubota, N., Kubota, T., Itoh, S., Kumagai, H., Kozono, H., Takamoto, I., Mineyama, T., Ogata, H., Tokuyama, K., Ohsugi, M., Sasako, T., Moroi, M., Sugi, K., Kakuta, S., Iwakura, Y., Noda, T., Ohnishi, S., Nagai, R., Tobe, K., Terauchi, Y., Ueki, K., and Kadowaki, T. (2008). Dynamic functional relay between insulin receptor substrate 1 and 2 in hepatic insulin signaling during fasting and feeding. Cell Metab 8, 49-64.
Kuriyama, H., Liang, G., Engelking, L.J., Horton, J.D., Goldstein, J.L., and Brown, M.S. (2005). Compensatory increase in fatty acid synthesis in adipose tissue of mice with conditional deficiency of SCAP in liver. Cell Metab 1, 41-51.
Le Bacquer, O., Petroulakis, E., Paglialunga, S., Poulin, F., Richard, D., Cianflone, K., and Sonenberg, N. (2007). Elevated sensitivity to diet-induced obesity and insulin resistance in mice lacking 4E-BP1 and 4E-BP2. J Clin Invest 117, 387-396.
Lee, W.N., Bassilian, S., Ajie, H.O., Schoeller, D.A., Edmond, J., Bergner, E.A., and Byerley, L.O. (1994a). In vivo measurement of fatty acids and cholesterol synthesis using D2O and mass isotopomer analysis. Am J Physiol 266, E699-708.
Lee, W.N., Bassilian, S., Guo, Z., Schoeller, D., Edmond, J., Bergner, E.A., and Byerley, L.O. (1994b). Measurement of fractional lipid synthesis using deuterated water (2H2O) and mass isotopomer analysis. Am J Physiol 266, E372-383.
Lee, W.N., Bassilian, S., Lim, S., and Boros, L.G. (2000). Loss of regulation of lipogenesis in the Zucker diabetic (ZDF) rat. Am J Physiol Endocrinol Metab 279, E425-432.
Lelliott, C.J., Medina-Gomez, G., Petrovic, N., Kis, A., Feldmann, H.M., Bjursell, M., Parker, N., Curtis, K., Campbell, M., Hu, P., Zhang, D., Litwin, S.E., Zaha, V.G., Fountain, K.T., Boudina, S., Jimenez-Linan, M., Blount, M., Lopez, M., Meirhaeghe, A., Bohlooly, Y.M., Storlien, L., Stromstedt, M., Snaith, M., Oresic, M., Abel, E.D., Cannon,

B., and Vidal-Puig, A. (2006). Ablation of PGC-1beta results in defective mitochondrial activity, thermogenesis, hepatic function, and cardiac performance. PLoS Biol 4, e369.
Leone, T.C., Lehman, J.J., Finck, B.N., Schaeffer, P.J., Wende, A.R., Boudina, S., Courtois, M., Wozniak, D.F., Sambandam, N., Bernal-Mizrachi, C., Chen, Z., Holloszy, J.O., Medeiros, D.M., Schmidt, R.E., Saffitz, J.E., Abel, E.D., Semenkovich, C.F., and Kelly, D.P. (2005). PGC-1alpha deficiency causes multi-system energy metabolic derangements: muscle dysfunction, abnormal weight control and hepatic steatosis. PLoS Biol 3, e101.
Li, S., Brown, M.S., and Goldstein, J.L. (2010). Bifurcation of insulin signaling pathway in rat liver: mTORC1 required for stimulation of lipogenesis, but not inhibition of gluconeogenesis. Proc Natl Acad Sci U S A 107, 3441-3446.
Li, X., Grundy, S.M., and Patel, S.B. (1997). Obesity in db and ob animals leads to impaired hepatic very low density lipoprotein secretion and differential secretion of apolipoprotein B-48 and B-100. J Lipid Res 38, 1277-1288.
Li, X., Monks, B., Ge, Q., and Birnbaum, M.J. (2007). Akt/PKB regulates hepatic metabolism by directly inhibiting PGC-1alpha transcription coactivator. Nature 447, 1012-1016.
Liang, C.P., and Tall, A.R. (2001). Transcriptional profiling reveals global defects in energy metabolism, lipoprotein, and bile acid synthesis and transport with reversal by leptin treatment in ob/ob mouse liver. J Biol Chem 276, 49066-49076.
Liang, G., Yang, J., Horton, J.D., Hammer, R.E., Goldstein, J.L., and Brown, M.S. (2002). Diminished hepatic response to fasting/refeeding and liver X receptor agonists in mice with selective deficiency of sterol regulatory element-binding protein-1c. J Biol Chem 277, 9520-9528.
Liao, W., Hui, T.Y., Young, S.G., and Davis, R.A. (2003). Blocking microsomal triglyceride transfer protein interferes with apoB secretion without causing retention or stress in the ER. J Lipid Res 44, 978-985.
Lin, J., Handschin, C., and Spiegelman, B.M. (2005). Metabolic control through the PGC-1 family of transcription coactivators. Cell Metab 1, 361-370.
Luong, N., Davies, C.R., Wessells, R.J., Graham, S.M., King, M.T., Veech, R., Bodmer, R., and Oldham, S.M. (2006). Activated FOXO-mediated insulin resistance is blocked by reduction of TOR activity. Cell Metab 4, 133-142.

Mao, J., DeMayo, F.J., Li, H., Abu-Elheiga, L., Gu, Z., Shaikenov, T.E., Kordari, P., Chirala, S.S., Heird, W.C., and Wakil, S.J. (2006). Liver-specific deletion of acetyl-CoA carboxylase 1 reduces hepatic triglyceride accumulation without affecting glucose homeostasis. Proc Natl Acad Sci U S A 103, 8552-8557.

Matsuda, M., Korn, B.S., Hammer, R.E., Moon, Y.A., Komuro, R., Horton, J.D., Goldstein, J.L., Brown, M.S., and Shimomura, I. (2001). SREBP cleavage-activating protein (SCAP) is required for increased lipid synthesis in liver induced by cholesterol deprivation and insulin elevation. Genes Dev 15, 1206-1216.

Matsumoto, M., Han, S., Kitamura, T., and Accili, D. (2006). Dual role of transcription factor FoxO1 in controlling hepatic insulin sensitivity and lipid metabolism. J Clin Invest 116, 2464-2472.

Matsumoto, M., Ogawa, W., Akimoto, K., Inoue, H., Miyake, K., Furukawa, K., Hayashi, Y., Iguchi, H., Matsuki, Y., Hiramatsu, R., Shimano, H., Yamada, N., Ohno, S., Kasuga, M., and Noda, T. (2003). PKClambda in liver mediates insulin-induced SREBP-1c expression and determines both hepatic lipid content and overall insulin sensitivity. J Clin Invest 112, 935-944.

Matsumoto, M., Ogawa, W., Teshigawara, K., Inoue, H., Miyake, K., Sakaue, H., and Kasuga, M. (2002). Role of the insulin receptor substrate 1 and phosphatidylinositol 3-kinase signaling pathway in insulin-induced expression of sterol regulatory element binding protein 1c and glucokinase genes in rat hepatocytes. Diabetes 51, 1672-1680.

Matsumoto, M., Pocai, A., Rossetti, L., Depinho, R.A., and Accili, D. (2007). Impaired regulation of hepatic glucose production in mice lacking the forkhead transcription factor Foxo1 in liver. Cell Metab 6, 208-216.

Matsusue, K., Haluzik, M., Lambert, G., Yim, S.H., Gavrilova, O., Ward, J.M., Brewer, B., Jr., Reitman, M.L., and Gonzalez, F.J. (2003). Liver-specific disruption of PPARgamma in leptin-deficient mice improves fatty liver but aggravates diabetic phenotypes. J Clin Invest 111, 737-747.

Matsusue, K., Kusakabe, T., Noguchi, T., Takiguchi, S., Suzuki, T., Yamano, S., and Gonzalez, F.J. (2008). Hepatic steatosis in leptin-deficient mice is promoted by the PPARgamma target gene Fsp27. Cell Metab 7, 302-311.

McCabe, B.J., Bederman, I.R., Croniger, C., Millward, C., Norment, C., and Previs, S.F. (2006). Reproducibility of gas chromatography-mass spectrometry measurements of 2H

labeling of water: application for measuring body composition in mice. Anal Biochem 350, 171-176.
McGarry, J.D. (1992). What if Minkowski had been ageusic? An alternative angle on diabetes. Science 258, 766-770.
Michael, M.D., Kulkarni, R.N., Postic, C., Previs, S.F., Shulman, G.I., Magnuson, M.A., and Kahn, C.R. (2000). Loss of insulin signaling in hepatocytes leads to severe insulin resistance and progressive hepatic dysfunction. Mol Cell 6, 87-97.
Millar, J.S., Cromley, D.A., McCoy, M.G., Rader, D.J., and Billheimer, J.T. (2005). Determining hepatic triglyceride production in mice: comparison of poloxamer 407 with Triton WR-1339. J Lipid Res 46, 2023-2028.
Mittendorfer, B., and Sidossis, L.S. (2001). Mechanism for the increase in plasma triacylglycerol concentrations after consumption of short-term, high-carbohydrate diets. Am J Clin Nutr 73, 892-899.
Miyake, K., Ogawa, W., Matsumoto, M., Nakamura, T., Sakaue, H., and Kasuga, M. (2002). Hyperinsulinemia, glucose intolerance, and dyslipidemia induced by acute inhibition of phosphoinositide 3-kinase signaling in the liver. J Clin Invest 110, 1483-1491.
Miyazaki, M., Flowers, M.T., Sampath, H., Chu, K., Otzelberger, C., Liu, X., and Ntambi, J.M. (2007). Hepatic stearoyl-CoA desaturase-1 deficiency protects mice from carbohydrate-induced adiposity and hepatic steatosis. Cell Metab 6, 484-496.
Nelson, D.L., and Cox, M.M. (2008). Lehninger Principles of Biochemistry. (New York, NY: W.H. Freeman and Company).
Neschen, S., Morino, K., Hammond, L.E., Zhang, D., Liu, Z.X., Romanelli, A.J., Cline, G.W., Pongratz, R.L., Zhang, X.M., Choi, C.S., Coleman, R.A., and Shulman, G.I. (2005). Prevention of hepatic steatosis and hepatic insulin resistance in mitochondrial acyl-CoA:glycerol-sn-3-phosphate acyltransferase 1 knockout mice. Cell Metab 2, 55-65.
Ntambi, J.M., Miyazaki, M., Stoehr, J.P., Lan, H., Kendziorski, C.M., Yandell, B.S., Song, Y., Cohen, P., Friedman, J.M., and Attie, A.D. (2002). Loss of stearoyl-CoA desaturase-1 function protects mice against adiposity. Proc Natl Acad Sci U S A 99, 11482-11486.
Ono, H., Shimano, H., Katagiri, H., Yahagi, N., Sakoda, H., Onishi, Y., Anai, M., Ogihara, T., Fujishiro, M., Viana, A.Y., Fukushima, Y., Abe, M., Shojima, N., Kikuchi, M., Yamada, N., Oka, Y., and Asano, T. (2003). Hepatic Akt activation induces marked hypoglycemia,

hepatomegaly, and hypertriglyceridemia with sterol regulatory element binding protein involvement. Diabetes 52, 2905-2913.
Oosterveer, M.H., van Dijk, T.H., Tietge, U.J., Boer, T., Havinga, R., Stellaard, F., Groen, A.K., Kuipers, F., and Reijngoud, D.J. (2009). High fat feeding induces hepatic fatty acid elongation in mice. PLoS One 4, e6066.
Parekh, P.I., Petro, A.E., Tiller, J.M., Feinglos, M.N., and Surwit, R.S. (1998). Reversal of diet-induced obesity and diabetes in C57BL/6J mice. Metabolism 47, 1089-1096.
Parekh, S., and Anania, F.A. (2007). Abnormal lipid and glucose metabolism in obesity: implications for nonalcoholic fatty liver disease. Gastroenterology 132, 2191-2207.
Parks, E.J., Skokan, L.E., Timlin, M.T., and Dingfelder, C.S. (2008). Dietary sugars stimulate fatty acid synthesis in adults. J Nutr 138, 1039-1046.
Pende, M., Kozma, S.C., Jaquet, M., Oorschot, V., Burcelin, R., Le Marchand-Brustel, Y., Klumperman, J., Thorens, B., and Thomas, G. (2000). Hypoinsulinaemia, glucose intolerance and diminished beta-cell size in S6K1-deficient mice. Nature 408, 994-997.
Petersen, K.F., Dufour, S., Savage, D.B., Bilz, S., Solomon, G., Yonemitsu, S., Cline, G.W., Befroy, D., Zemany, L., Kahn, B.B., Papademetris, X., Rothman, D.L., and Shulman, G.I. (2007). The role of skeletal muscle insulin resistance in the pathogenesis of the metabolic syndrome. Proc Natl Acad Sci U S A 104, 12587-12594.
Petersen, K.F., Laurent, D., Rothman, D.L., Cline, G.W., and Shulman, G.I. (1998). Mechanism by which glucose and insulin inhibit net hepatic glycogenolysis in humans. J Clin Invest 101, 1203-1209.
Petersen, K.F., Oral, E.A., Dufour, S., Befroy, D., Ariyan, C., Yu, C., Cline, G.W., DePaoli, A.M., Taylor, S.I., Gorden, P., and Shulman, G.I. (2002). Leptin reverses insulin resistance and hepatic steatosis in patients with severe lipodystrophy. J Clin Invest 109, 1345-1350.
Petro, A.E., Cotter, J., Cooper, D.A., Peters, J.C., Surwit, S.J., and Surwit, R.S. (2004). Fat, carbohydrate, and calories in the development of diabetes and obesity in the C57BL/6J mouse. Metabolism 53, 454-457.
Porstmann, T., Griffiths, B., Chung, Y.L., Delpuech, O., Griffiths, J.R., Downward, J., and Schulze, A. (2005). PKB/Akt induces transcription of enzymes involved in cholesterol and fatty acid biosynthesis via activation of SREBP. Oncogene 24, 6465-6481.

Porstmann, T., Santos, C.R., Griffiths, B., Cully, M., Wu, M., Leevers, S., Griffiths, J.R., Chung, Y.L., and Schulze, A. (2008). SREBP activity is regulated by mTORC1 and contributes to Akt-dependent cell growth. Cell Metab 8, 224-236.
Postic, C., Dentin, R., Denechaud, P.D., and Girard, J. (2007). ChREBP, a transcriptional regulator of glucose and lipid metabolism. Annual review of nutrition 27, 179-192.
Postic, C., and Girard, J. (2008). Contribution of de novo fatty acid synthesis to hepatic steatosis and insulin resistance: lessons from genetically engineered mice. The Journal of clinical investigation 118, 829-838.
Punga, T., Bengoechea-Alonso, M.T., and Ericsson, J. (2006). Phosphorylation and ubiquitination of the transcription factor sterol regulatory element-binding protein-1 in response to DNA binding. J Biol Chem 281, 25278-25286.
Raghow, R., Yellaturu, C., Deng, X., Park, E.A., and Elam, M.B. (2008). SREBPs: the crossroads of physiological and pathological lipid homeostasis. Trends Endocrinol Metab 19, 65-73.
Ramnanan, C.J., Edgerton, D.S., Rivera, N., Irimia-Dominguez, J., Farmer, B., Neal, D.W., Lautz, M., Donahue, E.P., Meyer, C.M., Roach, P.J., and Cherrington, A.D. (2010). Molecular characterization of insulin-mediated suppression of hepatic glucose production in vivo R2. Diabetes.
Rebuffe-Scrive, M., Surwit, R., Feinglos, M., Kuhn, C., and Rodin, J. (1993). Regional fat distribution and metabolism in a new mouse model (C57BL/6J) of non-insulin-dependent diabetes mellitus. Metabolism 42, 1405-1409.
Reilly, M.P., and Rader, D.J. (2003). The metabolic syndrome: more than the sum of its parts? Circulation 108, 1546-1551.
Repa, J.J., Liang, G., Ou, J., Bashmakov, Y., Lobaccaro, J.M., Shimomura, I., Shan, B., Brown, M.S., Goldstein, J.L., and Mangelsdorf, D.J. (2000). Regulation of mouse sterol regulatory element-binding protein-1c gene (SREBP-1c) by oxysterol receptors, LXRalpha and LXRbeta. Genes Dev 14, 2819-2830.
Ribaux, P.G., and Iynedjian, P.B. (2003). Analysis of the role of protein kinase B (cAKT) in insulin-dependent induction of glucokinase and sterol regulatory element-binding protein 1 (SREBP1) mRNAs in hepatocytes. Biochem J 376, 697-705.
Roach, P.J. (2002). Glycogen and its metabolism. Current molecular medicine 2, 101-120.

Sajan, M.P., Standaert, M.L., Nimal, S., Varanasi, U., Pastoor, T., Mastorides, S., Braun, U., Leitges, M., and Farese, R.V. (2009). The critical role of atypical protein kinase C in activating hepatic SREBP-1c and NFkappaB in obesity. J Lipid Res 50, 1133-1145.
Saltiel, A.R. (2001). New perspectives into the molecular pathogenesis and treatment of type 2 diabetes. Cell 104, 517-529.
Sarbassov, D.D., Guertin, D.A., Ali, S.M., and Sabatini, D.M. (2005). Phosphorylation and regulation of Akt/PKB by the rictor-mTOR complex. Science 307, 1098-1101.
Savage, D.B., Choi, C.S., Samuel, V.T., Liu, Z.X., Zhang, D., Wang, A., Zhang, X.M., Cline, G.W., Yu, X.X., Geisler, J.G., Bhanot, S., Monia, B.P., and Shulman, G.I. (2006). Reversal of diet-induced hepatic steatosis and hepatic insulin resistance by antisense oligonucleotide inhibitors of acetyl-CoA carboxylases 1 and 2. J Clin Invest 116, 817-824.
Schreiber, S.N., Knutti, D., Brogli, K., Uhlmann, T., and Kralli, A. (2003). The transcriptional coactivator PGC-1 regulates the expression and activity of the orphan nuclear receptor estrogen-related receptor alpha (ERRalpha). J Biol Chem 278, 9013-9018.
Schultz, J.R., Tu, H., Luk, A., Repa, J.J., Medina, J.C., Li, L., Schwendner, S., Wang, S., Thoolen, M., Mangelsdorf, D.J., Lustig, K.D., and Shan, B. (2000). Role of LXRs in control of lipogenesis. Genes Dev 14, 2831-2838.
Schwarz, J.M., Linfoot, P., Dare, D., and Aghajanian, K. (2003). Hepatic de novo lipogenesis in normoinsulinemic and hyperinsulinemic subjects consuming high-fat, low-carbohydrate and low-fat, high-carbohydrate isoenergetic diets. Am J Clin Nutr 77, 43-50.
Schwarz, J.M., Neese, R.A., Turner, S., Dare, D., and Hellerstein, M.K. (1995). Short-term alterations in carbohydrate energy intake in humans. Striking effects on hepatic glucose production, de novo lipogenesis, lipolysis, and whole-body fuel selection. J Clin Invest 96, 2735-2743.
Semple, R.K., Sleigh, A., Murgatroyd, P.R., Adams, C.A., Bluck, L., Jackson, S., Vottero, A., Kanabar, D., Charlton-Menys, V., Durrington, P., Soos, M.A., Carpenter, T.A., Lomas, D.J., Cochran, E.K., Gorden, P., O'Rahilly, S., and Savage, D.B. (2009). Postreceptor insulin resistance contributes to human dyslipidemia and hepatic steatosis. J Clin Invest 119, 315-322.

Shimano, H., Horton, J.D., Hammer, R.E., Shimomura, I., Brown, M.S., and Goldstein, J.L. (1996). Overproduction of cholesterol and fatty acids causes massive liver enlargement in transgenic mice expressing truncated SREBP-1a. J Clin Invest 98, 1575-1584.

Shimano, H., Horton, J.D., Shimomura, I., Hammer, R.E., Brown, M.S., and Goldstein, J.L. (1997a). Isoform 1c of sterol regulatory element binding protein is less active than isoform 1a in livers of transgenic mice and in cultured cells. J Clin Invest 99, 846-854.

Shimano, H., Shimomura, I., Hammer, R.E., Herz, J., Goldstein, J.L., Brown, M.S., and Horton, J.D. (1997b). Elevated levels of SREBP-2 and cholesterol synthesis in livers of mice homozygous for a targeted disruption of the SREBP-1 gene. J Clin Invest 100, 2115-2124.

Shimano, H., Yahagi, N., Amemiya-Kudo, M., Hasty, A.H., Osuga, J., Tamura, Y., Shionoiri, F., Iizuka, Y., Ohashi, K., Harada, K., Gotoda, T., Ishibashi, S., and Yamada, N. (1999). Sterol regulatory element-binding protein-1 as a key transcription factor for nutritional induction of lipogenic enzyme genes. J Biol Chem 274, 35832-35839.

Shimomura, I., Bashmakov, Y., and Horton, J.D. (1999a). Increased levels of nuclear SREBP-1c associated with fatty livers in two mouse models of diabetes mellitus. J Biol Chem 274, 30028-30032.

Shimomura, I., Bashmakov, Y., Ikemoto, S., Horton, J.D., Brown, M.S., and Goldstein, J.L. (1999b). Insulin selectively increases SREBP-1c mRNA in the livers of rats with streptozotocin-induced diabetes. Proc Natl Acad Sci U S A 96, 13656-13661.

Shimomura, I., Hammer, R.E., Ikemoto, S., Brown, M.S., and Goldstein, J.L. (1999c). Leptin reverses insulin resistance and diabetes mellitus in mice with congenital lipodystrophy. Nature 401, 73-76.

Shimomura, I., Matsuda, M., Hammer, R.E., Bashmakov, Y., Brown, M.S., and Goldstein, J.L. (2000). Decreased IRS-2 and increased SREBP-1c lead to mixed insulin resistance and sensitivity in livers of lipodystrophic and ob/ob mice. Mol Cell 6, 77-86.

Shimomura, I., Shimano, H., Horton, J.D., Goldstein, J.L., and Brown, M.S. (1997). Differential expression of exons 1a and 1c in mRNAs for sterol regulatory element binding protein-1 in human and mouse organs and cultured cells. J Clin Invest 99, 838-845.

Shimomura, I., Shimano, H., Korn, B.S., Bashmakov, Y., and Horton, J.D. (1998). Nuclear sterol regulatory element-binding proteins activate genes responsible for the

entire program of unsaturated fatty acid biosynthesis in transgenic mouse liver. J Biol Chem 273, 35299-35306.
Simmgen, M., Knauf, C., Lopez, M., Choudhury, A.I., Charalambous, M., Cantley, J., Bedford, D.C., Claret, M., Iglesias, M.A., Heffron, H., Cani, P.D., Vidal-Puig, A., Burcelin, R., and Withers, D.J. (2006). Liver-specific deletion of insulin receptor substrate 2 does not impair hepatic glucose and lipid metabolism in mice. Diabetologia 49, 552-561.
Song, S., Zhang, Y., Ma, K., Jackson-Hayes, L., Lavrentyev, E.N., Cook, G.A., Elam, M.B., and Park, E.A. (2004). Peroxisomal proliferator activated receptor gamma coactivator (PGC-1alpha) stimulates carnitine palmitoyltransferase I (CPT-Ialpha) through the first intron. Biochim Biophys Acta 1679, 164-173.
Sonoda, J., Mehl, I.R., Chong, L.W., Nofsinger, R.R., and Evans, R.M. (2007). PGC-1beta controls mitochondrial metabolism to modulate circadian activity, adaptive thermogenesis, and hepatic steatosis. Proc Natl Acad Sci U S A 104, 5223-5228.
Sparks, J.D., and Sparks, C.E. (1994). Insulin regulation of triacylglycerol-rich lipoprotein synthesis and secretion. Biochim Biophys Acta 1215, 9-32.
Sparks, J.D., Sparks, C.E., and Miller, L.L. (1989). Insulin effects on apolipoprotein B production by normal, diabetic and treated-diabetic rat liver and cultured rat hepatocytes. Biochem J 261, 83-88.
Stephens, L., Anderson, K., Stokoe, D., Erdjument-Bromage, H., Painter, G.F., Holmes, A.B., Gaffney, P.R., Reese, C.B., McCormick, F., Tempst, P., Coadwell, J., and Hawkins, P.T. (1998). Protein kinase B kinases that mediate phosphatidylinositol 3,4,5-trisphosphate-dependent activation of protein kinase B. Science 279, 710-714.
Stiles, B., Wang, Y., Stahl, A., Bassilian, S., Lee, W.P., Kim, Y.J., Sherwin, R., Devaskar, S., Lesche, R., Magnuson, M.A., and Wu, H. (2004). Liver-specific deletion of negative regulator Pten results in fatty liver and insulin hypersensitivity [corrected]. Proc Natl Acad Sci U S A 101, 2082-2087.
Stoeckman, A.K., and Towle, H.C. (2002). The role of SREBP-1c in nutritional regulation of lipogenic enzyme gene expression. J Biol Chem 277, 27029-27035.
Sun, Y., Liu, S., Ferguson, S., Wang, L., Klepcyk, P., Yun, J.S., and Friedman, J.E. (2002). Phosphoenolpyruvate carboxykinase overexpression selectively attenuates insulin signaling and hepatic insulin sensitivity in transgenic mice. J Biol Chem 277, 23301-23307.

Sundqvist, A., Bengoechea-Alonso, M.T., Ye, X., Lukiyanchuk, V., Jin, J., Harper, J.W., and Ericsson, J. (2005). Control of lipid metabolism by phosphorylation-dependent degradation of the SREBP family of transcription factors by SCF(Fbw7). Cell Metab 1, 379-391.

Surwit, R.S., Feinglos, M.N., Rodin, J., Sutherland, A., Petro, A.E., Opara, E.C., Kuhn, C.M., and Rebuffe-Scrive, M. (1995). Differential effects of fat and sucrose on the development of obesity and diabetes in C57BL/6J and A/J mice. Metabolism 44, 645-651.

Surwit, R.S., Kuhn, C.M., Cochrane, C., McCubbin, J.A., and Feinglos, M.N. (1988). Diet-induced type II diabetes in C57BL/6J mice. Diabetes 37, 1163-1167.

Taghibiglou, C., Carpentier, A., Van Iderstine, S.C., Chen, B., Rudy, D., Aiton, A., Lewis, G.F., and Adeli, K. (2000). Mechanisms of hepatic very low density lipoprotein overproduction in insulin resistance. Evidence for enhanced lipoprotein assembly, reduced intracellular ApoB degradation, and increased microsomal triglyceride transfer protein in a fructose-fed hamster model. J Biol Chem 275, 8416-8425.

Tamemoto, H., Kadowaki, T., Tobe, K., Yagi, T., Sakura, H., Hayakawa, T., Terauchi, Y., Ueki, K., Kaburagi, Y., Satoh, S., and et al. (1994). Insulin resistance and growth retardation in mice lacking insulin receptor substrate-1. Nature 372, 182-186.

Tamura, S., and Shimomura, I. (2005). Contribution of adipose tissue and de novo lipogenesis to nonalcoholic fatty liver disease. J Clin Invest 115, 1139-1142.

Taniguchi, C.M., Emanuelli, B., and Kahn, C.R. (2006a). Critical nodes in signalling pathways: insights into insulin action. Nat Rev Mol Cell Biol 7, 85-96.

Taniguchi, C.M., Kondo, T., Sajan, M., Luo, J., Bronson, R., Asano, T., Farese, R., Cantley, L.C., and Kahn, C.R. (2006b). Divergent regulation of hepatic glucose and lipid metabolism by phosphoinositide 3-kinase via Akt and PKClambda/zeta. Cell Metab 3, 343-353.

Taniguchi, C.M., Ueki, K., and Kahn, R. (2005). Complementary roles of IRS-1 and IRS-2 in the hepatic regulation of metabolism. J Clin Invest 115, 718-727.

Taskinen, M.R. (2003). Diabetic dyslipidaemia: from basic research to clinical practice. Diabetologia 46, 733-749.

Teleman, A.A., Chen, Y.W., and Cohen, S.M. (2005). 4E-BP functions as a metabolic brake used under stress conditions but not during normal growth. Genes Dev 19, 1844-1848.

Timlin, M.T., and Parks, E.J. (2005). Temporal pattern of de novo lipogenesis in the postprandial state in healthy men. Am J Clin Nutr 81, 35-42.

Tobe, K., Suzuki, R., Aoyama, M., Yamauchi, T., Kamon, J., Kubota, N., Terauchi, Y., Matsui, J., Akanuma, Y., Kimura, S., Tanaka, J., Abe, M., Ohsumi, J., Nagai, R., and Kadowaki, T. (2001). Increased expression of the sterol regulatory element-binding protein-1 gene in insulin receptor substrate-2(-/-) mouse liver. J Biol Chem 276, 38337-38340.

Tontonoz, P., and Mangelsdorf, D.J. (2003). Liver X receptor signaling pathways in cardiovascular disease. Mol Endocrinol 17, 985-993.

Um, S.H., Frigerio, F., Watanabe, M., Picard, F., Joaquin, M., Sticker, M., Fumagalli, S., Allegrini, P.R., Kozma, S.C., Auwerx, J., and Thomas, G. (2004). Absence of S6K1 protects against age- and diet-induced obesity while enhancing insulin sensitivity. Nature 431, 200-205.

West, D.B., Boozer, C.N., Moody, D.L., and Atkinson, R.L. (1992). Dietary obesity in nine inbred mouse strains. Am J Physiol 262, R1025-1032.

WHO (2008). Fact Sheet: The Top Ten Causes of Death. In http://www.who.int/mediacentre/factsheets/fs310/en/index.html. M.C. World Health Organization, ed.

Wiegman, C.H., Bandsma, R.H., Ouwens, M., van der Sluijs, F.H., Havinga, R., Boer, T., Reijngoud, D.J., Romijn, J.A., and Kuipers, F. (2003). Hepatic VLDL production in ob/ob mice is not stimulated by massive de novo lipogenesis but is less sensitive to the suppressive effects of insulin. Diabetes 52, 1081-1089.

Withers, D.J., Gutierrez, J.S., Towery, H., Burks, D.J., Ren, J.M., Previs, S., Zhang, Y., Bernal, D., Pons, S., Shulman, G.I., Bonner-Weir, S., and White, M.F. (1998). Disruption of IRS-2 causes type 2 diabetes in mice. Nature 391, 900-904.

Wolfrum, C., Asilmaz, E., Luca, E., Friedman, J.M., and Stoffel, M. (2004). Foxa2 regulates lipid metabolism and ketogenesis in the liver during fasting and in diabetes. Nature 432, 1027-1032.

Wolfrum, C., and Stoffel, M. (2006). Coactivation of Foxa2 through Pgc-1beta promotes liver fatty acid oxidation and triglyceride/VLDL secretion. Cell Metab 3, 99-110.

Yahagi, N., Shimano, H., Hasty, A.H., Matsuzaka, T., Ide, T., Yoshikawa, T., Amemiya-Kudo, M., Tomita, S., Okazaki, H., Tamura, Y., Iizuka, Y., Ohashi, K., Osuga, J., Harada, K., Gotoda, T., Nagai, R., Ishibashi, S., and Yamada, N. (2002). Absence of sterol

regulatory element-binding protein-1 (SREBP-1) ameliorates fatty livers but not obesity or insulin resistance in Lep(ob)/Lep(ob) mice. The Journal of biological chemistry 277, 19353-19357.

Yamashita, H., Takenoshita, M., Sakurai, M., Bruick, R.K., Henzel, W.J., Shillinglaw, W., Arnot, D., and Uyeda, K. (2001). A glucose-responsive transcription factor that regulates carbohydrate metabolism in the liver. Proc Natl Acad Sci U S A 98, 9116-9121.

Yang, D., Diraison, F., Beylot, M., Brunengraber, D.Z., Samols, M.A., Anderson, V.E., and Brunengraber, H. (1998). Assay of low deuterium enrichment of water by isotopic exchange with [U-13C3]acetone and gas chromatography-mass spectrometry. Anal Biochem 258, 315-321.

Yang, J., Goldstein, J.L., Hammer, R.E., Moon, Y.A., Brown, M.S., and Horton, J.D. (2001). Decreased lipid synthesis in livers of mice with disrupted Site-1 protease gene. Proc Natl Acad Sci U S A 98, 13607-13612.

Zhang, L., Rubins, N.E., Ahima, R.S., Greenbaum, L.E., and Kaestner, K.H. (2005). Foxa2 integrates the transcriptional response of the hepatocyte to fasting. Cell Metab 2, 141-148.

Zhang, W., Patil, S., Chauhan, B., Guo, S., Powell, D.R., Le, J., Klotsas, A., Matika, R., Xiao, X., Franks, R., Heidenreich, K.A., Sajan, M.P., Farese, R.V., Stolz, D.B., Tso, P., Koo, S.H., Montminy, M., and Unterman, T.G. (2006). FoxO1 regulates multiple metabolic pathways in the liver: effects on gluconeogenic, glycolytic, and lipogenic gene expression. J Biol Chem 281, 10105-10117.

Zhang, Y., Castellani, L.W., Sinal, C.J., Gonzalez, F.J., and Edwards, P.A. (2004a). Peroxisome proliferator-activated receptor-gamma coactivator 1alpha (PGC-1alpha) regulates triglyceride metabolism by activation of the nuclear receptor FXR. Genes Dev 18, 157-169.

Zhang, Y.L., Hernandez-Ono, A., Ko, C., Yasunaga, K., Huang, L.S., and Ginsberg, H.N. (2004b). Regulation of hepatic apolipoprotein B-lipoprotein assembly and secretion by the availability of fatty acids. I. Differential response to the delivery of fatty acids via albumin or remnant-like emulsion particles. J Biol Chem 279, 19362-19374.

Addendum:

Akt2$^{-/-}$ mice have improved glucose tolerance on Surwit HFD due to increased β-cell compensation

Figure A-1: *Akt2*$^{-/-}$ mice have improved glucose tolerance on Surwit HFD by over-compensating for insulin resistance by dramatically increasing insulin secretion.

Akt2$^{+/+}$ and *Akt2*$^{-/-}$ male mice were put on a Surwit HFD or maintained on chow at approximately 5 weeks of age.

A. Glucose tolerance tests (1g/kg IP) were performed every 5 weeks beginning at start of HFD (week 0).

B. Insulin levels at 0 (left) and 15 (right) minutes post glucose load during GTTs.

All values are expressed as mean ± SEM. n=8-12.

Figure A-1

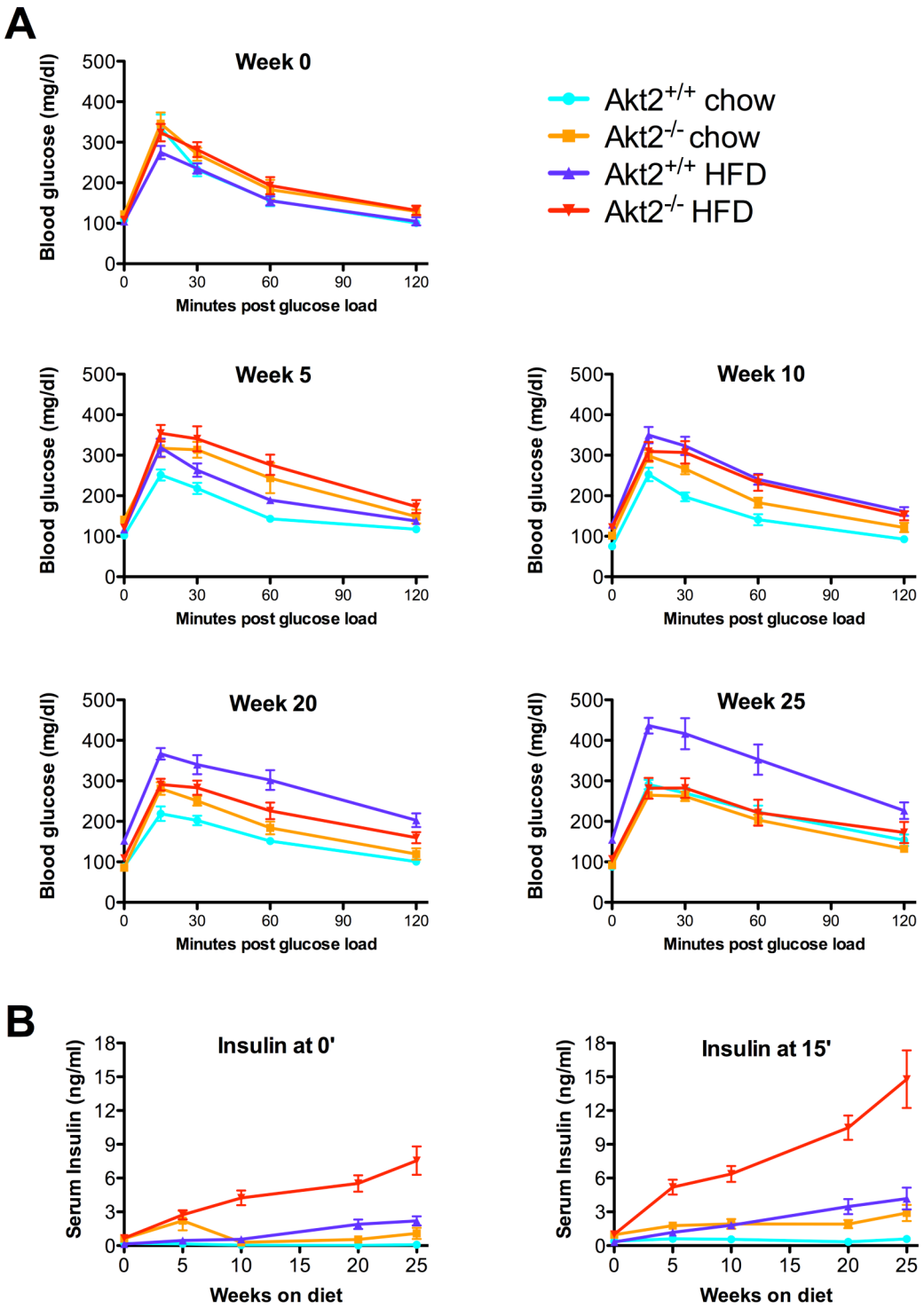
A
Week 0
Week 5
Week 10
Week 20
Week 25
Blood glucose (mg/dl)
Minutes post glucose load
Akt2+/+ chow
Akt2-/- chow
Akt2+/+ HFD
Akt2-/- HFD
B
Insulin at 0'
Insulin at 15'
Serum Insulin (ng/ml)
Weeks on diet

Figure A-2: *Akt2*$^{-/-}$ mice on Surwit HFD appear to have dramatically increased β-cell mass compared with their *Akt2*$^{+/+}$counterparts.

Akt2$^{+/+}$ and *Akt2*$^{-/-}$ male mice were put on a Surwit HFD or maintained on chow at approximately 5 weeks of age for 28 weeks.

A. Composite picture of pancreatic section from *Akt2*$^{+/+}$ and *Akt2*$^{-/-}$ mouse on Surwit HFD. Sections were fixed in 4% paraformaldehyde, embedded in paraffin, and immunohistochemistry was performed against insulin.

B. Hematoxylin and eosin stain of pancreatic sections. 100x magnification.

C. Preliminary quantification of β-cell mass from 4 mice (2 *Akt2*$^{+/+}$ and 2 *Akt2*$^{-/-}$). Each bar represents the mean ± SEM of mass from 3 pancreatic images (like those shown in A) of a single mouse. β-cell mass was determined using Metamorph software (Molecular Devices, INC).

Figure A-2

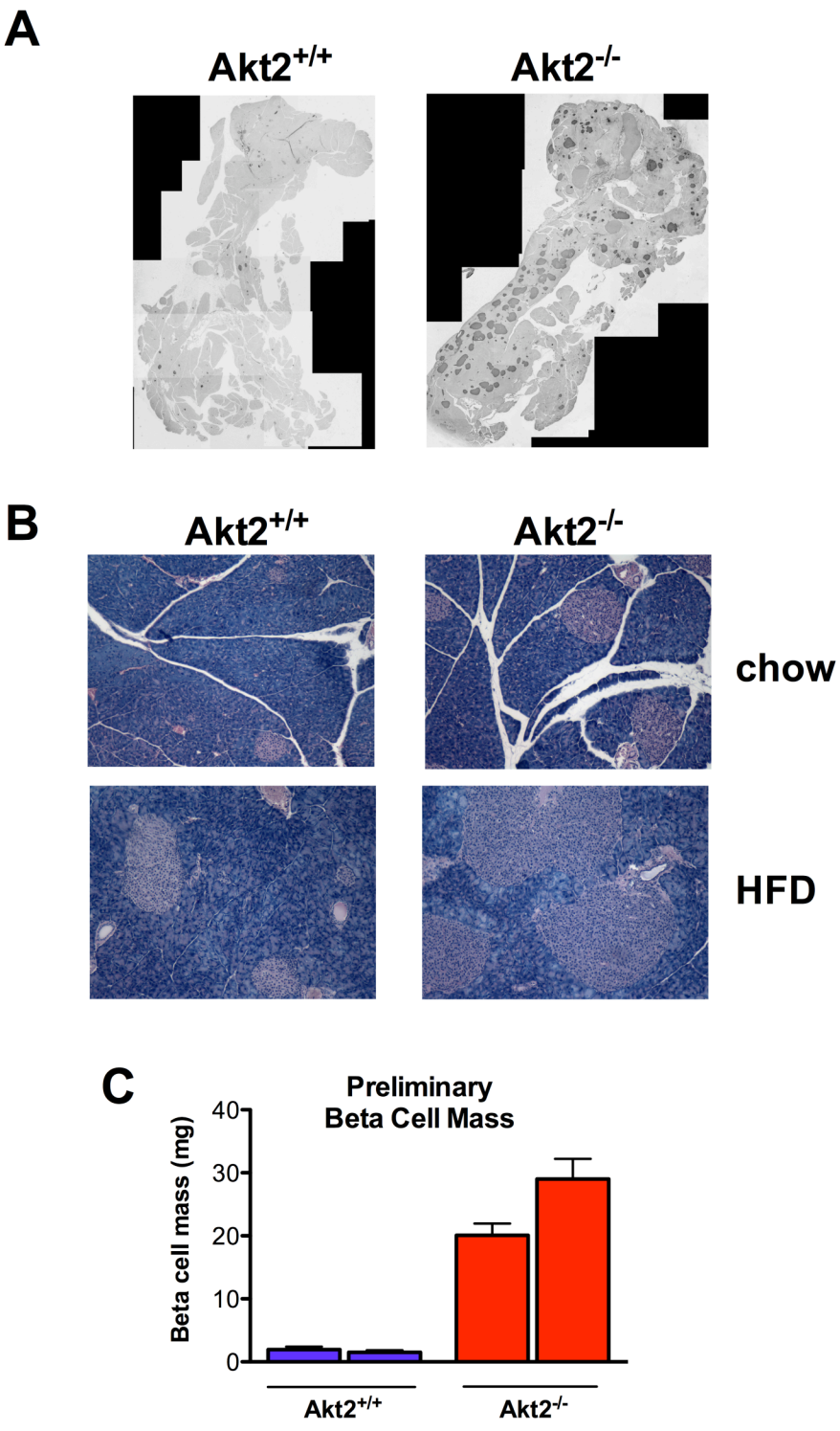
A
Akt2+/+
Akt2-/-
B
Akt2+/+
Akt2-/-
chow
HFD
C
Preliminary
Beta Cell Mass
Beta cell mass (mg)
40
30
20
10
0
Akt2+/+
Akt2-/-

Figure A-3: Improvement in GTT of *Akt2*$^{-/-}$ mouse on Surwit HFD is not due to cell-autonomous loss of Akt2 in the β-cell.

Akt2$^{lox/lox}$ and *Pdx;Akt2*$^{lox/lox}$ male mice were put on a Surwit HFD or maintained on chow at approximately 5 weeks of age.

A-B. Glucose tolerance tests (1g/kg IP) were performed at 10 (A) and 25 (B) weeks after the start of HFD. Insulin levels were measured at 0 and 15 minutes post glucose load during GTTs.

All values are expressed as mean ± SEM. n=5-7.

Figure A-3

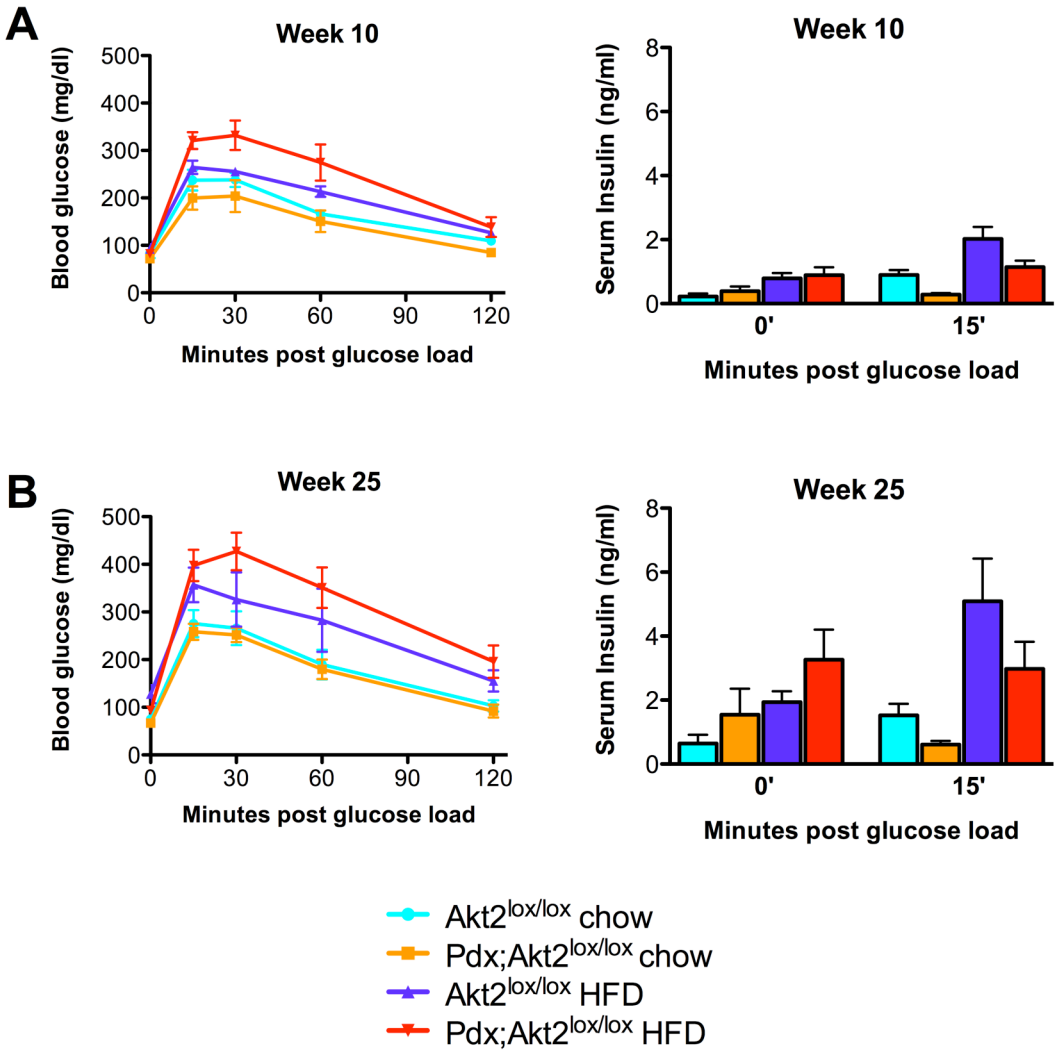
A
Week 10
Blood glucose (mg/dl)
500
400
300
200
100
0
0
30
60
90
120
Minutes post glucose load
Week 10
Serum Insulin (ng/ml)
8
6
4
2
0
0'
15'
Minutes post glucose load
B
Week 25
Blood glucose (mg/dl)
500
400
300
200
100
0
0
30
60
90
120
Minutes post glucose load
Week 25
Serum Insulin (ng/ml)
8
6
4
2
0
0'
15'
Minutes post glucose load
Akt2lox/lox chow
Pdx;Akt2lox/lox chow
Akt2lox/lox HFD
Pdx;Akt2lox/lox HFD